A SIZE-BASED MODEL OF CARBON AND NITROGEN FLOWS IN PLANKTON COMMUNITIES

by

Coleen Lyn Moloney

Submitted in fulfilment of the requirements for the degree of Doctor of Philosophy in the Faculty of Science (Department of Zoology), University of Cape Town

Supervisors: Professor John G. Field

Dr Michael I. Lucas

September 1988

DECLARATION

This thesis reports the results of original research which I have carried out in the Marine Biology Research Institute, University of Cape Town between 1985 and 1988, and has not been submitted for a degree at any other university. Any technical and other assistance which I have received is fully acknowledged. Most of the data that are presented were obtained from published studies, and are referenced as such.

Coleen Lyn Moloney

For Peter and our parents

In the absolute universe all events can be regarded as absolutely deterministic, and if we can't perceive the greater structures, it's because our vision is faulty

Robert Silverberg, The Stochastic Man (1975)

TABLE OF CONTENTS

ABSTRACT

Moloney, Coleen L. 1988. A size-based model of carbon and nitrogen flows in plankton communities. Ph.D. Thesis, Marine Biology Research Institute, University of Cape Town, Rondebosch 7700, South Africa, (ix)+256pp.

A generic, size-based simulation model is developed to investigate the dynamics of carbon and nitrogen flows in plankton communities. All parameters in the model are determined by body size using empirically-determined relationships calculated from published data. The model is robust with respect to most parameters and assumptions. Because the model is based on general ecological principles, it can be used to simulate microplankton community interactions in any planktonic ecosystem. Two coastal ecosystems from the southern Benguela region in South Africa are simulated; one typical of the relatively stable surface waters on the Agulhas Bank and one typical of upwelling plumes, usually found off the west coast of South Africa. Simulated communities compare well with field observations in terms of standing stocks and size composition, and simulation results indicate that the small-scale structure of the two ecosystems and the processes occurring within them are relatively well understood. Consequently, the dynamic functioning of the two systems is investigated at the ecosystem level, using the simulation results. Hypothetical carbon flow networks are constructed, and the average importance of different flow pathways at different times is assessed. In both ecosystems, the vast majority of carbon flows pass through short, efficient-transfer pathways, although longer pathways are potentially possible. Simulation analyses are extended from coastal to oceanic food webs, and the model results are consistent with the hypothesis that oceanic phytoplankton have rapid rates of primary production. At-sea sampling of a phytoplankton bloom is mimicked by "sampling" from simulation output, and interpretation of the data using standard techniques is compared with the model output. The dangers of extrapolating from snapshot measurements is highlighted, and the experiment emphasizes the importance of size-fractionated sampling of phytoplankton. A hypothetical pelagic food web is described, consisting of at least five different trophic pathways from phytoplankton to pelagic fish. It is suggested that coastal waters probably have all the different pathways, and the relative importance and efficiency of the different pathways will determine the total fish production in an ecosystem.

SUMMARY

1. The dynamics of carbon and nitrogen flows in planktonic food webs can be adequately simulated using a size-based simulation model. Such a model is developed, and is unique in that it is not based on any specific data set or ecosystem; all parameters are derived from empirical body size-relationships that were calculated from published data.
2. Simulation results are presented for two coastal areas in the southern Benguela region off South Africa. The Agulhas Bank simulation describes the dynamics of a microplankton community in conditions typical of the stable, stratified waters of the Agulhas Bank, in which nitrate-nitrogen is assumed to diffuse into the euphotic zone across the thermocline. The resulting community consists of an initially fluctuating phytoplankton crop, which stabilizes to a pico-phytoplankton-dominated assemblage. This steady state probably does not occur in nature, because physical- and other factors continually disrupt the steady-state conditions.
3. A second simulation describes the development of a phytoplankton bloom after an upwelling event, characteristic of the west coast. The results depict a typical "net-phytoplankton" bloom, which lasts for approximately seven days. However, this simulated bloom is preceded by rapid blooms of pico- and nano-phytoplankton, which have not been recorded in the field. It is suggested that such blooms may have been overlooked, or may be depressed by other factors such as light, which are not included in the simulation model.
4. Output from the two simulations is used to investigate the dynamics of the systems from a whole-system perspective. The average pathways of carbon flow through the two systems are assessed, by integrating the flows over time. The results suggest that short trophic pathways (i.e. those with a minimum number of trophic steps) are responsible for channelling most energy through planktonic systems, even though long pathways are present.
5. In the simulations, much carbon is lost from the two systems through respiration, chiefly because temporal mismatches occur between predators and prey. Predator populations do not utilize all prey efficiently, because nutrient- or food-limitation often retards prey-population growth before predators have had time to respond. This occurs as a result of differences in growth rates between small prey organisms and their larger-sized predators.
6. A simple oceanic community in warm, oligotrophic, surface waters is simulated, assuming a small, continuous input of new-nitrogen into the euphotic zone from depth. The results are consistent with the hypothesis that oceanic phytoplankton have fast primary production rates, and community P:B ratios of up to 5 d^{-1} occur in the simulation. However, despite their fast turnover rates, the model populations do not grow maximally, because ambient nitrogen concentrations are too low to support their very rapid potential growth rates.

7. A numerical experiment is carried out to assess whether current methods of analysing and interpreting field data are valid. The results emphasize the importance of size-fractionated sampling of phytoplankton production. Under conditions mimicking a typical incubation experiment, it is shown how the total model community production is almost entirely due to pico-phytoplankton, which have a very small biomass, whereas the large standing stock of model net-phytoplankton depletes its carbon reserves, and has a negative production.
8. The dangers of extrapolating from snapshot measurements are highlighted. It is very difficult to extrapolate to system processes and dynamics from such measurements, because appropriate averaging procedures are not known. The use of simulation models to assist in constructing and testing working hypotheses should be an integral part of any field program, because they force one to consider the total dynamics of the whole system.
9. An average planktonic / pelagic food web is described, in which up to five trophic pathways are possible. It is suggested that eutrophic coastal waters have more complex food webs than oligotrophic oceanic waters, because a number of different pathways for carbon transfer are possible in coastal waters which support a diverse assemblage of cell sizes. In oceanic waters, only the long pathways are possible, because phytoplankton cells are generally small, and cannot be grazed by large zooplankton such as copepods.
10. It is suggested that upwelling food webs have productive fish stocks because of very efficient, short food chains, even though much of primary production may not be directly utilized. Trophic efficiencies can be as high as 50 % at times, because the dense food aggregations that can occur in these regions favour efficient feeding by predators, resulting in efficient trophic transfers.

ACKNOWLEDGEMENTS

Financial and logistical support was provided by the South African National Committee for Oceanographic Research through the Systems Analysis Project of the Benguela Ecology Programme (BEP), and the University of Cape Town.

Many colleagues and friends assisted in the preparation of this thesis. John Field introduced me to the field of systems analysis, and directed my interest in size relationships. I am grateful for his encouragement and support. Mike Lucas patiently listened to many of my ideas, and was always willing and available to tell me about "real data" when I needed it. I thank him and John for the many useful comments they made on the first draft of the thesis. Richard Newell was largely responsible for initiating my modelling studies of carbon and nitrogen flows in the plankton, and his enthusiasm and guidance is gratefully acknowledged.

The Monday lunchtime talks of the BEP gave me a broad perspective of the system I was modelling, as did the many workshops and discussions in which I participated, and I am very grateful to all fellow-researchers in the BEP with whom I worked. I had many useful discussions with colleagues at the University of Cape Town and the Sea Fisheries Research Institute. In particular, Mike Lucas, Suzanne Painting, Trevor Probyn, Frieda Verheye-Dua, Caire Davis, Dave Muir, Andy James, Betty Mitchell-Innes, Larry Hutchings, Penny Brown, Grant Pitcher and Hans Verheye advised me on the structure of the model and the appropriateness of the output. Tony Starfield guided me towards parsimony, and Peter Shelton, Rob Crawford and Mike Bergh offered useful advice.

I am very grateful to the staff of the Computing Centre and the Information Technology Services at the University of Cape Town. The operators kept the COLMOL's running, were sympathetic when the computer was "down" and were unfailingly helpful when it misbehaved. Tommy Williams retrieved "lost" files when I believed them irretrievable. The staff of the Hot Seat uncomplainingly guided me through the development of my programs. The assistance of Gerard Boulle, Roger Haylett, Marietta Swart, Dan Franco and Marius du Toit is gratefully

acknowledged. Marius du Toit went beyond the call of duty in finding bugs where I insisted there were none, and I am grateful for the efforts he put into helping me debug my programs.

All my friends kept me sane by providing an anti-thesis environment, especially fellow members of "JLAB". Patti Wickens and Carlos Villacastin-Herrero uncomplaining assisted in solving big and small technical problems, and Jillian Burbidge assisted in counting most of the phytoplankton samples presented in Chapter 4. I am grateful to Sue Jackson for her companionship during our many lunch-time running sessions when I ran out my thesis frustrations.

Peter Ryan changed my writing style for the better by critically reading most of the initial drafts of the chapters of this thesis, and served as a sounding board for many of the ideas presented. I thank him for his patience and help through all stages of the preparation, and for encouraging me to have the strength of my convictions.

GENERAL INTRODUCTION

The role of bacteria and other micro-organisms in carbon transfer and nitrogen cycling in planktonic ecosystems is a topic currently invoking much debate. There is controversy as to where most of the primary production is channelled. Some studies have implicated bacteria as a link from phytoplankton production to zooplankton and fish (e.g. Cole *et al.* 1982, Laake *et al.* 1983), whereas others have placed emphasis on the role of large herbivores (e.g. Falkowski *et al.* 1983, Holligan *et al* . 1984). The role of these different-sized organisms in the remineralization of nitrogen is also uncertain. Bacteria traditionally are regarded as remineralizers, and some studies have implicated them in the remineralization of nitrogen in the water column (e.g. Harrison 1978, Billen 1984, Newell and Linley 1984). More recently, this has been questioned, and other microheterotrophs (especially bactivores) have been suggested as being the main remineralizers (e.g. Goldman *et al.* 1985). The role of macrozooplankton also is controversial (e.g. Holligan *et al.* 1984, Newell and Linley 1984).

There is little consensus as to how planktonic ecosystems function (cf. Williams 1981). The tendency has been for field workers to collect and analyse data from their areas of interest, and then use these data to support or refute one of the conflicting hypotheses regarding the roles of different micro-organisms. Thus there is a plethora of data, but few coherent hypotheses to explain the different results obtained. As with all controversies, many of the differences arise from the fact that different workers view the ecosystem from different perpectives, and thus reach different conclusions from their data. These above approaches typify reductionist models, in which attempts are made to explain system properties from detailed studies of components of the system. This thesis adopts a whole-system approach, and general system properties are used to analyse the functioning of planktonic ecosystems. In this regard, the systems model developed here synthesises some current understanding of planktonic ecosystem processes and functioning; predictions made by the model allow rigorous tests of hypotheses. More pragmatically, model predictions can be used to direct field research, to either invalidate or further strengthen current theory.

The most universally applicable system property that has been identified is the influence of organism size on rates of processes in and interactions among planktonic (and other) organisms (Peters 1983, Dickie *et al.* 1987). Consequently, I have developed a size-based model of a generalized plankton community to address the controversies regarding carbon and nitrogen flows through plankton communities.

The thesis is divided into three sections. The first section, consisting of two chapters, formalizes and quantifies the most important body-size relationships from empirical observations gleaned from the plankton literature. In Chapter 1 the allometric relationships describing the influence of body size on maximum specific nitrogen uptake rates, maximum specific ingestion rates and specific respiration rates are standardized with a common scaling factor, and allometric parameters are calculated. This allows these relationships to be used to predict rate parameters for a wide variety of sizes in general ecological models. In Chapter 2 four other factors affecting carbon and nitrogen flows in the plankton are related to organism size and quantified. These are 1) predator : prey size ratios, 2) parameters affecting the ability of phytoplankton and bacterioplankton to take up nutrients at low ambient concentrations, 3) parameters affecting the predation pressure on organisms when present in small numbers, and 4) sinking velocities of phytoplankton and faecal material through the water column.

The second section describes the development of the simulation model and presents some results. The section consists of four chapters. In Chapter 3 the model functions are described in detail, and a standard simulation is executed to demonstrate the output from the model and to serve as a basis for a sensitivity analysis. The sensitivity analysis is used to identify areas in which the model output is particularly sensitive to parameter values or the structure of the model. In Chapter 4 the model is used to simulate two contrasting plankton communities in the southern Benguela region; an Agulhas Bank community and a community off the west coast in an upwelling area. Having simulated the two Benguela communities, the model is used to analyse the functioning of the ecosystems in Chapter 5. In particular, the partitioning of primary production between the different sizes of heterotrophs is estimated, and the roles of different components in regenerating nitrogen is investigated. The model output is used to assess the trophic position of pelagic fish in

the two food webs. In Chapter 6 a food web of oligotrophic oceanic waters is simulated, to investigate the rate of primary production in such areas, based on a systems approach.

The third section uses the simulation model to derive general principles governing carbon and nitrogen flows in plankton communities. Chapter 7 uses the model in a numerical experiment, in which "snapshot samples" are taken from the simulation model output, analogous to current field measurements. The "results" are then compared with what actually occurs in the model system, where all of the processes are known. Problems arising from using current data-analysis techniques are identified. In Chapter 8, the different controversies regarding carbon and nitrogen flows are examined in the light of simulation model output. These controversies include the role of bacterioplankton as carbon consumers and nitrogen remineralizers in the plankton, and the "efficiencies" of different food webs. An attempt is made to resolve these controversies by showing that they result primarily from artefacts of snapshot sampling and inappropriate extrapolations, rather than fundamental differences in the functioning of the different systems. A general descriptive model of plankton food webs is presented, which summarizes the main conclusions resulting from the dynamic simulations described in the thesis.

SECTION 1

BODY-SIZE RELATIONSHIPS

CHAPTER 1

GENERAL ALLOMETRIC EQUATIONS FOR RATES OF NUTRIENT UPTAKE, INGESTION AND RESPIRATION IN PLANKTONIC ORGANISMS

ABSTRACT

General allometric equations are derived for rates of nutrient uptake, ingestion and respiration by planktonic organisms. Previous studies commonly calculated parameters a and b in the allometric equation $R = aW^b$ by linear regressions on log-transformed data. This results in variability between data sets in estimates of both a and b, making meaningful comparisons difficult. To overcome this problem, the mass-specific form of b is assumed to be -0.25, based on accumulated empirical evidence. Values of a are then re-calculated from published data by power-transforming all body masses by this exponent. Resulting functional regressions predict values of a ($\pm$ 95 % C.I.) (in pg $C^{0.25}.d^{-1}$) at 20°C as follows: 5.1 ± 0.3 for nutrient uptake by phytoplankton and bacteria; 78 ± 8.0 and 15 ± 1.5 respectively for ingestion and respiration by particle-feeding heterotrophs. In addition to standard statistical proofs, theoretical arguments are used to support calculated values. The validity of separating unicellular from multicellular organisms for allometric respiration models is questioned. Instead, it is hypothesized that organisms that take up dissolved nutrients from solution (autotrophs and osmotrophs e.g. phytoplankton and bacterioplankton) have lower specific respiration rates (i.e. smaller a) than do organisms (either unicellular or multicellular) that ingest particulate material.

INTRODUCTION

Body size is an important determinant of many physiological and ecological rates (Blueweiss *et al.* 1978, Peters 1983, Calder 1985, Dickie *et al.* 1987). Allometric equations have been derived *inter alia* for metabolic rates (Kleiber 1932, 1947, Brody *et al.*1934, Hemmingsen 1960), respiration rates (Ikeda 1970, Banse 1976, 1982, Humphreys 1979, Ivleva 1980), ingestion rates (Dagg 1976, Ikeda 1977, Lampert 1977, Cammen 1980, Ross 1982a), excretion rates (Brody *et al.* 1934), photosynthetic rates (Banse 1976, Taguchi 1976) and growth rates (Fenchel 1974, Banse 1976, 1982, Baldock *et al.* 1980, Schlesinger *et al.* 1981, Taylor and Shuter 1981) for a wide variety of organisms, ranging in size from viruses to large mammals (Blueweiss *et al.*1978, Peters 1983). As a consequence of the many studies estimating allometric equations, there are several different allometric models, often for the same process and group of organisms (see Table 1.1). This can lead to distracting arguments as to which model is "best" (Economos 1979, Heusner 1982a), as well as making it difficult to decide which model to use. Rather than emphasizing differences between models, there is a need to synthesize existing information and derive general allometric equations which highlight similarities in allometric processes, and make the models useful for predictive purposes (Platt 1985).

This chapter aims to simplify comparisons among published allometric regressions for planktonic organisms, by using literature data to derive general allometric equations and calculate confidence limits for estimates of rate coefficients. A novel approach is adopted in fitting parameters to allometric equations; body masses are power-transformed by an unchanging exponent, in keeping with theoretical and empirical evidence as to the power-form of the general allometric equation. Rate coefficients are then calculated. This procedure avoids the problem of obtaining dissimilar estimates of both allometric parameters for different data sets, and allows comparisons to be made between rate coefficients for different allometric processes.

Table 1.1. "General" allometric equations for different groups of organisms. Parameters were converted to values compatable with carbon masses (pg C) and mass-specific rates (d^{-1}) at 20°C.

Parameter	Organisms	*a*	*b*	Reference
Growth	Virus - mammals	20	-0.25	Fenchel (1974)
Growth	Virus - mammals	16.5	-0.26	Blueweiss *et al.* (1978)
Growth	Ciliates & amoebae	9.45	-0.311	Baldock *et al.* (1980)
Growth	Ciliates	12	-0.247	Taylor and Shuter (1981)
Growth	Copepod	9.2	-0.15	Ross (1982)
Ingestion	Marine amphipod	68	-0.25	Dagg (1976)
Ingestion	Detritivores	76	-0.258	Cammen (1980)
Ingestion	Invertebrates	54	-0.306	Capriulo (1982)
Respiration	Rat - steer	-	-0.25	Kleiber (1932)
Respiration	Mouse - elephant	-	-0.266	Brody *et al.* (1934)
Respiration	Bacteria - mammals	-	-0.25	Hemmingsen (1960)
Respiration	Marine plankton	33	-0.309	Ikeda (1970)
Respiration	Unicellular algae	0.4	-0.10	Banse (1976)
Respiration	Marine amphipod	11.6	-0.225	Dagg (1976)
Respiration	Daphnia	10	-0.15	Lampert (1977)
Respiration	Zooplankton	15.4	-0.312	Ikeda and Motoda (1978)
Respiration	Crustacea	16	-0.268	Ivleva (1980)
Respiration	Copepod	17	-0.25	Ross (1982)

METHODS AND DATA

General allometric equation

The earliest work in quantifying allometric processes was done chiefly on body size-metabolic rate relationships (e.g. Kleiber 1932, Brody *et al.* 1934 and Hemmingsen 1960). These studies found that a simple power function best described the relationship; the general allometric equation has the form

$$R = a W^{b} \quad \text{.....(1.1)}$$

where R can be one of many rates, W is body mass, *a* is the rate coefficient and *b* is the scaling parameter. R has dimensions $[T]^{-1}$ for mass specific rates, W has dimensions [M] and *b* is dimensionless, therefore *a* has dimensions $[T]^{-1}[M]^{-b}$.

Derivation of *b*

There is considerable debate as to the "true" value of *b*. Attempts have been made to derive *b* theoretically, initially from the now discredited *surface law* (for a review see Schmidt-Nielsen 1970), but more recently from the results of dimensional analysis and the theory of biological similitude (Economos 1979, Platt and Silvert 1981, Heusner 1982b). The latter studies are based on the theorem that all natural laws can be expressed as relationships between dimensionless quantities (Stahl 1962). Using this theorem, Heusner (1982b) calculated a value of -0.33 for *b* as a mathematical consequence of homomorphism, but Platt and Silvert (1981) calculated values of -0.33 for aquatic organisms and -0.25 for terrestrial organisms. Empirical evidence, however, chiefly indicates a value of -0.25, both for aquatic and terrestrial organisms (e.g. Brody *et al.* 1934, Kleiber 1947, Hemmingsen 1960, Fenchel 1974, Blueweiss *et al.*1978, Cammen 1980). In the absence of consensus as to the true value of *b* or its underlying theoretical basis, the value supported best by real data should be used (Lavigne 1982). Estimated values of *b* range between about -0.1 and -0.4 (Table 1.1). However, most values of *b* are close to -0.25, thus a value of -0.25 for *b* has been used in all calculations described below.

Calculation of *a*'s

Most studies have been primarily concerned with estimating *b*, with little attention being paid to *a* (Platt 1985). Literature estimates of *a* are influenced by the corresponding estimates of *b*, because of the practice of estimating these two parameters simultaneously (by using linear regressions on log/log transformed data). To obtain ecologically useful allometric models, appropriate data were extracted from the literature, body weights transformed by the exponent -0.25, and regression estimates of *a* were calculated independently of *b*.

Data were obtained from a number of sources, in some cases second-hand, having been converted to different units and temperatures by other authors. Some data were obtained from figures, which may have resulted in some error in estimation, especially because axes are usually logarithmic. Calculations were done to two significant figures throughout. Units were not always comparable between studies. Where necessary, data were converted to standard units of mass (pg C) and specific rates (d^{-1}) using the conversions presented in Table 1.2.

Table 1.2. Conversions used to standardize all body mass data to units of pg C. esd = equivalent spherical diameter, RQ = respiratory quotient (see text)

Conversion			Reference
1 μm^3	=	1 pg wet	Fenchel and Finlay (1983)
1 pg dry	=	0.4 pg C	Peters (1983)
1 pg wet	=	0.07 pg C	Peters (1983)
1 pg C	=	1 pl O_2 x 12 + 22.4 x RQ	Parsons *et al.* (1977)
1 nJ	=	0.05 pl O_2	Peters (1983)

The respiratory quotient (RQ) (Table 1.2) was assumed to equal one (Parsons *et al.* 1977), because the majority of the respiration data were for unstarved animals (Ikeda 1970, Ross 1982a, Fenchel and Finlay 1983). Hourly rates were converted to daily rates by multiplying by 24, and all data were standardized to 20°C using Q_{10} values from the appropriate sources (see below). Where practical, data were combined into a single set. Often the raw data were not readily available (not presented or difficult to extract from graphical representations). When this occurred and the published exponent was close to -0.25, the published rate coefficients were compared to the ones calculated below. Data sources are described in detail below, and summarized in Table 1.3.

Maximum uptake rates (V_{max})

Bacteria and phytoplankton are grouped together in this study, because both take up dissolved nutrients from solution (Azam *et al.* 1983); they are distinguished from particle-feeding heterotrophs (see **DISCUSSION**). Growth rates (μ) of phytoplankton and bacteria are often limited by nutrient availability (Eppley 1981, McCarthy 1981, Laake *et al.* 1983b, Fenchel 1987). Uptake rates (V) of the limiting nutrient therefore may be equated approximately to growth rates on an ecological time scale. Data for calculated maximum values of V and μ with corresponding cell sizes were used to estimate the uptake coefficient in the allometric equation.

Cell dimensions (μm) and maximum specific growth rates (d^{-1}) for four strains of bacteria (n = 4) at 2°C were taken from Tables 1 and 3 respectively of Laake *et al.* (1983b). Cell volumes were estimated using the formula for a cylinder, and converted to carbon masses using the relationship 1 μm^3 = 0.121 pg C (Laake *et al.* 1983b). Growth rates were standardized to 20°C using a Q_{10} of 2.45. In pure cultures, bacterial isolates of these strains followed the Arrhenius curve from 5°C to > 15°C (Laake *et al.* 1983b), so the extrapolation to 20°C is justified. Cell carbon (pg C) and specific growth rates (h^{-1}) of unicellular algae (n = 14) were read from Fig. 1 of Banse (1976), who used data from a number of sources and standardized them to 20°C. Cell carbon (pg C) and maximum specific growth rates (h^{-1}) for freshwater green algae (n = 26) were similarly read from Fig. 1 of Schlesinger *et al.* (1981). All these data span a size range from 0.3 - 100 μm esd (equivalent spherical diameter), and were combined into a single data set (N = 44) for parameter estimation (Table 1.3). Data from Taguchi (1976) for specific phytosynthetic rates of marine diatoms, converted to 20°C using a Q_{10} of 2.0, were an order of magnitude faster than those for similar-sized phytoplankton cells in the data sets described above, and therefore were omitted from the regression.

Maximum ingestion rates (I_{max})

Maximum specific ingestion rates have been shown to decrease with increasing body size both within species (Dagg 1976) and between species (Fenchel 1980b, Paffenhöfer 1971, Ikeda 1977, Ross 1982a, Capriulo 1982). Maximum ingestion rates (h^{-1}) and cell volumes (μm^3) for 17

Table 1.3. Sources of data used in calculating rate coefficients (*a*) in allometric equations ($R = a\ W^{b}$) for rates of nutrient uptake, ingestion and respiration

Rate	Approximate size range (µm esd)	Organisms	Original units: Rate	W	Temperature	Q_{10}	n	Reference
V_{max}	0.3 - 0.5	Bacteria	d^{-1}	μm^3	2°C	2.45 (Laake *et al.* 1983)	4	Laake *et al.* 1983b
V_{max}	4 - 32	Unicellular algae	h^{-1}	pg C	20°C	-	14	Banse 1976
V_{max}	5.3 - 100	Freshwater algae	h^{-1}	pg C	20°C	-	26	Schlesinger *et al.* 1981
I_{max}	8 - 340	Ciliates	h^{-1}	μm^3	20-22°C	-	18	Fenchel 1980
I_{max}	208 - 985	Copepod	d^{-1}	µg C	15°C	3.0 (Ross 1982)	5	Paffenhöfer 1971
I_{max}	190 - 420	Marine copepods	d^{-1}	µg dry	20°C	-	24	Ikeda 1977
I_{max}	390 - 4 450	Copepod	µg $C.d^{-1}$	µg C	12°C	3.0 (Ross 1982)	27	Ross 1982
R_I	5 - 620	Ciliates	nl $O_2.h^{-1}$	μm^3	20°C	-	48	Fenchel & Finlay 1983
R_I	960 - 4 600	Marine plankton	µl $O_2.d^{-1}$	mg dry	5-30°C	2.0 (Ross 1982)	103	Ikeda 1970
R_I	340 - 1 430	Copepods	µl $O_2.mg^{-1}.h^{-1}$	mg wet	20-25°C	2.14 (Gaudy & Boucher 1983)	16	Gaudy & Boucher 1983
R_I	330 - 3 880	Copepod	µg $C.d^{-1}$	µg C	12°C	2.0 (Ross 1982)	92	Ross 1982

species of ciliates at 20-22°C (n = 18) were read from Fig. 2 of Fenchel (1980b). Daily rations and body masses (µg C) for the copepod *Calanus helgolandicus* at 15°C (n = 5) were taken from Table 5 of Paffenhöfer (1971), and rates were standardized to 20°C using a Q_{10} of 3.0 (Ross 1982a). Maximum daily rations (d^{-1}) and dry masses (µg) for five species of marine copepod at 20°C (n = 24) were obtained from Table 2 of Ikeda (1977). Ingestion rates (µg $C.d^{-1}$) and body masses (µg C) for the euphausiid *Euphausia pacifica* at 12°C (n = 27) were read from Fig. 2 of Ross (1982a) and standardized to 20°C using a Q_{10} of 3.0 (Ross 1982a). All these data were combined into a single data set (N = 74) with ingestion rates for body sizes ranging from 8 - 4 450 µm equivalent spherical diameter (esd) (Table 1.3).

Respiration rates (R_V and R_I)

Banse (1982) presented allometric equations for respiration rates of unicellular organisms from data in Hemmingsen (1960) (for prokaryotes and eukaryotes combined) and Dewey (1976) (for eukaryotes). These equations yield estimates of *b* of -0.24 and -0.26 respectively, which is very close to the value of -0.25 adopted here. The mean (1.7) of the two estimated values of *a* (1.54 and 1.89) was therefore used as the respiration rate coefficient (R_V) for phytoplankton and bacteria.

Data for respiration rates (R_I) and body masses of particle-feeding heterotrophs over a wide range of body sizes were taken from the literature and combined into one data set (see Table 1.2). Respiration rates (nl $O_2.cell^{-1}.h^{-1}$) and cell volumes (μm^3) for growing, free-living protozoa at 20°C (n = 48) were extracted from Table 1 of Fenchel and Finlay (1983), and converted to standard units of mass and specific rates. Respiration rates (µg $C.d^{-1}$) and body masses (µg C) for the euphausiid *Euphausia pacifica* at 12°C (n = 92) were read from Fig. 2 of Ross (1982a) and a Q_{10} of 2.0 (Ross 1982a) was used to convert the rates to 20°C. Respiration rates (µl $O_2.d^{-1}$) and dry masses (mg dry) for marine plankton (n = 103) were obtained from Table 3 of Ikeda (1970). The measurements were made at temperatures ranging from 5.1 to 30.3°C; they were standardized to 20°C using a Q_{10} of 2.0 (Ross 1982a). Specific respiration rates (µl $O_2.mg^{-1}.h^{-1}$) and body masses (mg wet) for 27 species of marine copepods were taken from Table 1 of Gaudy

and Boucher (1983), and converted to 20°C using their Q_{10} of 2.14. These four data sets (N = 270) cover a range of body sizes from 5 to 4 600 µm esd (Table 1.3).

Regression procedure

Body masses were power-transformed by the exponent -0.25. Straight line regressions through the origin were fitted to specific rate versus power-transformed body mass data. Regression slopes were calculated as:

$$a` = \frac{\sum XY}{\sum X^2} \quad \text{.....(1.2)}$$

(Zar 1984)

Because both X and Y variables are subject to estimation error, functional regressions are required; functional regression slopes a were calculated by dividing $a`$ by correlation coefficients r (Ricker 1984). These slopes provide estimates of rate coefficients for each data set. Significance of regressions was investigated using ANOVA, and 95 % confidence limits for a were calculated using the t distribution (Zar 1984).

RESULTS

Allometric equations calculated for rates of nutrient uptake, ingestion and respiration are presented in Table 1.4. All regressions are statistically significant ($p < 0.001$). Exponents b were fixed at -0.25, and calculated values for rate coefficients a are presented with 95 % confidence intervals. The estimated rate coefficient for uptake rates of phytoplankton and bacteria V_{max} is an order of magnitude smaller than that for ingestion rates I_{max} of particle feeders. Similarly, the rate coefficient for phytoplankton and bacterial respiration rates (R_V) is much smaller than the coefficient for respiration rates of particle-feeding heterotrophs (R_I). The implications of this are discussed below.

Table 1.4. Allometric equations for maximum nutrient uptake rates (V_{max}) of phytoplankton and bacteria, and maximum ingestion rates (I_{max}) and respiration rates (R_I) of particle-feeding heterotrophs. The equation for respiration rates of phytoplankton and bacteria (R_V), modified from Banse (1982), is also presented. Significance of regressions (p) was calculated using ANOVA (Zar 1984). Units of *a* are pg $C^{0.25}.d^{-1}$

Equation	N	r	p
$V_{max}\ (d^{-1}) = 5.1\ (\pm\ 0.3)\ W\ (pg\ C)^{-0.25}$	44	0.98	< 0.001
$I_{max}\ (d^{-1}) = 78\ (\pm\ 8)\ W\ (pg\ C)^{-0.25}$	74	0.89	< 0.001
$R_I\ (d^{-1}) = 15\ (\pm\ 1.5)\ W\ (pg\ C)^{-0.25}$	270	0.56	< 0.001
$R_V\ (d^{-1}) = 1.7\ W\ (pg\ C)^{-0.25}$	-	-	-

Regression plots are presented of specific rates against power-transformed body masses for uptake rates (Fig. 1.1a), ingestion rates (Fig. 1.2a) and respiration rates of particle-feeding heterotrophs (Fig. 1.3a). The relationship between cell size and respiration rates of phytoplankton and bacteria, modified from equations presented by Banse (1982), is presented graphically in Fig. 1.4. It is apparent that there is much scatter about the regression lines. This appears exaggerated when compared with similar studies, because linear scales are used here for the Y axes. The scatter is partially due to natural variability; not all organisms are exactly alike, and cells in different physiological states will have different reaction times for physiological processes (see Fenchel and Finlay 1983). Some of the variability is also probably due to measurement error and errors in estimating body carbon using general conversions (Table 1.2). Similar conversions are used by most authors (e.g. Finlay 1977, Banse 1982, Fenchel and Finlay 1983, Peters 1983) because it is not always possible to take measurements in units that are useful for ecological interpretation, and the same limitations and potential sources of error probably apply to many physiological studies. Despite this, the forms of the allometric relationships remain remarkably consistent, giving some confidence in the "average" rate constants calculated here.

If log scales are used in plotting the data, as is usually the case (Peters 1983), the scatter appears reduced (Figs 1.1b to 1.3b), and resembles more closely "usual" plots presented in the

literature (e.g. Fenchel 1974, Blueweiss *et al.* 1978, Banse 1982). This can be misleading (see Smith 1980), and the linear vertical scale is preferred. Regression lines shown on these plots (Figs 1.1b, 1.2b and 1.3b) are log-transformed versions of those presented in Table 1.4, and show reasonable fits to the data. Linear regressions for log-transformed data were not calculated (see below for discussion of appropriate regression techniques for allometric equations).

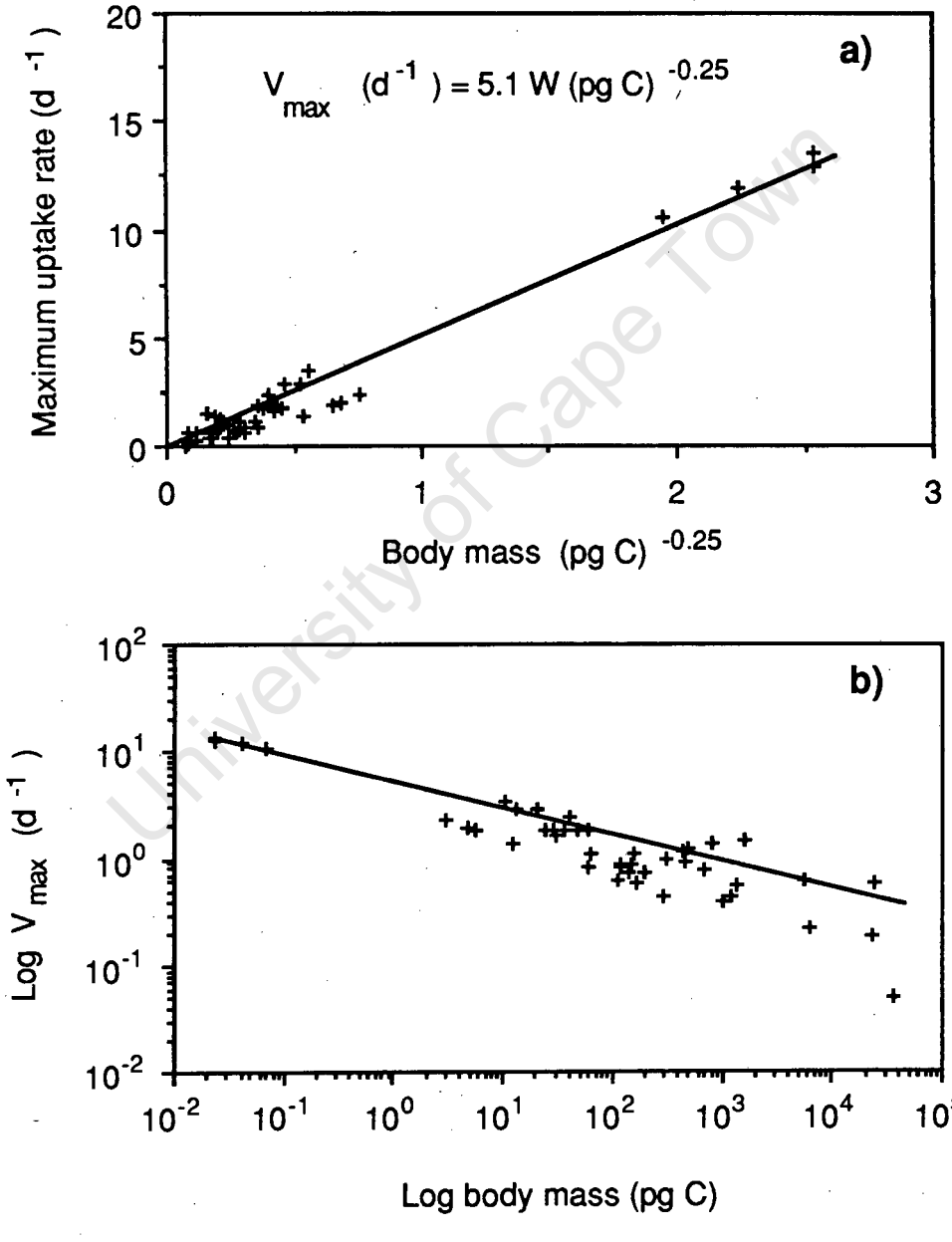

Fig. 1.1. Size dependence of maximum specific uptake rates (V_{max}) of phytoplankton and bacteria. a) Power-transformed body masses with functional regression line. b) Log axes and log-transformed functional regression line.

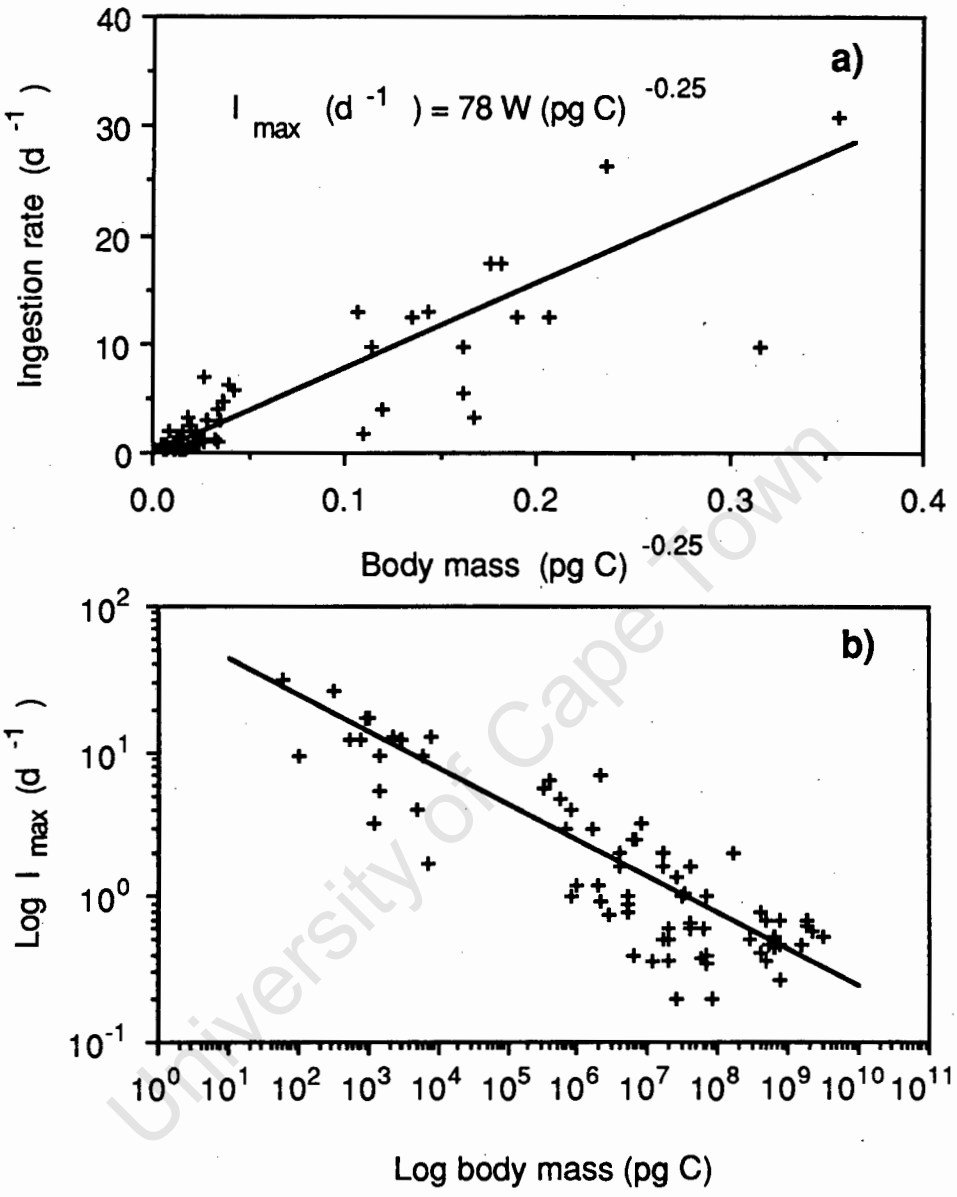

Fig. 1.2. Size dependence of maximum specific ingestion rates (I_{max}) of particle-feeding heterotrophs. a) Power-transformed body masses with functional regression line. b) Log axes and log-transformed functional regression line.

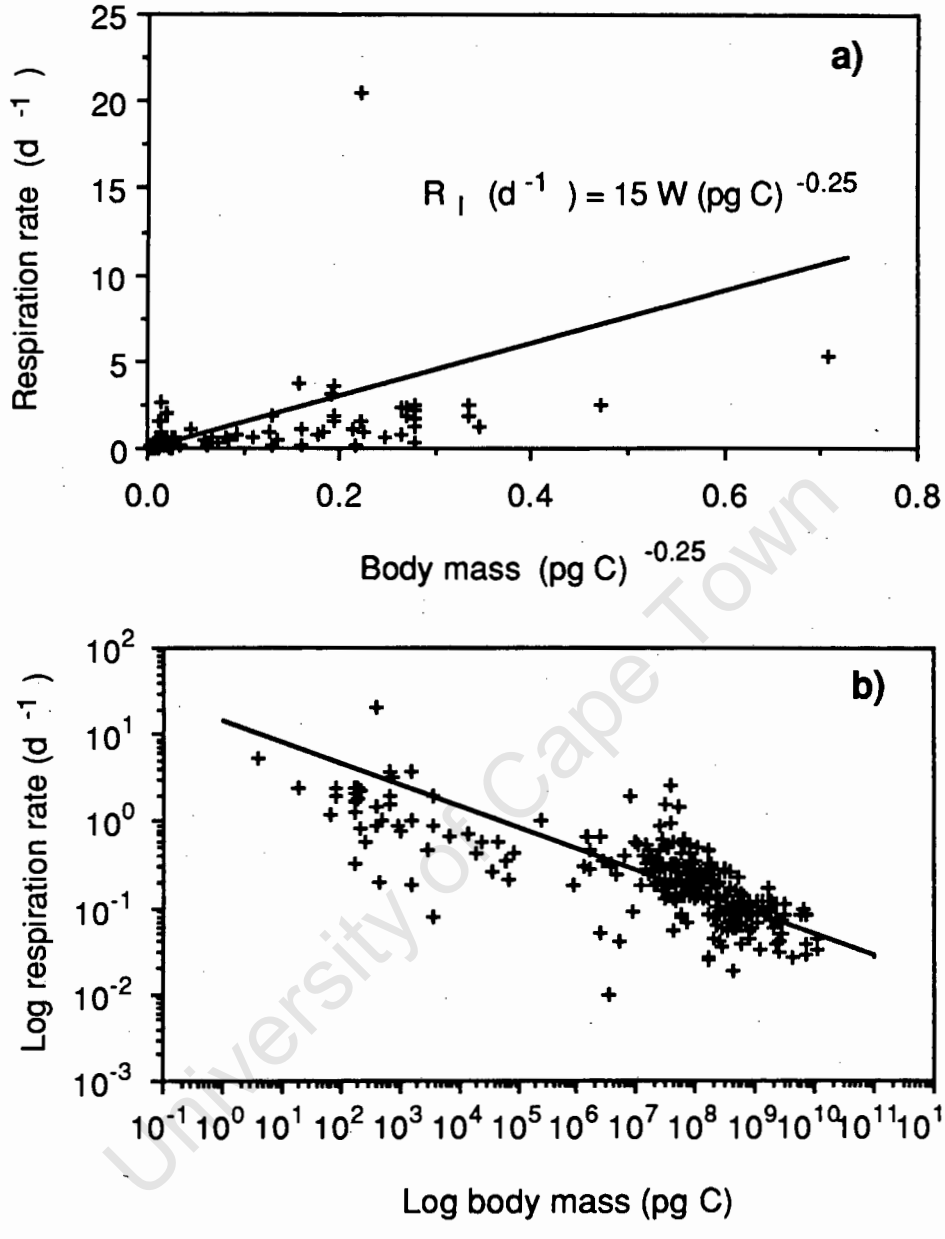

Fig. 1.3. Size dependence of specific respiration rates of particle-feeding heterotrophs (R_I). a) Power-transformed body masses with functional regression line. b) Log axes and log-transformed functional regression line. Note that the steep slopes are due to the use of functional regressions with small r values.

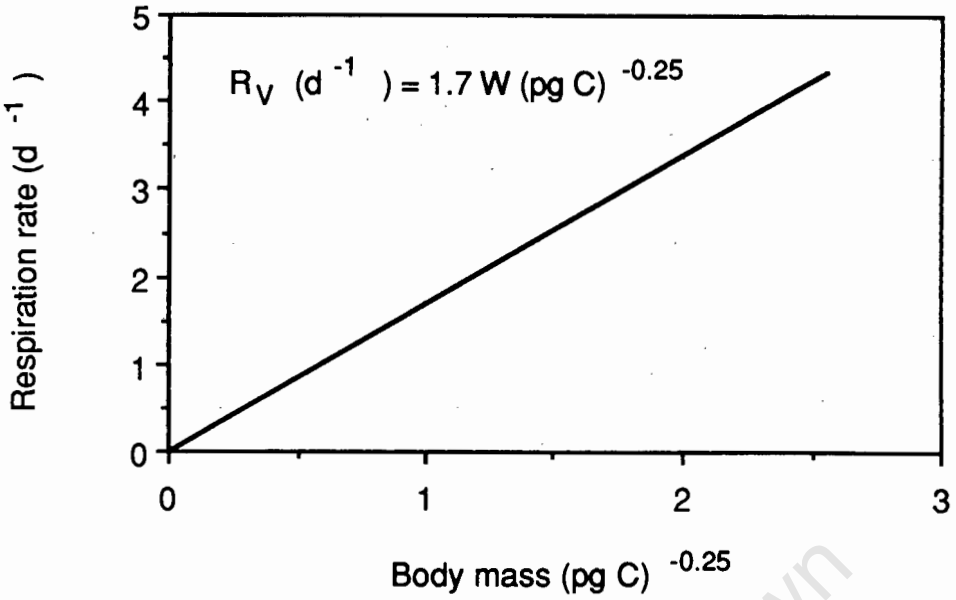

Fig. 1.4. Phytoplankton-bacterial respiration model, modified from Banse (1982), and plotted on the same axes as Figs 1.1 to 1.3. Specific respiration rates (R_V) are presented as a function of power-transformed body masses.

DISCUSSION

Limitations of previous studies

When allometric equations calculated in previous studies are compared (Table 1.1), it is evident that there is not always agreement between parameter estimates. This is not unexpected, taking into account potential sources of error in measurements and conversion factors used. In most studies in which *a* and *b* values have been estimated, this has been done by least squares linear regression on log-transformed values of body masses and the corresponding rates. Such transformations are not statistically ideal (Zar 1968); neither are the standard predictive regressions that have been employed (Laws and Archie 1981). A functional regression is recommended for analysing such data (Ricker 1973, 1984), but it has only recently come into general use (e.g. Humphreys 1979) and is seldom applied (Laws and Archie 1981, Peters 1983, Ricker 1984). Ideally, non-linear regressions would be preferred (Zar 1968), but readily available statistical packages with the necessary capabilities are a relatively recent occurrence. All these factors

confound the problem of deciding which allometric model is appropriate for use in mass budgets and energy balance equations in ecological studies of plankton communities.

Effect of using constant b

Complications in applying allometric models arise from the fact that allometric equations for different rate processes for the same group(s) of organisms often have different values for the exponent *b* (Table 1.1). For example, the model of Capriulo (1982) for ingestion rates of invertebrates has an exponent of -0.306 and the model of Ivleva (1978) for respiration rates of crustaceans has an exponent of -0.268. For two animals with body masses of 10 and 10^6 pg C, these models predict maximum specific ingestion rates of 27 and 0.39 d^{-1} respectively, and specific respiration rates of 8.6 and 0.21 d^{-1} respectively. Percentage respiration relative to ingestion for the smaller species is thus 32 %, and for the larger one 54 %, with this difference becoming larger as the size difference increases. This implies that growth and respiration do not change among species in the same fashion with body size, which is unrealistic because growth efficiencies are generally size invariant from species to species (Humphreys 1979). It should be noted that these arguments do not apply to ingestion, respiration and growth efficiencies within species, because changes in physiological relationships during growth result in characteristic growth curves within individual species. By standardizing the value of *b* to -0.25 in this study, this unrealistic source of interspecific variation has been removed. A similar procedure was advocated by Smith (1984) to analyse allometric data. He discussed a number of problems associated with allometric techniques, and suggested some alternative methods, among which was the use of *a priori* models (e.g. setting the exponent to a constant value) instead of *post priori* ones derived solely from the data.

Validation of estimates of a's

Values of rate coefficients for particle feeders calculated in regressions in Table 1.4 can be compared with literature values (estimated from data not used in the regressions) after these have been converted to standard units and a temperature of 20°C. These values are all associated with exponents of (or very close to) -0.25. The rate coefficient for ingestion rates was estimated to be

66 (μg $C^{0.25}.d^{-1}$) by Dagg (1976) for a marine copepod, 54 (μg $C^{0.25}.d^{-1}$) by Capriulo (1982) for a range of invertebrates, and 82 (μg $C^{0.25}.d^{-1}$) by Cammen (1980) for benthic deposit feeders and detritivores. The second value was associated with an exponent of -0.306, and the value of *a* would increase above 54 if the true value of *b* is -0.25. Our estimate of 78 ± 8 (μg $C^{0.25}.d^{-1}$) is comparable to these estimates. The rate coefficient for respiration rates of particle feeders was estimated to be 15 ± 1.5 (μg $C^{0.25}.d^{-1}$) (Table 1.4). Values of 13.7 (μg $C^{0.25}.d^{-1}$) for poikilotherms (Banse 1982) and 16 (μg $C^{0.25}.d^{-1}$) for crustaceans (n = 247) (Ivleva 1980), are similar to this estimate.

Net and gross growth efficiencies

Values of rate coefficients (*a*'s) are important in ecological models and mass budgets. Relative magnitudes of *a*'s for different processes affect growth efficiencies. Comparisons of relative values of *a*'s (calculated in this study) with theoretical and measured growth efficiencies make it possible to assess how realistic the calculated values are. For the discussion below, only organisms growing maximally are considered, because intraspecific growth efficiencies change as individuals age, usually peaking and then decreasing as organisms reach maturity (Parsons *et al.* 1977). Therefore, all relationships described are for maximum rates and are intended for use in interspecific comparisons among a large size range of organisms. In growing organisms, a substantial proportion of the daily carbon mass balance is comprised of consumption and respiration:

$$\text{PRODUCTION} = \text{CONSUMPTION} - \text{RESPIRATION} \quad \text{.....(1.3)}$$

All three above processes are body-size dependent. Equation (1.3) can be rewritten in allometric terms:

$$a_P W^b = a_C W^b - a_R W^b \quad \text{.....(1.4)}$$

If it is assumed that the scaling parameter *b* is the same for all rates for organisms growing maximally, it follows that the rate coefficient for production (a_P) depends on the difference between the rate coefficients for consumption (a_C) and respiration (a_R):

$$a_P = a_C - a_R \quad \text{..... (1.5)}$$

Values of a's for rates of uptake and respiration (Table 1.4) can be substituted into (1.5). Therefore, for a phytoplankton or bacterial cell growing under optimal conditions at 20°C in the absence of grazing, maximum net carbon production will be (5.1 - 1.7) ÷ 5.1 = 67 % of gross carbon production, i.e. maximum net growth efficiency (MNGE) for carbon will be 67 %. This is supported by theoretical arguments; Fenchel and Finlay (1983) propose that MNGE should be 67 % for prokaryotic micro-organisms, and Penning de Vries *et al.* (1974) theoretically derive general MNGE values between 60 % and 70 % for autotrophs. These relationships are appropriate for cells growing optimally, and NGE will decrease as conditions become sub-optimal. Measured NGE's for bacteria growing on a variety of substrates range from 26 % to 70 %. (Linley and Newell 1984, Lucas 1986), and phytoplankton respiration is generally accepted as comprising some 10 % to 45 % of photosynthesis (Raymont 1980), which ranges include values estimated using equation (1.5).

For grazers and predators similar calculations can be made, although efficiencies of heterotrophs should be greater than those of autotrophs and osmotrophs, because autotrophs and osmotrophs incur extra metabolic costs in assembling organic monomers from their inorganic constituents (Calow 1977). Particle-feeding heterotrophs grazing optimally with abundant food supply, have MNGE's for carbon calculated as:

$$\text{MNGE} = 1 - \frac{R_I}{U`I} = 1 - \frac{a_R W^b}{U` a_I W^b} \quad \text{..... (1.6)}$$

where R_I is respiration rate, I is ingestion rate, U` is assimilation efficiency and a_R and a_I are rate coefficients estimated empirically above for respiration and ingestion of particle-feeding heterotrophs. Because body mass terms in allometric equations for R_I and I cancel, the equation reduces to

$$\text{MNGE} = 1 - \frac{a_R}{U` a_I} \quad \text{..... (1.7)}$$

Substituting values of a_I and a_R (Table 1.4) in (1.7) and assuming U$\hat{}$ = 90 % (Dagg 1976, Barthel 1983, Miller and Landry 1984), MNGE is calculated to be size-independent, and has a value of 79 % for particle-feeding heterotrophs growing optimally at 20°C. This value is larger than that calculated for autotrophs and osmotrophs, in keeping with the prediction of Calow (1977). He estimated that "the best possible efficiency" that can be expected from any growing heterotroph is between 70 % and 80 %, which theoretical range includes the value estimated here. These theoretical estimates are also supported by measured values. Ross (1982b) measured NGE's of up to 74 % for larval stages of *Euphausia pacifica*. The copepod *Eurytemora affinis* was predicted to have a gross growth efficiency (GGE) of 60 % when growing at 15°C (Ikeda and Motoda 1978), and maximum GGE for *Daphnia pulex* was estimated to be 60 % at 20°C (Sushchenya 1970). Assuming 90 % assimilation efficiency, these GGE's are equivalent to NGE's of 67 %.

Comparing the two respiration models

It has frequently been stated that respiration rates for similar-sized unicells and multicellular poikilotherms differ by a factor of eight or nine (Hemmingsen 1960, Banse 1982), with unicells believed to have slower rates. In this study, two different allometric equations for respiration rates have been presented. One was obtained from the literature, and can be applied to unicellular phytoplankton and bacteria (Fig. 1.4). The other was calculated from combined data of unicellular protozoa and marine invertebrates (Table 1.1, Fig. 1.3). These equations thus do not conform to the usual unicell-multicell division. The grouping of protozoan respiration rates into a "unicell" line has recently been questioned by Fenchel and Finlay (1983), because the majority of the protozoan respiration rates were faster than predicted for unicells. After selecting only those data for actively growing protozoa, these authors showed that the protozoan line is similar to that calculated by Hemmingsen (1960) for multicellular organisms. Ciliate assimilation rates can be calculated from ingestion rates I_{max} (Table 1.4), using the calculated rate coefficient (a = 78), and an assimilation efficiency of 80 % (Stoecker 1984). If one adopts the "unicell" respiration equation with a coefficient of 1.7 (Table 1.3), NGE's are calculated from equation (1.7) to be 97 %, an impossibly large value (Calow (1977) predicted theoretical maximum efficiencies of 90-95 %).

Fenchel (1980) questioned the application of a "unicell" respiration rate to ciliates by Laybourn and Finlay (1976), because their estimates were an order of magnitude too small. Therefore, when the mass balance of organisms is taken into account, it is clearly unrealistic to describe all unicell respiration rates by a single "unicell" respiration model.

It is proposed that respiration rates for planktonic organisms be distinguished on the basis of method of food uptake. On the one hand, organisms that rely chiefly on dissolved nutrients from solution (autotrophs and osmotrophs, e.g. phytoplankton and bacterioplankton) conform to the traditional "unicell" model and have slower respiration rates than similar-sized organisms that feed mainly on particulate material. On the other hand, unicellular predators such as ciliates and phagotrophic flagellates have fast respiration rates (Fenchel and Finlay 1983), similar to the size-specific rates observed for multicellular animals. They are therefore grouped with other particle feeders. This grouping resolves the problem of apparently unrealistically large net growth efficiencies of ciliates, and is consistent with the hypothesis that maximum net growth efficiencies for organisms grazing under optimal food conditions, whether ciliates or copepods, remain constant (Humphreys 1979).

CHAPTER 2

SIZE-DEPENDENCE OF SOME FACTORS AFFECTING MATERIAL FLOWS IN PLANKTON COMMUNITIES

ABSTRACT

Data from the literature are used to develop empirical models which relate 1) prey sizes to predator zooplankton sizes, 2) half saturation constants for nitrogen uptake to phytoplankton and bacterial cell sizes, 3) half saturation constants for ingestion by predators to prey sizes, and 4) sinking velocities to phytoplankton cell masses and faecal pellet volumes. In general, zooplankton eat prey organisms roughly 4 to 13 % of predator size expressed in linear dimensions, or 0.002 to 0.06 % of predator mass. Half saturation constants for nitrogen uptake are described as a function of cell size by a hyperbolic relationship, K_S (μg N.l^{-1}) = 73 W pg C / ((W + 940) pg C), with maximum predicted K_S values of 73 μg N.l^{-1}. A power function is used to predict half saturation constants for ingestion of prey organisms, such that K (μg C.l^{-1}) = 54 W (pg C)$^{0.08}$. Thus, for a wide range of predator and prey sizes, small prey items are more susceptible to predation at low concentrations than are large prey items. Sinking velocities of phytoplankton cells and faecal pellets increase with increasing size, and these relationships are described by power functions. Faecal material sinks at a much faster rate than live cells, which have maximum sinking velocities of approximately 2 m.d^{-1}, compared with > 3 km.d^{-1} for large faecal pellets. Relating these factors to body size allows objective parameter estimation and generalization for use in dynamic simulation models of a wide range of planktonic organisms.

INTRODUCTION

Particle size can be used to predict many physical and ecological processes (Chapter 1, Peters 1983). Chapter 1 estimated allometric equations for body size - rate process data of planktonic organisms. However, other factors cannot be described by the general allometric model, because they are not related to intrinsic processes and do not scale in the same fashion with body mass. Such factors often depend on the organism's interaction with its environment. This chapter uses published data to derive empirical models relating particle size to four ecological processes in the planktonic environment. By quantifying the relationships, I attempt to make the estimation of parameters for use in ecological models a more rigorous process than has been used in the past.

Predator-prey size relationships.

In the marine pelagic environment, body size usually determines an organism's position in the food chain (Sheldon *et al.* 1972). This characteristic of pelagic food webs has been used in biomass spectrum models, where it is assumed that predators are roughly an order of magnitude larger than prey items (Sheldon and Kerr 1972, Sheldon *et al.* 1977, Azam *et al.* 1983, Moloney and Field 1985). However, in practice, predators are capable of ingesting a range of prey sizes, and relationships between predator sizes and minimum, optimum and maximum prey sizes can be determined for planktonic organisms.

Half saturation constants for nitrogen uptake

Phytoplankton and bacterioplankton rely on the uptake of dissolved nutrients for growth. The uptake process often is described by Michaelis-Menten models (Monod 1949, MacIsaac and Dugdale 1969), although this is probably an oversimplification for detailed understanding (see Shuter 1978, Eppley 1981, Morita 1984, Nissen *et al.* 1984). However, for the purpose of general ecological models, the Michaelis-Menten model is sufficient. The model has two parameters, the maximum uptake rate V_{max} and the half saturation constant K_s. It has been shown that V_{max} is body-size dependent, with small organisms having faster mass-specific uptake rates

than large organisms (Chapter 1). The ability to take up nutrients at low ambient nutrient concentrations is determined by K_S, which also is dependent on body size; small cells are more proficient (i.e. have smaller K_S) than are large cells (Eppley *et al.* 1969, Gray *et al.* 1984). This is important in environments where nutrients are scarce (Gray *et al.* 1984).

Half saturation constants for ingestion

Ingestion rates are a function of prey concentration and prey size. Various models have been used to relate ingestion rates to prey densities (see Mullin *et al.* 1975). Most of these models have a maximum or saturation rate at high prey densities, and a density-dependent rate at low prey densities (Mullin *et al.* 1975). In Michaelis-Menten ingestion models (e.g. Fenchel 1982b), ingestion rates at low prey densities are determined by half saturation constants K (equivalent to K_S above, but termed K throughout to avoid confusion). K is the ratio of the maximum uptake rate to the maximum clearance rate for filter feeders (Fenchel 1980b). Because both these rates scale to predator body size, the effect of predator size on K cancels (Fenchel 1980a), and K is predator-size independent. However, there is evidence to suggest that K is affected by prey size, and it may be possible to predict this parameter from prey-size data.

Sinking velocities

The rate at which organisms and particles sink through the water column depends to some extent on particle size, although sinking velocities are also affected by factors such as buoyancy, shape, orientation and physical features of the water column (Anderson *et al.* 1985). Measured sinking rates of live phytoplankton cells (S_P) are much slower than those of faecal and detrital material (S_F), presumably because of buoyancy mechanisms operating in live cells (Smayda 1970). The effect of particle size on sinking velocities will be investigated here, both for phytoplankton and for faecal pellets.

DATA SOURCES

Predator-prey size relationships

Prey sizes for different sizes of predator were obtained from the literature, and average esd's (equivalent spherical diameters) were estimated for each predator and prey species. "Prey" in this context is assumed to comprise all potential food items, and includes autotrophs, heterotrophs and detritus. Data used are summarized in Table 2.1. The esd of the copepod *Pseudocalanus minutus* (Table 2.1) was estimated by assuming a wet mass : carbon conversion of 7 % (Chapter 3, Peters 1983), and approximate volumes of the three copepod species obtained from Cowles (1979) were calculated using dimensions estimated from diagrams in Newell and Newell (1963).

Half saturation constants for nitrogen uptake

No half saturation constants for nitrogen uptake with corresponding cell sizes were found for bacteria. Most published half saturation constants for bacterial uptake of a variety of substrates are in the μM range, but the data are generally not collected from low-nutrient waters (Morita 1984). Because bacteria can have more than one K_s (Nissen *et al.* 1984), these calculated values probably do not reflect the ability of bacteria to function in low-nutrient conditions (Morita 1984). Thus it is assumed that the phytoplankton model can be extrapolated to bacterial-sized organisms. Cell diameters (μm) and K_s values (μg at.l^{-1}) for NO_3 and NH_4 uptake were obtained from Table 2 of Eppley *et al.* (1969). Cell volumes were calculated using the formula for a sphere, and converted to pg carbon using the equations of Strathmann (1967). K_s values for NO_3 and NH_4 were averaged, giving one K_s value for nitrogen uptake per species.

Half saturation constants for ingestion

A half saturation constant of 5 x 10^6 bacteria.ml^{-1} was estimated for microflagellates feeding on bacteria (Fenchel 1982b). Using an average bacterial cell size of 0.11 μm^3 and a conversion of 1 μm^3 = 0.121 pg C (Laake *et al.* 1983b), this is equivalent to a K value of 55 μg C.l^{-1}. Prey sizes (μm esd) and half saturation constants ($\mu m^3.l^{-1}$) of ciliates were obtained from Fenchel (1980c). Only prey larger than 2 μm were used, because ciliates probably do not feed on

Table 2.1 Summary of predator sizes (µm esd) and estimated minimum, optimum and maximum food-particle sizes (µm esd). Ratios of food size : predator size are given as $ratio_{min}$, $ratio_{opt}$ and $ratio_{max}$. µFlag = microflagellates, Ci = ciliates, Co = copepods and Met = other metazoa

Predator	Predator size	minimum prey size	optimum prey size	maximum prey size	$ratio_{min}$	$ratio_{opt}$	$ratio_{max}$
Monosiga sp. (µFlag)	3[g]	0.2[g]	-	-	0.07	-	-
Actinomonas sp. (µFlag)	5[g]	1 - 2[g]	-	-	0.2-0.4	-	-
Cyclidium glaucoma (Ci)	10[f]	0.2[d]	0.4[d]	2[d]	0.02	0.04	0.2
Colpoda steini (Ci)	12[f]	0.4[e]	1.1[f]	2[e]	0.03	0.09	0.2
Colpoda cucullus (Ci)	18[f]	0.2[e]	0.4[f]	1[e]	0.01	0.02	0.06
Glaucoma scintillans (Ci)	35[f]	0.1[d]	0.4[f]	4[d]	0.002	0.01	0.1
Colpidium campylum (Ci)	35[f]	0.1[d]	0.4[f]	2[d]	0.002	0.01	0.06
Colpidium colpoda (Ci)	40[f]	-	0.4[f]	-	-	0.01	-
Euplotes moebiusi (Ci)	50[f]	1[d]	5[f]	10[d]	0.02	0.1	0.2
Stylonychia mytilus (Ci)	50[f]	-	10[f]	-	-	0.2	-
Blepharisma americanum (Ci)	60[f]	1[d]	6[f]	10[d]	0.02	0.1	0.2
Paramecium caudatum (Ci)	70[f]	0.2[d]	1[f]	6[d]	0.003	0.01	0.09
Bursaria truncatella (Ci)	400[f]	10[d]	35[f]	80[d]	0.03	0.09	0.2
Pseudocalanus minutus (Co)	570[b]	4[b]	25 - 57[b]	100[b]	0.01	0.04-0.1	0.2
Calanus chilensis (Co)	880[a]	12[c]	-	57[c]	0.01	-	0.06
Centropages brachiatus (Co)	880[a]	10[c]	-	50[c]	0.01	-	0.06
Eucalanus inermis (Co)	920[a]	8[c]	-	57[c]	0.01	-	0.06

a Newell and Newell (1963); b Poulet (1973); c Cowles (1979) d Fenchel (1980b, Fig. 6); e Fenchel (1980b, Fig. 7); f Fenchel (1980c); g Fenchel (1984)

small, free-living bacteria in open waters (Fenchel 1980c). Food particle sizes and their half saturation constants for ingestion were obtained for copepods (*Calanus pacificus* (Frost 1972), *Euchaeta elongata* (Yen 1983) and *Oithona nana* (Lampitt and Gamble 1982)), and a euphausiid (*Euphausia lucens* (Stuart 1986)). All prey sizes are expressed as pg C, using Strathmann's (1967) conversions from volume to carbon when necessary. Half saturation constants are expressed as $\mu g\ C.l^{-1}$.

Sinking velocities

Data were partitioned into live cells and dead or detrital material. Sinking rates ($m.d^{-1}$) of particulate organic carbon and phytoplankton in three discrete size classes were obtained from Burns and Rosa (1980). Geometric mean sizes were estimated for each size class, and sizes were converted to carbon masses (pg C) using an average conversion of 1 μm^3 = 0.07 pg C (Chapter 3). Sinking rates of particulate carbon (Bienfang 1985) were similarly treated (n = 4), and cell carbon (pg) and sinking rates ($m.d^{-1}$) of 29 species of nutrient-replete marine phytoplankton were obtained from Bienfang and Harrison (1984). The data for live cells were combined into one data set (N = 36). Logarithmic values of sinking rates ($m.d^{-1}$) and particle volumes (μm^3) for faeces of gelatinous zooplankton (n = 232) were read from Fig. 2 of Bruland and Silver (1981), and the data were converted to a linear scale.

ANALYSIS AND RESULTS

Predator-prey size relationships

Relationships between individual predator and prey sizes were established as simple proportions (Table 2.1). Minimum, optimum and maximum prey:predator size ratios (mean ± 95% C.I.) were calculated as 0.04 ± 0.04 (n = 15), 0.06 ± 0.04 (12) and 0.13 ± 0.04 (13) respectively. Thus each predator ingests, on average, prey organisms ranging from 4 % to 13 % of its body size calculated in linear dimensions, or from 0.002 % to 0.06 % of predator mass, the latter range spanning some two orders of magnitude. Optimum prey sizes are estimated to be 6 % of predator linear dimensions or 0.006 % of body mass.

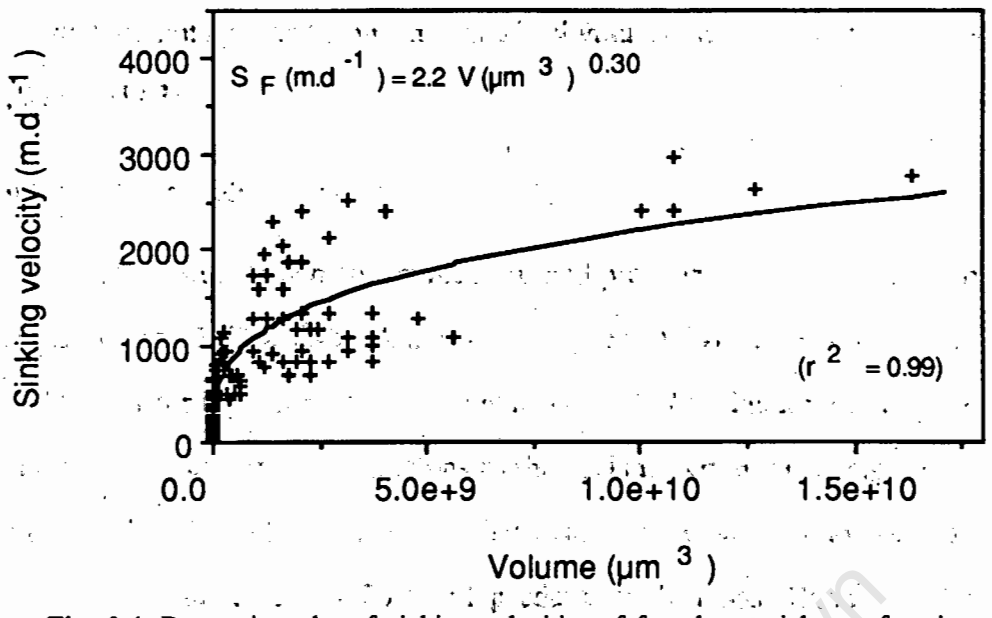

Fig. 2.4. Regression plot of sinking velocities of faecal material as a function of particle volume

DISCUSSION

There are obvious drawbacks to generalizing biological and ecological processes. For every general rule that is formulated, there will always be a species or group of organisms which have specialized in such a fashion as to negate the rule. Thus the relationships presented here will not apply to all cases. However, they are not intended for use by biologists studying details of the biology of individual species. They have been developed to assist ecologists in estimating parameters for use in ecological models of plankton communities. Isaacs (1973) described unstructured food webs as ones in which organisms feed on whatever available food is suitable in terms of size and their mode of feeding. This concept can be used to develop flow pathways of carbon and nitrogen in size-based models. Maximum rates of transfer processes can be calculated using allometric equations (Chapter 1), and factors modifying the maximum rates are also body-size dependent, as has been shown in this chapter. By formulating quantitative relationships for these factors, it is possible to construct a size-based model of a microplanktonic food web which allows unbiased assessment of food web structure and interconnections, and is not dependent on trophic levels or preconceived ideas of how specific systems function, apart from the general size-dependency. Such a model can be used to explore community structure, and identify properties of

Half saturation constants for ingestion.

There has been no previous attempt to relate half saturation constants for ingestion to prey sizes over a large range of organisms. The relationship used here was calculated primarily on an empirical basis, because no *a priori* theoretical basis for the form of the function was intuitively obvious. The curve levels off at about 300 $\mu g\ C.l^{-1}$, and K values from literature studies of large copepod predators generally range between 200 and 300 $\mu g\ C.l^{-1}$ (O'Connors *et al.* 1976, Lampert 1977), indicating that this ceiling is realistic. For small prey organisms such as bacteria, natural densities are about 0.5 to $2x10^6$ $cells.ml^{-1}$ (Azam *et al.*1983) or 5.5 to 22 $\mu g\ C.l^{-1}$, and seldom exceed 200 $\mu g\ C.l^{-1}$, which implies that half saturation constants for ingestion by predators should at least be of this order of magnitude. Thus we would expect smaller values of K for small prey than for large prey.

In contrast to the function derived here, intraspecific feeding studies have shown that large prey items are more susceptible to predation at low concentrations than are small prey items (Paffenhöfer 1971, Frost 1972; 1975, Boyd 1976, Cowles 1979, Fenchel 1980a, Capriulo 1982, Quetin and Ross 1985). A similar trend was found for the threshold feeding response of the copepod *Calanus pacificus*, the response occurring at progressively smaller concentrations as the sizes of food particles increase (Frost 1975) . This implies that K should decrease as prey size increases, which is the reverse of the pattern found here for a range of species (Fig. 2.2). Individuals apparently utilize prey items at the large end of their prey size range more efficiently than small prey items, but for the general interspecific trend K values increase as prey size increases. This implies that small predators generally are more proficient than are large ones when prey are scarce.

Sinking velocities

Many workers relating sinking velocities to particle volumes have fitted a linear regression to log-transformed data (e.g. Bruland and Silver 1981, Arashkevich *et al.* 1986). When considering a large range of particle sizes, sinking velocities of large particles tend towards a maximum value (Figs 2.3 and 2.4), as expected from physical theory of sinking bodies in a fluid

medium when gravitational forces are the most important component affecting the sinking velocity. A viscous or drag component is more important in small particles than large particles, small particles having a low Reynolds number and thus sinking more slowly than large particles (Anderson *et al.* 1985). Most data sets cover only the small end of the size range and/or a limited range of sizes, and thus do not detect this trend.

The maximum sinking velocity of live cells (approximately 2 $m.d^{-1}$) is some three orders of magnitude slower than that of detrital material (approximately 3 000 $m.d^{-1}$). Thus only big phytoplankton cells will be important in the loss of material through sinking out of the euphotic zone. Conversely, only very small faecal pellets (e.g. minipellets produced by protozoans, Gowing and Silver 1985) will be important as sources of nutrients regenerated by bacteria in the euphotic zone, because big particles rapidly sink out of the system. Very fast sinking rates of faecal material have been measured for pellets produced by salps (Madin 1982), copepods (Turner 1977, Small *et al.* 1979) and mysids (Arashkevich *et al.* 1986). Robison and Bailey (1981) present a range of sinking rates of a variety of particles, including faecal pellets from crustaceans and fish, carcasses of different organisms and dead phytoplankton cells. The maximum sinking rate they found is 1 200 $m.d^{-1}$ for fish faecal pellets, which falls in the range of values presented above for faecal pellets of gelatinous zooplankton. All of the detrital material has sinking velocities much faster (range from 15 to 2700 $m.d^{-1}$) than those calculated here for live cells.

Anderson *et al.* (1985) measured sinking rates of marine dinoflagellate cysts; mean velocities ranged from 6 to 11 $m.d^{-1}$. This is faster than the maximum of 2 $m.d^{-1}$ calculated from Fig. 2.3, because the cysts are denser than most vegetative phytoplankton cells, presumably as an adaptation to sink rapidly (Anderson *et al.* 1985).

CONCLUSIONS

The size of organisms is probably the most important factor affecting their roles in pelagic ecosystems. I have demonstrated (Chapter 1, this chapter) that quantitative relationships can be derived which relate important parameters used in modelling interactions and processes in plankton communities to organism size. These size relationships are objective estimators of ecological parameters, and therefore have wide-ranging applications in the study and understanding of pelagic ecosystems.

SECTION 2

MODEL DEVELOPMENT AND OUTPUT

CHAPTER 3

DEVELOPMENT OF A SIZE-BASED SIMULATION MODEL OF A GENERALIZED MICROPLANKTON COMMUNITY

ABSTRACT

A dynamic simulation model is described of carbon and nitrogen flows in a generalized microplankton community. The model is size-based, with community structure and transfer processes all size-dependent. Major flows include carbon fixation, release of photosynthetically-produced dissolved organic carbon (PDOC), nitrogen uptake, respiration, excretion, predation and sinking. A standard simulation is produced which serves as the basis for comparing output from a sensitivity analysis. The model is robust with respect to most parameters. Important factors to which model output is sensitive include estimates of PER (percentage extracellular release), factors affecting ingestion rates, shapes of initial biomass distributions (seeding effects), wet mass to carbon conversion functions, and the form of the ingestion function. The model can be used to simulate microplankton community interactions in any planktonic ecosystem.

INTRODUCTION

Planktonic ecosystems commonly are described by compartmental models, each compartment representing a trophic level or taxonomic group (e.g. Steele 1974, Wroblewski 1977, Kiefer and Atkinson 1984, Newell and Linley 1984, Jones and Henderson 1987). Such models primarily are descriptive, because the most important components of the ecosystem are represented by compartments, and interactions are described by linking compartments. However, when using these models as the basis for dynamic simulation models (e.g. Moloney *et al.* 1986), a number of problems are encountered. For example, unrealistic lumping of all phytoplankton sizes with widely disparate rates of growth and metabolism often results in the use of inappropriate rate parameters. In a model of a planktonic ecosystem in an enclosed water column, Andersen *et al.* (1987) found it necessary to divide the phytoplankton compartment into diatoms and flagellates, which in turn necessitated subdividing zooplankton herbivores into copepods and appendicularians. Despite this added complexity, they concluded that further subdivision probably was necessary to make model output more realistic. This is a problem commonly encountered with trophic-level-based compartment models, and has the effect of making models increasingly unwieldy and parameter estimation very difficult, especially if there are not sufficient data available from which to estimate the parameters.

An alternative to the above reductionist approach is to use an holistic approach to modelling planktonic ecosystems (Platt *et al.* 1981). The structure of marine pelagic food chains is largely dependent on organism size (Chapter 2, Sheldon *et al.* 1972, 1977, Platt and Denman 1978, Silvert and Platt 1980, Cousins 1985, Platt 1985). Furthermore, rates of many processes occurring in planktonic ecosystems are body-size dependent (Chapter 1). Problems of parameter estimation are obviated to a large extent by the fact that an independent criterion, viz. body size, may be used to estimate nearly all parameters. Organism size thus serves as a convenient theoretical and practical basis for developing a system model of a marine plankton community.

Cousins (1980) developed a trophic continuum model (Fig. 3.1) in which an ecosystem is divided into three basic components: autotrophs, heterotrophs and detritus. Each component

represents a size continuum from small to large organisms or particles, and links between components are represented by a double cylinder (Fig. 3.1). This model can be used to describe processes occurring in planktonic/pelagic ecosystems (Cousins 1985), and appears to be universally applicable as a descriptive model. However, system dynamics of planktonic communities throughout the world's oceans vary. Simulation models are required which can be used to investigate factors affecting community structure and dynamics, and thus serve as a basis for understanding marine planktonic ecosystems.

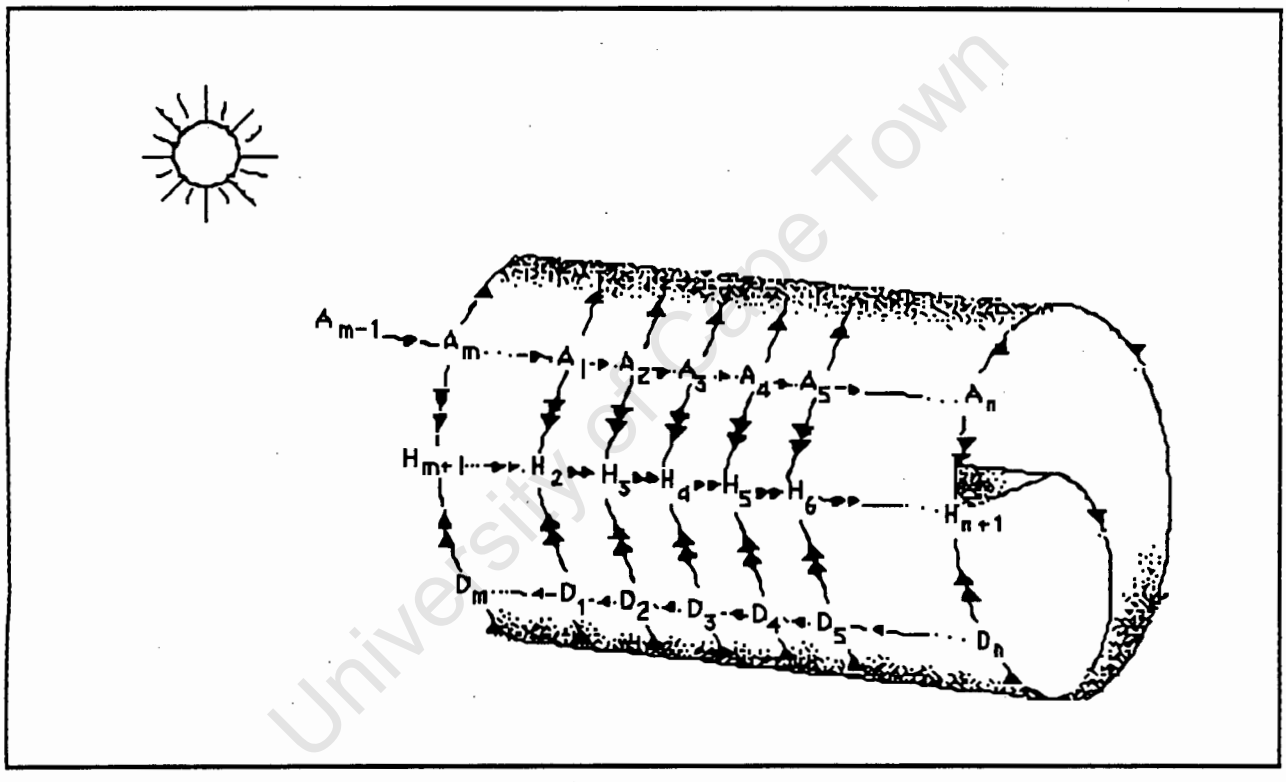

Fig. 3.1. Double cylinder representation of a trophic continuum of a pelagic ecosystem. The three components are autotrophs (A), heterotrophs (H) and detritus (D). Subscripts refer to different sizes within the continuums, with smallest particles on the left and largest on the right. The arrows represent the flows of energy through and between the three continuums. Single arrows represent growth (from small to large organisms in the autotroph and heterotroph continuums), breakdown of particulate material (from large to small particles in the detritus continuum), and production of detrital material by autotrophs and heterotrophs. Double arrows represent trophic interactions.

This chapter describes the structure and functioning of a dynamic trophic continuum model. In contrast to size-based energy flow models (Silvert and Platt 1980, Parkin and Cousins 1981), the model simulates flows of carbon (C) and nitrogen (N) through a microplankton community. The double currency is necessary because, although N is usually believed to be the limiting

nutrient, C can also limit growth of bacterioplankton, and there are close couplings between growth of bacterioplankton and phytoplankton. Output from the model is validated against real data from planktonic ecosystems in Chapter 4.

MODEL DESCRIPTION

In the model, microplankton communities are represented as a trophic continuum (Fig. 3.1) (Cousins 1985). Cousins' (1985) model represents energy flows, whereas my model simulates flows of C and N. To accommodate material flows, the model has been adapted to include dissolved C and N pools in addition to the detrital pool (Fig. 3.2).

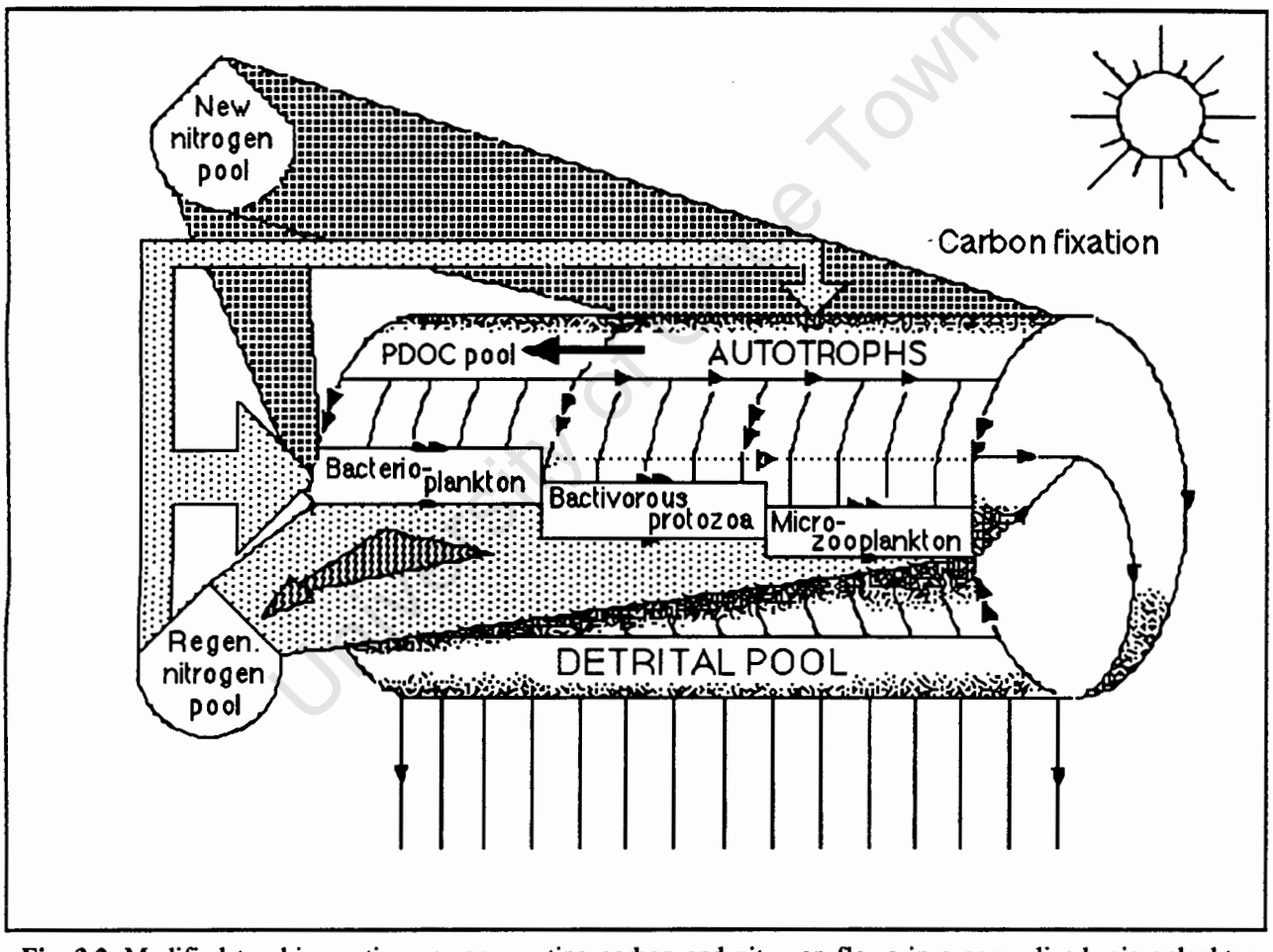

Fig. 3.2. Modified trophic continuum representing carbon and nitrogen flows in a generalized microplankton community. The autotroph continuum is extended to include a PDOC pool, and the heterotroph continuum is divided into convenient trophic categories. The solid arrow represents the excretion of PDOC by autotrophs. The stippled areas represent flows of dissolved nitrogen between the nitrogen pools and the living components. Solid arrow-heads represent carbon and nitrogen flows within the trophic continuum, through growth (single horizontal arrow-heads), ingestion (double arrow-heads) and death/sinking (single vertical arrow-heads). Respiratory losses are not shown.

Living organisms are assigned to two major groups: autotrophs and heterotrophs. Some organisms are ambiguous in life-style, and apparently fall into both groups; e.g. phagotrophic phytoflagellates and photosynthetic ciliates. Until mechanisms governing such modes of life are identified and quantified, these organisms cannot be accommodated in the model. Within groups all further classification is done on the basis of body size. The size continuums are divided into discrete size classes; the model is essentially a compartmental model (*contra* the continuous trophic continuum described by Cousins 1980, 1985, Parkin and Cousins 1981). The discrete form of the model was chosen to reduce mathematical complexity.

In this chapter, autotroph and heterotroph continuums are assumed to comprise organisms in size ranges from 0.2 to 200 µm esd (equivalent spherical diameter) and 0.2 to 2 000 µm esd respectively (Table 3.1).

Table 3.1 Categorization of the model community on the basis of size and trophic function

Category	Size range (µm esd)	No. of size classes
Autotrophs	0.2 - 200	3
Pico-phytoplankton	0.2 - 2	1
Nano-phytoplankton	2 - 20	1
Net-phytoplankton	20 - 200	1
Heterotrophs	0.2 - 2 000	4
Bacterioplankton	0.2 - 2	1
Bactivorous protozoa	2 - 20	1
Micro/mesozooplankton	20 - 2 000	2

For simplicity, large zooplankton and fish have not been included. Large fauna are difficult to incorporate, because of the large temporal and spatial scales required to adequately describe their behaviour (Field *et al.*1985, Fenchel 1987). Microplankton populations fluctuate many times in a time period during which large zooplankton and fish will grow slowly. If the entire size range

from bacteria to fish is included in a deterministic simulation, it is found that the time horizon is either too short to adequately simulate large organisms, or, if their standing stocks are initially large, they exert an unrealistic controlling force on the phytoplankton, preventing these from increasing (pers. obs). Consequently, it is inappropriate to include the entire size spectrum in a deterministic simulation model. Large mobile organisms may be better represented by a stochastic model with a longer time horizon. The role of large organisms is discussed in Chapter 5.

Within the heterotroph size continuum, three sub-groups are distinguished (Fig. 3.2). Smallest organisms are bacterioplankton (approximately 0.2-2 μm esd). These are preyed on by bactivorous protozoa (2-20 μm esd), which also ingest the smallest autotrophs (0.2-2 μm). All heterotrophs larger than 20 μm are placed in the micro-mesozooplankton group. These three sub-groups are designated as non-overlapping segments along the continuum, and allow for comparison of model output with traditional trophic categories in the literature.

A double currency of C and N is used in the model. Major flow pathways are represented diagrammatically in Fig. 3.3. Autotroph C is obtained by carbon fixation during photosynthesis, and N through uptake from solution. C is released as PDOC (photosynthetically-produced dissolved organic carbon), and further losses occur as a result of respiration, grazing, sinking, death and growth (Fig. 3.3). Uptake and ingestion by bacterioplankton and grazers respectively results in autotroph C entering the heterotroph continuum. Bacterioplankton obtain C and N from solution, whereas large heterotrophs obtain them by ingesting particulate material. Heterotrophs incur losses as a result of egestion, respiration, excretion, predation and growth. The detrital pool receives inputs from faecal material and senescent phytoplankton cells, and loses material as a result of sinking and utilization of organic material by attached (epi-) bacteria. The PDOC pool is supplied by autotrophs and sustains losses to bacterioplankton. The dissolved N pool is separated into new N (chiefly nitrate-N) and regenerated N (e.g. ammonia, urea) pools. Both lose N to autotrophs and bacterioplankton. New N is the only external input to the model system, whereas regenerated N results from the cycling of reduced N by heterotroph size classes. The forms of all functions describing fluxes are described below.

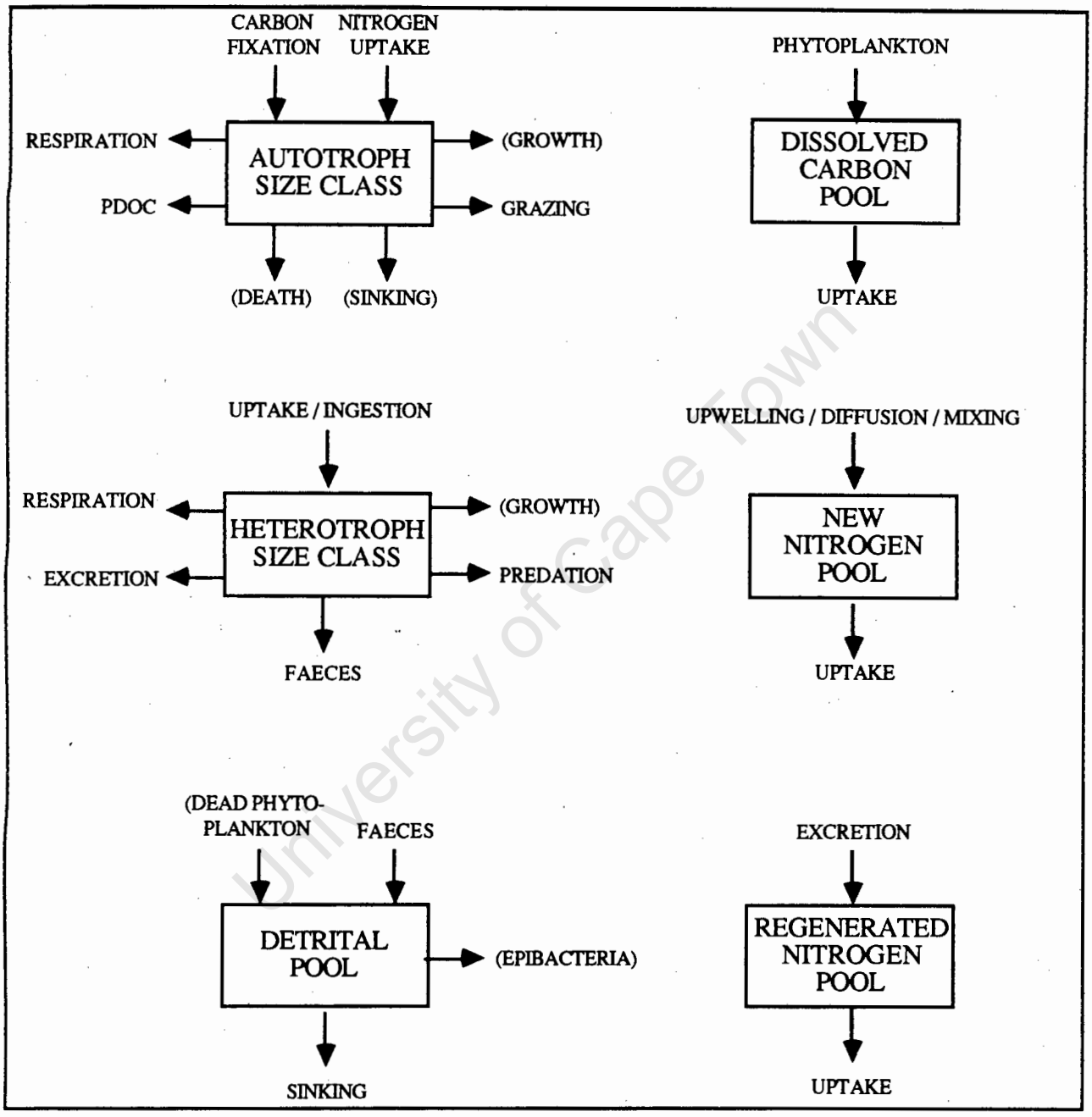

Fig. 3.3. Diagrammatic representation of major carbon and nitrogen flows into and out of model compartments. Flows in parentheses are excluded from the standard simulation.

DEVELOPMENT OF THE SIMULATION MODEL

Logarithmic scale and size classes

All organism sizes are expressed in linear dimensions as equivalent spherical diameters (esd's). Autotroph and heterotroph continuums are divided into size classes using a logarithmic scale. In executing the model, the user is able to set the value of the base used for the logarithmic scale. In this chapter the base is set to ten, because the resulting size classes are similar to traditional categories described by Sieburth *et al.* (1978), and the total number of size classes is manageable for the sensitivity analysis (see below). However, the log-10 scale does not separate, for example, heterotrophic flagellates and ciliates, and a smaller scale to the base five is used in subsequent chapters. The logarithmic base used has the effect of increasing or decreasing the number of size classes and consequently the mean size of organisms per size class.

An average size is calculated for each size class using a geometric mean:

$$esd_{average} = \sqrt{esd_{min} \times esd_{max}} \quad \text{.....(3.1)}$$

Spherical volumes are calculated and the conversion from volume to wet mass is 1 pg = 1 μm^3, assuming a specific density of one. Peters (1983) used factors of between 0.1 and 0.3 to convert from wet to dry mass, and 0.4 to convert from dry mass to C mass. His conversions from wet mass to C mass were thus between 0.04 and 0.13. An intermediate factor of 0.07 is used here. However, it should be noted that the equations of Strathmann (1967) for marine phytoplankton do not predict a linear conversion as assumed above, but one of body mass to the power 0.75. Taguchi (1976) estimated a similar relationship for marine diatoms. No equivalent relationship presently exists for bacterio- or zooplankton, and the effect of these dissimilar conversion factors will be investigated in the sensitivity analysis.

Relating carbon and nitrogen flows

Because the model uses a double currency of C and N, it is necessary to relate the fluxes of the two. This is done by assuming constant C:N ratios for different trophic categories; 6 for autotrophs, 4 for bacteria, and 4.5 for bactivorous protozoa and micro/mesozooplankton. This may not always be realistic, but mechanisms causing different rates of uptake and/or release of C and N are complex and poorly understood (Terry 1982, Syrett 1981). Furthermore, the Redfield ratio for phytoplankton is commonly used to convert C estimates to N and vice versa (e.g. Probyn and Lucas 1987), indicating that many ecologists implicitly assume constant C:N ratios in their calculations. Mass units are mg C and mg N.

Modelling procedure

Rates of change of standing stocks for biotic and abiotic compartments are determined by rates of input and output of C and N to and from each compartment. All instantaneous rates are averaged over one day, and diurnal effects are not included in the model. Mass flows are described by mathematical functions (described below), and the rates of change of standing stocks are described by differential equations (Table 3.2) which are solved numerically using a second order Runge-Kutta method (Lapidus and Seinfeld 1971).

Table 3.2 Differential equations describing rates of change of state variables. AC = autotroph carbon, AN = autotroph nitrogen, HC = heterotroph carbon, HN = heterotroph nitrogen, DET = detrital carbon and nitrogen, NEWN = new nitrogen, REGN = regenerated nitrogen, PDOC = dissolved carbon pool, j = size class subscript

dAC_j / dt	=	carbon fixation - PDOC - respiration - grazing - sinking + growth in - growth out
dAN_j / dt	=	nitrogen uptake - grazing - sinking + growth in - growth out
dHC_j / dt	=	ingestion/uptake - egestion - respiration - predation + growth in - growth out
dHN_j / dt	=	ingestion/uptake - egestion - excretion - predation + growth in - growth out
dDET / dt	=	sinking/death + faeces - ingestion - sinking
dPDOC / dt	=	PDOC production - uptake
dNEWN / dt	=	(Upwelling / diffusion) - uptake
dREGN / dt	=	excretion - uptake

Primary production

Many factors can limit phytoplankton growth (see Raymont 1980). In the model described here, it is assumed that only nitrogen is limiting. *Thus the model describes the carbon and nitrogen flows of a hypothetical microplankton community in a small, closed body of water, in which light and other nutrients are not limiting*. This should be borne in mind when extrapolating from the simulation results to field conditions, because other factors (such as light) will be important in the field, and will modify the results accordingly. Primary production rates are assumed to be limited by N uptake rates, which are governed by Michaelis-Menten kinetics (MacIsaac and Dugdale 1969):

$$V_j(d^{-1}) = V_{max_j}(d^{-1}) \frac{N\ (mg.m^{-3})}{K_{s_j}(mg.m^{-3}) + N\ (mg.m^{-3})} \quad \text{.....(3.2)}$$

where V_j is the mass-specific uptake rate for size class j, V_{maxj} is the maximum mass-specific uptake rate for size class j, K_{sj} is the half saturation constant for size class j, and N is the ambient N concentration. V_j and N are variables, and V_{maxj} and K_{sj} are size-dependent parameters. N uptake rates are thus modified by ambient N concentrations; if N is large V_j tends to V_{maxj}, and if N is small V_j is slower than V_{maxj}. Net C fixation rates (P_j) are calculated as the specific uptake rate (V_j), calculated in equation 3.3, times the C standing stock (B_j) in each size class j

$$P_j\ (mg\ C.m^{-3}.d^{-1}) = V_j\ (d^{-1}) \times B_j\ (mg\ C.m^{-3}) \quad \text{.....(3.3)}$$

C fixation rates are thus determined by N uptake rates.

PDOC production

Phytoplankton exude some fraction of primary production as PDOC (Berman and Holm-Hansen 1974). The percentage of primary production released in this fashion is believed to be relatively large, some authors believe as much as 70 % (Johnson *et al.* 1981, Lancelot 1983), although it is very difficult to measure, because the labile fraction of PDOC is rapidly taken up by bacteria. PER (percentage extracellular release) has been related to ambient N concentrations, with large PER associated with small concentrations and small PER with large concentrations (Azam *et*

al. 1983). The implication is that phytoplankton fix C at an optimal rate, but under N-limiting conditions insufficient N is taken up to meet the demand, and excess C has to be excreted. However, the situation is far more complex. PER is affected also by light levels, age of cells, etc (Lancelot 1983). N concentrations and PER are correlated (Azam *et al.* 1983), but the relationship cannot be interpreted as being causative, so N levels alone cannot be used to predict PER. Many authors assume a constant value for PER. Although this is probably not realistic at all times, a constant fraction has been used in the model. This fraction refers only to the labile portion, because the refractory material has a much longer residence time (Lucas 1986). It is assumed that only the labile fraction is important on the time scales that are used in the simulations. The effect of varying the value of PER is investigated in the sensitivity analysis.

Heterotroph uptake / ingestion

Two sources of input to heterotroph compartments are simulated. Bacterioplankton take up N from solution (organic and inorganic N) in much the same way as do phytoplankton, and are assumed to obtain C solely from the PDOC pool. Particulate carbon (POC) such as faecal material and senescent phytoplankton cells sinks rapidly (Chapter 2). Consequently, it is assumed that bacterial utilization of POC occurs below the euphotic zone, and a pathway from POC to attached bacteria is not included in the model. Uptake of both C and N is governed by Michaelis-Menten models; equation (3.2) for N (Monod 1949) and equation (3.4) for C (Parsons and Strickland 1962):

$$V_j\,(d^{-1}) = V_{max_j}(d^{-1})\,\frac{PDOC\,(mg.m^{-3})}{K_{s_j}(mg.m^{-3}) + PDOC\,(mg.m^{-3})} \qquad \text{.....(3.4)}$$

where V_j is the mass-specific growth rate of bacteria as determined by C availability, V_{maxj} is the size-dependent maximum uptake rate as in equation (3.3), PDOC is the ambient dissolved C concentration and K_{sj} is the size-dependent half saturation constant for PDOC uptake (assumed equal to K_{sj} for N uptake times the C : N ratio for bacterioplankton). Bacterioplankton growth ($P`_j$) is thus limited by C or N, depending on which uptake rate V_j (3.2 or 3.4) is slower:

$$P`_j \text{ (mg C/N.m}^{-3}\text{.d}^{-1}) = V_j \text{ (d}^{-1}) \text{ x } B_j \text{ (mg C/N.m}^{-3}) \quad \text{.....(3.5)}$$

When nitrogen is limiting, carbon uptake may be underestimated by the model, because bacteria often do not modulate their rates of carbon uptake sufficient just to meet their biosynthetic or bioenergetic demands (Tempest and Neijssel 1978), and "excess" carbon is frequently taken up.

Particle-feeding heterotrophs obtain C and N by ingestion of autotrophs or heterotrophs. Food available to each size class of predator is calculated on a size basis; predators may ingest a range of food-particle sizes, dependent on their own sizes. The ingestion model is of the form:

$$\text{Ingestion}_{j_k}(d^{-1}) = a_{j_k} \text{ x } I_{max_j}(d^{-1}) \frac{B'_k}{K_{s_k} + \sum_{r=min}^{max} B'_r} \quad \text{.....(3.6)}$$

where the specific ingestion rate of size class k by size class j is determined by the maximum mass-specific size-dependent ingestion rate of size class j (I_{maxj}), modified by a preference index *a* which takes a value between 0 and 1. The optimum prey size class for each predator size class is assigned a value of 1 for *a*, and *a* decreases by a pre-determined factor (a_1) with each additional size class separating it from the optimum class. For example, if ø is the position of the optimum prey size class and the factor a_1 is 2, $a_ø = 1$, $a_{ø+1}$ and $a_{ø-1} = 0.5$, $a_{ø+2}$ and $a_{ø-2} = 0.25$ and so on. $B`_k$ is the standing stock of size class k available to size class j, and r represents the range of size classes available to each predator class j. K_{sk} is the half saturation constant dependent on the size of the prey k (see Chapter 2).

Egestion

Heterotrophs do not assimilate all they ingest. A proportion of ingested material is released as faeces. Hall *et al.* (1976) were not able to show any size-dependence of absorption efficiencies, which are assumed to be 90 % for all particle-feeding heterotrophs (Dagg 1976, Barthel 1983, Miller and Landry 1984), and 100 % for bacteria.

Respiration

C losses as a result of respiration are modelled as a constant fraction of size-class standing stock:

$$\text{Respiration (mg C.m}^{-3}\text{.d}^{-1}) = R_j\ (d^{-1}) \times B_j\ (\text{mg C.m}^{-3}) \quad \text{.....(3.7)}$$

where R_j is the mass-specific size-dependent respiration rate, and B_j the C standing stock of size class j. Respiration rates change during feeding and other activities, but these effects are not included in the model. This may result in an underestimate of respiratory losses, but is probably only important for large size classes of heterotrophs, because motility of protozoans requires an insignificant fraction of their energy budget (Fenchel and Finlay 1983).

Excretion

Metabolic C losses through respiration are matched by equivalent N losses in order to maintain constant C:N ratios for heterotrophs. The required excretion rates are calculated as:

$$\text{Excretion (mg N.m}^{-3}\text{.d}^{-1}) = R_j\ (d^{-1}) \times B_j\ (\text{mg N.m}^{-3}) \quad \text{.....(3.8)}$$

where R_j is the same as for equation (3.7), and B_j is the N standing stock in size class j. For bacteria this may not be realistic. Bacteria can take up N and C separately, because the dissolved pools consist of both inorganic and organic material, and a variety of different substrates. Bacterial C and N uptake rates are therefore not necessarily coupled, as is assumed here. When N is limiting, bacteria may conserve this nutrient. An alternative approach to modelling this process would be to consider only the net uptake of N, i.e. assume that bacteria only take up sufficient N for their requirements, and excrete none. However, this approach makes the *a priori* assumption that bacteria excrete *no* nitrogen at all. The real situation is probably intermediate between these two extremes. As it stands (equation 3.8), the model will probably overestimate nitrogen excretion by bacteria (see Chapters 4 and 5).

Sinking

C and N losses through sinking of phytoplankton and faecal material are calculated as:

$$\text{Sinking losses (mg C / N.d}^{-1}) = \frac{S_j (\text{m.d}^{-1})}{D\,(\text{m})} \times B_j (\text{mg C / N}) \quad \ldots\ldots\ldots\ldots\ldots\ldots (3.9)$$

where S_j is the sinking velocity of size class j, D is the depth of the water mass / euphotic zone in question, and B_j is the C / N standing stock of size class j.

Growth through size classes

Growth along the continuums is a complicated process to model. Not all organisms in a size class will grow into the next size class - some will divide and remain in the same size class. Also, bacteria do not grow into whales (Cousins 1985), so restrictions are required. The simplest way to model growth is as a simple proportion (G) of standing stock (B) growing out of each size class (j) and in to the next.

$$\text{Growth}_j \text{ (mg C/N.m}^{-3}\text{.d}^{-1}) = G\ (\text{d}^{-1}) \times B_j \text{ (mg C/N.m}^{-3}) \quad \ldots\ldots\ldots\ldots\ldots\ldots (3.10)$$

However, equation (3.10) does not take into account faster growth rates in smaller size classes, and also does not include the effect of food availability on growth. For simplicity, growth was not included in the standard simulation, but its effect is investigated in the sensitivity analysis.

ESTIMATION OF MODEL PARAMETERS

Many of the processes described above are size-dependent and parameters thus vary between size classes. General allometric equations relating body size to mass-specific rates were calculated in Chapter 1, and empirical relationships between body size and other factors of importance to ecological processes and interactions were calculated in Chapter 2. Equations derived in these two chapters are used to calculate size-dependent parameters for each size class. Allometric and other parameters used in the computer program are presented in Table 3.3. Resulting size-dependent parameters of autotrophs and heterotrophs (Table 3.4) are presented with associated size classes and C masses. There is a large difference in rate parameters

Table 3.3. Parameter values used in the standard simulation (size-dependent parameters in bold). See equations (3.1) to (3.9) for explanations of symbols.

Process	Size-dependent parameters	Parameter	Values	Units
Uptake = $B_j \mathbf{V_{max_j}} \frac{N}{{}_V\mathbf{K_{s_j}} + N}$	$\mathbf{V_{max_j}} = a W_j^b$	a	5.1+0.3	$pgC^{0.25} d^{-1}$
		b	-0.25	-
	$_V\mathbf{K_{s_j}} = {}_VK_{s_1} \frac{W_j}{{}_VK_{s_2} + W_j}$	$_VK_{s_1}$	73	$mgNm^{-3}$
		$_VK_{s_2}$	940	$mgCm^{-3}$
Ingestion = $B_j \mathbf{I_{max_j}} \frac{S}{{}_I\mathbf{K_{s_k}} + S}$	$\mathbf{I_{max_j}} = a W_j^b$	a	78+8.0	$pgC^{0.25} d^{-1}$
		b	-0.25	-
	$_I\mathbf{K_{s_k}} = {}_IK_{s_1} W_j^{\,{}_IK_{s_2}}$	$_IK_{s_1}$	54	$pgC^{-0.08}$
		$_IK_{s_2}$	0.08	-
Respiration = $\mathbf{R_{V_j}} B_j$ (phytoplankton and bacterioplankton)	$\mathbf{R_{V_j}} = a W_j^b$	a	1.7	$pgC^{0.25} d^{-1}$
		b	-0.25	-
Respiration = $\mathbf{R_{I_j}} B_j$ particle-feeding heterotrophs	$\mathbf{R_{I_j}} = a W_j^b$	a	15+1.5	$pgC^{0.25} d^{-1}$
		b	-0.25	-
$Sinking_P = \frac{\mathbf{S_{P_j}}}{D}$ $Biomass_j$ (live phytoplankton cells)	$\mathbf{S_{P_j}} = S_{P_1} W^{\,S_{P_2}}$	S_{P_1}	0.029	$pgC^{-0.42} m.d^{-1}$
		S_{P_2}	0.42	-
$Sinking_F = \frac{\mathbf{S_{F_j}}}{D}$ $Volume_j$ (faecal and detrital material)	$\mathbf{S_{F_j}} = S_{F_1} W^{\,S_{F_2}}$	S_{F_1}	2.2	$(\mu m^3)^{-0.30} m.d^{-1}$
		S_{F_2}	0.30	-
Absorption = A x Ingestion	-	A	0.90	-
PDOC = PER x primary production	-	PER	0.30	-
Minimum prey size = r_{min} x pred size	-	r_{min}	0.125	-
Optimum prey size = r_{opt} x pred size	-	r_{opt}	0.125	-
Maximum prey size = r_{max} x pred size	-	r_{max}	0.125	-
Preference index for ingestion	-	a	1	-
Preference index factor for ingestion	-	a_I	1	-

between the smallest and largest organisms, highlighting the necessity for some form of size differentiation among system components. For example, phytoplankton comprise four size classes, with thirty-fold differences in rate parameters (Table 3.4). Such differences are realistic. Specific growth rates of 8.9 d^{-1} have been calculated for pico-phytoplankton (Douglas 1984), whereas net-phytoplankton growth rates are usually < 1 d^{-1} (Parsons *et al.* 1977). Prey-size dependent half saturation constants (equation 3.6) for prey size classes (autotrophs and heterotrophs) are presented in Table 3.5, together with the predator size class ingesting each prey size class.

Table 3.4. Autotroph and heterotroph size classes, size-dependent parameters and initial standing-stocks

Size class (μm)	Average esd (μm)	Carbon mass (pg)	$V_{max}^{\#}$ / I_{max}^{*} (d^{-1})	Resp (d^{-1})	K_S (uptake) (mg $N.m^{-3}$)	Sinking ($m.d^{-1}$)	Initial values (mg $C.m^{-3}$)
Autotrophs							
Pico-phytoplankton (0.2-2)	0.63	0.0093	16#	5.5	0.00072	0.004	0.00001
Nano-phytoplankton (2-20)	6.3	9.3	2.9#	0.97	0.72	0.074	0.008
Net-phytoplankton (20-200)	63	9300	0.52#	0.17	66	1.3	5.9
Heterotrophs							
Bacterioplankton (0.2-2)	0.63	0.0093	16#	5.5	0.00072	-	0.00001
Bactivores (2-20)	6.3	9.3	45*	8.6	-	-	0.008
Microzooplankton (20-200)	63	9300	8.0*	1.5	-	-	5.9
Mesozooplankton (200-2000)	632	$9.3x10^6$	1.4*	0.27	-	-	4.2

Table 3.5 Prey-size dependent half saturation constants (mg $C.m^{-3}$) for ingestion of prey (columns, autotrophs and heterotrophs) by predators (rows, heterotrophs)

		PREY SIZE CLASSES		
		Picoplankton *(0.2 - 2 μm)*	*Nanoplankton* *(2 - 20 μm)*	*Microplankton* *(20 - 200 μm)*
PREDATOR SIZE CLASSES	*Nanozooplankton* *(2 - 20 μm)*	37.1	-	-
	Microzooplankton *20 - 200 μm)*	-	64.5	-
	Mesozooplankton *(200 - 2000 μm)*	-	-	112

INITIALIZATION OF STATE VARIABLES

Values assigned to standing stocks in each model compartment at the start of a simulation to some extent determine the behaviour of the model system. A general functional form is used to calculate initial biomasses (B) in each size class (j) from body masses (W):

$$B_j(\text{mg C.m}^{-3}) = {}_1\psi \times W_j(\text{mg C.m}^{-3})^{{}_2\psi} \quad \text{.....(3.11)}$$

If ${}_2\psi$ is made zero, initial biomasses are set to ${}_1\psi$, and if ${}_2\psi$ is made 1, initial biomasses are calculated as a linear function of size class body mass. An equation of this form, relating steady-state biomasses in subtropical oceanic waters to organism size was calculated by Rodriguez and Mullin (1986):

$$B_j\ (\text{mg C.m}^{-3}) = 0.108\ W_j\ (\mu\text{g C})^{-0.16} \quad \text{.....(3.12)}$$

This relationship (3.12) predicts that, on average, small organisms will have larger standing stocks than large organisms. However, in executing simulations, it was found that large organisms

generally had to be initialized with higher standing stocks than small organisms, to prevent small organisms from dominating. The values of the initial standing stocks in the autotroph and heterotroph size classes were therefore arbitrarily designated (Table 3.4). PDOC and regenerated nitrogen concentrations are started at zero, and new-nitrogen concentrations, which effectively "drive" the model, are set to different starting values, depending on the kind of water body that is simulated. The effect of changing initial values of standing stocks is investigated in the sensitivity analysis.

MODEL EXECUTION

The simulation model consists of two computer programs. The first sets up the structure of the model community. It quantifies certain attributes of model compartments, calculates parameters and initializes state variables, which consist of C and N standing stocks in each biotic size class and in the abiotic pools.The second program simulates the dynamics of the model system. It traces changes in standing stocks over time, resulting from the movements of C and N within- and between- components of the trophic continuum. Both programs are written in FORTRAN V for use on the Sperry 1100 Series mainframe computer at the University of Cape Town. Copies of the programs and associated documentation are presented in Appendices I and II. Details of calculations performed by the two programs are described below.

The simulation model is executed by running the two computer programs in sequence. Example runstreams are presented in Appendix II. A number of options are available when executing the simulations. These were included to allow some system complexity, and are selected by setting pre-defined values to program parameters. They include a parameter which sets the method of new-N input at a constant unchanging value, a continuous input simulating diffusion into the euphotic zone, or a single initial input followed by zero input which simulates upwelling and subsequent stratification of the water column. Similarly, by changing a second parameter, PER can be changed from a constant to a variable proportion of primary production. Although diurnal effects are not included in simulations, a diurnal structure has been incorporated into the model. This is "activated" by setting a parameter to a pre-defined value, which results in carbon

fixation being made zero for half the day, with all other processes left unchanged. Output resulting from using the diurnal effect is presented in the sensitivity analysis.

STANDARD SIMULATION

A standard simulation is exercised to serve as a basis for comparing output from a sensitivity analysis. For simplicity, new N concentrations are set to an unchanging value of 200 mg $N.m^{-3}$ (15 mg-at.m^{-3}). Although this is unrealistic, the purpose of the standard simulation is to assess model output, not to validate it, and simple systems are easiest to use for comparisons. Realistic simulations are described in Chapters 4, 5 and 6.

Standing stocks in each autotroph and heterotroph size class are initialized using equation (3.11), with $\psi_1 = 1000$ and $\psi_2 = 0.95$, except for the largest heterotoph size class (200-2000 μm), which had $\psi_1 = 1$. Regenerated N and PDOC pools are initialized with zero concentrations, and the pools later receive inputs from biotic compartments during growth. The standard simulation is kept as simple as possible by assuming that PER is constant, and by not including sinking of phytoplankton cells and growth through size classes.

Output of the standard simulation

Changes with time of the standing stocks of model compartments in the standard simulation are presented in Fig. 3.4. The biotic size classes are divided into three groups to facilitate presentation of the results. Populations of pico-phytoplankton, bacterioplankton and nanozooplankton (zooflagellates) cycle within 3-5 days (Fig. 3.4a), and are plotted on different axes from the nano-phytoplankton and microzooplankton (Fig. 3.4b) and net- phytoplankton and mesozooplankton (Fig. 3.4c). There is a succession from small to large organisms with time in the standard simulation. The sensitivity analysis will assess to what degree the results depicted in Fig. 3.4 depend on the parameter values and model assumptions.

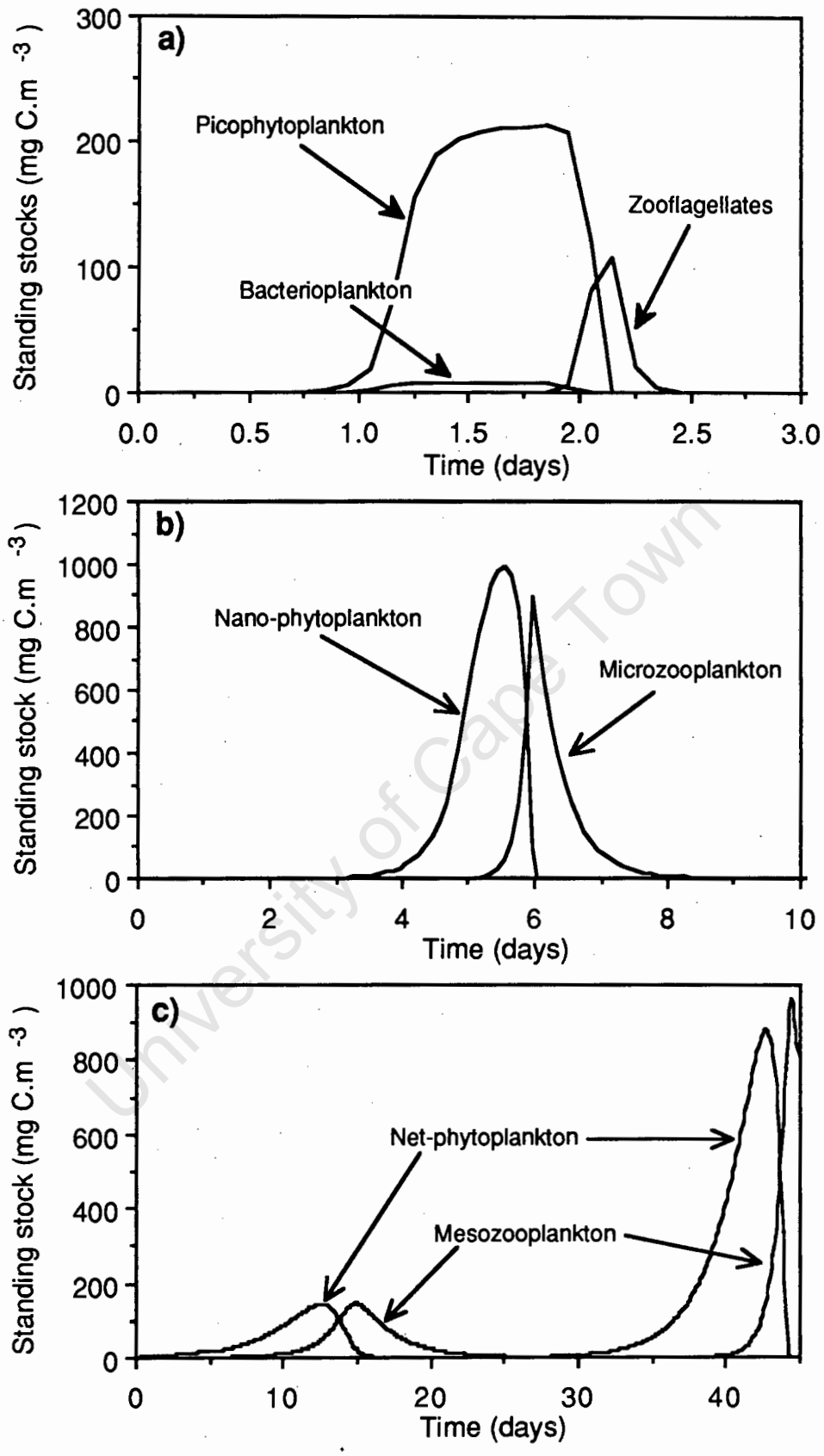

Fig. 3.4. Output from the standard simulation. Changes in standing stocks with time of a) pico-phytoplankton (0.2-2 μm), bacterioplankton (0.2-2 μm) and predators of both (zooflagellates, 2-20 μm), b) nano-phytoplankton (2-20 μm) and their microzooplankton predators (20-200 μm), c) net-phytoplankton (20-200 μm) and their mesozooplankton predators (200-2000 μm).

SENSITIVITY ANALYSIS

Platt *et al.* (1981) list four areas in which model sensitivity should be tested: i) sensitivity to parameters, ii) sensitivity to initial values, iii) sensitivity to functional form and iv) sensitivity to model structure. In the sensitivity analysis described below, all four areas of sensitivity are explored to some extent. A "brute-force" approach is used, whereby parameters are varied one at a time and the effect on output of the standard simulation assessed (Platt *et al.* 1981). This is done descriptively, using graphical displays of output. As a result, a number of different qualitative responses of the simulations have been identified, and some factors that may produce these responses are summarized in Table 3.6.

i) Sensitivity to parameter values

Allometric equation parameters

Values of parameters are halved and doubled for each parameter in turn. Changes in output resulting from varying the values of allometric equation parameters are presented in Fig. 3.5, and the major effects are summarized in Table 3.6. All results are compared with those of the standard simulation (Fig. 3.5a). The succession of size classes observed in the standard simulation is repeated in the sensitivity analysis output, but the time scales and magnitudes of standing stocks vary. Most of the changes are predictable and are not substantial. For example, doubling the value of the nitrogen uptake rate, V_{max}, results in phytoplankton and bacterial standing stocks increasing faster than in the standard simulation (Fig. 3.5b), and the converse is true when V_{max} is halved (Fig. 3.5c). Doubling the ingestion rate, I_{max}, of predators allows small predators to attain large standing stocks (Fig. 3.5d, left panel), but large predators do not flourish, because the fast predation rate prevents their phytoplankton prey from increasing. When I_{max} is halved (Fig. 3.5e), the durations of the phytoplankton and bacterioplankton blooms increase. Similarly, when the respiration rates of predators are doubled, the durations of the blooms of their prey increase (Fig. 3.5f). Increasing respiration rates retards predator growth; thus the parameters that affect predation rates or predator standing stocks influence the time scales of prey population fluctuations. The

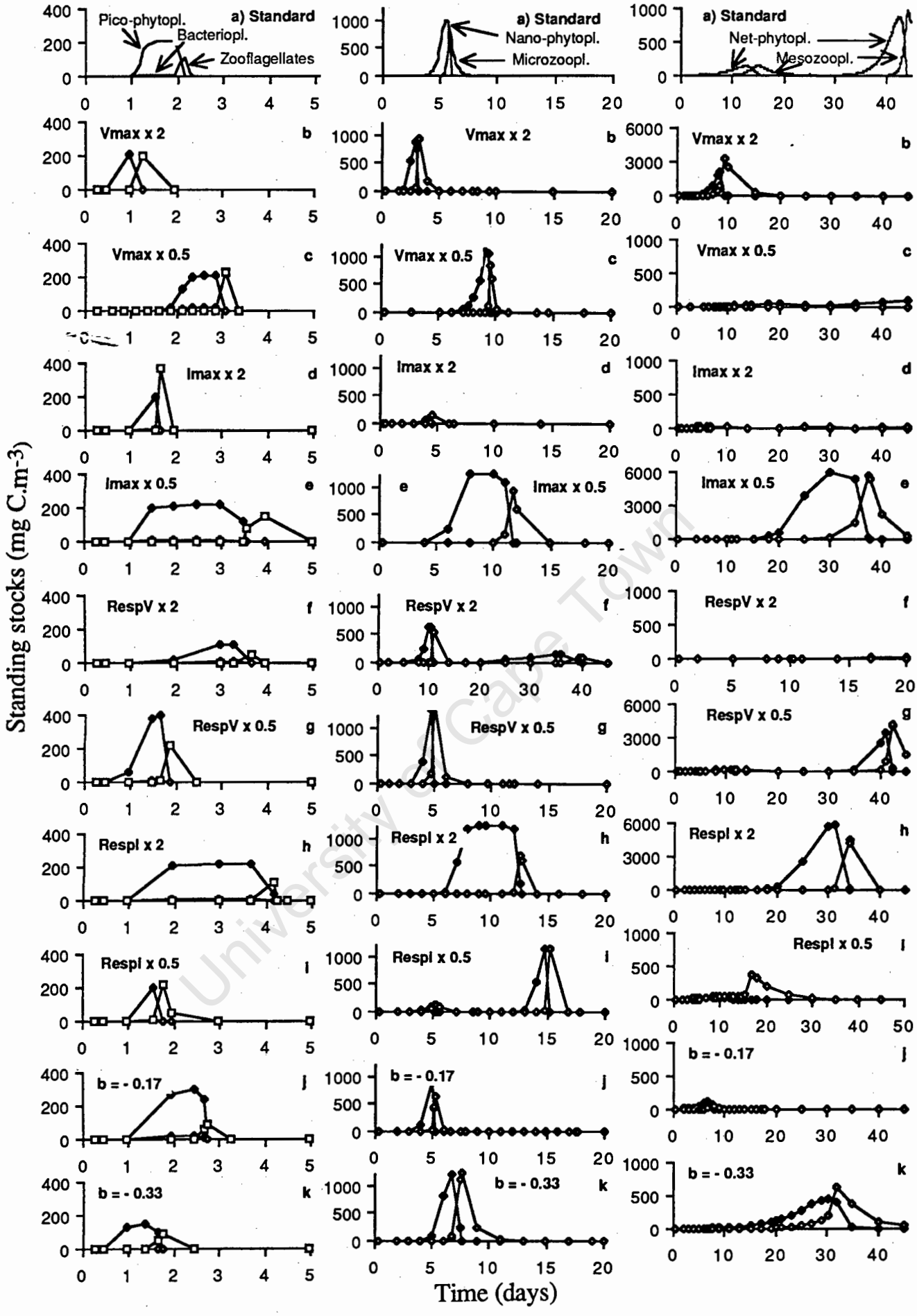

Fig. 3.5. Effects of altering allometric equation parameters in the standard simulation (see text for explanation of symbols). Each parameter in turn is doubled (x 2) and halved (x 0.5). Note that the scales vary on the vertical axes in the right panel.

magnitudes of standing stocks are affected by the values of the respiration rate parameters R_V and R_I (Figs. 3.5f-i), as would be expected. Altering the value of the allometric exponent from the assumed value of -0.25 (Chapter 1) has a small effect on standing stocks. When *b* is increased to -0.17 (Fig. 3.5j), small organisms are favoured, because their rate parameters are faster relative to those of large organisms. The reverse is true when *b* is decreased to -0.33 (Fig. 3.5k). Largest organisms then have the fastest relative rates, and standing stocks of net-phytoplankton and microzooplankton increase, whereas the other biotic components decrease.

Half saturation constant parameters

The half saturation constants in the nitrogen uptake function (equation 3.2) and the ingestion function (equation 3.6) are calculated using two parameters for each function (Table 3.3). The effects of doubling and halving these parameters are presented in Fig. 3.6. Changing the nitrogen uptake parameters has very little effect (Figs. 3.6b-e), whereas altering the values of the ingestion parameters has a pronounced effect. When these parameters are altered in such a way as to make the net effect one of increasing predation rates (i.e. ${}_IK_{s1}$ and ${}_IK_{s2}$ are halved), the most obvious effect is to decrease the standing stocks of net-phytoplankton and their mesozooplankton predators (Figs. 3.6f-g, third panel). When these parameters are doubled, the standing stocks of net-phytoplankton and mesozooplankton increase (Figs. 3.6h-i, third panel). Only these two components are affected substantially, indicating that grazing can be an important factor limiting net-phytoplankton growth.

Absorption efficiencies

Absorption efficiencies determine the proportion of ingested food that may be used for maintenance and growth. When the absorption efficiencies (*A*) of heterotrophs are altered, the effects are predictable (Fig. 3.7). A reduced efficiency of 45 % slows down predation rates because predator standing stocks take longer to increase. Furthermore, the maximum standing stocks of predators are reduced (Fig. 3.7b). Conversely, an almost perfect absorption efficiency of

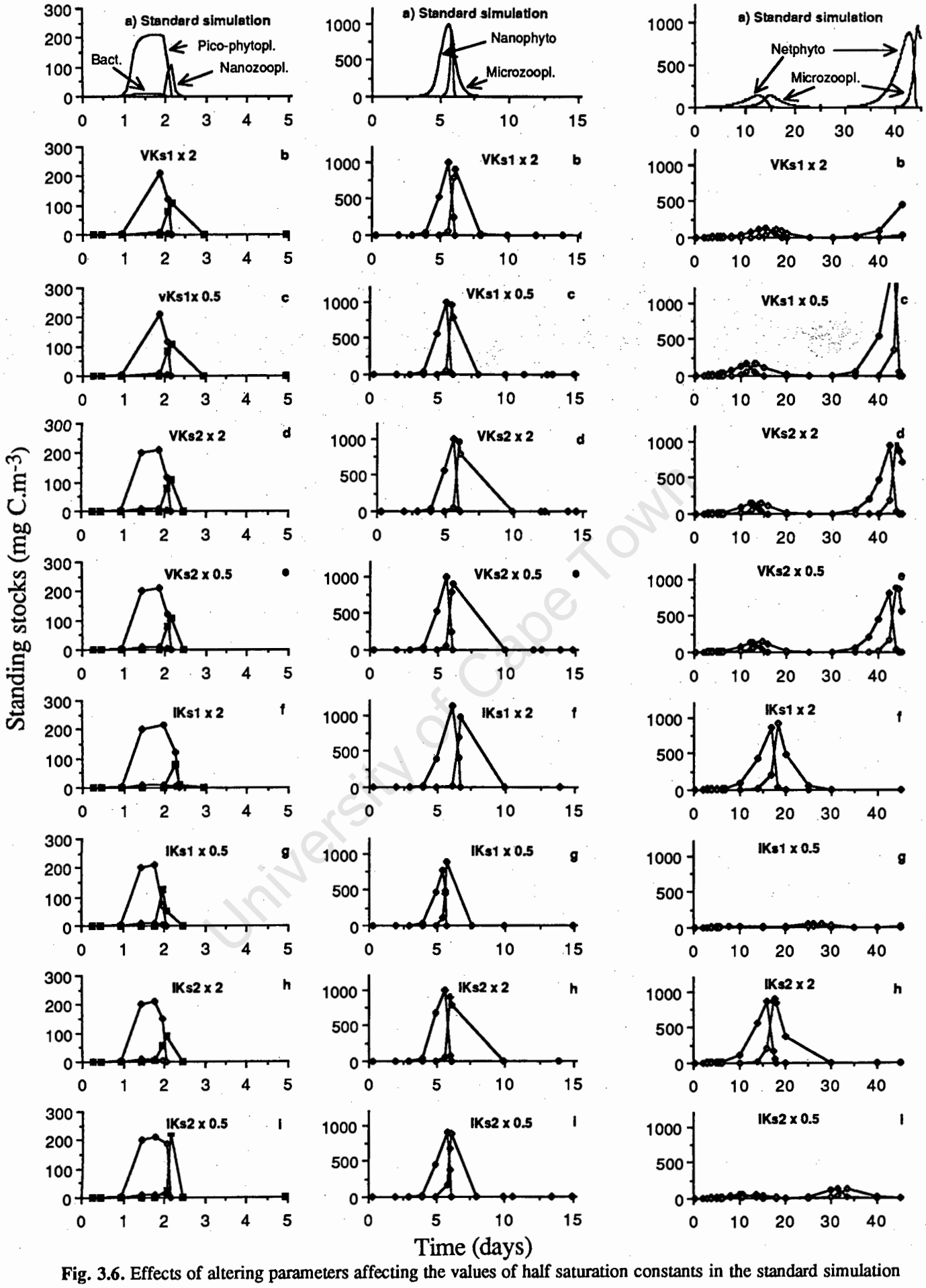

Fig. 3.6. Effects of altering parameters affecting the values of half saturation constants in the standard simulation (a) for nitrogen uptake by phytoplankton and bacterioplankton (b-e) and ingestion by predators (f-i). Each parameter in turn is doubled (x 2) and halved (x 0.5).

99% increases predation rates and predator standing stocks (Fig. 3.7d), whereas an efficiency of 60 % results in an effect intermediate between the previous two (Fig. 3.7c). Thus, as *A* decreases, so the durations of the blooms of the biotic components increase, and the lag before they develop decreases. (The second bloom in the third panel does not always occur, because the time scales depicted are sometimes too short.)

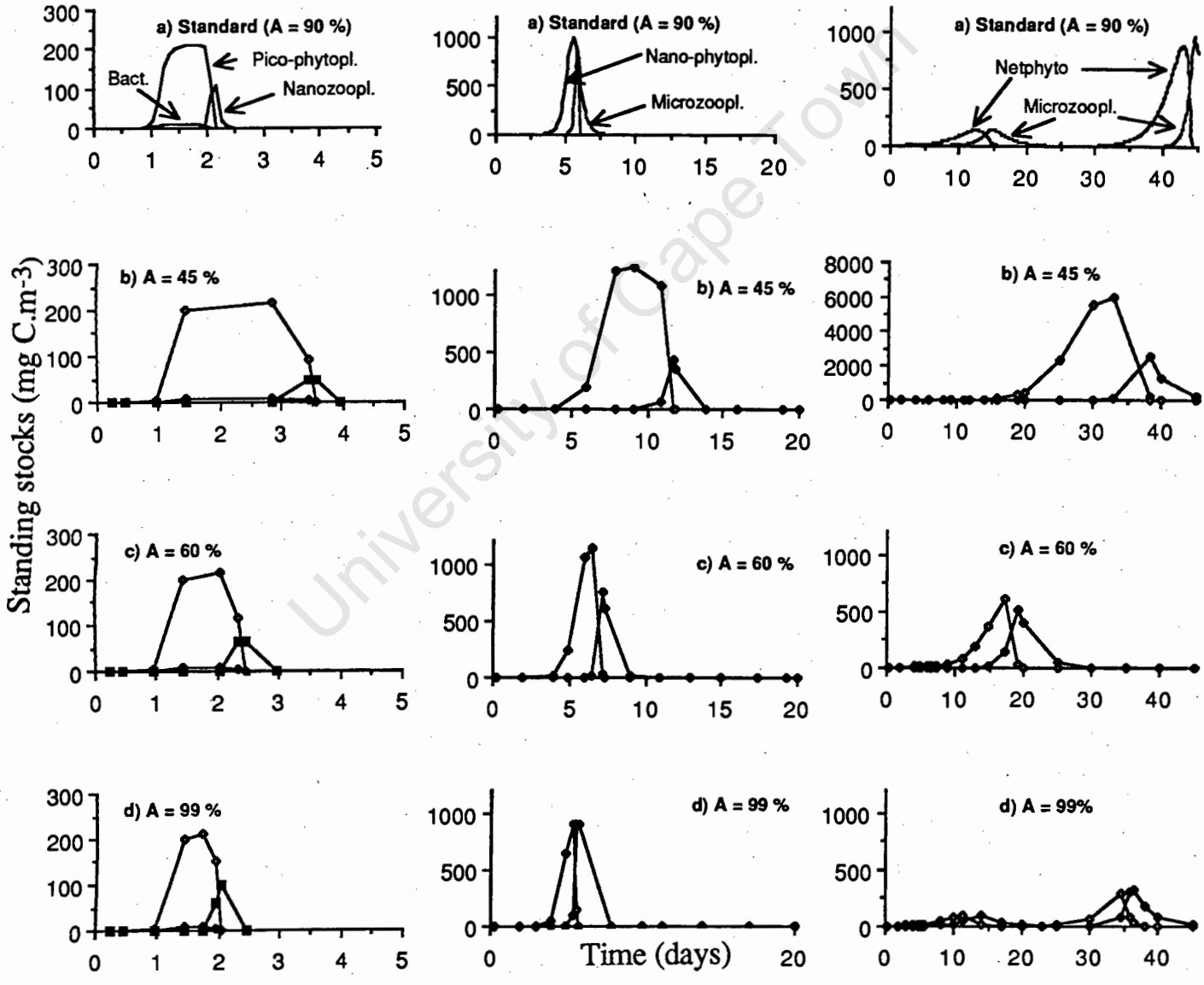

Fig. 3.7. Effects of altering the values of the absorption efficiency of particle-feeding heterotrophs in the standard simulation.

Percentage extracellular release (PER)

Changing the value of PER affects only the bacterioplankton population (Fig. 3.8), which increases when PER is increased, because more carbon is made available. Nitrogen does not limit bacterioplankton growth at the start of the standard simulation, because nitrogen concentrations are high, and there is little competition for nitrogen, because all standing stocks are low.

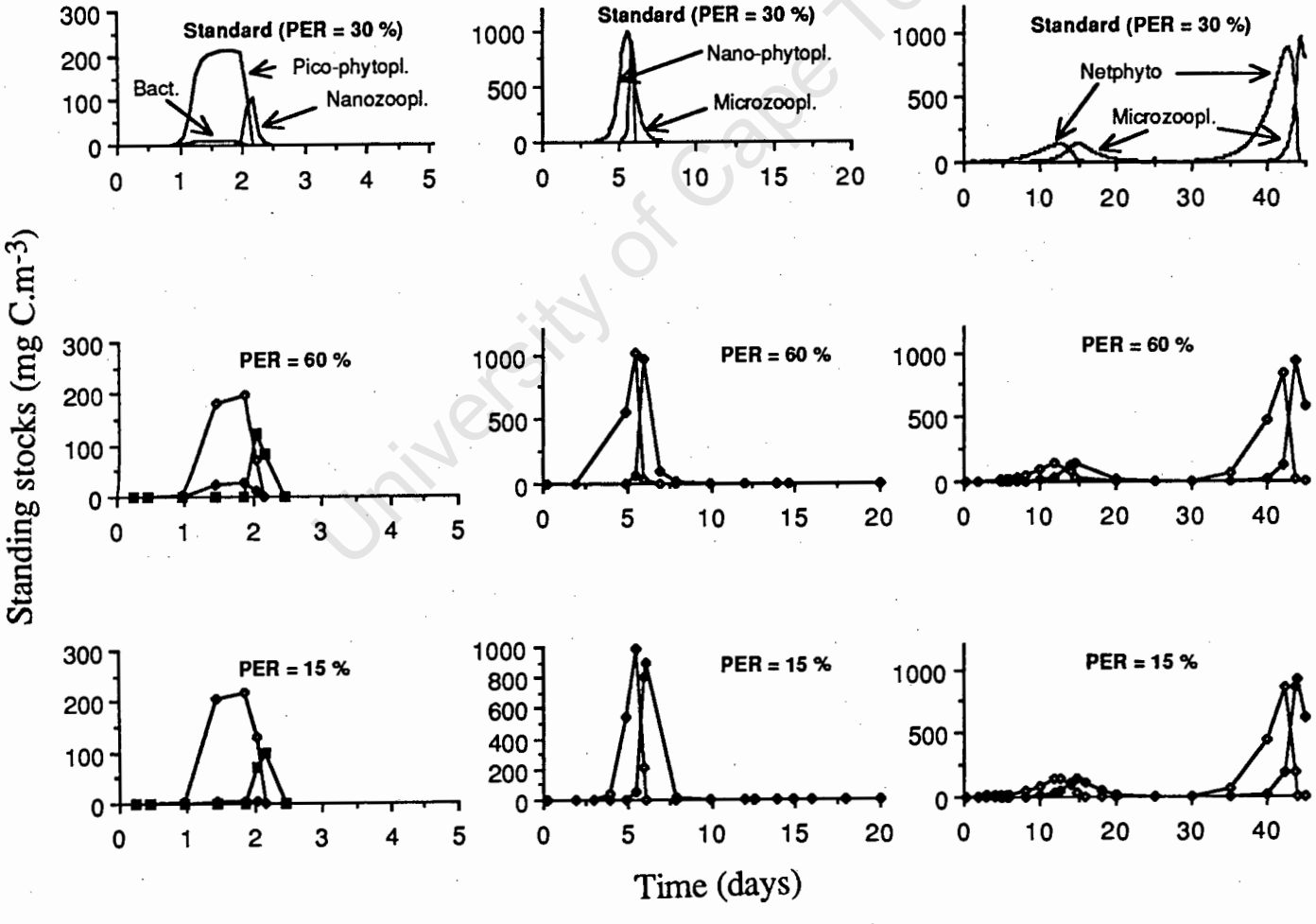

Fig. 3.8. Effects of altering the value of PER in the standard simulation.

ii) Sensitivity to initial values

Initial values assigned to standing stocks at the start of each simulation may be important in determining model output. A number of simulations have been executed in which the initial biomass spectra were altered (Fig. 3.9). There are some marked differences (mainly quantitative) between the different simulations. These include changes in magnitudes of standing stocks and in the time scales of model-population increases.

In the first two simulations, the initial biomass spectra were flat, with standing stocks of 1 and 10 mg $C.m^{-3}$ respectively (Figs. 3.9b-c). The standing stocks of the small components of the model community increase rapidly in these two simulations, and their blooms are shifted to the left relative to those of the standard simulation, but standing stocks are smaller. The initial values of the small size classes in Fig. 3.9b and c are larger than those in the standard simulation, whereas those of the large phytoplankton and zooplankton are relatively unchanged.

In the third simulation (Fig. 3.9d), the biomass spectrum is initialized with a positive slope, and the output is very similar to that of the standard simulation (Fig. 3.9a), although the time scales are slightly different. In the remaining five simulations the standing stocks of different components are altered relative to those of Fig. 3.9d. The initial standing stocks are increased by a factor of 10 for pico-phytoplankton and bacterioplankton (Fig. 3.9e) and nano-phytoplankton and zooflagellates (Fig. 3.9f), and decreased by a factor of 10 for mesozooplankton (Fig. 3.9g). In all three cases the output is similar to that of Fig. 3.9d, except for differences in the magnitudes of standing stocks.

The initial standing stocks of bacterioplankton are increased by a factor of 100 (Fig. 3.9h) and 1000 (Fig. 3.9i), to assess whether bacterioplankton standing stocks in the simulations are depressed due to the control of predators. However, similar results are obtained to those of Fig. 3.9d, suggesting that some other factor (probably carbon limitation) retards the growth of bacterioplankton at the start of the simulations.

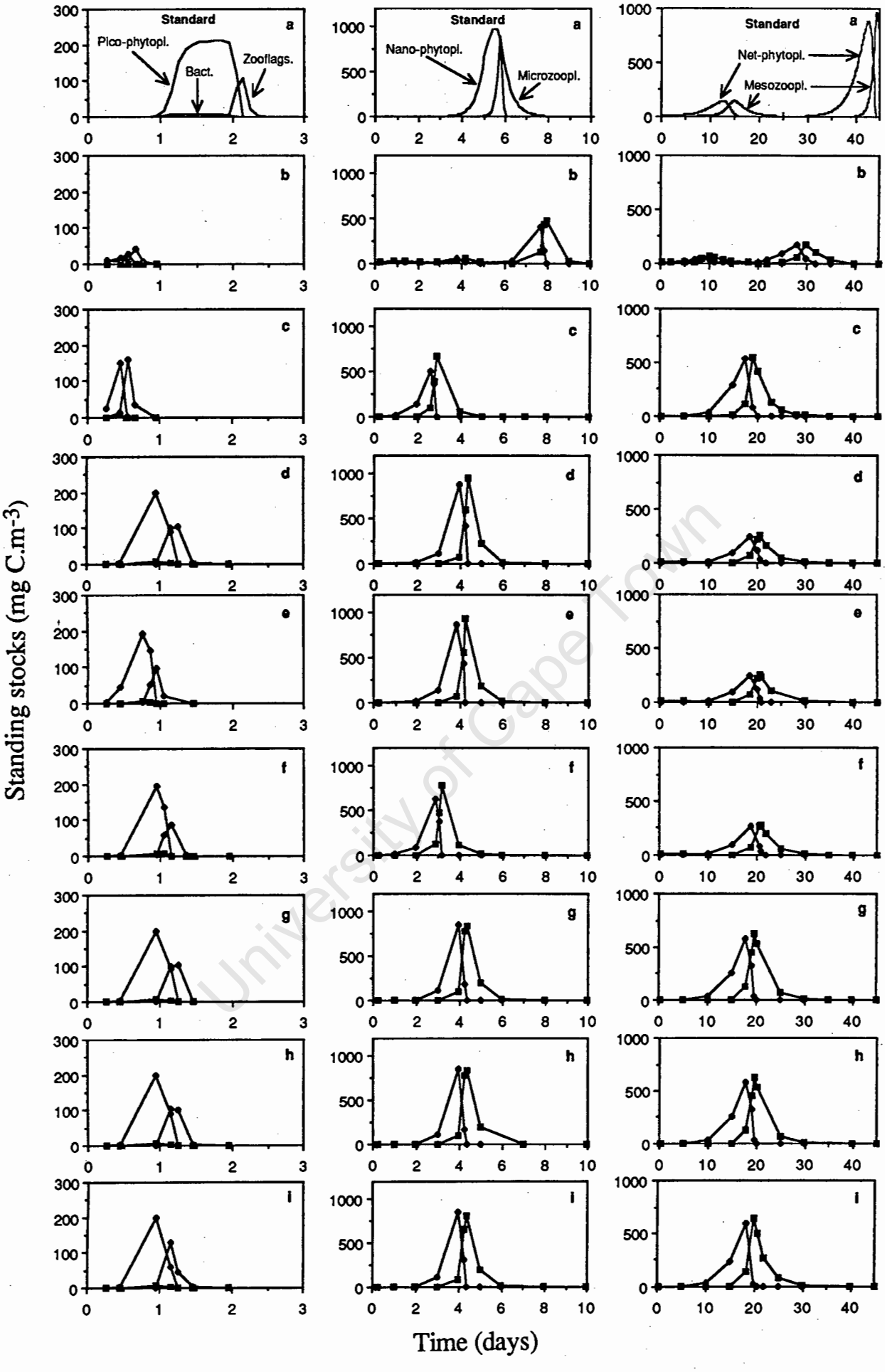

Fig.3.9. Effects of altering the initial biomass spectrum in the standard simulation

iii) Sensitivity to functional form

Wet mass : carbon conversions

Linear conversions have been used to convert wet mass to C for autotrophs and heterotrophs in the standard simulation. However, volume : carbon relationships for phytoplankton are non-linear, and the following relationships have been estimated for diatoms:

$$W \text{ (pg C)} = 0.378 \text{ V } (\mu m^3)^{0.758} \text{ (Strathmann 1967)} \quad (3.13)$$

$$W \text{ (pg C)} = 0.26 \text{ V } (\mu m^3)^{0.74} \text{ (Taguchi 1976)} \quad (3.14)$$

and for non-diatom phytoplankton:

$$W \text{ (pg C)} = 0.347 \text{ V } (\mu m^3)^{0.866} \text{ (Strathmann 1967)} \quad (3.15)$$

The non-linear equations of Strathmann (1967) are widely used to calculate phytoplankton C from cell volumes, whereas linear conversions are used for all heterotrophs (e.g. Rodriguez and Mullin 1986). Because the model uses size classes and not weight classes, it is confusing to use different conversions. Heterotrophs could then ingest autotroph and heterotroph prey of the same physical size but with different C masses. Furthermore, allometric equations typically use C masses as an indicator of organism size, and autotrophs and bacteria of the same physical size would have different C masses and thus different physiological rates.

The effect of using the assumed linear conversion for all groups is compared with a simulation in which equation (3.13) is used for autotrophs and heterotrophs (Fig. 3.10). It is apparent that the standing stocks of small organisms increase, whereas those of large organisms are depressed. The non-linear conversion results in bigger C masses for small organisms, whereas large organisms are assigned smaller C masses, the changeover occurring at 1066 μm^3 (12.7 µm esd). If a non-linear conversion were used for phytoplankton and a linear conversion for all heterotrophs, as is usually the case, this would substantially affect the differences in uptake rates between similar-sized autotrophs and bacteria.

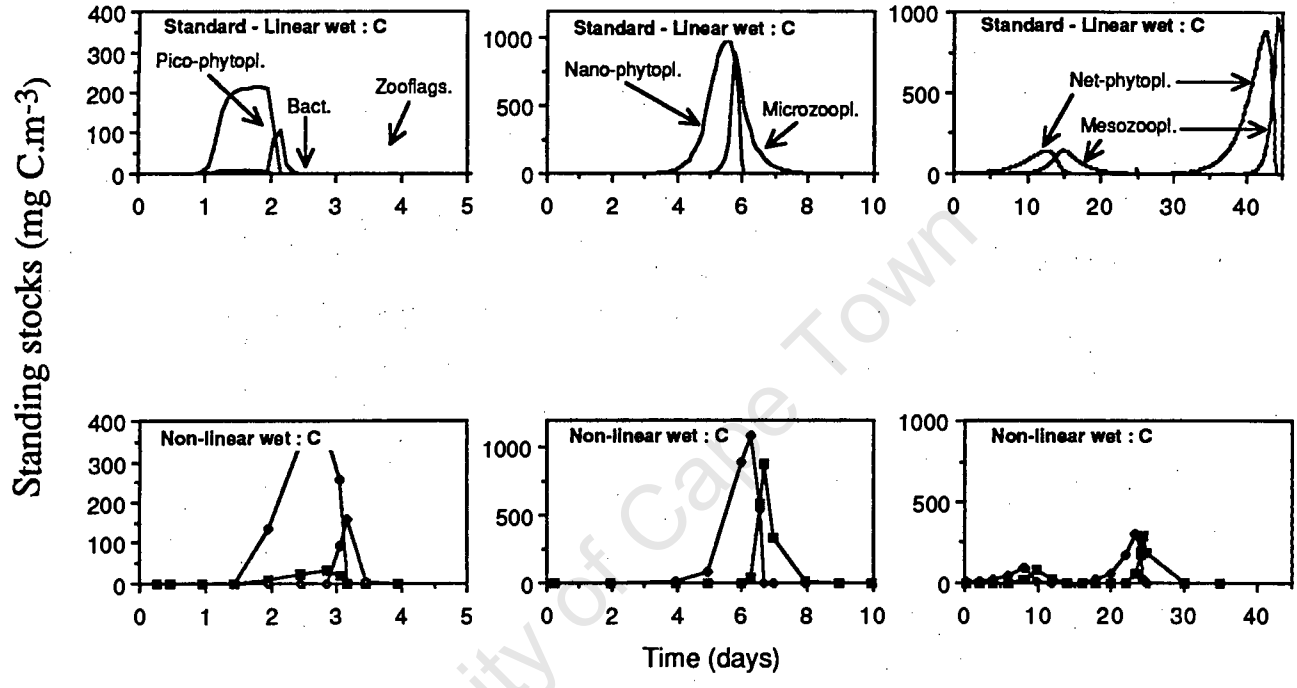

Fig. 3.10. The effect of using non-linear wet mass to carbon conversion functions in the standard simulation.

The complexity that would be introduced to the model structure if apparent differences between wet mass to C conversions for autotrophs and heterotrophs were accommodated, does not warrant their inclusion (Starfield and Bleloch 1986), and simple linear conversions are used throughout. Thus C masses in the model may be underestimated for small autotrophs and overestimated for large autotrophs. The reason why autotrophs should display this non-linearity between volume and C mass whereas heterotrophs apparently do not is unclear. It is possible that a non-linear conversion should be applied to all organisms, but has not yet been calculated for heterotrophs, because a large enough size range has not yet been studied.

Varying percentage extracellular release (PER)

Phytoplankton production and bacterioplankton growth are believed to be closely coupled (Azam *et al.* 1983). Bacterioplankton compete with phytoplankton for dissolved N, but at the same time rely on phytoplankton for PDOC, resulting in a paradoxical situation (Bratbak and Thingstad 1985), in which phytoplankton supply bacteria with one nutrient while competing with them for another. A number of studies have attempted to elucidate the relationship between phytoplankton production of PDOC and its subsequent utilization by bacterioplankton (e.g. Azam and Hodson 1977, Bell 1980, Bell and Sakshaug 1980, Cole *et al.* 1982, Jensen 1983, Laake *et al.* 1983a; b, Hagstrom *et al.* 1984), but PER is very difficult to estimate, largely because PDOC is rapidly taken up by bacteria. The problem becomes even more complex when one considers that PER is probably not a constant proportion of primary production, but varies with a number of factors (Lancelot 1983).

A constant PER of 30 % for labile PDOC is assumed in the standard simulation. The effect of halving and doubling this value has been shown (Fig. 3.8), and this parameter has been identified as being important in determining the standing stocks of bacterioplankton. The effect of using a variable PER determined by ambient N levels, as suggested by Azam *et al.* (1983), is investigated in this section. Azam *et al.* (1983) presented a plot of PER versus ambient N concentrations, and calculated a linear relationship. However, the linear function is not realistic because at nitrate concentrations greater than about 480 $mg.m^{-3}$ PER becomes negative. I fitted an exponential decay function to the data to give the following relationship:

$$PER\ (d^{-1}) = e^{-0.004 \times N} \quad \text{.....(3.16)}$$

where N is nitrogen concentration measured in $mg.m^{-3}$, and PER changes as ambient nitrogen concentrations change. The result of making PER variable was similar to having constant PER (Fig. 3.11), because new-N levels in the standard simulation are set to be constant, and do not decline to zero. PER thus does not become very large, varying between 13 and 44 %. Initially, PER is greater than 30 %, resulting in a larger bacterioplankton standing stock than that observed in the standard simulation (Fig. 3.11). The importance of PER is manifested through its effect on

bacterioplankton, because PER determines the amount of C available for bacterioplankton growth. The assumption of constant PER is valid for the standard simulation, but may not be valid in a dynamic system.

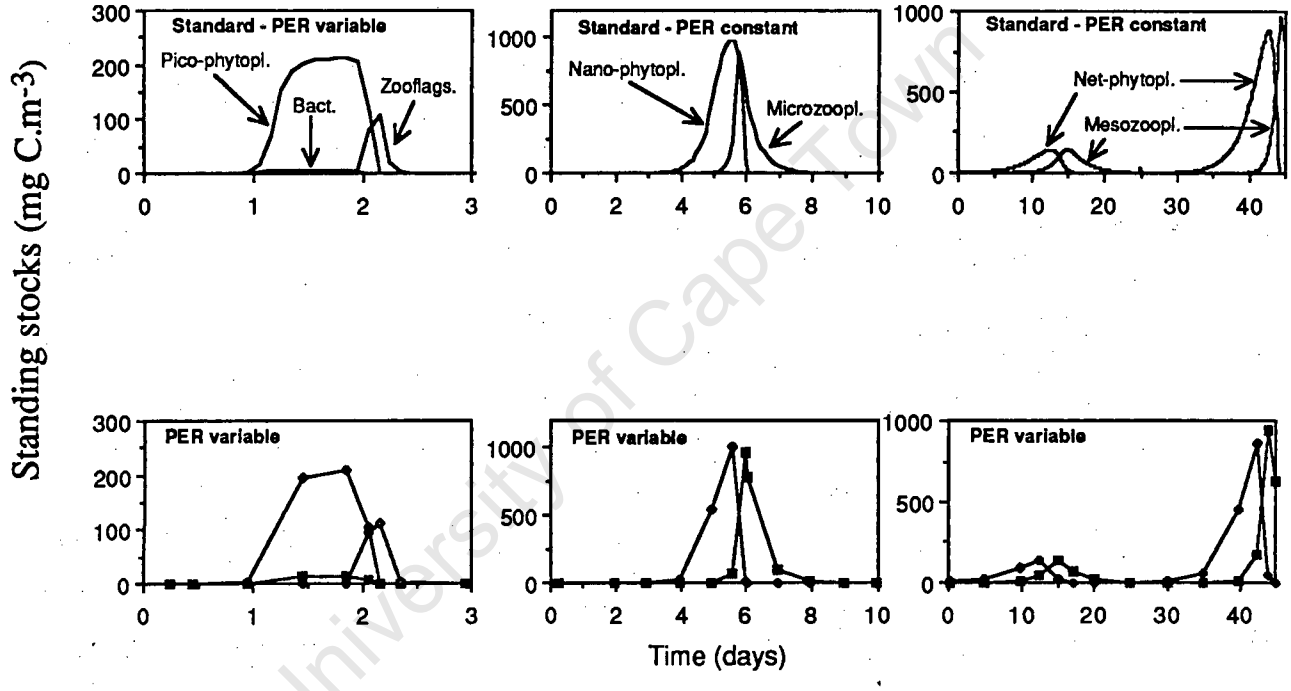

Fig. 3.11. The effect of making PER a variable in the standard simulation, dependent on the ambient nitrogen concentrations

Threshold densities for ingestion of prey

Predators often display a threshold response in their feeding behaviour; feeding may cease when the density of prey items falls below a threshold value (e.g. Frost 1975). Such a functional response has been included in the structure of the ingestion functions in the simulation model (see Appendix II), but the threshold concentrations were set to zero in the standard simulation, to reduce model complexity. The effect of including a threshold density of 10 mg $C.m^{-3}$ for ingestion

of all prey size classes is demonstrated in Fig. 3.12. It is evident that the simulation output stabilizes when threshold densities are included. This result may be more realistic than that of the standard simulation, but the values of the threshold concentrations are not known for all size classes. The strength of the model lies in the fact that all of its parameters are estimated objectively, using size-dependent relationships. Rather than lose this objectivity by including subjective estimates of threshold parameters, the threshold densities were reset to zero for all subsequent simulations. However, the effect of including threshold densities in the model (Table 3.6) should be borne in mind when interpreting "realistic" simulations in Chapters 4, 5, and 6.

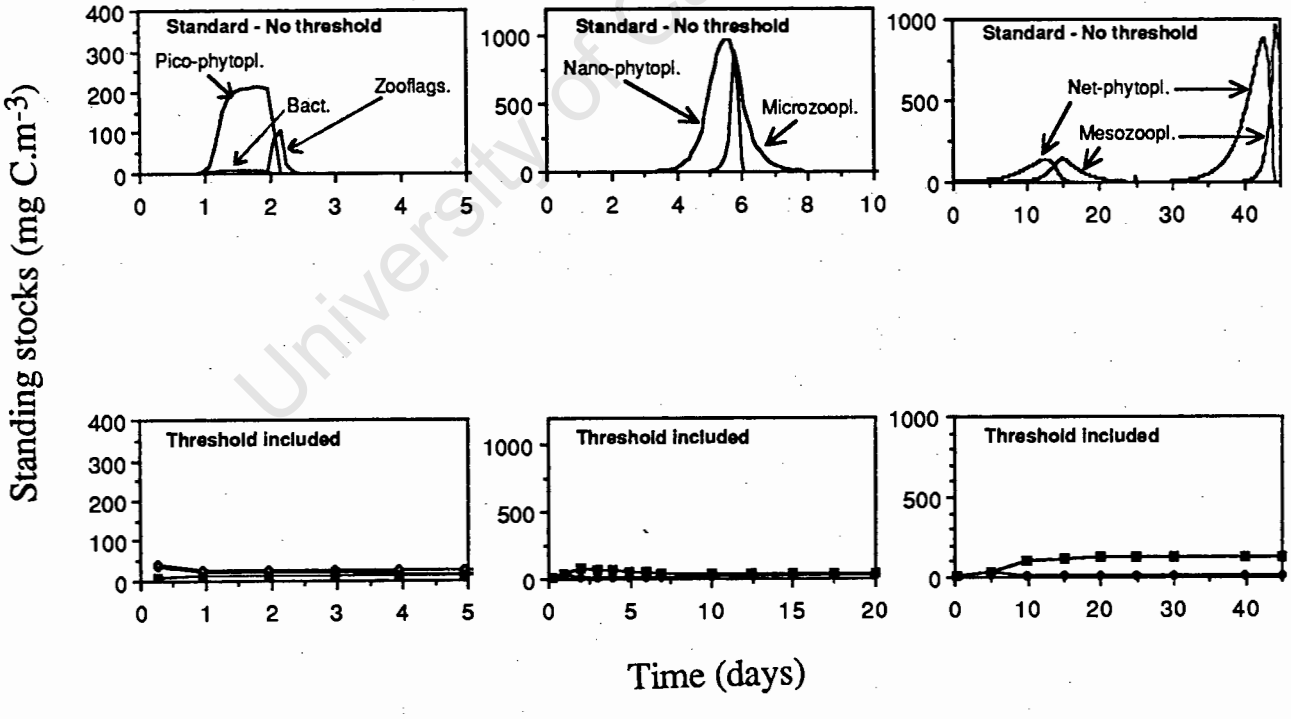

Fig. 3.12. The effect of including a threshold concentration of 10 mg $C.m^{-3}$ for ingestion in the standard simulation for all prey size classes.

iv) Sensitivity to model structure

Growth

In the standard simulation, growth along the continuums was ignored. The effect of allowing a linear transfer of standing stock from small to large size classes is investigated. A transfer of 10 % per day results in increases in magnitudes of heterotroph standing stocks (Fig. 3.13b), and a greater transfer of 30 % per day causes a greater relative increase, and results in stable populations of the largest heterotrophs (Fig. 3.13c). By growing into a larger size class, an organism slows down all process rates, so the net effect is for standing stocks to increase. This may be important in systems in which food is not abundant.

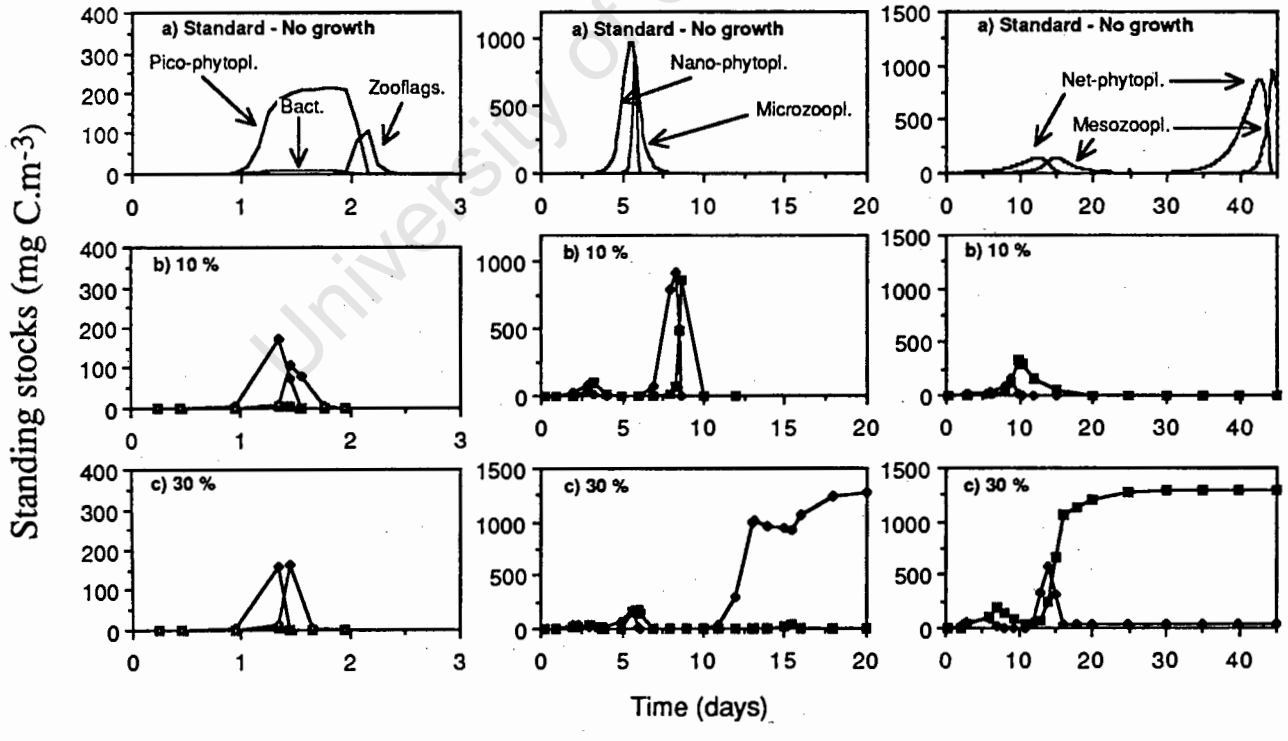

Fig. 3.13. The effects of including growth from small to large size classes in the standard simulation. a) Standard simulation, no growth. b) Growth factor of 10 % per day. c) Growth factor of 30 % per day.

Sinking

Sinking losses are included in the standard simulation by assuming a 1 m deep zone, and calculating the amount of autotroph C and N that would be lost through sinking (equation 3.9). Inclusion of sinking losses from the autotroph continuum has very little effect on standing stocks of autotrophs less than 20 μm (Fig. 3.14b, first two panels), and changing the values of the sinking parameters has no further effect (Figs. 3.14c-f, first two panels). This is because the small autotrophs have very slow sinking velocities (Table 3.4). However, the large-celled autotrophs and their grazers are affected dramatically by the inclusion of sinking losses in the simulations (Fig. 3.14b-f, third panel), with standing stocks barely increasing before decreasing to zero, except in the last simulation (Fig. 3.14f), in which the effect of increasing the exponent in the power function (Chapter 2) results in slower sinking velocities. These sinking velocities are applicable in a water column in which water densities are uniform and there is no upward transport. This is obviously unrealistic, and in nature sinking velocities will change as the physical and chemical structure of the water body changes.

Diurnal effects

All processes in the model are assumed to occur continuously, i.e. there are no diurnal effects. Obviously this is not realistic. Assuming that photosynthesis is averaged over a day, gives an indication of the magnitude of primary production, but does not reflect the true dynamic pattern. The effect of including a simple diurnal pattern is shown in Fig. 3.15, in which it has been assumed that carbon is fixed for one half of every day, but all other processes remain unchanged throughout the day. This results in a jagged pattern of standing stocks with time, which is more pronounced for small size classes than for large size classes. The pico-phytoplankton (Fig. 3.15, left panel) oscillate more frequently than in the standard simulation. Because no carbon is fixed during the "night" but respiration continues, the autotroph standing stocks take longer to increase than in the standard simulation, which also affects the rate of increase of heterotroph grazers.

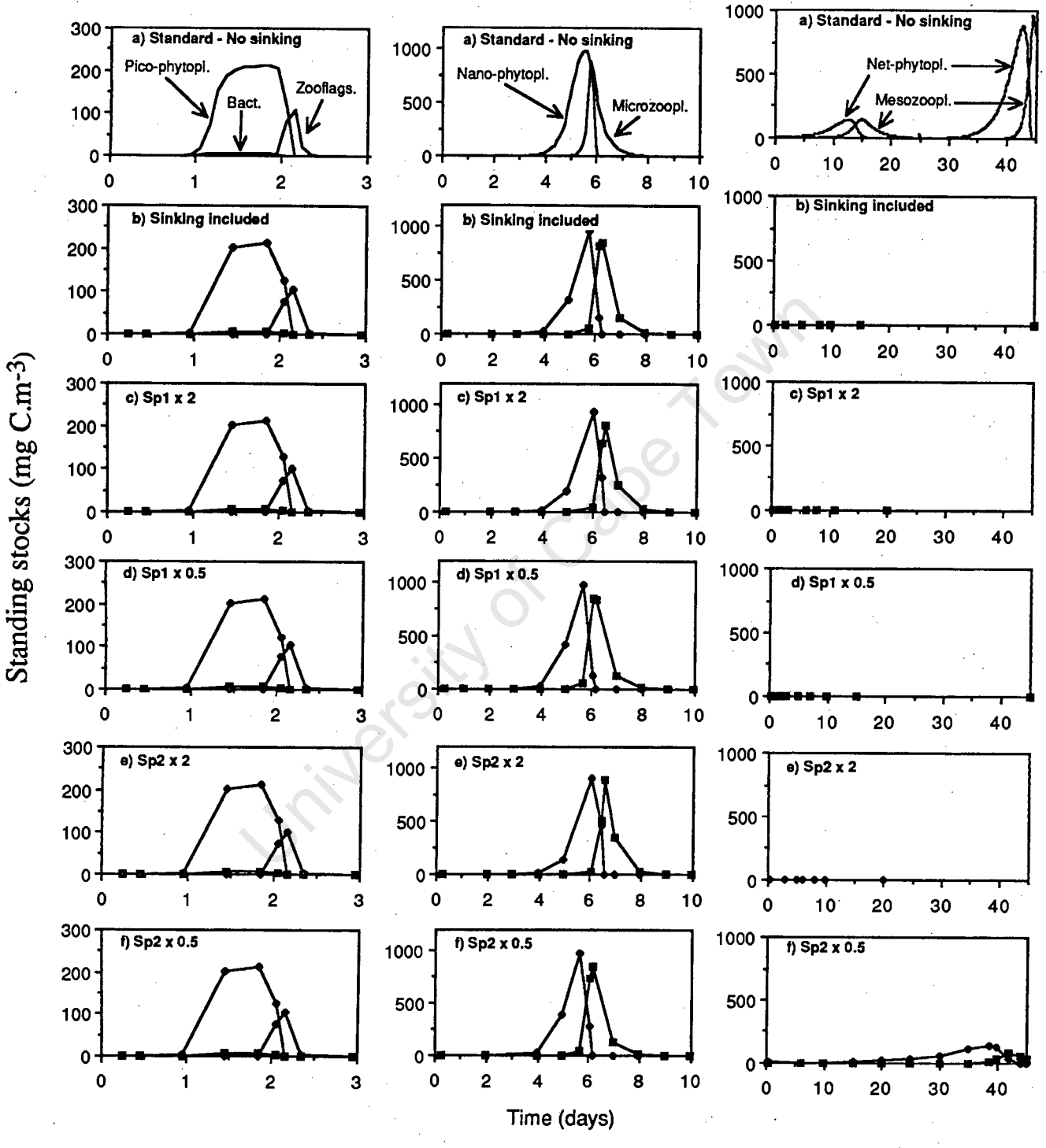

Fig. 3.14. The effect of including sinking losses of phytoplankton cells in the standard simulation (a-b). The values of each of the two sinking parameters in turn are doubled and halved(c-f).

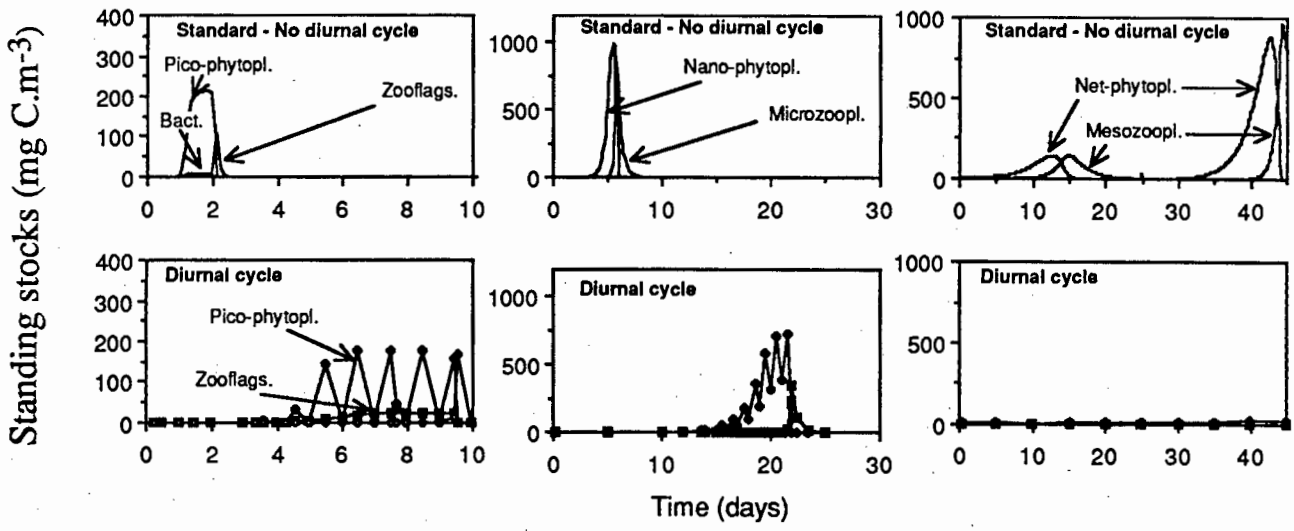

Fig. 3.15. The effect of including a simple diurnal cycle in the standard simulation.

Number of size classes

The number and size range of size classes in the model community is variable, and is set at the start of each simulation, when the total size ranges of autotrophs and heterotrophs are defined and the log scale is set. In the standard simulation, the log scale was set to 10, but in subsequent chapters a scale of 5 is used, resulting in more size classes. By increasing the number of size classes within a fixed size range, the structure of the model becomes more complex. Predators are able to utilize more than one size class, and competition for nitrogen between phytoplankton size classes become more pronounced. Successions involving different sizes of organisms still occur, but not necessarily in a strict sequence from small to large organisms. In nature, it appears that a log scale of 5 is more realistic than one of 10, because it allows for the separation of, for example, heterotrophic flagellates and ciliates. Heterotrophic flagellates are generally < 5 µm (Fenchel 1982a), whereas ciliates can range from approximately 10 to greater than 50 µm (Fenchel 1980c). These two groups play different roles in the marine pelagic environment, and it is useful to separate them on a size basis. Adopting a log scale smaller than 5, e.g. 2, results in an unmanageable number of sizes classes. Organism size is probably not continuous in nature. In benthic environments, it has been found that sizes of organisms fall into discrete size categories

(Schwinghamer 1983, Warwick 1983), and this may also be true for pelagic environments (e.g. Sprules *et al.* 1983). A log scale of 5 appears to be realistic in separating trophic categories in the plankton, although further, detailed studies are required.

Table 3.6. Summary of some of the different effects that may be achieved in simulations by altering the values of certain parameters, or changing certain assumptions of the model. Note that the "desired effects" may occur in nature if some factor other than those included in the model were to influence the "sensitive" parameters.

Desired effect	Sensitive parameter(s) and/or assumptions
Change the absolute magnitudes of standing stocks	Values of respiration rates Values of absorption efficiencies *A* Change organism growth parameters Diurnal effects
Change bacterioplankton standing stocks	Values of PER Include "refuge" densities (threshold densities for ingestion by bactivores)
Change the relative magnitudes of standing stocks	Values of the half saturation constants for ingestion of different sized organisms (chiefly affects predators larger than 200 µm and their prey) Starting values Wet mass : carbon conversion functions Include organism growth through size classes Change organism growth parameters Include sinking losses
Accelerate or delay the rates of bloom "increases"	Values of nitrogen uptake rates V_{max} Factors affecting nitrogen uptake rates V Values of absorption efficiencies Starting values Diurnal effects
Change the durations of population "blooms"	Values of maximum ingestion rates I_{max} Factors affecting ingestion rates I Values of respiration rates of heterotrophs R_v Factors affecting respiration rates R_v Values of absorption efficiencies *A* Diurnal effects
Stabilise predator-prey oscillations	Include growth through size classes Include threshold densities for ingestion

CONCLUSIONS

The model is robust with respect to many of its parameters, because most changes that occur on altering parameter values are quantitative, not qualitative, and are predictable. The model appears to be sensitive to ingestion rates, to the value of PER, to the shape of the initial biomass spectrum at the start of each simulation, and to wet mass:carbon conversion functions (Table 3.6). Parameters such as these, identified as being important in affecting model output, can be used to analyse system behaviour, and to try to isolate factors that may be instrumental in structuring plankton communities.

Model structure is largely hypothetical; the model is essentially a synthesis of hypotheses describing processes occurring in microplankton communities. Functions describing flows of C and N through the model community are not necessarily linear. This is in contrast to most other whole-system models, which usually abandon non-linearity because linear transfers between state variables are easier to handle. However, this may result in over-simplification, and it is believed that non-linearity is an integral part of complex systems (Prigogine 1987).

This model, based primarily on body size criteria, obviates many of the problems of parameter estimation common in ecological modelling. As a result, model output can be validated against any system study or data series, because parameters in the model are not specifically related to any ecological system. The model can therefore be applied to any microplankton community, to test ideas on structure and functioning of different systems. This is a major advantage over most previous models which are largely area- or system-specific, and whose predictive capacities are often in question.

CHAPTER 4

MODELLING TWO CONTRASTING SOUTHERN BENGUELA FOOD WEBS. I. STANDING STOCKS AND SIZE STRUCTURE

ABSTRACT

Size-based models are used to simulate planktonic food webs of the Agulhas Bank and an upwelling area off the west coast in the southern Benguela region. In both models the phytoplankton are divided into four size categories, and the microzooplankton into five size categories, and all parameters are determined using body-size relationships. It is assumed that nitrogen is limiting in both ecosystems, and other physical factors such as light are ignored. A continuous small input of new nitrogen into the Agulhas Bank model simulates diffusion into the euphotic zone across the thermocline, whereas an initial large pulse of new nitrogen in the west coast model simulates upwelling. Simulated model communities compare well with field observations in terms of standing stocks and size composition. The Agulhas Bank simulations depict an initially fluctuating standing stock of phytoplankton, which stabilizes to a pico-phytoplankton dominated community. This steady state probably never occurs in nature. The west coast model predicts that net-phytoplankton blooms after upwelling will be preceded by rapid blooms of pico-phytoplankton, and it is suggested that such blooms may have been overlooked in field studies, or may be depressed by other factors such as light. Simulation results indicate that understanding of the structure of the two ecosystems and the processes occurring are relatively well understood. The models provide useful tools for exploring the relationships between different components of the plankton communities.

INTRODUCTION

The Benguela system is situated off the west coast of southern Africa (Shannon 1985). It is dominated by a coastal upwelling system which, in common with upwelling systems in other eastern boundary current regions, supports productive commercial fisheries (Cushing 1971). The Benguela system generally is divided into northern and southern sections (Shannon 1985), the southern Benguela extending offshore between Hondeklip Bay and Cape Agulhas (Shannon 1985) (Fig. 4.1). This southern area supports an important pelagic fishery, with pilchard *Sardinops ocellatus* and anchovy *Engraulis capensis* dominating purse-seine catches at different stages in the history of the fishery (Crawford *et al.* 1987). At present, both species spawn on the Agulhas Bank (Fig. 4.1), but larval development takes place chiefly on the west coast, in the upwelling region of the southern Benguela.

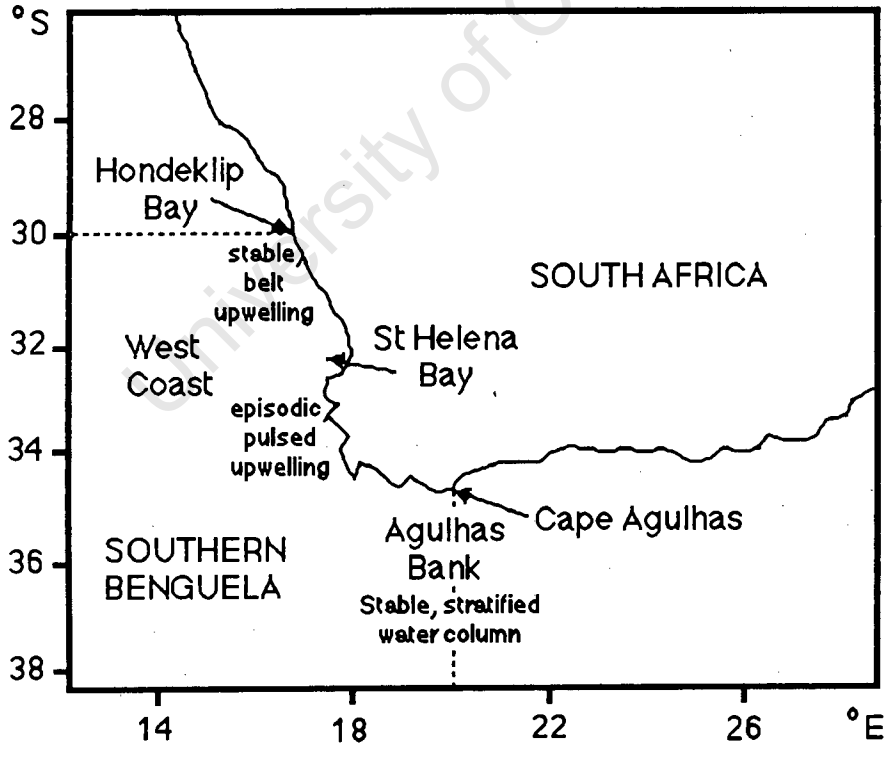

Fig. 4.1. Location of the two model ecosystems off South Africa

The spawning and recruitment areas have markedly different physical and biotic environments, which display variations on a number of time scales. During summer, the period during which spawning of pelagic fish takes place, the water column of the Agulhas Bank is characterized by strong thermal stratification with a well developed chlorophyll maximum at the thermocline (Carter *et al.* 1986). Primary production is limited by nitrogen availability and by light when self shading occurs in the chlorophyll maximum (Shannon and Pillar 1986, Carter *et al.* 1987). Nitrate is believed to enter the euphotic zone by diffusion from nitrate-rich water below the thermocline (Carter *et al.* 1986, 1987). The structure of the water column and its associated phytoplankton community appears to be stable compared with that of the active upwelling areas off the west coast (Carter *et al.* 1987), and it is believed that this structure is important to anchovy spawning success (Carter *et al.* 1987).

In contrast, the upwelling region of the southern Benguela is characterized by episodic upwelling events during spring and summer (Brown and Hutchings 1987a), and has a cold, variable and unpredictable environment. Nitrate is the limiting nutrient in this system (Andrews and Hutchings 1980). Nitrate-rich water is brought to the surface during upwelling, allowing the rapid development of phytoplankton blooms, usually of short duration (Olivieri 1985, Brown and Hutchings 1987b). The upwelling region generally supports larger standing stocks of phytoplankton than are found on the Agulhas Bank (De Decker 1973), and has a larger primary production than the Agulhas Bank (Shannon and Field 1985).

The pelagic ecosystems in these two regions of the southern Benguela are subjects of research aimed at understanding trophic processes affecting pelagic fish. Seasonal and monthly variations in phytoplankton and zooplankton standing stocks have been demonstrated in both regions (see Shannon and Pillar 1986 for a review). However, shorter time scales than these are probably required to understand trophic processes, of the order of days and weeks. "Snapshot" measurements are difficult to extrapolate, and existing time series of data (e.g. Carter *et al.* 1987, Brown and Hutchings 1987b, Lucas *et al.* 1987, Painting *et al.* 1988, Verheye-Dua and Lucas 1988) allow for the construction of working hypotheses as to how the ecosystems function, but cannot be used to test these hypotheses. In this chapter I test the hypothesis that differences in the

mechanics of nutrient supply to the phytoplankton populations on the Agulhas Bank and the upwelling area are responsible for the different communities that occur in the two regions. I use a generalized model of a microplankton community, developed in Chapter 3, to simulate food webs and processes for the two regions. Output from the simulations is compared with field data, to assess whether model communities are realistic. A detailed analysis of the functioning of the model ecosystems is discussed in Chapter 5.

SIMULATIONS

Nutrient dynamics of microplankton communities are simulated for hypothetical food webs at the chlorophyll maximum on the Agulhas Bank (AB) and for an upwelling area on the west coast (WC). Identical size-based simulation models are used for both regions. Details of the model structure are described elsewhere (Chapter 3), as are the derivations of model parameters (Chapters 1 and 2). The simulations are executed over a time horizon of up to 50 days, with time increments of 0.05 days.

The model microplankton communities consist of four phytoplankton and five zooplankton size classes (Fig. 4.2). To facilitate discussion the zooplankton size classes are categorized according to familiar groups of animals that fall in those size classes, but it should be remembered that these categories are not exclusive, and the representative taxa are not necessarily the dominant ones in that size category. Transfers of carbon and nitrogen are simulated within the communities. Carbon is assumed to enter the system through carbon fixation by phytoplankton, and to leave the system as a result of sinking of faecal material and dissipation through respiration (Fig. 4.2a). Carbon flows into and out of compartments occur through uptake of PDOC (photosynthetically-produced dissolved organic carbon) and ingestion of carbon as biomass. Nitrogen inputs into the system occur through upwelling or diffusion of new nitrogen into the new nitrogen pool, and nitrogen is lost from the system through sinking of faecal material. Nitrogen flows within the communities occur by uptake, ingestion and excretion (Fig. 4.2b), with soluble excreted nitrogen being recycled into the regenerated nitrogen pool.

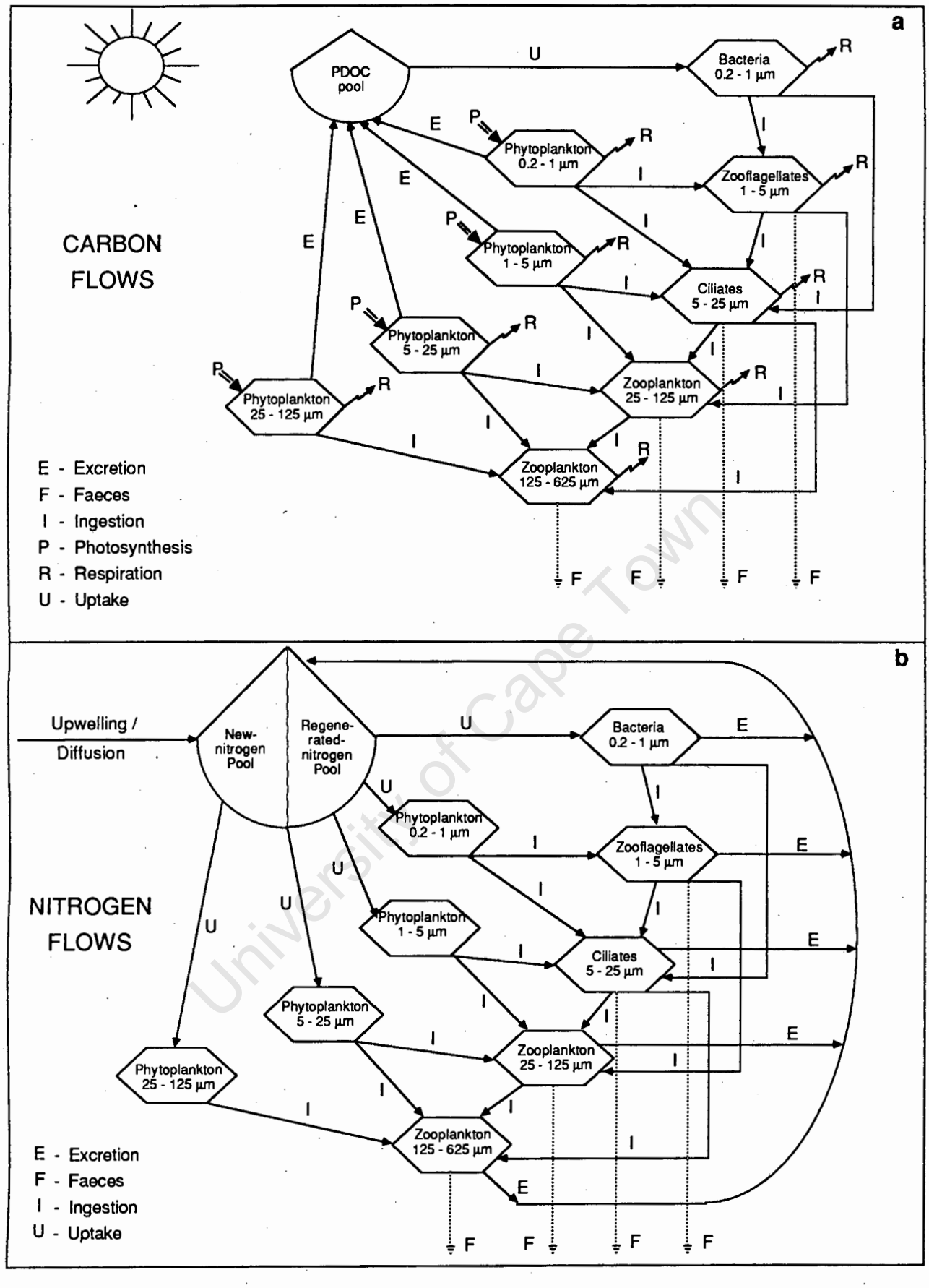

Fig. 4.2. Diagrammatic representations of a) carbon and b) nitrogen flows of the simulation models of microplankton communities of the Agulhas Bank and a west coast upwelling region.

The models are kept as simple as possible by assuming optimal light conditions in the euphotic zone, with only nitrogen limiting phytoplankton growth. Simulations of AB and WC environmental conditions differ only in terms of two factors: 1) method and amount of new nitrogen input to the systems and 2) ambient temperatures, which affect the values of rate parameters (see below). All parameters are presented in Table 4.1.

Agulhas Bank (AB) model.

Carter *et al.* (1986) estimated that a daily nitrate flux of 6.2 $mM.m^{-2}.d^{-1}$ was necessary to sustain primary production in the euphotic zone on the Agulhas Bank. The chlorophyll maximum for which this flux was estimated is approximately 2 m thick. Most primary production occurs in the chlorophyll maximum (Carter *et al.* 1986, 1987), and the nitrate flux is thus equivalent to 3.1 $mg\text{-}at.m^{-3}.d^{-1}$ or 42.3 $mg\ N.m^{-3}.d^{-1}$. In the AB model, new nitrogen is introduced continuously at a rate of 20 $mg\ N.m^{-3}.d^{-1}$ (1.5 $mg\text{-}at\ N.m^{-3}.d^{-1}$), simulating diffusion into the chlorophyll maximum layer. This rate is less than that estimated by Carter *et al.* (1986), but larger values resulted in unrealistically large phytoplankton standing stocks. Temperatures of the surface waters on the Agulhas Bank are relatively warm (19-22°C, Swart and Largier 1987), and an ambient temperature of 20°C is assumed for the model system. Initial phytoplankton and zooplankton biomass spectra are set with large organisms dominating (Table 4.1). Simulation output for only 10 days is presented for the AB model, because the system stabilizes to a steady state from day 10 onwards.

West coast (WC) model

In the WC model, upwelling of nutrient-rich water into the euphotic zone is simulated by introducing a large initial concentration (350 $mg\ N.m^{-3}$ or 25 $mg\text{-}at\ N.m^{-3}$) of new-nitrogen at the start of the simulation, after which new-nitrogen input is zero. This value corresponds to the largest measured concentrations of nitrogen in newly upwelled water off the Cape Peninsula (Armstrong *et al.* 1987, Brown and Hutchings 1987a). Conditions in cold upwelled water are simulated by assuming an ambient temperature of 10°C (Brown and Hutchings 1987a). A Q_{10} of 2.0 is assumed, and rate parameters for uptake, ingestion and respiration are half those of the

Agulhas Bank simulation (Table 4.1). As upwelled water ages, its temperature increases, which affects the values of rate parameters, but this effect is ignored in the simulation to reduce model complexity. However, ignoring temperature changes may underestimate production rates. The phytoplankton and zooplankton biomass spectra are initialized with large organisms dominant (as for the AB model), simulating the seeding of newly upwelled water (Table 4.1). Zooplankton larger than 25 μm are set to very small starting values, because it is believed that organisms in these size classes probably are not abundant in newly upwelled water, and grazing losses from phytoplankton blooms are estimated to be as little as 2% of total production (Olivieri 1985).

Table 4.1. Values of parameters used to simulate carbon and nitrogen flows through microplankton communities in the Agulhas Bank model and the west coast upwelling model. 1 x 10^{-5} mg C.m^{-3} is the smallest standing stock by default in the model community (Appendix I)

	Agulhas Bank size classes (μm)					West coast size classes (μm)				
Parameter	0.2-1	1-5	5-25	25-125	125-625	0.2-1	1-5	5-25	25-125	125-625
AUTOTROPHS										
Maximum growth rate (d^{-1})	21	6.4	1.9	0.57	-	11	3.2	1.0	0.29	-
Respiration rate (d^{-1})	7.1	2.1	0.64	0.19	-	3.6	1.1	0.32	0.09	-
Half saturation constant for N uptake (mg N.m^{-3})	0.00026	0.032	3.8	64	-	0.00026	0.032	3.8	64	-
PDOC production rate (d^{-1})	0.3	0.3	0.3	0.3	-	0.3	0.3	0.3	0.3	-
Initial standing stocks (mg C.m^{-3})	1x10^{-5}	1x10^{-5}	2	36	-	1x10^{-5}	1x10^{-5}	2	36	-
HETEROTROPHS										
Maximum uptake rate (d^{-1})	21	-	-	-	-	11	-	-	-	-
Maximum ingestion rate (d^{-1})	-	98	29	8.7	2.6	-	49	15	4.4	1.3
Respiration rate (d^{-1})	7.1	19	5.6	1.7	5.0	3.6	9.4	2.8	0.84	0.2
Half saturation constant for N uptake (mg N.m^{-3})	0.00026	-	-	-	-	0.00026	-	-	-	-
Half saturation constant for predation (mg C.m^{-3})	34	50	74	110	160	34	50	74	110	160
Faecal production rate (d^{-1})	-	0.1	0.1	0.1	0.1	-	0.1	0.1	0.1	0.1
Initial standing stocks (mg C.m^{-3})	1x10^{-5}	1x10^{-5}	2	3.6	1.2	1x10^{-5}	1x10^{-5}	2	1x10^{-5}	1x10^{-5}

RESULTS AND DISCUSSION

Agulhas Bank

Autotrophs.

The model system initially has a distinct cyclical nature due primarily to predator-prey interactions, but then stabilizes after 10 days. The steady state is artificial, because conditions in the water column change continually. Thus the changes displayed up to the steady-state will be discussed in detail to assess the dynamics of the system, and the stable system is regarded as the underlying structure upon which fluctuations are imposed. Pico-phytoplankton (0.2-1 μm), increase rapidly at the start of the AB simulation (Fig. 4.3a), and cycle approximately 8 times during the 10-day simulation. The maximum standing stock of this size class is 30 mg $C.m^{-3}$. From day 9 onwards, this size class stabilizes at approximately 20 mg $C.m^{-3}$, when it dominates the phytoplankton assemblage. The second smallest phytoplankton size class (1-5 μm) does not increase during the 10-day simulation. The main phytoplankton bloom which occurs from days 6 to 9 is comprised of the phytoplankton size class 5 to 25 μm, and is grazed down by zooplankton. Although the biggest phytoplankton size class (25-125 μm) is initialized with a relatively large standing stock, its standing stock decreases slowly throughout the duration of the simulation (Fig. 4.3a).

Heterotrophs

Bacterioplankton standing stocks (size class 0.2 to 1 μm) display the same trends as the smallest phytoplankton size class, changing 8 times during the 10-day simulation, but have smaller standing stocks, attaining maximum values of about 1.6 mg $C.m^{-3}$ (Fig. 4.3b). In the steady-state system the bacterioplankton have standing stocks of 1.1 mg $C.m^{-3}$. Bactivorous "zooflagellates" (1-5 μm) increase at day 1 to a maximum standing stock of 13 mg $C.m^{-3}$, and then decrease by day 3, and remain at very small standing stocks for the remainder of the simulation. "Ciliates" (5-25 μm) feed on the two smallest phytoplankton size classes as well as bacterioplankton and zooflagellates. The ciliates increase after day 3, and undergo regular fluctuations until day 7, after

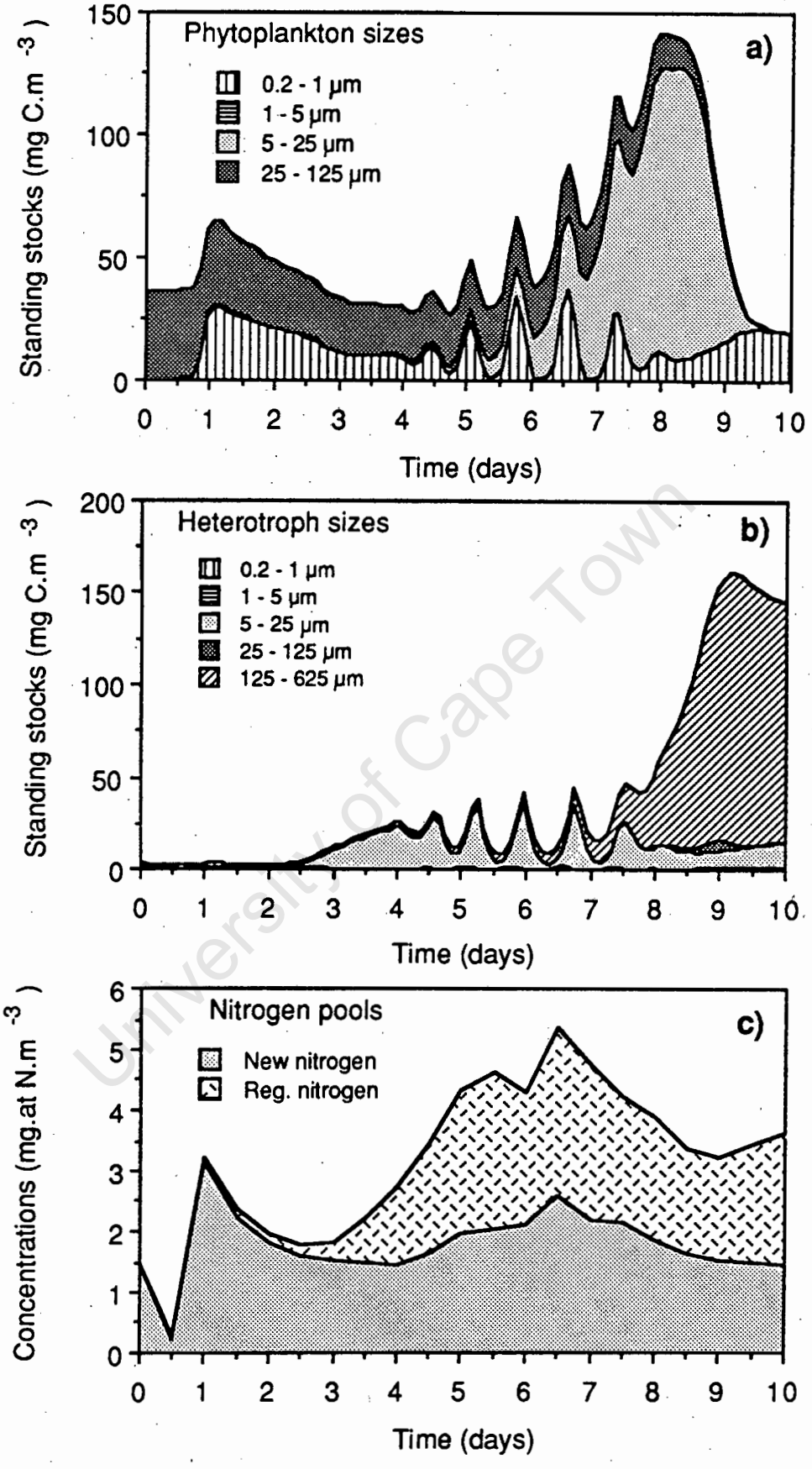

Fig. 4.3. Simulation results depicting changes in standing stocks of a) phytoplankton, b) micro-heterotrophs and c) nitrogen pool concentrations in an Agulhas Bank microplankton community. Note that the standing stocks of each size category are added on to those of the smaller categories

which time they remain stable at 20 mg C.m^{-3}. There is a small peak in the standing stock of the zooplankton size class 25-125 µm between days 8 and 9, and the biggest zooplankton size class (125-625 µm) increases from day 7 to a maximum persistent standing stock of 150 mg C.m^{-3} .

Dissolved nutrients

Changes in the concentrations of dissolved nitrogen in the new and regenerated nitrogen pools in the AB model are shown in Fig. 4.3c. New nitrogen concentrations increase and then stabilize at the input level of 1.43 mg-at N.m^{-3}. Because the concentrations do not increase, it can be concluded that all of the new nitrogen is taken up at each time step in the simulation, and that the ambient concentrations merely reflect the instantaneous input at the start of each time step. In practical terms this means that measurable new nitrogen concentrations would be zero. Regenerated nitrogen concentrations increase from zero to approximately 3.26 mg-at N.m^{-3}, and remain at this concentration in the steady state system. The nitrogen concentrations fluctuate as zooplankton standing stocks fluctuate.

Although concentrations in the dissolved nitrogen pools are relatively stable during the simulation (Fig. 4.3c), the PDOC pool concentrations (not shown in Fig. 4.3) increase steadily from zero concentrations throughout the simulation. Phytoplankton produce PDOC continuously, but model bacterioplankton do not utilize all the PDOC that is produced, allowing it to accumulate in the PDOC pool. This implies that carbon is not limiting to bacterioplankton, except perhaps in the initial stages of the simulation when PDOC concentrations are zero. This result is probably not correct, because in nature the PDOC concentrations will not continue increasing. Our knowledge of the factors affecting the production of PDOC under natural conditions is very poor and not quantitative, and this is reflected in the unrealistic result in the simulation output, in which constant percent extracellular release (PER) is assumed.

A number of different time scales operate in the model system before steady state. Picoplankton (< 1 µm) operate on time scales of hours (Table 4.1), and this is reflected in the periodicity of their fluctuations, which occur approximately every 0.8 days. The most important phytoplankton size class in terms of magnitude of standing stocks, the size class 5-25 µm,

"blooms" for 3-4 days. In steady state the pico-phytoplankton apparently are able to outcompete all other sizes. However, steady states are not reflected in field measurements (see below), and probably never occur in nature.

Comparison with field data.

Autotrophs

The dynamic nature of the Agulhas Bank has not been sufficiently emphasised in field studies, which have concentrated mainly on a snapshot approach to sampling programs. However, there are similarities between the data of Probyn and Lucas (1987) and different time segments of the simulation model output (Fig. 4.4). Largest standing stocks occur at station 133, and are estimated to be approximately 150 mg $C.m^{-3}$, based on the cell counts of Probyn and Lucas (1987), concentrated mainly in the size class 5-25 µm. This size class dominates at both stations where total standing stocks are relatively large (Fig. 4.4a). The maximum estimated standing stock is similar to the maximum simulated by the AB model (Fig. 4.4b), where the model size class 5-25 µm also dominates. The biggest phytoplankton size class (25-125 µm) is present in relatively large quantities in the simulation output only because it is initialized with a large standing stock. After 9 days standing stocks of this size class decrease to zero in the simulation (Fig. 4.4b). This is supported by field data, which indicate that large phytoplankton cells are not an important contributor to total phytoplankton biomass on the Agulhas Bank. This should be expected, because if nitrogen concentrations are as low as indicated by Carter *et al.* (1986) and the simulation output above, large cells will be at a disadvantage due to relatively slow uptake rates. The observed standing stocks of cells smaller than 5 µm range from practically zero to about 14 mg $C.m^{-3}$ (based on cell counts, Fig. 4.4a), which is of the same order of magnitude as the standing stocks of equivalent sizes in the simulation results (Fig. 4.4b). Phytoplankton cells smaller than 15 µm are difficult to identify and enumerate (Davis and Sieburth 1982), and there are no field data of pico-phytoplankton on the Agulhas Bank.

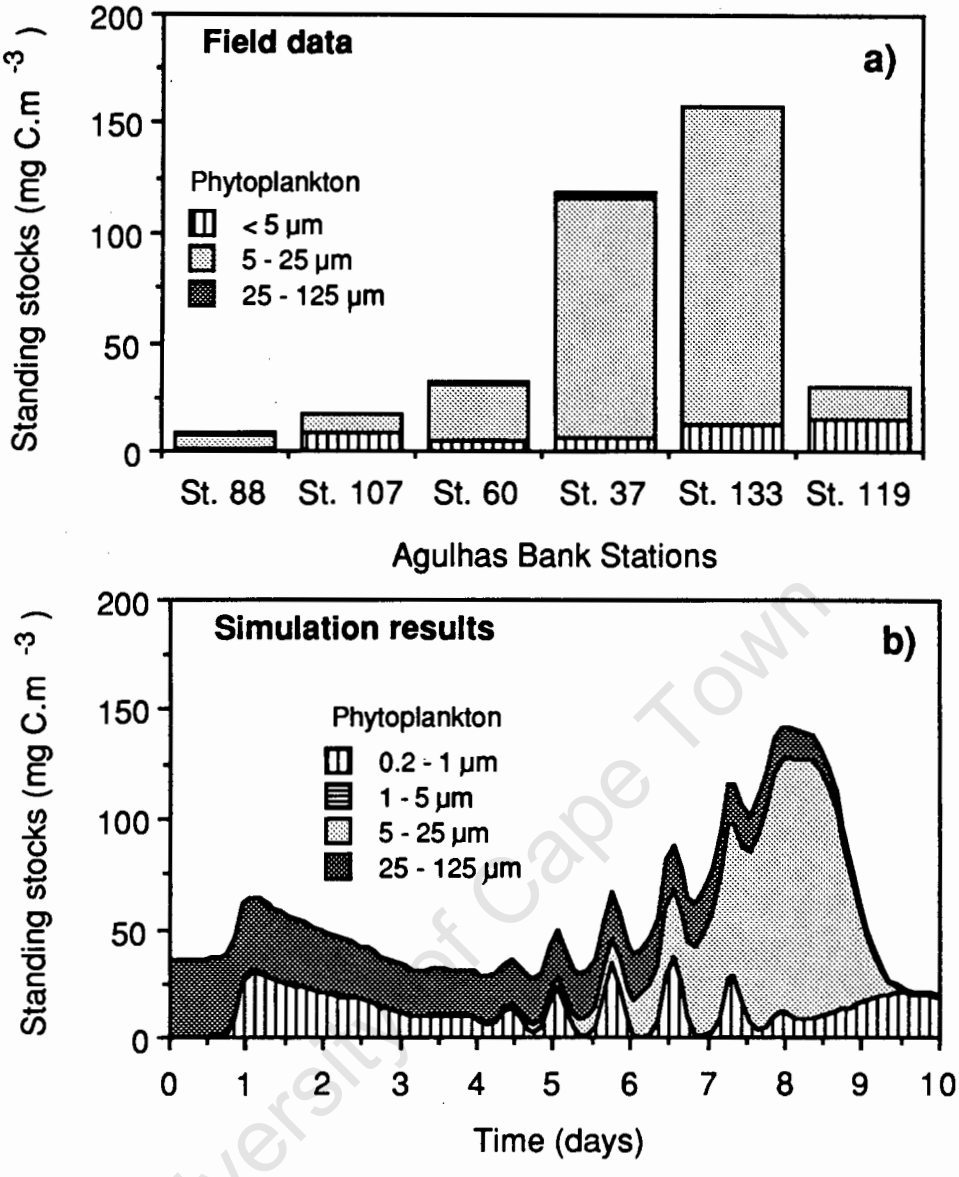

Fig. 4.4. Comparison of standing stocks of phytoplankton size classes from a) stations sampled at the chlorophyll maximum (not a time series) on the Agulhas Bank (based on cell counts from Probyn and Lucas 1987) and b) results of the Agulhas Bank simulation

The fluctuations in standing stocks simulated by the AB model are supported to some extent by a short time series of field observations from the Agulhas Bank presented by Carter *et al.* (1987). These data indicate that maximum measured chlorophyll concentrations at a sub-surface chlorophyll maximum fluctuated between 5 $mg.m^{-3}$ (about 335 mg $C.m^{-3}$) and greater than 10 $mg.m^{-3}$ (about 670 mg $C.m^{-3}$) over a period of 3 days. Two "peaks" occurred during this time. The first lasted for at least 1.5 days and the second for 0.5 days, and they were separated by an interval of approximately 0.5 days. This time scale is very similar to that shown in simulation

output (Fig. 4.4b), where pico-phytoplankton primarily are responsible for the rapid fluctuations in standing stock.

Heterotrophs

No time series are available of field measurements of heterotroph standing stocks on the Agulhas Bank. However, the range of standing stocks that have been estimated are similar to the ranges of values simulated by the model. At the chlorophyll maximum at a number of stations sampled on the Agulhas Bank, Probyn and Lucas (1987) present cell counts for heterotrophs < 5 μm ranging from 1017 to 48302 cells.ml^{-1}. Assuming most of these are 3 μm in diameter (Probyn and Lucas 1987), I converted these counts to approximate standing stocks of 1 to 50 mg C.m^{-3}. The simulated standing stocks of sizes < 5 μm in the simulation reach maximum values of 1.5 mg C.m^{-3}. I estimated that standing stocks of organisms 5-15 μm were approximately 2 to 90 mg C.m^{-3}, and standing stocks of ciliates (assumed to be 30 μm in diameter) were approximately 0.2 to 4.5 μg C.m^{-3}, based on the cell counts of Probyn and Lucas (1987). Thus estimated maximum standing stocks of heterotrophs < 30 μm were approximately 145 mg C.m^{-3}. The simulated maximum for these sizes is about 40 mg C.m^{-3}. However, all of the different sizes do not peak at the same time so instantaneous standing stocks should be smaller. The flagellate standing stocks are much larger in the field data than in the model, indicating that the bacteria and flagellates are underestimated by the Agulhas Bank model. This is probably due to predator control by the ciliate size class (5-25 μm), which is persistently present in the simulation and does not allow the heterotrophs < 5 μm to increase.

Counts of copepod nauplii from the Agulhas Bank are also presented by Probyn and Lucas (1987). When present in samples, they range from 0.1 to 1.6 nauplii.ml^{-1}, and rough conversions result in a biomass estimate of approximately 1 to 16 mg C.m^{-3}, assuming 150 μm length and the length-weight conversions of James (1987). The model size class 125-625 μm has a maximum standing stock of 170 mg C.m^{-3}. Pillar (1986) estimates average copepod standing stocks on the Agulhas Bank to be 610 mg dry wt.m^{-2} or 244 mg C.m^{-2}. If the simulation estimates are extrapolated to cover the depth of the chlorophyll maximum (about 2 m), the simulation results give potential integrated standing stocks of 340 mg C.m^{-2}. The model does not allow for increased

metabolic rates during activities such as feeding (see Chapter 3), and will underestimate respiratory losses and thus overestimate standing stocks in motile organisms.

West Coast

Autotrophs.

As expected from field observations, a phytoplankton bloom develops in the model system as a result of the input of a pulse of new nitrogen (Fig. 4.5). However, the structure of the bloom is more complex than has previously been observed. The model phytoplankton bloom displays a number of peaks (Fig. 4.5a). The first peak occurs at day 2, and is dominated by pico-phytoplankton (0.2-1 μm). This peak reaches a maximum standing stock of approximately 400 mg $C.m^{-3}$, before decreasing rapidly. It is followed by a bloom of nano-phytoplankton (0.2-5 μm) at day 4.5, and another bloom of pico-phytoplankton from days 7 to 9, after which the pico-phytoplankton increase only slightly from days 13 to 18. A protracted bloom of phytoplankton of sizes 5-25 μm occurs from approximately day 6 onwards, reaching a maximum standing stock at day 10 of approximately 300 mg $C.m^{-3}$ (Fig. 4.5a). The largest phytoplankton size class (25-125 μm) is essentially predator-free in the model system (their predator size class remains at very small standing stocks due to long generation times), and therefore does not exhibit the same rapid decreases in standing stock as do the three smaller phytoplankton size classes over a 20-day period.

Heterotrophs

Standing stocks of different size classes of heterotrophs show cyclical patterns in response to phytoplankton blooms (Fig. 4.5b). These cycles often have very short periods (often less than 1 day for a complete cycle), making it unlikely that they would be adequately recorded if they occur in the field, given that most sampling periods are longer than one day and that field studies are integrated over time and space. However, the durations of bacterioplankton (0.2-1 μm) and nano-zooplankton (1-25 μm) blooms were shown to increase if parameters affecting ingestion rates were altered (Chapter 3), so the time scales shown in simulation output may alter if some other factor, not included in the model, affected ingestion rates.

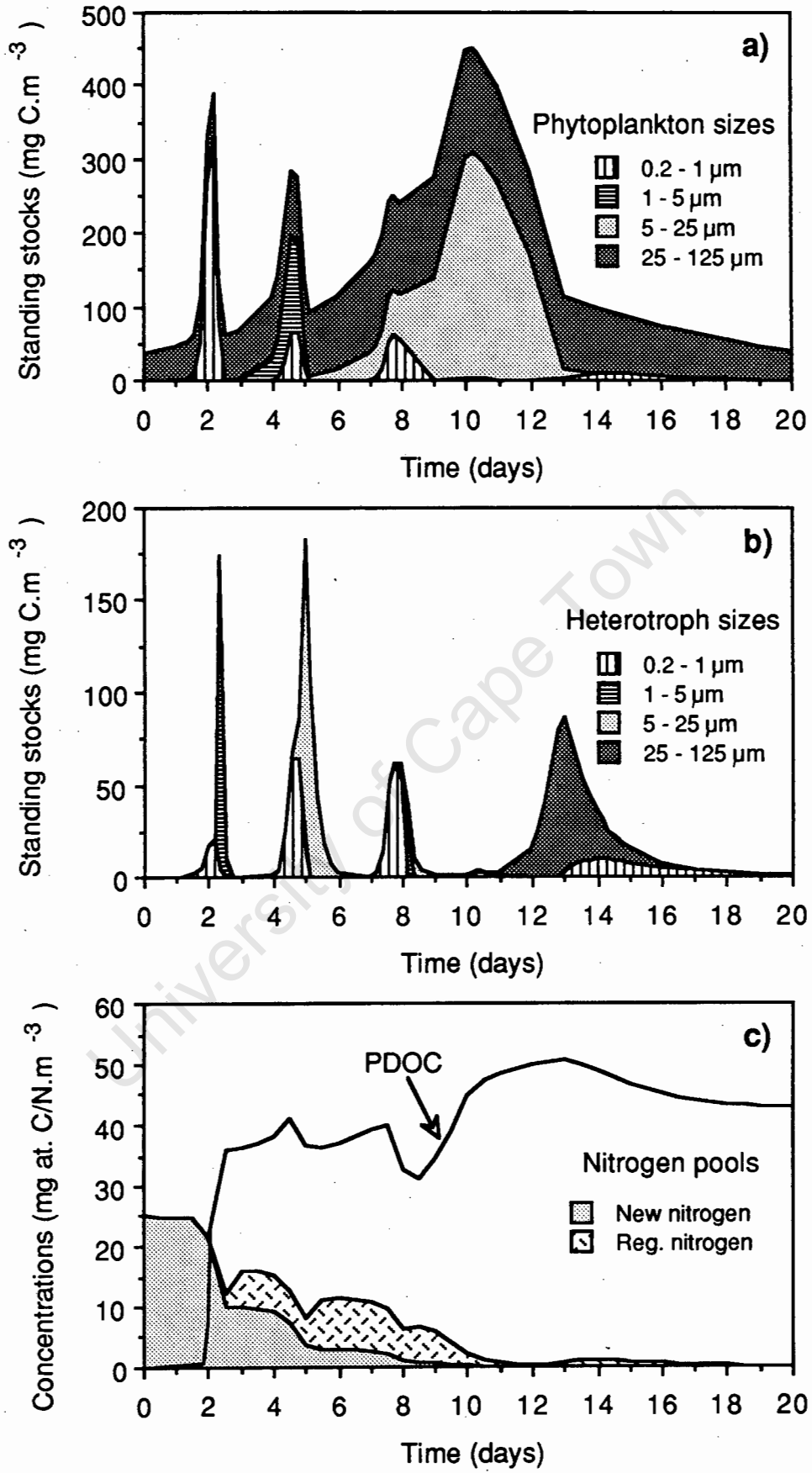

Fig. 4.5. Simulation results depicting changes in standing stocks of a) phytoplankton, b) micro-heterotrophs and c) nitrogen pools concentrations in a west coast microplankton community after upwelling

In general, in the model system there is a succession from small to large zooplankton with time, reflecting predator-prey relationships in the model, where small prey are eaten by large organisms (Fig. 4.2). Bacterioplankton (0.2-1 μm) increase first (Fig. 4.5b), reaching a peak of approximately 20 mg $C.m^{-3}$ by day 2, and then decrease. They increase again at day 4.5 and day 8, and display a small peak at day 10 and a protracted but small bloom from day 13 to 20. These trends are similar to those displayed by the pico-phytoplankton, but the initial bacterioplankton peak is much smaller than that of the pico-phytoplankton, presumably because bacterioplankton are carbon limited at the start of the bloom, because PDOC concentrations in the model are started at zero. The zooflagellates (1-5 μm), which ingest bacterioplankton and pico-phytoplankton, increase when the pico-phytoplankton increase. During the nano-phytoplankton (1-5 μm) bloom when bacterioplankton also increase (days 4-5), zooflagellate growth is retarded by predation pressure from ciliates (5-25 μm), which dominate at that time, feeding on bacterioplankton and phytoplankton < 5 μm. The microzooplankton (25-125 μm) increase from day 11 to 13, then decrease because all of their phytoplankton and zooplankton prey are grazed down (Figs 4.5a and b). The largest heterotrophs in the model community (125-625 μm) are initialized with a small standing stock, and this size class does not increase to significant levels in the simulation (not shown in Fig. 4.5b).

Dissolved nutrients

New nitrogen is introduced only once at the beginning of the upwelling simulation, and concentrations consequently decrease to zero with time. The new nitrogen pool initially decreases slowly (Fig. 4.5c), but after day 2 this process accelerates as a result of uptake by phytoplankton and bacterioplankton. The depletion of the new-nitrogen pool is stepped, because predators reduce picoplankton standing stocks during the initial stages of the bloom, and nitrogen uptake at these times is negligible. New-nitrogen concentrations are zero by day 10. However, the nitrogen pool is supplemented by regenerated nitrogen (Fig. 4.5c), excreted by all heterotroph size classes. The regenerated nitrogen pool becomes important after day 2, but is subsequently depleted by phytoplankton and bacterioplankton, decreasing to zero by day 20. The PDOC pool increases from initial concentrations of zero to a concentration of 400 mg $C.m^{-3}$ after 2.5 days, and then fluctuates

between about 400 and 600 mg $C.m^{-3}$ for the remainder of the simulation. These fluctuations correspond to increases in phytoplankton standing stocks (which replenish the pool) and in bacterioplankton standing stocks (which deplete the pool). The accumulated carbon in the PDOC pool is potentially utilizable by bacterioplankton, because only the production of labile carbon is simulated by the model. This carbon is not utilized because bacterioplankton are nitrogen-limited at the end of the simulation. Except for the PDOC pool, all other compartments in the model system eventually decline to zero, because some nitrogen (and carbon) continually is lost in faecal material, which rapidly sinks out of the system.

Comparison with field data.

Autotrophs

The counts of phytoplankton cells which I carried out on samples obtained from a phytoplankton bloom after an upwelling event were converted to carbon masses, and this time series is presented in Fig. 4.6a, together with simulation results (Fig. 4.6b). The field data have been shifted along the time axis so that the peaks in standing stocks coincide at day 11. Carbon estimates from cell counts (Fig. 4.6a) are presented as shaded areas, and the difference between these estimates and the total carbon estimated from chlorophyll measurements (Painting *et al.* 1988) is presented as the unshaded area. There are obvious discrepancies between the two standing stock estimates. A relatively small discrepancy occurs from about day 10 onwards, but prior to this the difference is large, indicating that a large proportion of phytoplankton crop may have been overlooked in the cell counts. The method used to count cells is not accurate for cells less than 15 μm (Davis and Sieburth 1982), and small cells were probably underestimated in the field bloom. This is consistent with simulation results, which show that small cells typically increase rapidly at the beginning of a phytoplankton bloom. Standing stocks in the simulation are of the right order of magnitude when compared to those of the real data (Fig. 4.6), as are the time scales for bloom duration. Large numbers of *Noctiluca* sp., a unicellular phagotroph (B. Mitchell-Innes, pers. comm.), were present in most samples, and these and other zooplankton probably were responsible for the decline of the bloom.

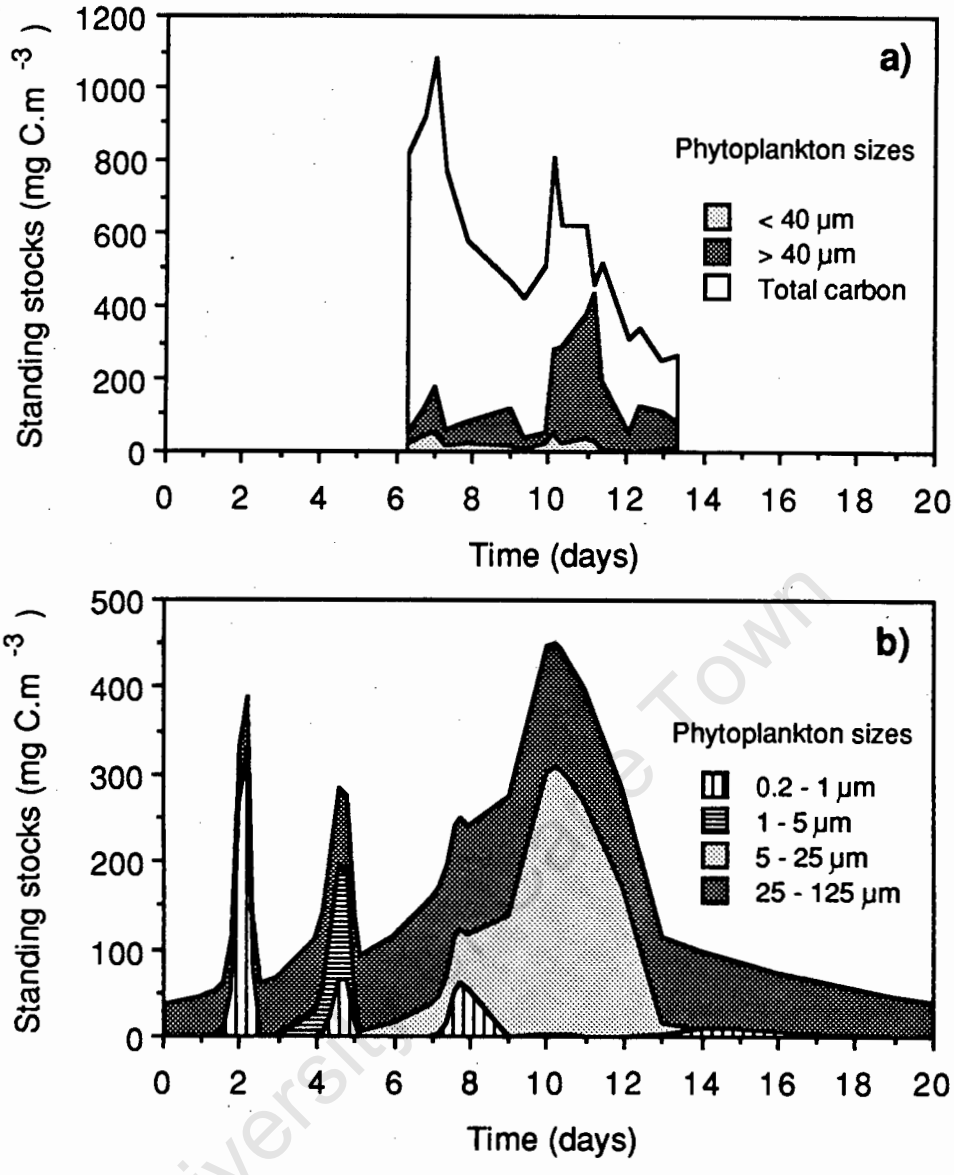

Fig. 4.6. Comparison of standing stocks of phytoplankton size classes from a) a time series of stations sampled in the southern Benguela, with standing stocks based on cell counts and b) results of the west coast simulation (note that the scales are different on the vertical axes)

The development of phytoplankton blooms after upwelling in the southern Benguela has been studied in detail by Brown and Hutchings (1987a, b). Their results for five different blooms indicate that these typically take about 3 days to develop and 3-4 days to decline, making total bloom duration about 7 days. Recent microcosm work by G. Pitcher (Sea Fisheries Research Institute, pers. comm.) has extended this period to 10-12 days, because of a much longer development time. This can be compared with simulation output, which depicts a bloom that lasts about 13 days. The simulation results are more consistent with the microcosm results than the field

measurements, probably because physical conditions in a microcosm more closely resemble those that are assumed for the simulation model.

It is probably not valid to compare quantitative aspects of the simulations in too much detail with field data, because time scales and standing stocks can change if, for example, different size categories are used. Also, the model does not include the effect of factors such as light and, at times, these factors may be more important than the effect of nitrogen in determining phytoplankton growth. This should be remembered when extrapolating from the model output to the field, where other factors may reduce the effects of certain phenomena produced in simulation results. Thus the two initial, rapid blooms of phytoplankton cells < 1 μm in the simulation may be an artefact of a model system in which the effects of light-limitation and photo-inhibition have been ignored. Alternatively, because the initial blooms are composed of very small cell sizes, they may have been overlooked in "snapshot" sampling, especially if their magnitude is somewhat less than that predicted by the model.

If these initial blooms are ignored, the "main" bloom in the simulation occurs from day 6 to 13 (i.e. a duration of 7 days), which conforms well with field obsevations (Brown and Hutchings 1987a,b), and the size composition of this bloom is similar to that observed in field studies (Olivieri 1985). There is some evidence to suggest that initial rapid blooms may have been overlooked in field studies. One of the field-observed blooms (series D, Brown and Hutchings 1987b), had an initial decrease in nitrogen concentrations without a concomitant increase in chlorophyll concentrations. The authors were unable to explain this phenomenon, but results of the simulation offer a plausible explanation. A rapid pico-phytoplankton bloom may have occurred, but would not have been detected because the authors used relatively large-pore sized (0.7 μm) glass fibre filters, which are believed to underestimate the chlorophyll in the < 1 μm size fraction (Takahashi and Bienfang 1983).

Heterotrophs

A number of measurements have been made of bacterioplankton and zooplankton standing stocks in the west coast upwelling region. Model bacterioplankton standing stocks range from

very small values to approximately 60 mg C.m^{-3} (Fig. 4.5). The minimum values appear to be unrealistic, probably because the ingestion function does not include a threshold concentration below which feeding stops (Chapter 3), allowing very small densities of bacterioplankton to be grazed, albeit at a very slow rate. The maximum value is comparable with estimates ranging from 10 to 80 mg C.m^{-3} (Lucas *et al.* 1986), 30 mg C.m^{-3} (Armstrong *et al.* 1987), 3.5 to 47 mg C.m^{-3} (Probyn 1987) and < 20 to 50 mg C.m^{-3} (Verheye-Dua and Lucas 1988), all of which were measured on the west coast. In addition, microcosm studies depicting the changes in bacterial standing stocks with time are presented by Lucas *et al.* (1987) and Painting *et al.* (1988), and these data are plotted with simulation data in Fig. 4.7. Although the short cycles depicted in the model output are not obvious in the microcosm data, the frequency of sampling may have precluded their detection. Some fluctuations may occur at days 3, 5 and 7, but it is difficult to decide whether these are significant or not.

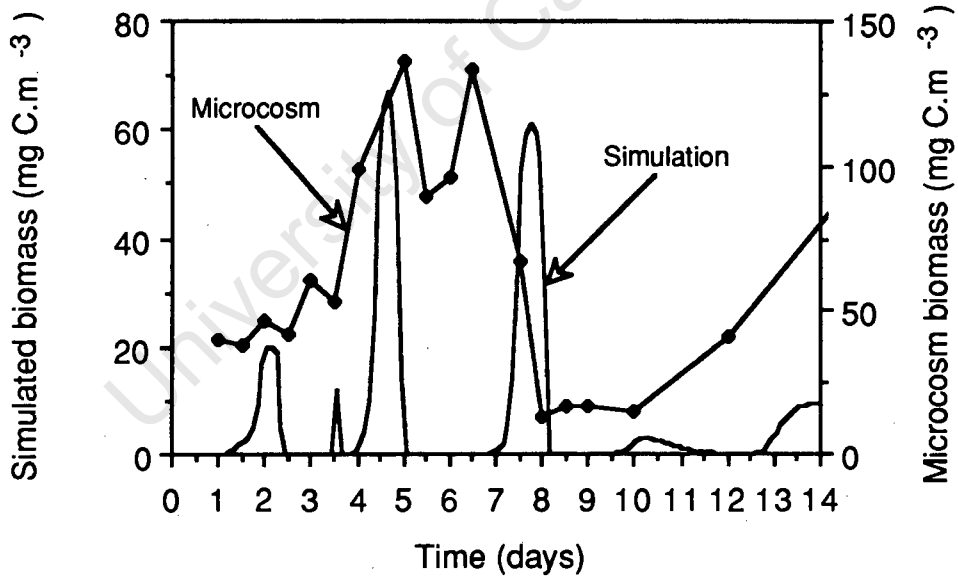

Fig. 4.7. Comparison of bacterioplankton standing stocks predicted by the west coast simulation with those from microcosm studies (after Lucas *et al.* 1987)

Zooflagellate (< 5 μm esd) standing stocks of up to 100 mg C.m^{-3} were observed by Lucas *et al.* (1987) and Painting *et al.* (1988) in the microcosm, which compares well with the maximum standing stock of the model size class 1-5 μm, approximately 150 mg C.m^{-3} at day 2 (Fig. 4.5). Standing stocks of large zooplankton are usually presented per unit sea surface area,

because they are sampled by mean of net hauls. Hutchings *et al.* (1984) present zooplankton data collected at monthly intervals over a number of years, and these standing stocks range from 1 to 5 g dry wt.m^{-2} or 400 to 2000 mg C.m^{-2}. Pillar (1986) estimated mean standing stocks of copepods and euphausiids in different areas of the southern Benguela, and his estimates for the Cape Peninsula area are 590 mg C.m^{-2} (1485 mg dry wt.m^{-2}) and for the Cape Columbine/St Helena Bay area 980 mg C.m^{-2} (2455 mg dry wt.m^{-2}). Zooplankton size categories were sampled by Verheye and Hutchings (1988), and they estimate standing stocks of 170 mg C.m^{-2} (200-500 μm), and 1400 mg C.m^{-2} for all zooplankton > 200 μm. Model zooplankton > 125 μm do not reach large standing stocks in the simulation, because they are initialized with small values. If their initial standing stocks are increased, they exert an unrealistic controlling effect on the growth of model phytoplankton of sizes 25-125 μm and microzooplankton (25-125 μm), possibly because of the absence of a threshold feeding concentration in the ingestion function (see Chapter 3), and the time scale of the simulation is too short to adequately simulate their growth.

System behaviour

Agulhas Bank model.

The results of altering initial biomass spectra are summarized in Table 4.2 for the AB model. Results are similar to those depicted in Fig. 4.3, although there are differences in values of standing stocks. The largest phytoplankton size class (25-125 μm) always decreases in the simulations, even when initialized with large standing stocks (Table 4.2). On the other hand, pico-phytoplankton (0.2-1 μm) are always present, increasing and decreasing a variable number of times in the 10-day simulations. The nano-phytoplankton (1-5 μm) occur sporadically in blooms, but only dominate when they are initialized with a large standing stock (Table 4.2). In most simulations, the main bloom comprises the phytoplankton of sizes 5-25 μm. The fluctuations in phytoplankton crop that occur in the first 10 days of the AB simulation occur in all of the simulations. The pico-phytoplankton (1-5 μm) and the nano-phytoplankton (5-25 μm) increase at different times, and comprise the most important constituents of total phytoplankton standing stock. The pico-phytoplankton are controlled by predators, and fluctuate regularly when the model

Table 4.2. The effect of altering initial standing stocks (mg $C.m^{-3}$) of phytoplankton size classes in Agulhas Bank simulations. Results are for 10-day simulations, and the biomasses are the maximums attained by each size class in each simulation

Initial phytoplankton standing stocks (µm esd)				0.2 - 1 µm		1 - 5 µm		5 - 25 µm		size composition of the main bloom
0.2 - 1	1 - 5	5 - 25	25 - 125	no. of blooms	Biomass (mg $C.m^{-3}$)	no. of blooms	Biomass (mg $C.m^{-3}$)	Biomass (mg $C.m^{-3}$)	duration (days)	
0.00001	0.0003	0.1	37	9	30	1	23	110	6	5 - 25 µm
0.00001	0.0003	37	0.1	7	32	0	-	90	4.5	5 - 25 µm
0.00001	37	0.1	0.0003	5	43	3	275	5	2	1 - 5 µm
37	0.0003	0.1	0.00001	8	50	0	-	95	4.5	5 - 25 µm
0.00001	0.1	37	37	8	37	0	-	60	6.5	5 - 25 µm
1.2	1.2	1.2	1.2	6	31	0	-	75	4	5 - 25 µm
12	12	12	12	4	60	0	-	18	5	0.2 - 1 µm

Table 4.3. The effect of altering initial standing stocks (mg $C.m^{-3}$) of phytoplankton size classes in west coast upwelling simulations. Results are for 25-day simulations. "Pre-" and "post-" blooms refer to rapid blooms, dominated by pico- and nano- phytoplankton, which occur before and after the main net-phytoplankton bloom.

Initial phytoplankton standing stocks (µm esd)				Maximum biomass	No. of pre-	No. of post-	Duration of main	Dominant size classes
0.2 - 1	1 - 5	5 - 25	25 - 125	(mg $C.m^{-3}$)	blooms	blooms	bloom (days)	
0.00001	0.0003	0.1	37	450	3	0	6-13	5 - 25 µm, 25 - 125 µm persists to end
0.00001	0.0003	37	0.1	850	1	3	0-6	5 - 25 µm
0.00001	37	0.1	0.0003	450	3	4	4 -12	5 - 25 µm
37	0.0003	0.1	0.00001	400	3	1	6-14	5 - 25 µm, 25 - 125 µm persists to end
0.00001	0.1	37	37	900	1	3	0-6	5 - 25 µm
1.2	1.2	1.2	1.2	500	3	2	4-11	5 - 25 µm
12	12	12	12	750	2	4	1-7	5 - 25 µm, 25 - 125 µm persists to end

system is not in steady state, whereas the largest size class never dominates in the simulations (Table 4.2).

West coast model.

The effects of altering initial biomass spectra in the WC model are presented in Table 4.3. Simulation results show an underlying trend, despite variations in standing stocks. A "main" bloom consisting of phytoplankton 5-25 μm occurs in all simulations (Table 4.3), and the duration of this bloom is generally 6-8 days. Superimposed on this bloom are a number of rapid pico- and nano- phytoplankton blooms ("pre-" and "post-" blooms, Table 4.3), the number, magnitude and duration of which are determined by initial biomass spectra. These pre- and post- blooms are the result of predator-prey oscillations; predator control prevents very small phytoplankton from dominating and using all of the available nitrogen before larger size classes can increase. The largest phytoplankton size class (25-125 μm) never dominates in simulations (Table 4.3), and only becomes abundant if present in large initial quantities. The magnitudes of maximum standing stocks depend on the initial biomass spectra (Table 4.3). The largest standing stocks occur when large phytoplankton (> 5 μm) are initialized with large standing stocks, and in these simulations the number of pre-blooms is reduced (Table 4.3).

SUMMARY AND CONCLUSIONS

The two models simulate general features of the Agulhas Bank and the west coast communities that are supported by data from field studies, although the model output is not totally realistic, because only the effect of nitrogen on phytoplankton growth has been simulated. Thus, hypothetical features that have not been explicitly described in field studies have been identified, but may reflect artefacts resulting from unrealistic assumptions e.g. ignoring the effects of light. On the Agulhas Bank, it appears that a "steady-state" community dominated by pico-phytoplankton serves as a baseline community, but the system probably is continually disrupted, so that fluctuations of the type depicted by the model are often found. This is similar to the situation described by Joint and Pomroy (1983) as being typical of a stratified water column on the

continental shelf in temperate regions in summer. These authors believe that pico-phytoplankton are probably important in many more areas than have thus far been reported.

The west coast simulation depicts a bloom consisting of a succession of phytoplankton of different sizes after upwelling. Traditionally, this succession has been viewed from a taxonomic viewpoint, and individual species and higher taxa have been used to describe the succession e.g. diatoms to dinoflagellates (Sukhanova *et al.* 1978). The simulation results show that, at least on one level, the succession can be described by size-dependent effects. Species-dependent effects will probably also be important, but these should be considered only after the size-effects have been accounted for when attempting to explain the succession phenomenon. The phytoplankton of the southern Benguela have been regarded as being diatom-dominated (Shannon and Pillar 1986). However, recent studies have shown that nano- and pico- phytoplankton may also be important, and may dominate both standing stocks (Hutchings *et al.* 1984, Probyn 1985, Mitchell-Innes and Winter 1987) and primary production (Norris 1983 quoted in Shannon and Pillar 1986, Probyn 1987). The dynamics of these different size fractions of phytoplankton only recently have been studied (e.g. Probyn and Lucas 1987). The simulation models can provide a framework within which future field programs in the two regions can be planned, illustrating the time scales required and the possible manifestations of interactions through the entire plankton community.

In both model systems, competition for nitrogen sets limits to phytoplankton growth, favouring dominant size classes unless some other factor limits their growth. Large cells are not as efficient as small cells in utilizing dissolved nitrogen at small concentrations, and the simulation results indicate that this is sufficient to restrict large-celled phytoplankton (25-125 μm) in the Agulhas Bank model. However, increased storage capacity and reduced metabolic demand of large cells relative to small cells (Laws 1975) may allow large cells to survive periods of reduced nutrient concentrations, and then capitalize at times when nutrient concentrations are enhanced, for example during sporadic and localized upwelling or mixing events. Such effects were not included in the model, and this is probably why pico-phytoplankton dominate the Agulhas Bank model community, when other sizes should probably also be present.

This chapter demonstrates the applicability of size-determined relationships and parameters for modelling microplankton communities in different physical and biotic environments. A frequently expressed and often valid criticism of simulation models is that the models can be made to produce almost any result; model parameters often are unknown, and choices of different parameters can affect model output. The models presented above are free from this criticism, because an independent criterion (body size) is used to estimate almost all parameters, and these are essentially the same for both models. Thus, even though no data of the two ecosystems were used in developing model parameters, by altering only the frequencies and amounts of new nitrogen input, and the values of rate parameters as determined by temperature, two totally different microplankton communities have been simulated. These communities are very similar to those observed in field studies, implying that many of the interactions that occur are well explained using size-criteria. The structure of the communities depends on the interplay of biotic (competition and predation) and abiotic (nutrient supply) influences, with the time scales of importance depending mainly on body-size. In Chapter 5, output from the models is used to analyse the functioning of the planktonic communities.

CHAPTER 5

MODELLING TWO CONTRASTING SOUTHERN BENGUELA FOOD WEBS. II. ANALYSIS OF THE FLOW NETWORKS AND TROPHIC STRUCTURE

ABSTRACT

Hypothetical carbon and nitrogen flow networks are constructed for food webs in the chlorophyll maximum in the surface waters of the Agulhas Bank and the surface waters of an upwelling area on the west coast of southern Africa, using output from simulation models. The importance of different flow pathways is assessed at different times in the two model systems. Average primary production is estimated to be approximately 0.54 g $C.m^{-2}.d^{-1}$ on the Agulhas Bank and 2 g $C.m^{-2}.d^{-1}$ in the upwelling area. The sizes of autotrophs responsible for primary production vary with time, although the smallest sizes generally are responsible for the greatest proportion of production in the models. Similarly, it is shown that different size classes of heterotrophs are important at different times in nutrient regeneration. On the Agulhas Bank, regenerated production is generally greater than new production. In the west coast model, new production is replaced by regenerated production as the phytoplankton bloom matures and the new nitrogen is used up. Competition between bacteria and phytoplankton for dissolved nitrogen may be important at times in the upwelling system, although control by predators generally prevents bacteria from "outcompeting" phytoplankton. Although a five step "food chain" may occur, neither model system has more than three effective trophic categories. The "inefficient microbial loop" hypothesis is of little consequence in the two systems, because the vast majority of flows pass through shorter, more efficient pathways. The importance of size- fractionated sampling of phytoplankton is emphasized, and the dangers of extrapolating from snapshot measurements is highlighted. It is recommended that field data be collected and analysed within a framework supplied by simulation model output.

INTRODUCTION

Much of marine ecological research is directed towards understanding the factors that affect the productivity of fish (Fenchel 1987). This is a central theme of the Benguela Ecology Programme, where the species of interest is the Cape anchovy *Engraulis capensis*, which forms the basis of an important purse seine fishery in the upwelling region of the southern Benguela. Extensive feeding studies by James (1987) indicate that anchovy selectively feed on meso-zooplankton, especially calanoid copepods and euphausiids. These zooplankton depend on phytoplankton for growth, but it is not known what proportion of primary production ends up as zooplankton carbon and is ultimately eaten by anchovy.

In the southern Benguela area, two regions are important to anchovy populations; the Agulhas Bank where anchovy spawn and the west coast upwelling area where anchovy recruit to the fishery (Crawford *et al.* 1987, Chapter 4). The structures of the food webs in these two areas are reasonably well understood (Shannon and Pillar 1986). Furthermore, a number of studies have been carried out on the important processes occurring in the plankton. Measurements have been made of primary production (Brown 1984, Brown and Field 1985, Brown and Hutchings 1987a; b, Carter *et al.* 1987), bacterioplankton production (Lucas *et al.* 1986; 1987, Painting *et al.* 1988, Verheye-Dua and Lucas 1988), microzooplankton regeneration rates (Probyn 1985; 1987, Probyn and Lucas 1987) and grazing by large zooplankton (Verheye and Hutchings 1988). However, although many of the components of the system have been studied in detail, it is still unclear how the whole system functions, because it is impossible to measure all of the processes occurring at all times. Different temporal and spatial scales in sampling programs make it inappropriate to treat all of the data as a "system sample".

In this chapter I use a systems approach to analyse the trophic structure of the food webs in the two systems. I attempt to assess the relative importance of different flow pathways through the food webs, and try to answer the question of how much of primary production eventually reaches pelagic fish, and the relative importance of different pathways, especially in recycling.

ANALYSES

Estimates of flow rates

Carbon and nitrogen flow networks were obtained from outputs of the Agulhas Bank and the west coast simulations described in Chapter 4. At each time step (0.05 d) in the simulations, the rates of carbon and nitrogen entering and leaving each model compartment were estimated. Primary production rates were estimated as the difference between carbon fixation rates and respiration rates, and production rates of bacterioplankton as the differences in rates between carbon taken up from the PDOC pool and carbon lost through respiration. Nitrogen regeneration rates are the rates at which nitrogen is excreted by heterotrophs as a result of metabolic activity, and were estimated as the nitrogen equivalents to carbon respiratory losses, although this may not be realistic for bacterioplankton (see Chapter 3). All rates are instantaneous, and are given in units of mg C / N.m^{-3}.d^{-1}. Note that it is not valid to assume that these instantaneous rates represent total daily production or excretion, because such a procedure assumes that the instantaneous rate is constant for the whole day. This assumption is incorrect, because the instantaneous rates can undergo substantial changes in less than one day.

Trophic structure

The program NETWRK3 of Ulanowicz (1986) is used to analyse the trophic structures of the flow networks at different times in the two simulations. The food webs are condensed into one-dimensional "food chains" termed Lindeman spines (Ulanowicz and Kemp 1979), by apportioning model compartments to integer trophic categories. These effective trophic categories describe the average trophic function of each model compartment (Levine 1980), and allow for the description of complex food webs in terms of steps in a food chain. They are particularly useful in identifying the most important pathways of material flows in the food webs. Inputs to the program are in the form of carbon and nitrogen flows integrated over quarter-day periods. In addition, all inputs and outputs are summed over the total simulation time horizon (14 days for the west coast model and 9 days for the Agulhas Bank model), and these flows are used to estimate a "time-averaged" trophic structure for each ecosystem.

RESULTS AND DISCUSSION

In the discussion below, the simulated output described in Chapter 4 is discussed in a systems context, i.e. the relative importance of different components and pathways in the total system are assessed. It is recognized that some features of the simulation output are not realistic when compared with field observations, e.g. the pico-phytoplankton blooms described in Chapter 4 for the west coast model. This is not surprising, because a large number of physical and biological effects operate under natural conditions, whereas the simulation models concentrate only on the nitrogen and carbon environments of the two model systems. Even in these simplified systems, further assumptions regarding the functional forms of different processes had to be made (Chapter 3). The simulation models cannot reproduce accurately all that occurs in the field. It is possible to change parameter values and model assumptions to produce output that is consistent with field measurements. However, a number of different factors may produce the same response (see Table 3.6, Chapter 3), and it is difficult to decide which factors to alter. Rather than increasing the complexity of the model, assuming causal effects which may not be correct, the output has been left unchanged for the analyses described below. The "problem areas" will be restated where necessary, as a reminder of why certain results apparently deviate from those observed in nature. The factors in the field that prevent the "anomalies" from occurring need to be identified.

Carbon flows

Primary production

The potential importance of small phytoplankton in primary production is demonstrated by simulation results. However, the model probably overestimates the role of pico-phytoplankton for natural conditions (Chapter 4), because the effects of factors other than nitrogen supply have not been simulated. In the simulated phytoplankton bloom after upwelling there are four production peaks (Fig. 5.1a) corresponding to the four peaks in standing stocks (Fig. 5.1b). Rates of production are fastest when small phytoplankton comprise most of the standing crop, even though standing stocks may be relatively small. During the main bloom from day 6 to 13, when standing

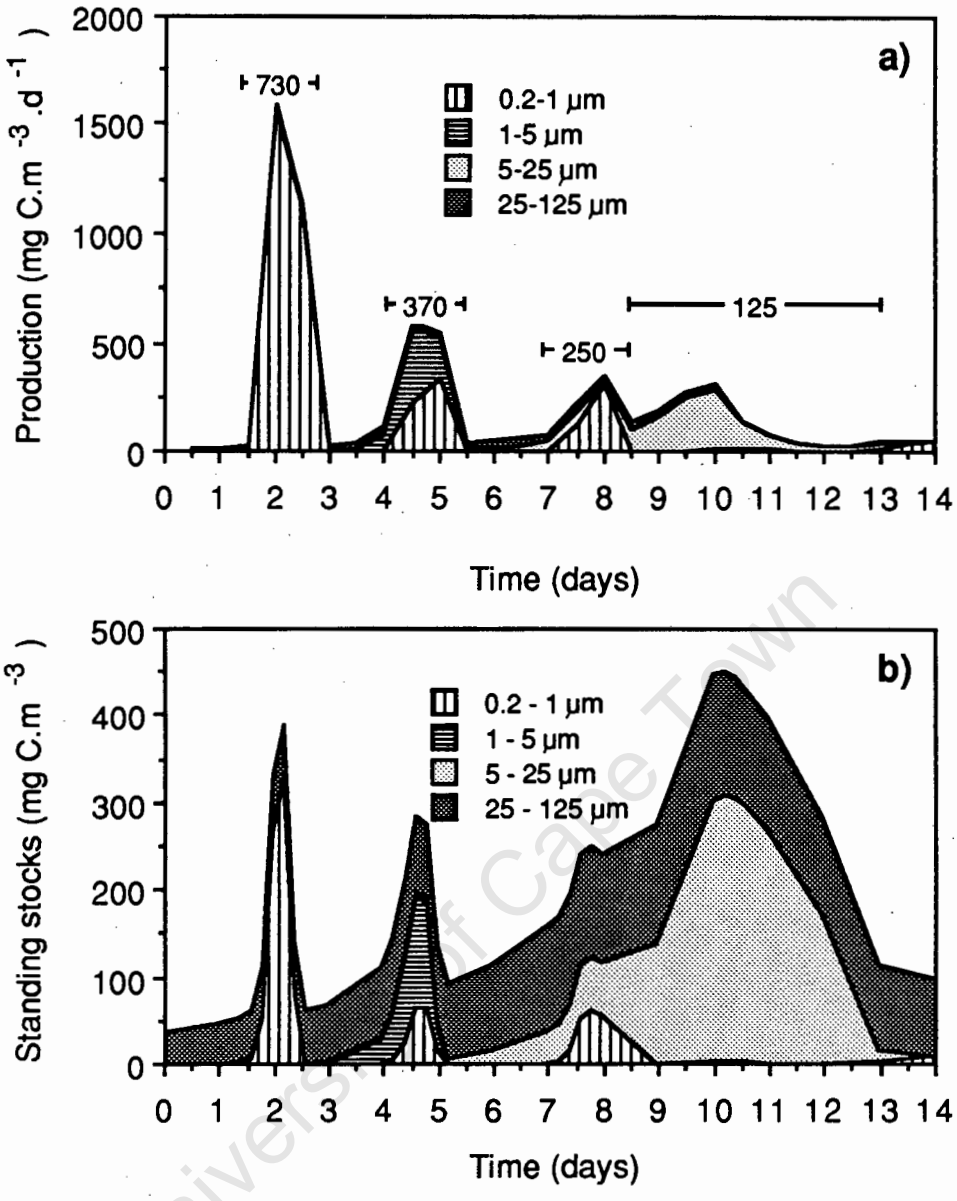

Fig. 5.1. The phytoplankton community of a simulated phytoplankton bloom after upwelling. a) Changes in primary production and the potential contribution by different size classes of phytoplankton. b) Changes in the size composition and standing stocks. Average daily production (mg $C.m^{-3}.d^{-1}$) is shown for selected time periods. Note that pico-phytoplankton standing stocks and production rates are probably overestimated for natural conditions, because the effects of factors other than nitrogen supply have not been modelled.

stocks are large, the rates of primary production are relatively slow, because the standing crop is dominated by large-celled phytoplankton. The maximum instantaneous rates in the model are compared with field measurements in Table 5.1. The model production rates fall within the range of measured primary production rates, but appear to be too low in mature upwelled water. This is

probably because nutrients in the model system are not replenished from an outside source after the single input of new nitrogen, whereas in reality mixing processes and diffusion can cause the advection of new nitrogen into the euphotic zone after the initial upwelling pulse. The additional input of new N would enhance primary productivity of the net-phytoplankton which typically dominate in mature upwelled waters.

Table 5.1. Comparison of maximum instantaneous rates of primary production in surface waters of the west coast upwelling region with model estimates. Water types are classified according to nitrate concentrations and temperatures after Barlow (1982).

Primary Production ($mg\ C.m^{-3}.h^{-1}$)	Water type	Reference
8.6	Newly upwelled	Brown (1984)
93	Mature upwelled (Oudekraal)	"
147	Mature upwelled (Robben Island)	"
167	Aged upwelled (Oudekraal)	"
181	Aged upwelled (Robben Island)	"
120	Mature upwelled	Brown and Field (1985)
147	Mature upwelled	Brown and Field (1986)
167	Aged upwelled	"
34.5	-	Lucas *et al.* (1986)
22	Mature upwelled	Armstrong *et al.* (1987)
142	Newly upwelled	This study, day 2
50	Mature upwelled	" day 4.5
28	Aged upwelled	" day 7
24	Aged upwelled	" day 13

The total primary production in the west coast model over the 14-day simulation is the total shaded area in Fig. 5.1a, and is estimated to be 2 800 mg $C.m^{-3}$ or an average daily production of approximately 200 mg $C.m^{-3}.d^{-1}$. Assuming a 20 m deep productive zone, this equals an

average daily production of 4000 mg $C.m^{-2}.d^{-1}$, which can be compared with the estimate of Brown (1984) of 4052 mg $C.m^{-2}.d^{-1}$. Obviously the depth factor that is used influences the production estimate, so the values are only rough approximations. They do, however, indicate that the model estimate of primary production, although variable in the short term, is similar to field estimates of primary production when averaged over time and space. Average daily production during each of the production peaks is presented in Fig. 5.1a. During the period when the size class 5-25 μm dominates (day 8.5 to 13), average production is approximately 125 mg $C.m^{-3}.d^{-1}$, some six times smaller than when the size class 0.2-1 μm dominates (day 1.5 to 3). This indicates that the pico-phytoplankton may be important primary producers, although their role is probably overestimated in the simulation output. Furthermore, additional inputs of new nitrogen would boost nutrient concentrations and enhance the productivity of net-phytoplankton (see above).

Primary production in the Agulhas Bank model (Fig. 5.2a) is relatively constant when compared with that of the west coast model. Small cells dominate primary production over most of the 9-day simulation (Fig. 5.2a). Instantaneous rates of primary production range between about 100 and 300 mg $C.m^{-3}.d^{-1}$. The total primary production for the 9-day simulation is 2 400 mg $C.m^{-3}$, corresponding to an average daily production of 270 mg $C.m^{-3}.d^{-1}$, which is larger than the daily average estimated for the west coast model. However, this production is confined to a 2 m thick chlorophyll maximum, so that total, integrated production (540 mg C. $m^{-2}.d^{-1}$) is less than that of the west coast model. Carter *et al.* (1986) estimated that primary production in the chlorophyll maximum was 630 mg $C.m^{-2}.d^{-1}$, which is similar to the model prediction. Much of the simulated primary production (> 90 %) is due to very small cells, so this production is not directly available to large zooplankton and fish. In general, only two size classes are important in primary production in the Agulhas Bank simulation (0.2-1 μm and 5-25 μm), with pico-phytoplankton (< 1μm) comprising between 40 % and 98 % of total production during the 9-day simulation.

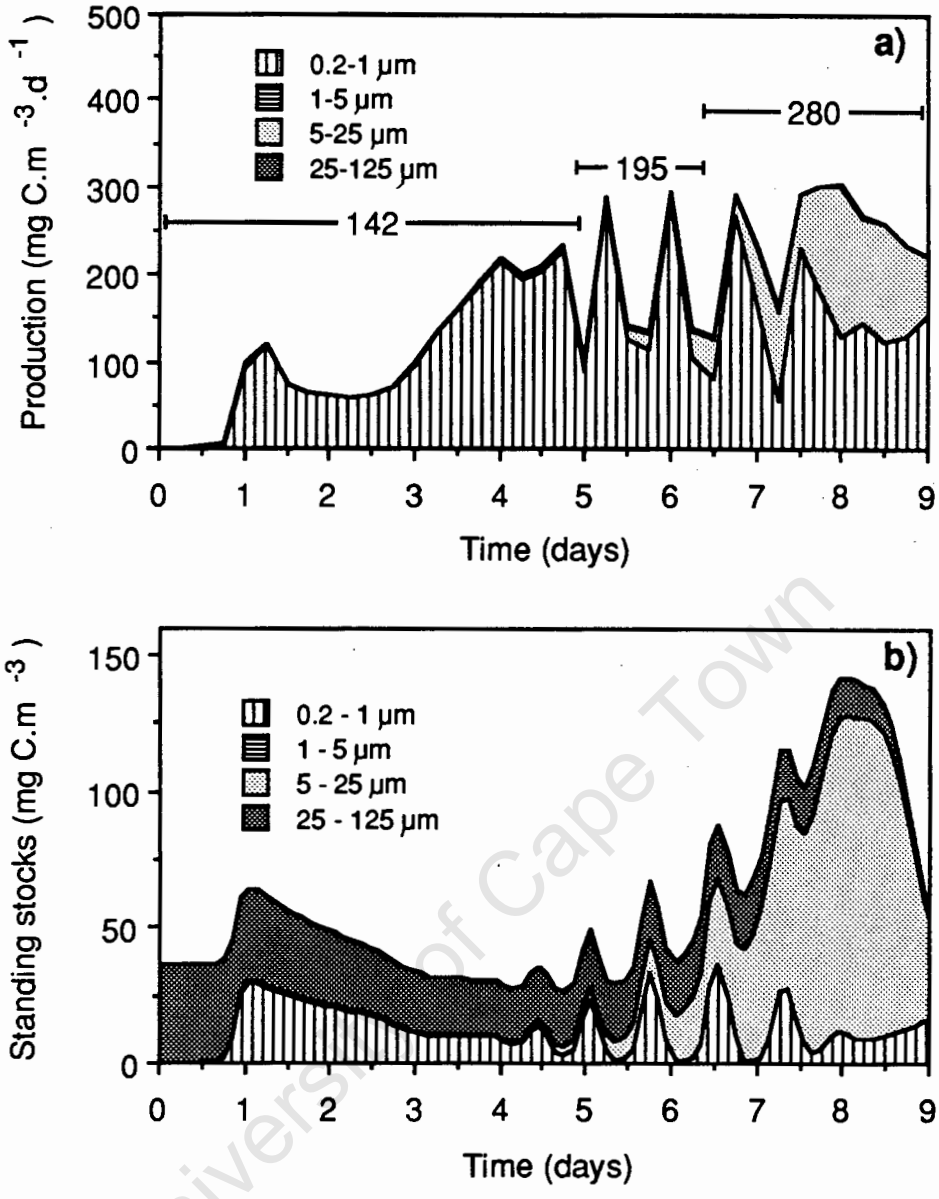

Fig. 5.2. A simulated phytoplankton community in the chlorophyll maximum layer of stratified waters on the Agulhas Bank. a) Changes in primary production and the potential contribution by different size classes of phytoplankton. b) Changes in the size composition and standing stocks. Average daily production (mg $C.m^{-3}.d^{-1}$) is shown for selected time periods.

Bacterioplankton production

Bacterioplankton production and standing stocks in the west coast model are roughly two orders of magnitude greater than those in the Agulhas Bank model (Fig. 5.3). The maximum bacterial production rate in the west coast model is estimated to be approximately 180 mg $C.m^{-3}.d^{-1}$ (Fig. 5.3), comparable to measured rates of 54 to 90 mg $C.m^{-3}.d^{-1}$ (Lucas *et al.* 1986) and 120

mg $C.m^{-3}.d^{-1}$ (Armstrong *et al.* 1987) in surface waters on the west coast. There are no field data for the Agulhas Bank. The temporal variations in bacterioplankton production and standing stocks differ in the two model systems. In the west coast model there are large fluctuations, with peaks in standing stocks and production lasting for about 1 to 1.5 days, whereas in the Agulhas Bank model the fluctuations are much smaller, and can have a cycle length of only 0.5 days. It should be noted that these fluctuations are overemphasised in the models, because threshold densities for predator ingestion are not included (Table 3.6, Chapter 3).

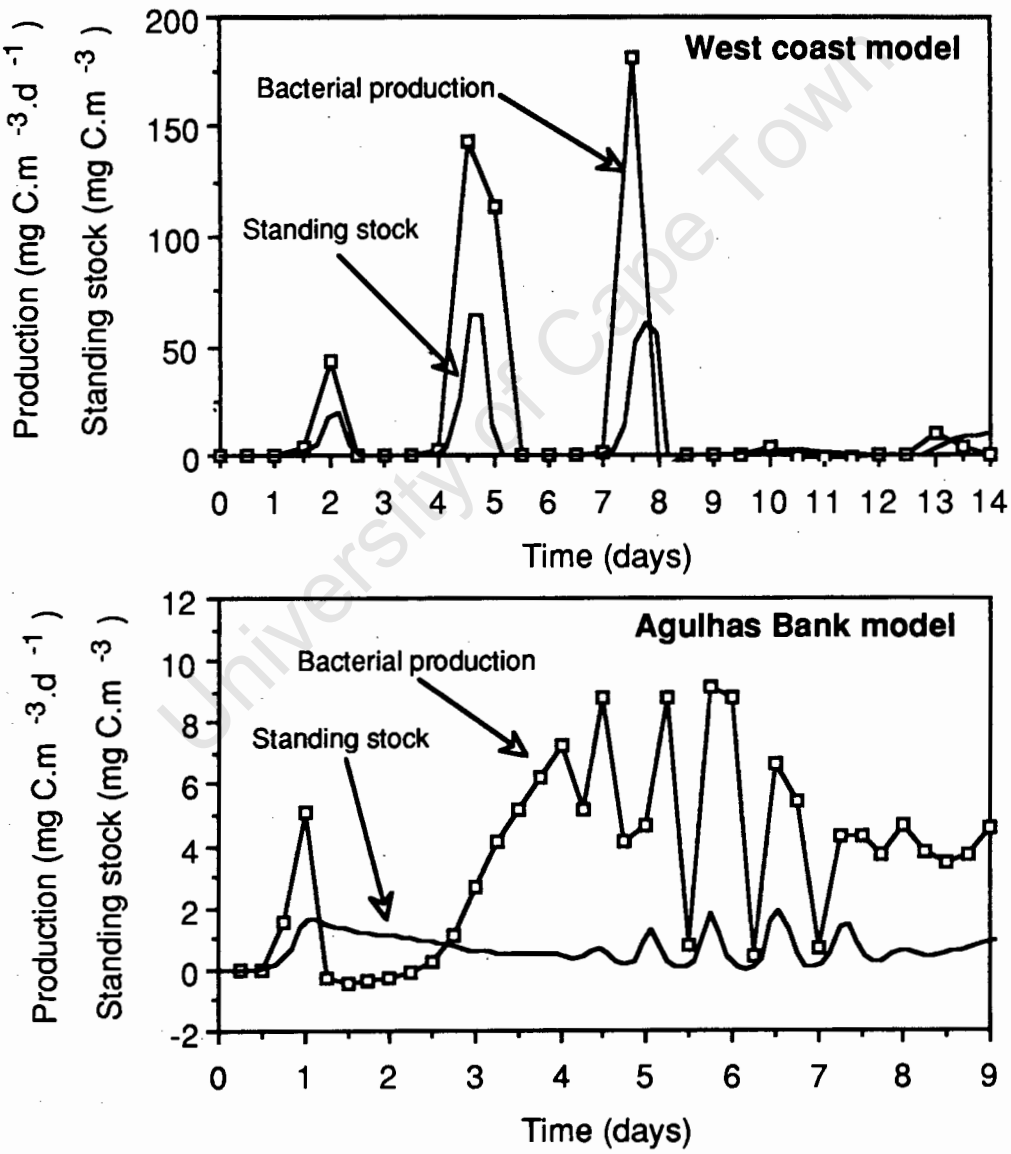

Fig. 5.3. Simulated standing stocks and potential production rates of bacterioplankton. Note that the fluctuations to zero are a model artefact, arising from the absence of a "refuge from predation" for bacterioplankton.

Thus the baseline of zero standing stocks and consequent zero production rates are unrealistic, because predators do not continue ingesting prey organisms when densities are very low, as occurs in the models. Production generally lags behind standing stocks, because production rates are fastest when standing stocks are still increasing, and are zero when standing stocks are at their peak.

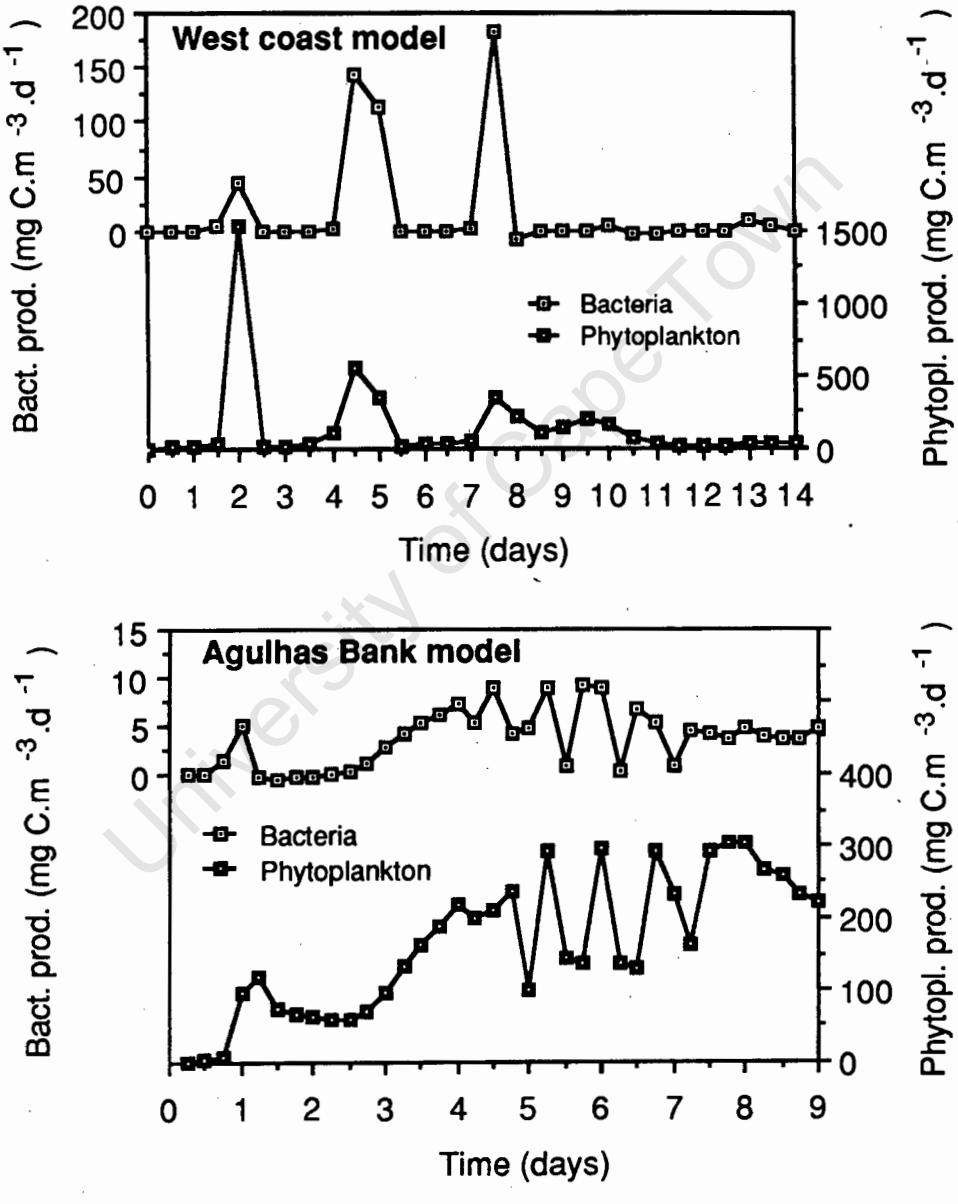

Fig. 5.4. Comparison between simulated production rates of phytoplankton and bacterioplankton in the two model communities.

Bacterioplankton production appears to be related to primary production in both models (Fig. 5.4), but this relationship is indirect, because it reflects predatory control of pico-phytoplankton (responsible for much of the primary production in the models) and bacterioplankton by the same size class of predators (zooflagellates). Nitrogen and not carbon limits bacterioplankton growth during most of the simulation periods, so one would not expect a direct (causal) relationship between primary production and bacterioplankton production in the model output. Maximum bacterial production rates are about 10 % of maximum primary production rates, but these maximum rates occur at different times; day 2 for primary production and day 8 for bacteria (Fig. 5.4). Primary production peaks get progressively smaller with time in the west coast model, whereas bacterial production peaks get progressively larger. This is related to the fact that carbon initially limits bacterial growth, because the PDOC pool is initialized with zero concentrations (Chapter 4), whereas towards the end of the bloom both phytoplankton and bacteria are limited by nitrogen. In the Agulhas Bank model there is little bacterioplankton production, reflecting their small standing stocks.

Nitrogen flows

Production of regenerated nitrogen

The proportion of regenerated nitrogen contributed by different heterotroph size classes changes with time in both model systems, reflecting the changing abundances of the size classes in the communities (Figs 5.5 and 5.6). These results are compared with data of Probyn (1987) and Probyn and Lucas (1987) respectively for the west coast area and for the Agulhas Bank. Model results are consistent with the conclusions of these authors that the sizes < 15 μm are the most important remineralizers, due to their rapid regeneration rates. However, the small organisms are not consistently important, and the temporal variations suggested by the models of Moloney *et al.* (1986) and Newell *et al.* (1988) are apparent. These temporal variations result in apparently conflicting evidence from "snapshot" sampling as to which size categories of heterotrophs are most important. In general, the smaller the organism, the shorter the duration of the period when that organism contributes most to regenerated nitrogen. Consequently, the contribution of small

organisms to the regeneration of nitrogen may be missed in some field studies, although the contributions of bacterioplankton may have been overestimated in Figs 5.5 and 5.6 (Chapter 3).

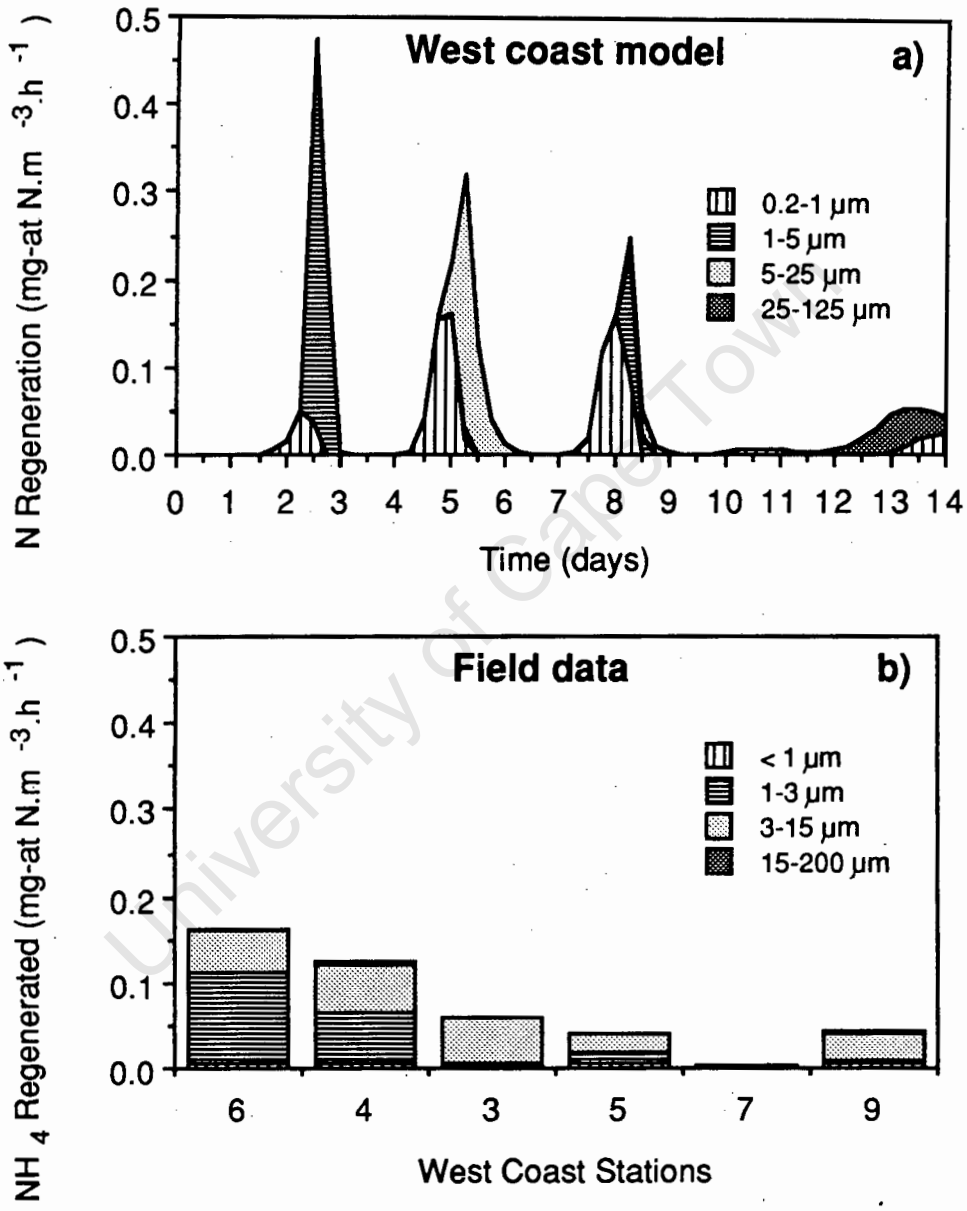

Fig. 5.5. Contributions of different size fractions of heterotrophs to regenerated nitrogen in the west coast upwelling region. a) Simulated regeneration rates. b) Field measurements of ammonium excretion rates (after Probyn 1987). Note that there is no time scale on the horizontal axis in b).

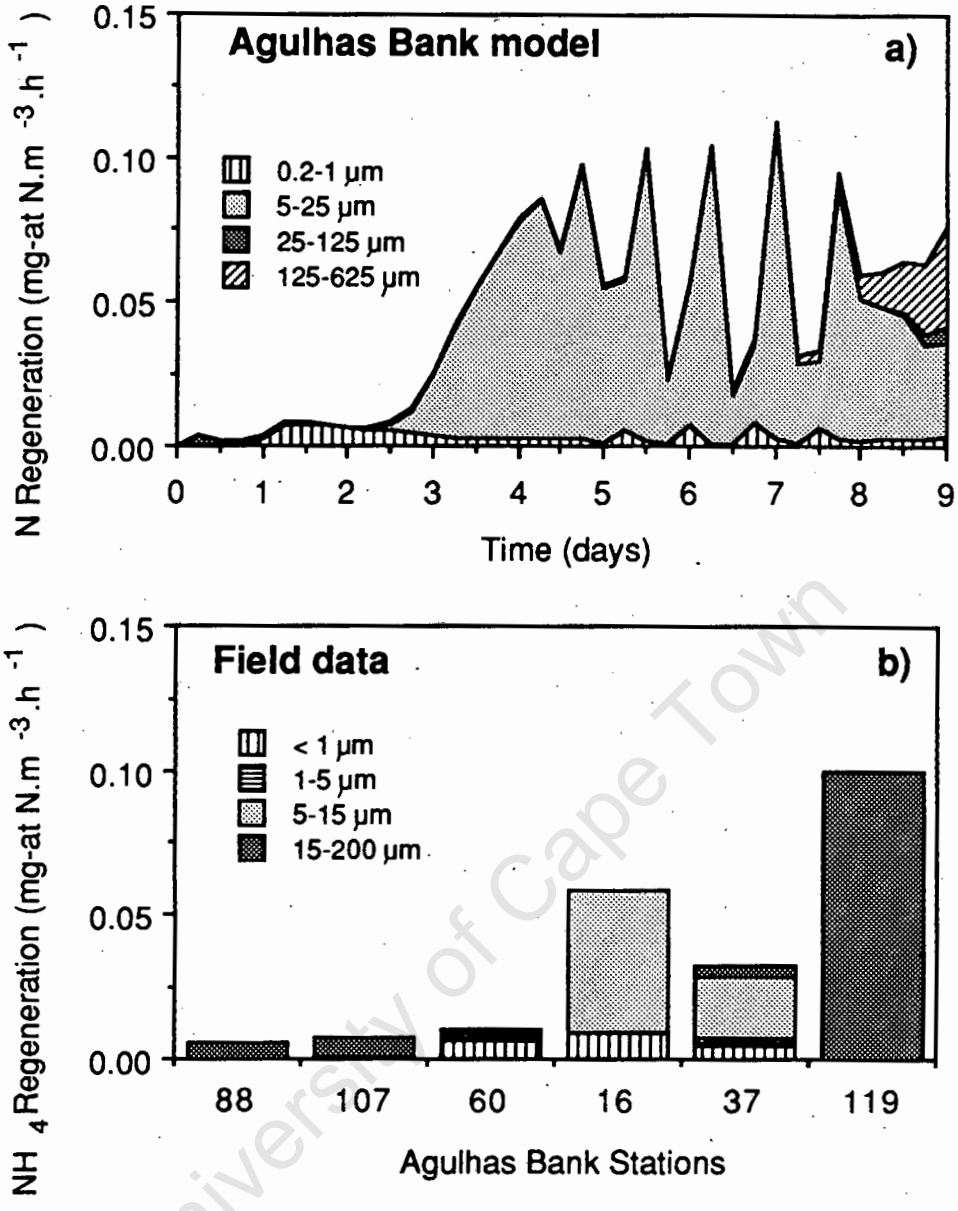

Fig. 5.6. Contributions of different size fractions of heterotrophs to regenerated nitrogen on the Agulhas Bank. a) Simulated regeneration rates. b) Field measurements of ammonium excretion rates (after Probyn and Lucas 1987). Note that there is no time scale on the horizontal axis in b).

Competition for dissolved nitrogen

The relative uptake of nitrogen from the dissolved pool by phytoplankton and bacteria in the two models is presented in Fig. 5.7. In the west coast model, relative uptake by bacteria may at times equal that by phytoplankton, whereas in the Agulhas Bank model bacteria take up < 10 % of

the total nitrogen utilized. The uptake pattern with time is more variable in the west coast model than in the Agulhas Bank model, where bacterial uptake is slow but persistent.

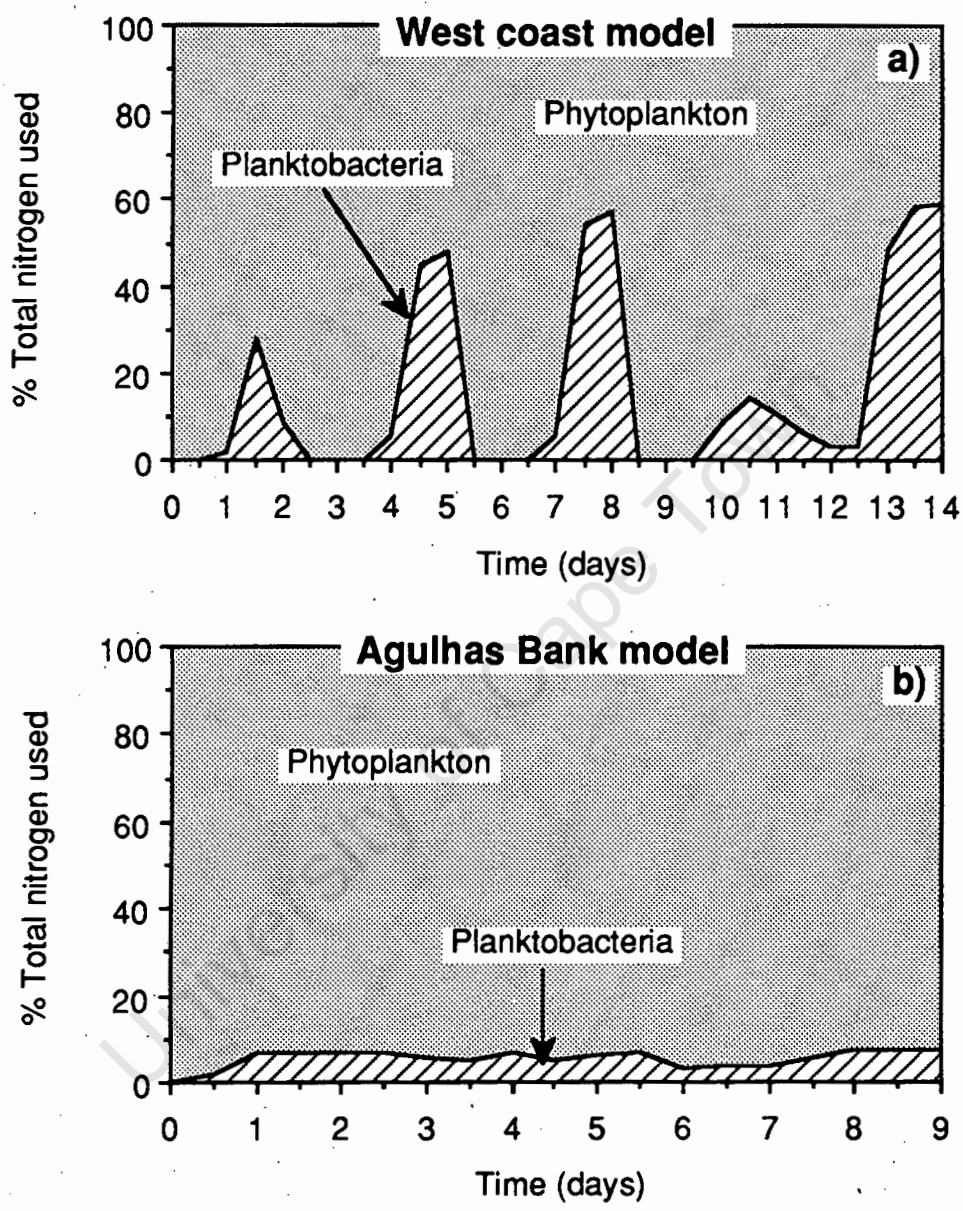

Fig. 5.7. The relative uptake of total dissolved nitrogen by phytoplankton and bacterioplankton in simulations of plankton communities. a) West coast upwelling model. b) Agulhas Bank model.

There has been some speculation in the literature about bacteria outcompeting phytoplankton for dissolved nitrogen (Gray *et al.* 1984), because of the fast uptake rates of bacteria and their ability to utilize nitrogen at small concentrations. Both of these attributes have been related to the small size of bacteria, and consequently their large surface : volume ratios (Gray *et al.* 1984,

Moloney *et al.* 1986). This line of argument overlooks the role of pico-phytoplankton, which are the same size as bacterioplankton and therefore have similar uptake capabilities. The competition between phytoplankton and bacterioplankton for nitrogen is probably less important than the competition between different sizes of phytoplankton, as has been demonstrated by the model output.

Utilization of regenerated nitrogen

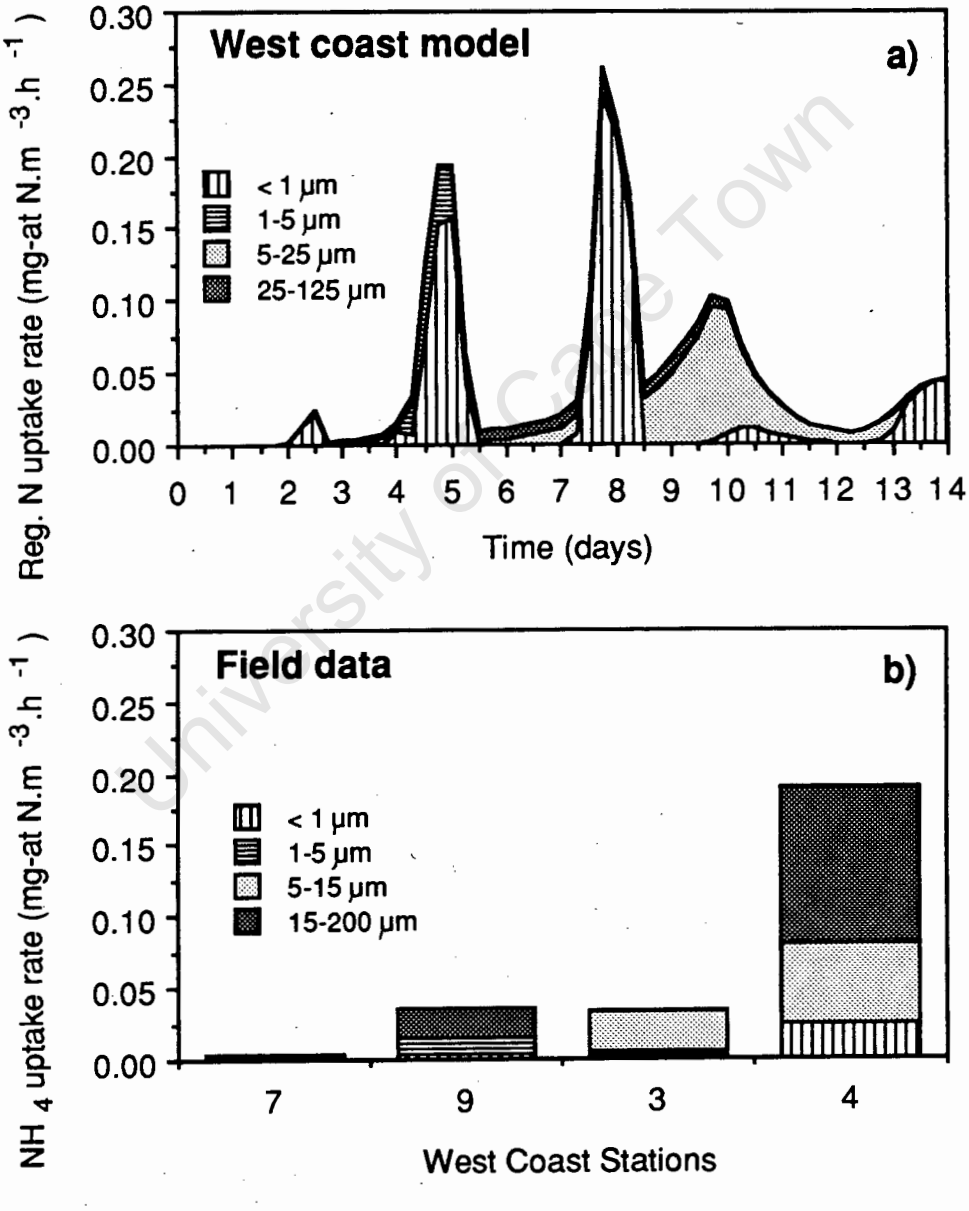

Fig. 5.8. Uptake of regenerated nitrogen by different size fractions of phytoplankton in the west coast upwelling region a) Simulated uptake rates. b) Field measurements of ammonium uptake rates (after Probyn 1987). Note that there is no time scale on the horizontal axis in b).

The simulated uptake of regenerated nitrogen by different phytoplankton size fractions is compared with field data from the upwelling area (Fig. 5.8) and the Agulhas Bank (Fig. 5.9).

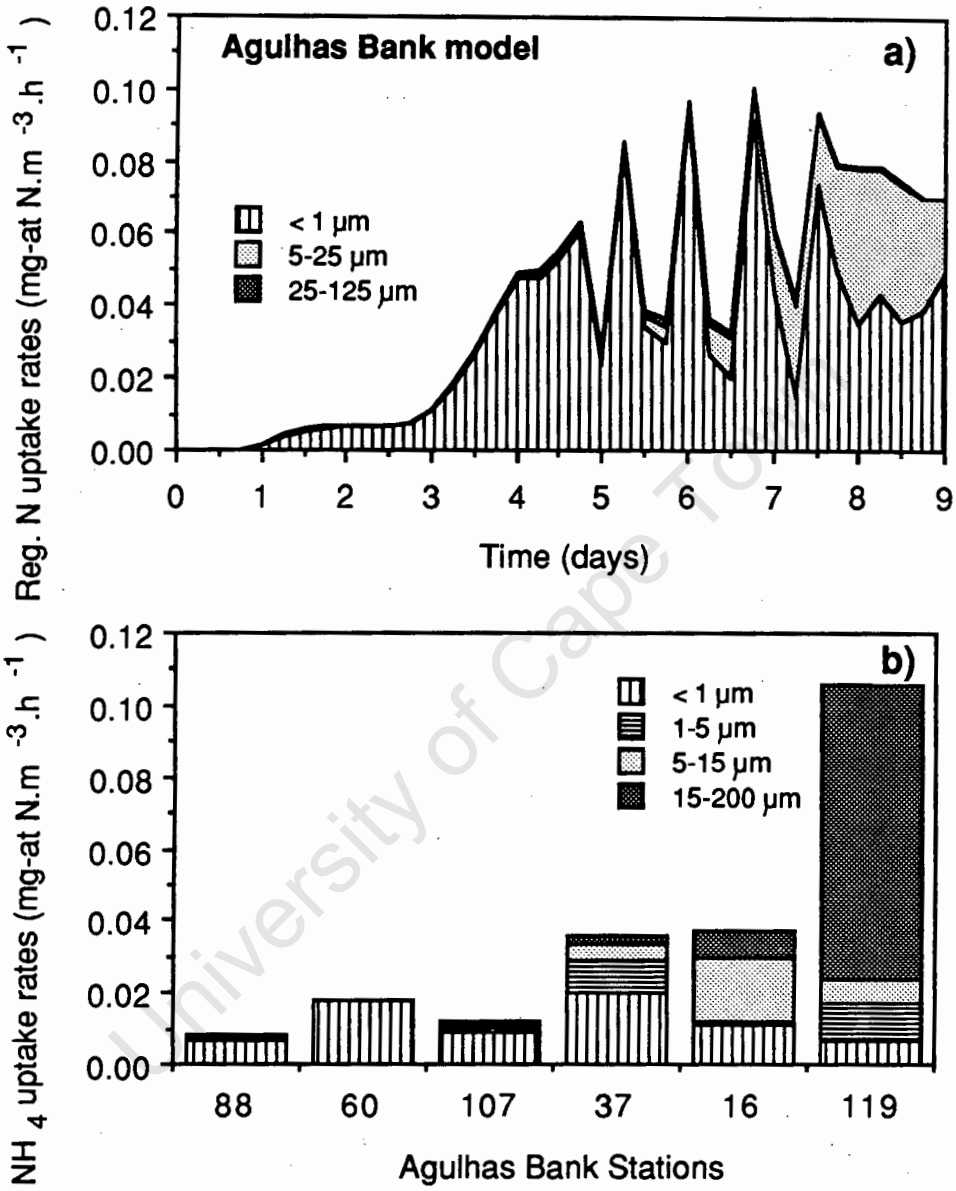

Fig. 5.9. Uptake of regenerated nitrogen by different size fractions of phytoplankton in the chlorophyll maximum layer on the Agulhas Bank. a) Simulated uptake rates. b) Field measurements of ammonium uptake rates (after Probyn and Lucas 1987). Note that there is no time scale on the horizontal axis in b).

In both model systems, pico-phytoplankton dominate nitrogen uptake. This is not supported by field studies on the west coast. Probyn (1985) found that pico-phytoplankton only accounted for

10 % of the nitrogen taken up by the total phytoplankton community in coastal waters, and in a more recent study (Probyn 1987) the uptake of ammonia by pico-phytoplankton was estimated to be small compared with that by phytoplankton > 5 μm (Fig. 5.8b). The west coast model has been shown to overestimate the contribution by pico-phytoplankton (Chapter 4), so the magnitudes of the uptake rates are probably overestimated. However, it is not known whether these peaks in uptake rates (corresponding to production peaks) occur in a more depressed form, or not at all, because their short duration makes it likely that they could be missed in field studies, which typically have been directed at larger cells. Very little is known of the short time-scale patterns of nitrogen uptake and regeneration (Probyn 1985).

The field data from the Agulhas Bank (Fig. 5.9b) agree with model predictions regarding the important role played by pico-phytoplankton in nitrogen uptake. Large-celled phytoplankton in the model appear to flourish only when nutrient concentrations are large enough to support growth. Large cells utilize food reserves under conditions of scarce nutrients, and then replenish reserves when nutrients are again abundant. The model does not include inactive, resting stages of large cells in the community; neither does it simulate variable physical conditions that presumably give large cells an advantage. It will thus underestimate the role of the large cells, as is indicated by the fast nitrogen uptake rate measured for the size fraction 15-200 μm, which is not duplicated in model output.

New versus regenerated production

The proportion of total primary production due to the utilization of new nitrogen (Dugdale and Goering 1967) is termed the f ratio (Eppley and Peterson 1979). This ratio provides an index of the degree of recycling in the euphotic zone. The changes with time of the relative proportions of new and regenerated production in the model systems are shown in Fig. 5.10. In both model systems regenerated nitrogen concentrations are started at zero, so regenerated production increases with time. In the west coast model the nitrogen pool is not replenished with new nitrogen, so regenerated nitrogen comes to dominate as the new nitrogen is used up, and after 14 days all of the primary production is regenerated production. This result is supported by the work

of Verheye-Dua and Lucas (1988), who estimated that regenerated production comprised < 26 % of primary production in newly upwelled waters, but in mature upwelled water the proportion increased to 65 %. The model does not incorporate diffusion and mixing processes, and new production is consequently underestimated during the latter stages of the simulated bloom.

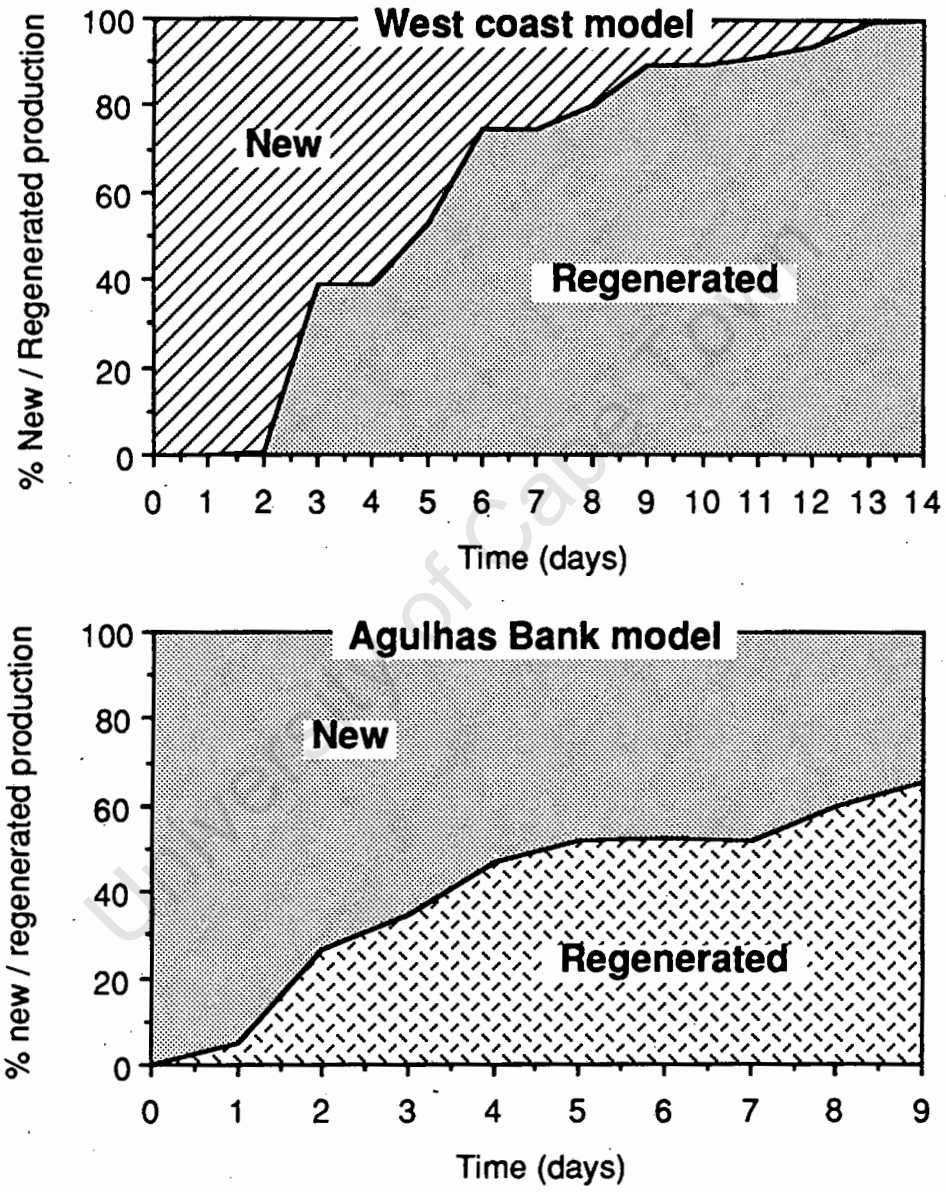

Fig. 5.10. Changes with time of the relative proportions of simulated new and regenerated production in the two model systems.

In the Agulhas Bank model new production comprises roughly 35 % of total production at the end of the simulation, similar to the value of 30 % estimated for inshore waters (Eppley and Peterson 1979). Although regenerated nitrogen produced by large zooplankton and fish is not included in the two models, the contributions by these large organisms are probably small compared to the contribution by micro-organisms (Azam *et al.* 1983), and this should not be a significant source of error.

Food web structure

Five Lindeman spines are presented from the west coast simulation (Fig. 5.11), corresponding to the four phytoplankton standing stock peaks (days 2, 5, 8 and 11) and a period of bloom decay (day 14). The Agulhas Bank model is used to produce four Lindeman spines (Fig. 5.12), corresponding to peaks in phytoplankton standing stocks (days 1, 3, 7 and 9). The importance and efficiency of different flow pathways changes considerably between days.

Trophic categories

In a traditional representation of a food chain, it is customary to place different species or groups of species into each trophic level, and in such a representation the trophic structure of the two models would be:

Phytoplankton -> Bacteria (0.2-1 μm)-> Flagellates (1-5 μm) -> Ciliates (5-25 μm) ->
Microzooplankton (25-125 μm) -> Mesozooplankton (125-625 μm)

In the west coast model, there are five effective trophic categories on all days except day 11, when there are only four. The compositions of the model trophic categories are shown beneath the boxes, as percentage contributions of the different model size classes to each trophic category (Fig. 5.11). These categories can be contrasted with the traditional series above. Trophic category I consists only of phytoplankton and the PDOC pool (produced by phytoplankton and utilized by bacterioplankton). The second trophic category comprises some fraction of all of the heterotroph size classes, assuming omnivory in the plankton. This is very different to the traditional "food

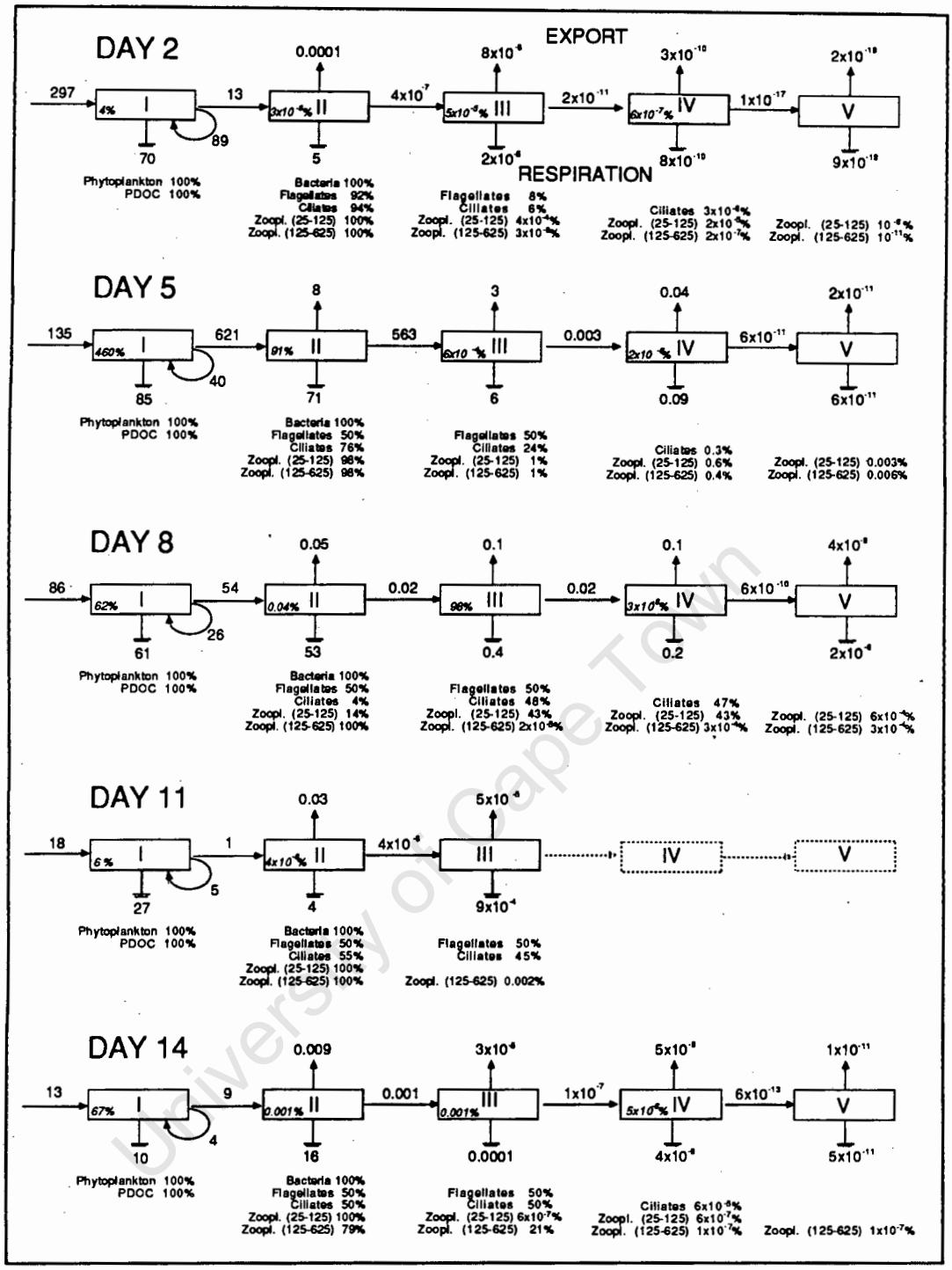

Fig. 5.11. Lindeman spines showing the collapsed carbon food webs of the west coast at selected times in the simulation. The flows represented in the diagram have been integrated over quarter-day periods, ending at the times shown in days. Roman numerals represent trophic categories. The distributions of the model compartments in the different trophic categories are given in percentages, which represent the relative dependence of that compartment on the previous trophic category. Within the boxes, italicized figures are the trophic efficiencies, calculated as the percentage of the input into each category that enters the next category. Arrows represent carbon flows (ingestion, export of faeces by sinking, and respiration), and the internal cycling within category I represents the production of PDOC by phytoplankton, which two model compartments both occur 100 % in category I.

chain" represented above. Bacterioplankton always occur only in the second trophic category, because in the model all of their carbon is obtained from the PDOC pool. Zooflagellates (1-5 μm) chiefly occupy categories II and III, and generally obtain half of their carbon from phytoplankton and half from bacteria. However, at the start of the simulation (day 2, Fig. 5.11) they obtain 92 % of their carbon from phytoplankton, because bacterial standing stocks are much smaller than those of pico-phytoplankton at that time (Chapter 4). "Ciliates" (5-25 μm) occur in categories II, III and IV in varying proportions, ranging from 94 % in II, 6 % in III and a very tiny fraction in IV (day 2, Fig. 5.11) to 4 % in II and 48 % and 47 % respectively in categories III and IV (day 8, Fig. 5.11). The two largest zooplankton size classes (25-125 and 125-625 μm) occupy all four consumer trophic categories. Much of the time they appear to occur almost entirely in category II, but it must be remembered that the results are only snapshot representations, and a different result may be obtained at different time periods. In general, the planktonic food web for organisms < 625 μm in the west coast model consists of five trophic categories, but only the first three appear to be consistently important in carbon flows.

In the Agulhas Bank model a maximum of five trophic categories is also obtained (Fig. 5.12), but for some periods in the simulation there are only three or four. Phytoplankton and the PDOC pool comprise the first trophic category, and bacterioplankton occur only in the second trophic category, as is the case in the west coast model. Zooflagellates (1-5 μm) occupy categories II and III, but occur in greater proportions in category II. This is not unexpected, because bacterial standing stocks in the Agulhas Bank model are consistently much smaller than are those of pico-phytoplankton, both of which are preyed upon by zooflagellates. "Ciliates" (5-25 μm) also fall almost exclusively into category II, indicating that they obtain most of their carbon from phytoplankton. Again, this can be explained by the small standing stocks of their zooflagellate prey compared with that of similar-sized phytoplankton cells. The two largest zooplankton size classes (25-125 and 125-625 μm) occur in categories II, III, IV and V, but are mainly found in categories II and III, thus utilizing chiefly phytoplankton and small zooplankton prey.

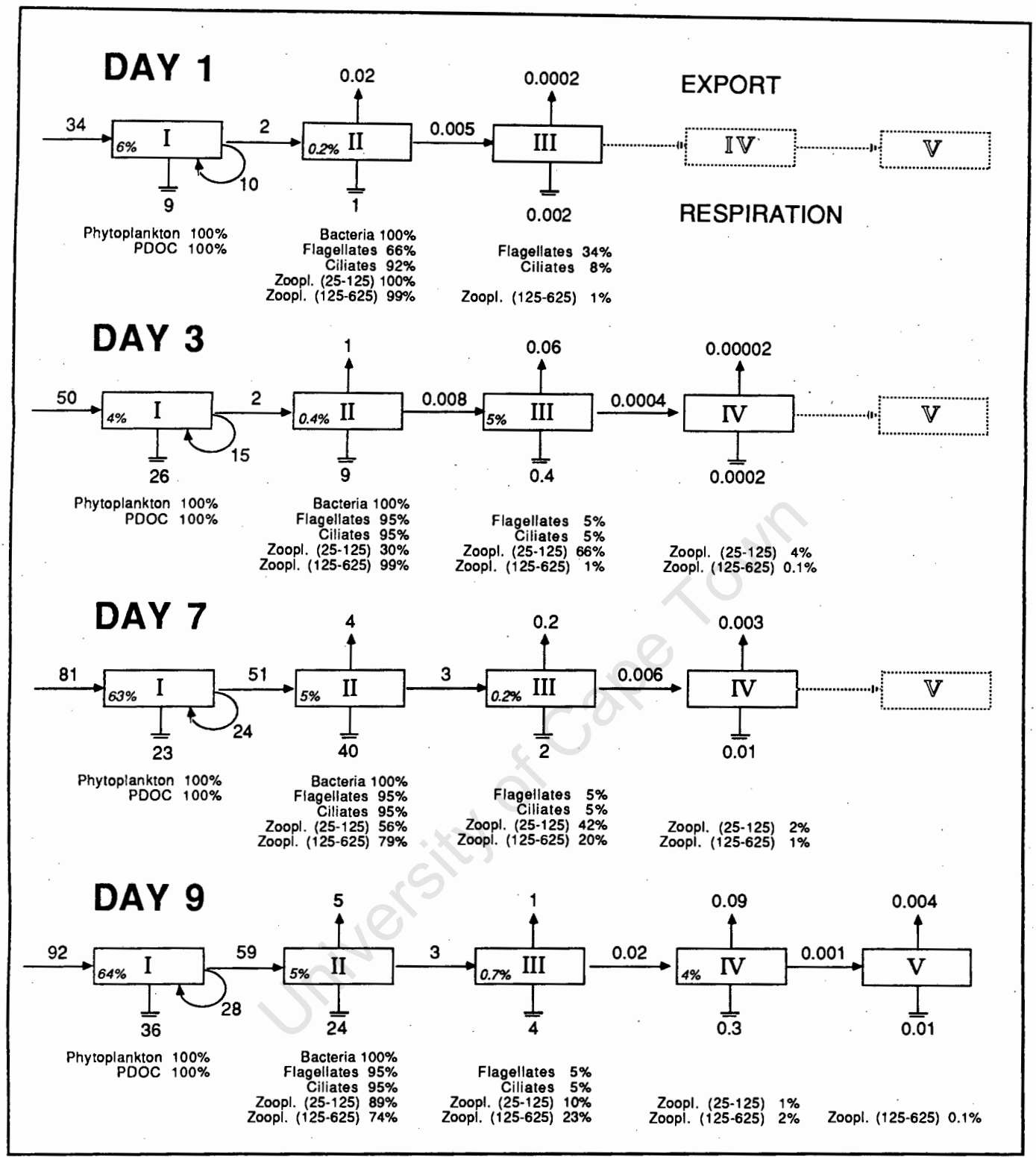

Fig. 5.12. Lindeman spines showing the collapsed carbon food webs of the Agulhas Bank at selected times in the simulation. The flows represented in the diagram have been integrated over quarter-day periods, ending at the times shown in days. Roman numerals represent trophic categories. The distributions of the model compartments in the different trophic categories are given in percentages, which represent the relative dependence of that compartment on the previous trophic category. Within the boxes, italicized figures are the trophic efficiencies, calculated as the percentage of the input into each category that enters the next category. Arrows represent carbon flows (ingestion, export of faeces by sinking, and respiration), and the internal cycling within category I represents the production of PDOC by phytoplankton, which two model compartments both occur 100 % in category I.

Trophic flows

Flow pathways in the Lindeman spines are represented by arrows. Input into category I represents carbon fixation, and the cycling of I into itself is the production of PDOC by phytoplankton. All other horizontal flows are due to grazing. Upward flows are carbon exports from the system, and in the examples in Figs 5.11 and 5.12 they are due entirely to the sinking of faecal material. The export flows from the two systems are generally small, because absorption efficiencies of zooplankton are assumed to be large (90 %, Chapter 3). Additional exports realistically should encompass the sinking of phytoplankton cells at times, but this pathway was not included in the models. Downward arrows represent respiratory carbon losses, and at times these losses are quite large. For example, at day 8 of the west coast model (Fig. 5.11), respiratory losses are 98 % of carbon inputs into trophic category II, and at day 3 of the Agulhas Bank simulation (Fig. 5.12) respiration of trophic category II exceeds carbon inputs by a factor of 4.5. Clearly such an imbalance cannot persist, and exists because inputs on previous days exceeded metabolic expenditure.

At each time period shown, the flows through the west coast food web do not always decrease with increasing trophic category, as would be expected from theory based on steady states (e.g. day 5, Fig. 5.11). This indicates that mismatches in time occur between production at two different trophic categories. This is realistic, because there will always be a time lag between photosynthesis and the passage of a molecule of carbon through the food web, which passage will be further delayed if storage products are synthesized (not modelled here). Similarly, the trophic efficiencies may be small at the start of the Lindeman spine but larger further along, again indicating lag effects. In dynamic systems the flows should always be considered together with the standing stocks because, for example, a large input into a trophic category can be interpreted in a different way if the receiving standing stock is large, rather than when the receiving standing stock is small. Also, outputs can exceed inputs (e.g. day 5, category I, Fig. 5.11), because grazers do not only utilize production but also biomass, which results in estimated trophic efficiencies greater than 100%.

In the early 1980s, the importance of measuring rate processes in order to understand the dynamic functioning of ecosystems was stressed (e.g. Platt *et al.* 1981). As a consequence, some studies consider only the flows when analysing data sets. This is only applicable when the systems are in steady state (probably seldom) or if integrated measurements over a time period are available. Few such data sets exist. In dynamic systems, both standing stocks and production measurements should be used in constructing hypothetical flow networks of the systems. Information about "past production" is contained in the standing stocks, as is the current "state" of the system. It is the standing stocks that the predators perceive at any time, whereas the probable future state is described by the instantaneous flows. Using this argument, on day 8 in the west coast model (Fig. 5.11), the respiratory loss from trophic category II relative to the inputs is not 98 % as indicated by the flows, but 47 % if the average standing stock is taken into account.

The trophic position of pelagic fish

The two simulated plankton communities contain only microplankton (< 625 μm). It is not realistic to include large, motile zooplankton and fish in a deterministic model in which the time scales are in days. Also, the spatial extent of the simulated systems is that of a cubic meter of water in the euphotic zone. Large-scale features of the water column have been ignored e.g. vertical migrations by zooplankton. The model systems are thus too small and have too short a time scale to be applicable to pelagic fish. An alternative approach is adopted here, in which the simulation results are integrated over time, in order to increase the time scale to that applicable to pelagic fish.

The flows in the west coast simulation were integrated over 14 days, and those of the Agulhas Bank simulation over 9 days. Average trophic structures of the two systems are presented in Fig. 5.13. The west coast model has three effective trophic categories, and the "trophic efficiencies" in these categories are large; 62.5 % for category I and 48.7 % for category II. Trophic categories further down the food web are far less important, and trophic efficiencies are very small. This Lindeman spine can be compared with that of the Agulhas Bank simulation. Here the trophic efficiencies in categories I and II are much smaller than those of the west coast model,

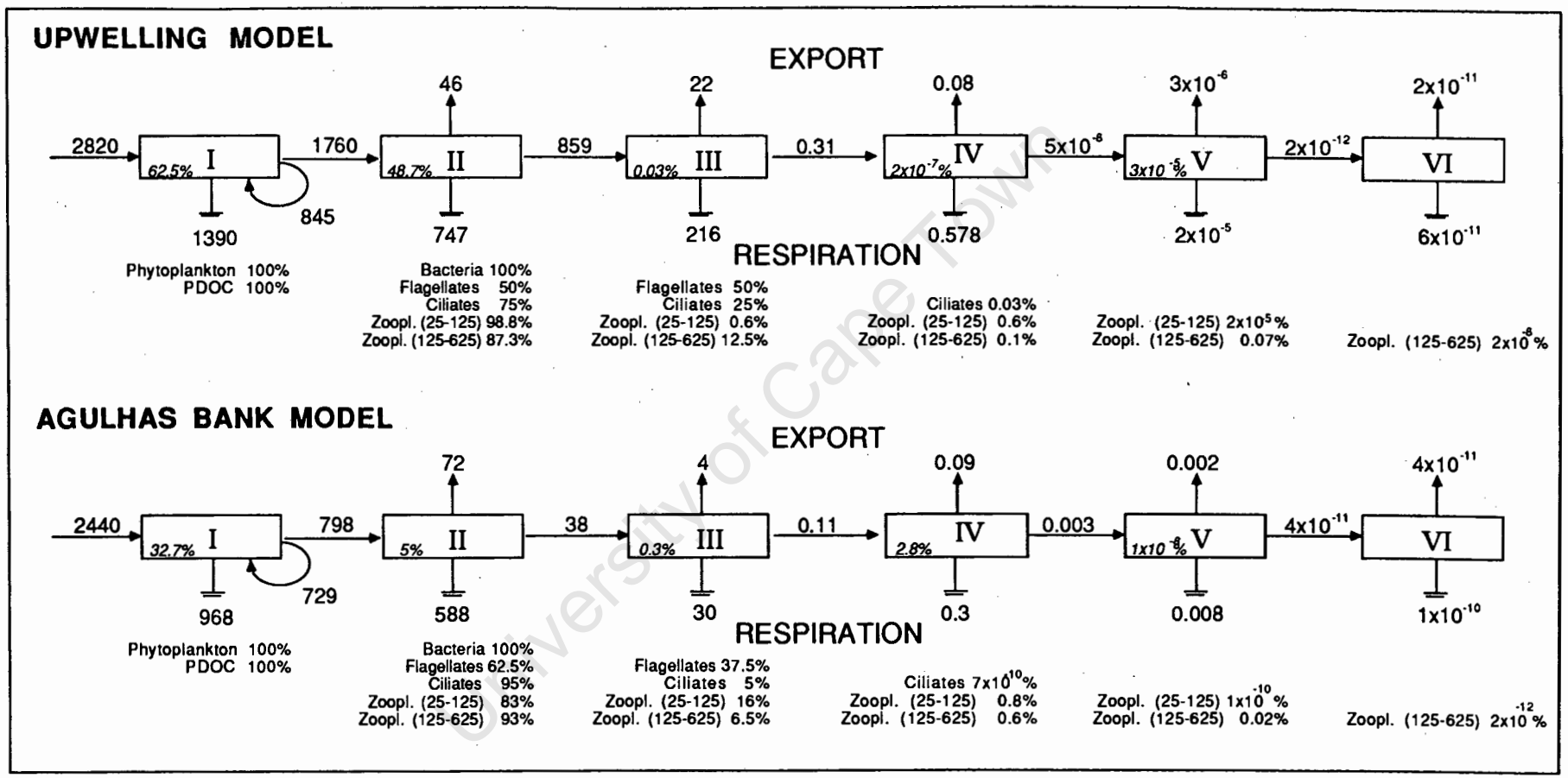

Fig. 5.13. Time-averaged Lindeman spines of the two model communities. The flows in the upwelling model are integrated over 14 days, and those of the Agulhas Bank model are integrated over 9 days

whereas the trophic efficiencies at categories III and IV are relatively large. There are effectively four trophic categories in this model.

Important pelagic fish in the southern Benguela region feed primarily on zooplankton (James 1987), possibly because most phytoplankton are too small. It is relatively simple to assess the trophic position of anchovy in the food web on the basis of where their food occurs. Assuming that they feed on the largest zooplankton size classes (125-625 μm), anchovy occupy trophic categories II, III, IV, V and VI in both model systems. However, most of their trophic function would be concentrated in category III, because their prey size class occurs mainly in category II (Fig. 5.13).

The proportion of primary production that reaches pelagic fish can also be assessed. In the simulations described above for the west coast and the Agulhas Bank microplankton communities, the integrated carbon flows have been summarized, and the relative proportions moving along various pathways are presented in Fig. 5.14. The flows from the pico-phytoplankton (0.2-1 μm) and bacterioplankton to heterotrophs of sizes 1-5 and 5-25 μm are overestimated, because during predator-prey population fluctuations an excess of carbon available is ingested. This unrealistic result does not affect model output drastically, because predator and prey populations go to zero immediately after this occurs. However, the cumulative effect of these excess flows are apparent in the integrated flows, which have therefore been corrected for them (figures in parentheses, Fig. 5.14).

The carbon flows are standardized to relative units, assuming that 100 units of carbon is fixed by autotrophs during the two simulations. In the west coast model, of the 100 units fixed during photosynthesis, a total of 83 units are respired by autotrophs and heterotrophs (Fig. 5.14a). 30 units enter the PDOC pool, of which 16 are passed on to bacterioplankton. Heterotrophs ingest 21 units of autotroph carbon, but most of this is respired. A small proportion moves along the heterotroph size continuum through ingestion, but only a tiny fraction eventually reaches the microzooplankton size classes (25-625 μm) in the simulation, making very little of the primary production available to pelagic fish. However, these results are incomplete, because large

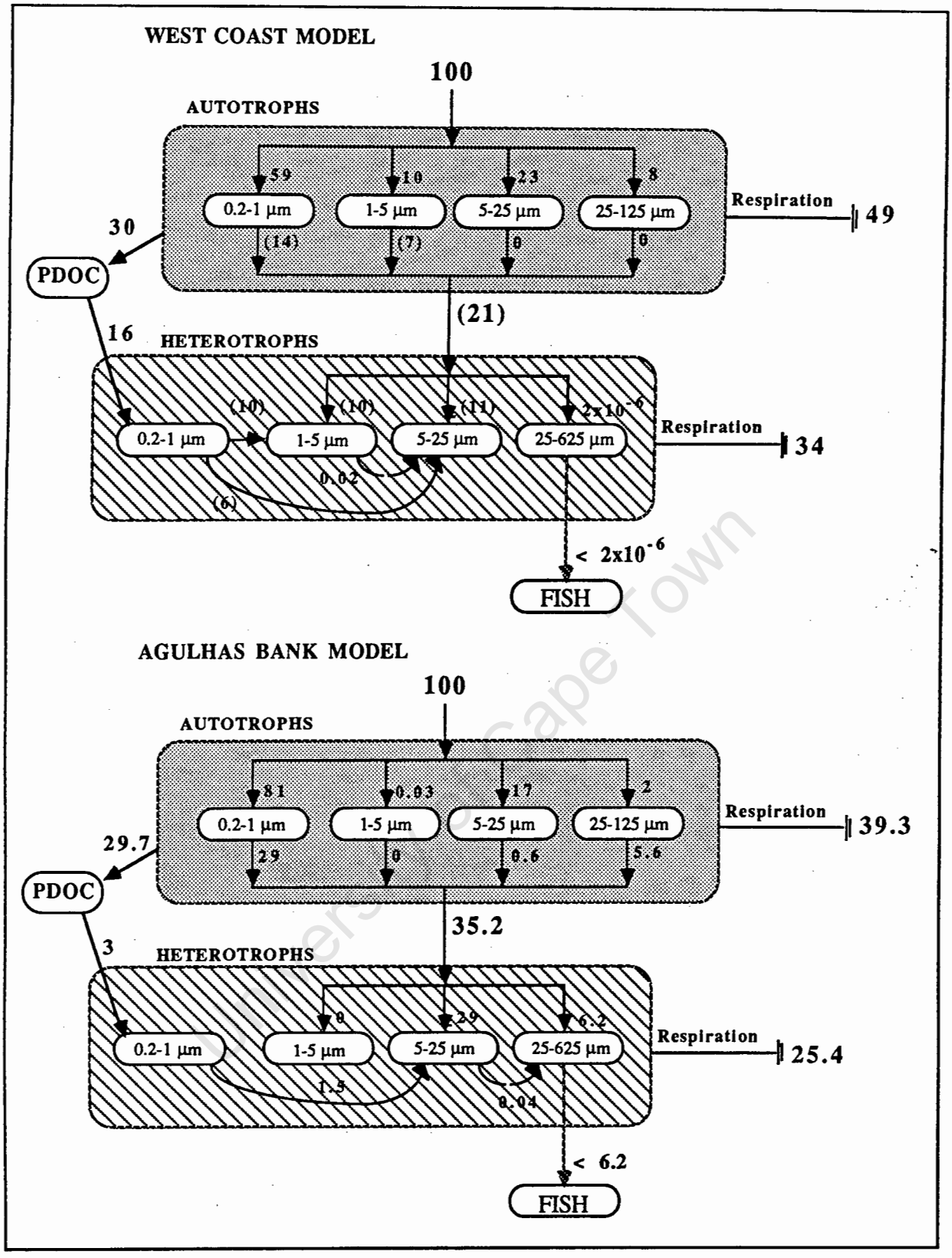

Fig. 5.14. Summary of simulated carbon flows through the microplankton communities of the west coast upwelling region and the Agulhas Bank, integrated over 14 days for the west coast model, and 9 days for the Agulhas Bank model. The flows have been standardized to 100 units of carbon.

zooplankton standing stocks are deliberately set to low values in the simulation, as they probably are of little importance in newly upwelled water (Olivieri 1985). In reality, zooplankton may encounter a dense phytoplankton patch after a bloom has developed, and the proportion of primary production moving into large organisms in the food web would obviously increase. Thus the model representing the west coast system represents an extreme example.

The results of the Agulhas Bank model are probably more representative than those of the west coast model, because the Agulhas Bank has a more stable physical environment. Stochastic processes are probably important on the west coast, where the environment is dynamic and unpredictable. In the Agulhas Bank simulation, 64.7 of the 100 units of carbon fixed by autotrophs are respired by autotrophs and heterotrophs. The PDOC pool receives 29.7 units, but only three of these are taken up by bacterioplankton, the remainder accumulating in the PDOC pool. 35.3 units pass from the autotroph to the heterotroph continuum, but only 6.2 units of autotroph carbon are ingested by microzooplankton of sizes 25-625 μm, and an even smaller amount (0.04 units) reaches this size range by predation within the heterotroph continuum. In this example (Fig. 5.14b), less than 6.2 % of primary production would be available to pelagic fish.

Although these results represent only one of a large set of possible conditions in the two systems, they are useful because they attempt to scale up from temporal and spatial scales relevant to microplankton, to scales that are required to understand the dynamics of larger organisms such as pelagic fish. In so doing, the carbon flows in the model systems have been integrated over relatively short time periods during which complex, non-linear interactions have occurred. It has been shown that most primary production in the two model systems occurs in pico- and nano-phytoplankton, and most primary production in these simulations does not reach large organisms. This is mainly due to temporal lags in food web flows. Because all of the consumer compartments do not occur in the system at the same time in the simulations, respiratory and other losses reduce the amounts available for trophic transfer, and respiratory losses are a relatively large proportion of total carbon flows in the two simulated systems (Fig. 5.14). This is an important effect which is often overlooked when extrapolations are made from snapshot samples to develop whole system models.

Despite the apparently small proportion of primary production reaching pelagic fish, the southern Benguela supports a relatively large pelagic-fish production (Crawford *et al.* 1987). The efficiency of transfer appears to be greater in the west coast model than in the Agulhas Bank model (Fig. 5.13), and this may be important for the total productivity of the system. Possible reasons for the efficient transfer are discussed in Chapter 8.

SUMMARY AND CONCLUSIONS

1. Primary production occurs in "bursts" in the west coast model, whereas it is more constant in the Agulhas Bank model.
2. Pico- and nano- phytoplankton are potentially important primary producers in both model systems. As a consequence, much of primary production is not directly available to large metazooplankton and fish.
3. Bacterioplankton production is larger in the west coast model than in the Agulhas Bank model.
4. The relationship between primary production and bacterioplankton production is not causative in the model systems, because it reflects predatory control of both populations by the same predators.
5. A relatively large proportion of primary production goes to heterotrophs of sizes 1-25 μm in the two model systems, but this transfer is chiefly through phytoplankton and not bacterioplankton.
6. The smallest heterotrophs are the most important in nitrogen regeneration, although temporal variations occur, reflecting changes in standing stocks of dominant heterotroph size classes.
7. Competition for dissolved nitrogen between bacterioplankton and phytoplankton is probably not extensive. The "competitive advantage" of bacterioplankton is probably fallacious, because pico-phytoplankton presumably have similar uptake capabilities.
8. New production is estimated to be > 60 % in the west coast model, and approximately 35 % in the Agulhas Bank model.
9. The structures of the two model food webs change considerably with time. This highlights the dangers of extrapolating from snapshot sampling. It is recommended that both standing stocks and flow rates be used to analyse snapshot samples of dynamic systems, and not just one or the other as is sometimes the case.
10. In the southern Benguela region, anchovy probably only utilize a small proportion of primary production, because most of it is channelled through small organisms, and lost through respiration.
11. The actual quantities of primary production that reach pelagic fish are difficult to estimate, because these will change with time and for different phytoplankton assemblages.
12. The exact role of pico-phytoplankton is not known from field studies, and the model predictions regarding the small cells need to be tested with field measurements of the appropriate time scales.

CHAPTER 6

PHYTOPLANKTON GROWTH RATES IN OCEANIC WATERS

ABSTRACT

An oceanic food web is simulated using a generic size-based model. It is assumed in the model system that new nitrogen diffuses into the euphotic zone at a rate of 0.35 mg $C.m^{-3}.d^{-1}$. The model is exercised and approached steady state after approximately 25 days, when pico-phytoplankton dominate standing stocks and production. Community production to biomass ratios are estimated to be 5 d^{-1} at steady state, supporting the hypothesis that oligotrophic oceanic waters have fast rates of primary production. However, despite their fast production rates, the cells are not growing maximally, because ambient nutrient concentrations are small.

INTRODUCTION

Central oceanic regions traditionally were regarded as biological deserts (Parsons *et al.* 1977, Eppley 1981), with small standing stocks of living organisms and correspondingly little productivity (Kerr 1986). Recently, however, studies have indicated that primary production rates in the open ocean may be rapid (Sheldon and Sutcliffe 1978, Morris 1981), and in oligotrophic waters off Hawaii production rates approach the maximum values measured in laboratory studies (Bienfang and Takahashi 1983, Laws *et al.* 1984). This has resulted in some controversy regarding the accuracy and reliability of the different methods used to measure primary productivity (Eppley 1981, Sheldon 1984, Smith *et al.* 1984), as well as the underlying processes determining production rates (McCarthy and Goldman 1979, Goldman *et al.* 1979, Jackson 1980, Landry *et al.* 1984, Kanda *et al.* 1985). I examine this controversy from a systems viewpoint, in which I assume that the underlying size-dependent relationships that have been used to simulate coastal food webs in preceding chapters (Chapters 4 and 5) also apply to oceanic systems.

SIMULATION OF AN OCEANIC FOOD WEB

Oceanic waters are characterised by a small but relatively constant nutrient supply (Kanda *et al.* 1985) resulting from the diffusion of nitrogen from below the thermocline in a water column that is persistently stratified (Bienfang 1985). It is difficult to estimate how fast nutrients are entrained from depth in oceanic waters (Dortsch *et al.* 1982, Kanda *et al.* 1985), and no information on the diffusion rates or new nitrogen supply rates could be found in the literature. I use the generic model described in Chapters 3 and 4 to simulate an oceanic plankton community by assuming a continuous new nitrogen input of 0.35 mg-at $N.m^{-3}.d^{-1}$ and a temperature of 25°C.

MODEL OUTPUT AND DISCUSSION

Ambient concentrations of nitrogenous nutrients such as ammonia and nitrate are often below detection limits in oligotrophic oceanic waters, implying that they are rapidly taken up (McCarthy and Goldman 1979). Dissolved nitrates typically have ambient concentrations of 0.01 mg-at $N.m^{-3}$, although they can reach concentrations of 3.22 mg-at $N.m^{-3}$ (Kanda *et al.* 1985). In

the North Pacific central gyre, nitrogen concentrations have been estimated to be < 0.05 mg-at.m^{-3} (Eppley *et al.* 1977), although urea concentrations of 0.35 mg-at N.m^{-3} have been measured in northwestern Pacific central waters (Mitamura and Saijo 1980). NH_4^+ concentrations in Hawaiian waters are approximately 0.16 mg-at N.m^{-3} (Bienfang and Takahashi 1983). These measured values are of the same order of magnitude as the simulated regenerated nitrogen concentrations of 0.011 mg-at.m^{-3} (Table 6.1).

Table 6.1. Standing stocks and production rates of different sizes of phytoplankton, and standing stocks and numbers of bacterioplankton in oligotrophic oceanic waters after a 25-day simulation, when the model system is approaching steady state. Ambient concentrations of regenerated nitrogen are presented. (New nitrogen is continually input at a rate of 0.35 mg-at. N.m^{-3}.d^{-1}).

	Standing stock (mg C.m^{-3})	Numbers	Production (mg C.m^{-3}.d^{-1})	Concentration (mg-at N.m^{-3})
Phytoplankton (Total)	3.026	-	1.25	-
Phytoplankton (0.2-1 µm)	2.972	-	-	-
Phytoplankton (1-5 µm)	0.054	-	-	-
Bacterioplankton	0.060	$1.6x10^6$	-	-
Regenerated Nitrogen	-	-	-	0.011

Phytoplankton size structure

The biomasses in each of the phytoplankton size classes in the simulation were initialized with values of $1x10^{-5}$ pg C (0.2-1 and 1-5 µm), and 2 pg C (5-25 and 25-125 µm). Despite the presence of large-celled phytoplankton at the start of the simulation, after 25 days a community of pico-phytoplankton (< 5 µm) results, comprising mainly cells in the size category 0.2-1 µm (Table 6.1). This is consistent with the size structure of oceanic phytoplankton, which are usually < 3 µm (Eppley *et al.* 1969, Bienfang and Takahashi 1983, Herbland *et al.* 1985). However, the simulation results appear to overestimate the relative importance of the cells < 1 µm. In Hawaiian

waters, 80 % of the total chlorophyll is contained in cells < 5 μm, and 50 % of the total chlorophyll in cells < 1 μm (Takahashi and Bienfang 1983, Bienfang 1985). This has been partially ascribed to the competitive advantage of small cells compared to large cells due to fast nutrient assimilation rates and growth rates, and negligible losses due to sinking (Parsons and Takahashi 1973, Bienfang and Takahashi 1983, Bienfang 1985). This competitive advantage is consistent with the simulation results.

"Steady state" standing stocks

The simulated phytoplankton standing stocks (approximately 3 mg $C.m^{-3}$, Table 6.1) are of the same order of magnitude as the varying field estimates. At six stations off Hawaii, Laws *et al.* (1984) measured phytoplankton standing stocks ranging from 3.2 to 150 mg $C.m^{-3}$, and in the equatorial Atlantic Ocean Herbland *et al.* (1985) measured chlorophyll standing stocks of approximately 5 mg $chl.m^{-3}$, which are equivalent to approximately 150 mg $C.m^{-3}$, assuming a carbon to chlorophyll ratio of 30 (Raymont 1980). The simulated phytoplankton crop is thus at the small end of the range of measured values. This may be due to the apparently unrealistic dominance of cells < 1 μm in the simulation; small cells have a smaller standing stock than large cells supported by the same nutrient concentrations (Chapter 3). Alternatively, the discrepancy may simply reflect the fact that the structure of the model system is very simple, and nutrient enhancements through excretion by zooplankton or fish passing through an area are of necessity excluded from the model.

Simulated bacterioplankton standing stocks are equivalent to $1.6x10^6$ $cells.l^{-1}$ (Table 6.1), which is less than measured counts of $6.5x10^8$ $cells.l^{-1}$ (Laws *et al.* 1984). Large bacterioplankton standing stocks are possible in the model system; a standing stock of up to $5.3x10^9$ $cells.l^{-1}$ occurs 2 days after the start of the simulation, from a very small initial standing stock. Only "steady-state" values are presented in Table 6.1.

Rates of primary production

Simulated rates of primary production are approximately 1.25 mg $C.m^{-3}.h^{-1}$ (Table 6.1). Measured phytoplankton production rates in Hawaiian waters range from 0.32 to 52 mg $C.m^{-3}.h^{-1}$ for the < 3 μm size fraction (Bienfang and Takahashi 1983, Takahashi and Bienfang 1983) and 0.35 to 11 mg $C.m^{-3}.h^{-1}$ for the total phytoplankton community (assuming a 12 hour day, Laws *et al.* 1984). In the Sargasso Sea, Sheldon *et al.* (1973) estimated primary production rates to be 2.8 mg $C.m^{-3}.h^{-1}$. Production to biomass ratios in the simulated community are large, approximately 5 d^{-1} assuming continuous growth through a 12-hour day. This value is slightly larger than other estimates of 0.89 to 1.50 d^{-1} (Laws *et al.* 1984) and 3 d^{-1} (Sheldon 1984), but this may be explained by the dominance of primary production in the model community by phytoplankton < 1 μm, which have fast production rates but small biomasses.

The model output is consistent with the evidence that specific production rates in oceanic waters are probably fast rather than slow, in keeping with the observation that small cells characteristically have fast specific growth rates. Jackson (1980) suggested that oceanic pico-phytoplankton have lost the ability to grow rapidly, but Bienfang and Takahashi (1983) refute this statement on the basis of their studies in Hawaiian waters. The maximum specific instantaneous growth rates of individual cells in the simulation are estimated to be 30 d^{-1} for sizes 0.2-1 μm and 9 d^{-1} for sizes 1-5 μm at 25 C (derived empirically, Chapter 1). This is faster than the simulated population growth rate of 5 d^{-1}, reflecting the damping influence of low nutrient concentrations on growth rates. The phytoplankton cells, although growing rapidly, grow at sub-optimal rates, as was inferred by Landry *et al.* (1984) for growth of bacteria and flagellates in Hawaiian waters. The ability of small cells to grow rapidly in low-nutrient conditions is due to their small half saturation constants, estimated empirically to be 0.00026 mg-at $N.m^{-3}$ for sizes 0.2-1 μm and 0.032 mg-at $N.m^{-3}$ for sizes 1-5 μm (Chapter 2).

CONCLUSIONS

The hypothesis that phytoplankton in warm, surface oceanic waters have fast primary production rates is supported by size-based arguments. Small ambient nutrient concentrations result in a phytoplankton community dominated by small cells, which have fast specific growth rates, even when growing sub-optimally. In real systems the basic model is complicated by other factors such as nutrient pulses caused by isolated mixing events and excretion by large zooplankton and fish, but these complications should modify the basic structure, not determine it. Sheldon *et al.* (1973) stated that if the definitive relationships that exist between growth rates, size and temperature could be formalized, it would not be necessary to rely on conventional measurements of rate processes to understand system functioning. This simple example shows how an holistic model can be used to analyse a system from a totally different perspective from that in which most data are collected, and thus provide an objective hypothesis with which field data can be compared.

SECTION 3

EXPLORING SYSTEM DYNAMICS

CHAPTER 7

AN EVALUATION OF CURRENT TECHNIQUES USED TO ESTIMATE PLANKTONIC PROCESSES FROM FIELD MEASUREMENTS

ABSTRACT

A numerical experiment is carried out in which at-sea sampling of a phytoplankton bloom is mimicked by "sampling" from the output produced by a simulation model. The aim of the experiment is to assess whether current methods of analysing field measurements to determine planktonic processes are valid. It is shown that size-fractionated sampling of primary production is essential to be able to identify the pathways and processes occurring in planktonic ecosystems. Pico-phytoplankton usually have fast production rates but small biomasses, and their model populations fluctuate on shorter time scales than do those of net-phytoplankton. Some of the assumptions that are implicit in the techniques used to analyse bacterioplankton - phytoplankton relationships are at times invalid, and result in erroneous conclusions. Some indices of community processes are similarly invalid unless integrated over time with a large enough data set. The use of simulation models as a tool to understand and analyse system behaviour, and to construct and test working hypotheses, should be an integral part of any field program, especially before field data are collected. Most inconsistencies and errors result from using a non-dynamic approach to analysing complex, dynamic biological systems.

INTRODUCTION

The proliferation of scientific journals and research programs in marine ecology without a concomitant increase in our comprehensive understanding of biological processes has been remarked upon by many authors (Sakshaug 1980, Peters 1983, Fenchel 1987). The collection of data *per se* appears to be the main aim of many field studies. Consequently, every data set is used to construct hypotheses, with little attempt being made to rigorously test these hypotheses or to develop new ones to accommodate disparate observations (Walsh *et al.* 1971). The tendency to collect data and then develop *a posteriori* hypotheses to account for the data is not only bad science, but also often results in inadequate data being collected (Eppley 1981, Harrison *et al.* 1983). For example, size fractionated measurements of phytoplankton crop and primary production routinely are carried out in many studies (e.g. Malone 1977, Furnas 1982, 1983, Bienfang and Takahashi 1983, Gieskes and Kraay 1983), but there are still many studies that do not distinguish phytoplankton on the basis of body size (e.g. Estrada 1980, Harding *et al.* 1982, Holligan *et al.* 1984). Pico- and nano-phytoplankton appear to be ubiquitous components of phytoplankton, but because of their small size they are generally not available as food for large grazers such as copepods. In food web studies it is necessary to measure the available production, and the result of ignoring size effects may result in errors in interpretation of the data.

Biological systems incorporate complex interactions, and it is necessary to take all of these into account when analysing the relationships of one component of the system to all the others (Lehman 1980, Lehman and Sandgren 1985, Pengerud *et al.* 1987). Although efforts are usually made to isolate aspects of the system in order to study them, this is not always possible. For example, the study of the production of dissolved organic carbon (PDOC) by phytoplankton during normal growth has been hampered by the rapid utilization of the PDOC by bacterioplankton in the experimental incubations (Joint and Morris 1982, Jensen 1983). This problem also applies to carbon-14 incubations which estimate primary production, but which cannot exclude predators of pico- and nano-phytoplankton (e.g. Furnas 1982). The predatory interactions often cannot be

separated from the production rates being measured, and the accuracy of the estimates is often questionable (Sheldon *et al.* 1973, Smith *et al.* 1984).

Simulation models are useful tools for critically examining sampling and analytical procedures; they provide readily available "data", the "true" nature of which is known, and against which the interpretation of the data can be compared. Furthermore, output can be obtained more than once i.e. sampling can be repeated. In this chapter I show that some of the current techniques used to analyse and interpret data result in erroneous conclusions, either because sampling is inadequate, or because the dynamics of the system are not taken into account. It is very difficult to conceptualize all of the loops and feedbacks occurring in planktonic ecosystem processes. By using specific examples I attempt to show how incorrect answers can be obtained, and motivate for a more dynamic approach, incorporating the use of simulation models.

METHODS

Data are obtained from the output of a simulated phytoplankton bloom after upwelling (Chapters 4 and 5). The simulated phytoplankton bloom develops and decays within 14 days. "Samples" are taken four times during the course of the bloom. Phytoplankton and bacterioplankton standing stocks are calculated from instantaneous measurements, and primary production is estimated by integrating instantaneous production rates over a quarter-day period, mimicking a standard incubation (Strickland and Parsons 1968). Bacterioplankton production is calculated as the difference between PDOC taken in and carbon respired, and is similarly integrated over a quarter-day time interval.

RESULTS AND DISCUSSION

Standing stocks

"Sampled" phytoplankton and bacterioplankton standing stocks are superimposed on the "real" data in Fig. 7.1. As is often done, the points have been joined by lines. This forces an unfounded dynamic pattern on the data, which is seen to be incomplete (Fig. 7.1).

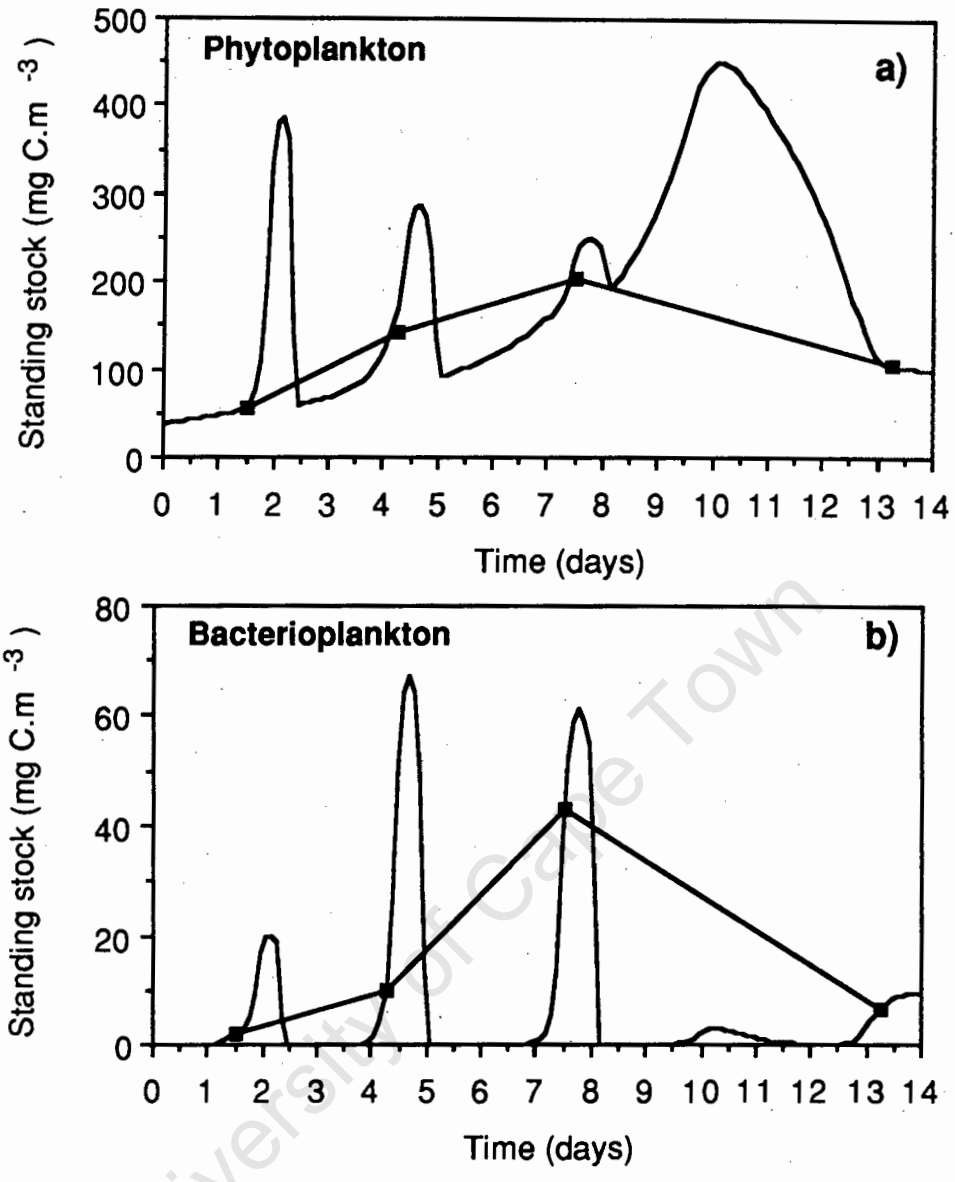

Fig. 7.1. Simulated ("real") standing stocks and four "samples" from a phytoplankton bloom after upwelling. a) Phytoplankton. b) Bacterioplankton.

This example reflects an extreme case in the sense that the samples were not taken randomly, but were selected to co-incide with certain features of the bloom. The magnitudes of the bacterioplankton fluctuations are probably not realistic (see Chapters 4 and 5), but the time scales of the changes (less than one day) have been observed in some field and experimental studies (e.g. Lochte 1985, Van Wambeke and Bianchi 1985). The intervals between sampling periods in Fig. 7.1 are not unusual for typical sampling programs, where conclusions are, of necessity, often based on samples collected at intervals of a few days (e.g. Holligan *et al.* 1984, Harrison *et al.* 1987) or weeks (e.g. Harrison *et al.* 1983, Hargrave *et al.* 1985). The results indicate that caution

should always be exercised in delineating continuity to data that have been collected as discrete samples.

Size-fractionated primary production

Size differences in primary production are shown in Table 7.1. At the four different sampling times, the instantaneous rates of primary production of the total phytoplankton community change dramatically. It is evident that in these samples most of the standing stock consists of the largest phytoplankton size class (25-125 μm), which has the slowest production rate. However, the major proportion of the primary production is due to pico-phytoplankton. These small cells may be overlooked in field studies, resulting in an overestimate of production by the large cells and incorrect conclusions about the carbon available to consumers such as copepods which consume the large-celled phytoplankton. In the sample of day 13, the net-phytoplankton (25-125 μm) have a negative production (i.e. respiration losses exceed carbon gains), but the total community has a positive P/B ratio. In a standard field experiment, the large, obvious cells could be inferred to be growing, whereas size fractionation indicates that their carbon reserves are actually being depleted.

The P/B ratios of pico-phytoplankton appear to be unrealistically large (Table 7.1). This is because primary production rates are *instantaneous* rates, and do not represent total *daily* production rates. This distinction seldom is made. Pico-phytoplankton may only have a daily production rate of 164.4 mg $C.m^{-3}.d^{-1}$ (day 4, Table 7.1) if their growth continues at the same rate for the entire day. In the model, pico-phytoplankton standing stocks decrease very rapidly, and their P/B becomes negative, so that actual daily production is much less than that indicated by the instantaneous rates.

In general, it is invalid to multiply measured instantaneous rates for any process by an hourly factor to obtain daily rates, unless the changes have been investigated through the entire day (Eppley 1981), and a correction factor has been estimated. Although researchers generally are aware of the dangers of extrapolations, these are often forgotten when data are used in a whole

system context, where units are standardized and simple linear conversions are used to change units from hours to days, with little cognisance of the assumptions implicit in such calculations.

Table 7.1. Size fractionated primary production and standing stock estimates of samples taken at different times during the simulated phytoplankton bloom. Standing stocks are those at the start of each time interval.

Time (days)	Phytoplankton (µm esd)	Production (mg $C.m^{-3}.d^{-1}$)	Standing stocks (mg $C.m^{-3}$)	P/B (d^{-1})
1.50 - 1.75	0.2 - 1	84.2	2.05	41
	1 - 5	0.20	0.038	5.3
	5 - 25	0.56	0.47	1.2
	25 - 125	13.6	51.8	0.26
	TOTAL	**98.6**	**54.4**	**1.8**
4.25 - 4.50	0.2 - 1	164.4	3.8	43
	1 - 5	266.0	52.4	5.1
	5 - 25	4.81	4.26	1.1
	25 - 125	17.5	81.6	0.22
	TOTAL	**453**	**142**	**3.2**
7.50 - 7.75	0.2 - 1	207.6	24.2	8.6
	1 - 5	-	-	-
	5 - 25	27.9	57.2	0.49
	25 - 125	7.84	126.4	0.062
	TOTAL	**243**	**205**	**1.2**
13.25 - 13.50	0.2 - 1	18.7	5.53	3.4
	1 - 5	-	-	-
	5 - 25	0.26	3.63	0.072
	25 - 125	-6.26	96.2	-0.065
	TOTAL	**12.96**	**105**	**0.123**

Relationships between bacterioplankton and phytoplankton

A number of "standard" calculations are commonly carried out in order to assess the role of bacterioplankton (and microzooplankton) in the plankton community. Correlations between the standing stocks of heterotrophs and phytoplankton are used to identify possible relationships (e.g. Fig. 7.2).

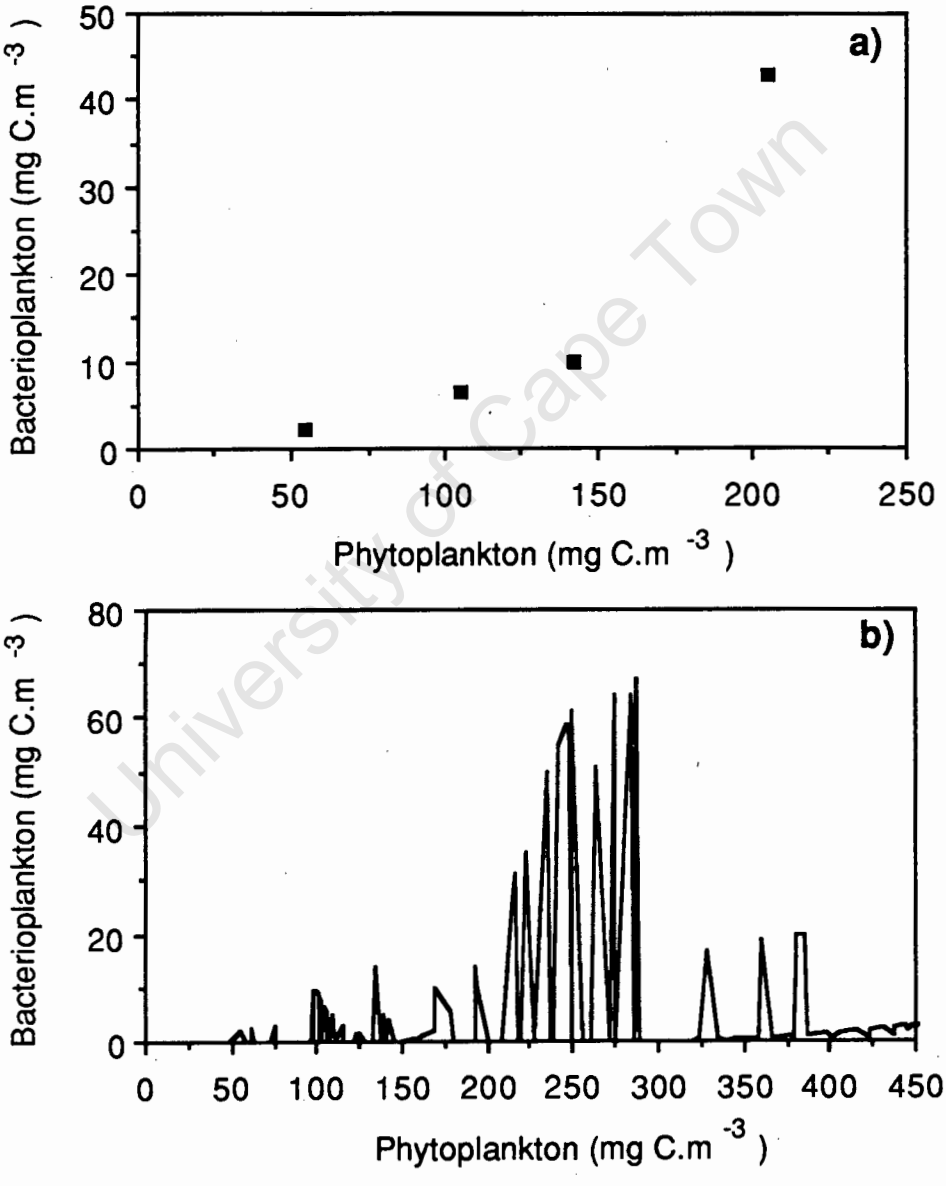

Fig. 7.2. Scatter plot showing the relationship between standing stocks of phytoplankton and bacterioplankton. a) "Samples" from the simulation. b) "Real" relationship (from simulation results).

Often, these relationships are assumed to be causal. For example, a relationship between bacterioplankton and phytoplankton may be expected, on the basis that bacterioplankton rely on carbon produced by phytoplankton for growth. This premise is only partially true, because bacterioplankton growth often is limited by nitrogen and not carbon, and predation by zooflagellates can also limit bacterioplankton populations (Pengerud *et al.* 1987). Simple correlations may overlook the effect of time lags, and assume that all effects take place instantaneously. Clearly, a relationship between the standing stocks of phytoplankton and bacterioplankton in the simulation results does occur (Fig. 7.2). However, this does not imply that the relationship is causal, because in the simulation the relationship is mainly due to the fact that pico-phytoplankton and bacterioplankton are controlled by the same predators. The fitting of simple functions (often linear) to such data is tempting, but should be carried out with caution, bearing in mind the assumption of continuity that is implicit in such a procedure.

The amount of primary production utilized by bacterioplankton is a subject that has received much attention in recent years (Joint and Morris 1982). In order to assess carbon utilization by bacterioplankton a simple procedure often is followed (e.g. Larsson and Hagstrom 1982, Eberlein *et al.* 1983, Lucas *et al.* 1987), using field measurements of phytoplankton and bacterial production (Table 7.2). Bacterial consumption is calculated by:

$$\text{Consumption} = \text{Production} / \text{Net Growth Efficiency (NGE)} \quad \ldots\ldots\ldots\ldots (7.1)$$

where NGE for bacterioplankton utilizing PDOC is assumed to equal 60 % (Lucas 1986). PDOC production usually is calculated as some fraction of primary production; this fraction is seldom known, and a value of 30 % has been used in the present simulations (Chapter 3). Comparing PDOC production with bacterial consumption rates (Table 7.2), it appears that consumption is larger than production on days 4, 7 and 13. This often leads to the conclusion that PER is larger than 30 % or that bacterioplankton are utilizing some other source of carbon, such as particulate carbon. This conclusion appears to be supported by the fact that the discrepancy becomes larger towards the end of the bloom, when bacteria are "expected" to be utilizing senescent phytoplankton cells.

Table 7.2. Estimated relationships between phytoplankton production and bacterioplankton production at different days during the simulated phytoplankton bloom. All production and consumption units are in mg $C.m^{-3}.h^{-1}$.

Time (days)	Bacterioplankton Production	Bacterioplankton [1]Consumption	Phytoplankton Production	[2]PDOC Production	% Primary Production
1.50-1.75	0.19	0.32	4.11	1.23	4.6
4.25-4.50	4.16	6.93	18.9	5.67	22.0
7.50-7.75	4.07	6.78	10.1	3.03	40.3
13.25-13.50	0.26	0.43	0.54	0.16	48.1

[1] Consumption = Production / 0.60 (Lucas 1986)
[2] PDOC Production = 0.30 x Primary Production (Chapter 3)

In the simulation, neither of these conclusions is correct; PER *is* 30 % and bacterioplankton are *only* utilizing PDOC. The misinterpretation arises because bacterioplankton not only utilize instantaneous production, they also use accumulated production in the form of ambient PDOC concentrations. Consequently, snapshot measurements of production rates do not contain sufficient information to be able to assess the carbon flow dynamics. Standing stocks and concentrations should also be included in the calculations.

The use of equation (7.1) or similar, involves two critical assumptions. The first is that NGE is a constant. When food is abundant, NGE may be large (Chapter 1). However, when food becomes limiting NGE decreases, and this index should only be applied if food is known to be non-limiting. The second assumption is more subtle. NGE is not a measurable quantity, but is a derived index, and consequently is dependent on the processes that have been used to define it viz. consumption and respiration (Lynch 1977). Production is the difference between net consumption and respiration. Equation (7.1) can be rewritten as:

$$NGE = (Consumption - Respiration) / Consumption \quad (7.2)$$

Total carbon consumption by an animal population per unit time depends both on the food concentration and the population size, whereas population respiration is dependent only on

population size. When food is abundant, the dependence of consumption rates on food concentrations is small. However, when food is scarce, respiration rates increase relative to consumption rates and NGE decreases, and can become negative. For this reason, community indices such as "% respiration" (Lochte and Turley 1985, Bauerfreind 1985), used to assess how much of production is respired, should only be used for periods when food is known to be abundant. Such conditions are probably not the norm in nature, and these indices of community dynamics should be used with caution, especially when making comparisons between different regions.

CONCLUSIONS

The interpretation of data has been described by Sakshaug (1980) as a "... so far ... underdeveloped field of phytoplankton ecology". The examples that have been discussed highlight problems that are found in many ecological studies. Plankton ecologists study complex biological systems with many rapid interactions. Because it is difficult to conceptualize all pathways and components, a static approach has been adopted by many researchers to analyse field data. This chapter has shown the dangers of such an approach. A feasible alternative is to make extensive use of simulation models, both in constructing hypotheses and in testing their feasibility.

SYNTHESIS - CHAPTER 8

TOWARDS AN UNDERSTANDING OF THE DYNAMICS OF MARINE PLANKTONIC FOOD WEBS

ABSTRACT

Output from size-based simulation models is used to examine the dynamics of food webs in the euphotic zone of coastal and oceanic waters. The roles of different sizes of phytoplankton in primary production are shown to change with the nutrient status of the water in simulation models. In coastal waters, pico-phytoplankton (< 1 μm) dominate in the model systems when nutrients are limiting, but when nutrients are abundant, model pico-phytoplankton populations are controlled by predators, and display rapid fluctuations. Net-phytoplankton populations (here defined as 5-125 μm) increase in eutrophic waters, because nutrient concentrations are large enough to sustain the large cells and they are no longer outcompeted by the predator-controlled small-celled pico-phytoplankton. In oceanic waters pico-phytoplankton dominate, and model output is consistent with the hypothesis that oceanic phytoplankton have rapid rates of primary production. Large amounts of carbon may be taken up by bacterioplankton, but much of this is rapidly respired, and thus lost to the rest of the food chain. Microheterotrophs (< 125 μm) are important in nitrogen regeneration, because of their rapid metabolism. A hypothetical planktonic food web is presented in which all size classes of micro-heterotrophs are capable of utilizing phytoplankton directly. Consequently, the microbial loop from bacterioplankton to large zooplankton and fish is the longest possible route in the food web, and probably only occurs in relatively stable environments. In upwelling systems, the components of the microbial loop and mesozooplankton seldom co-occur, because of rapid fluctuations in their populations, and most energy passes through short food chains. The large productivity of upwelling systems may be due to short-lived but very efficient matches in time and space between dense phytoplankton assemblages and their zooplankton and fish predators. Trophic efficiencies are predicted to be as large as 50 % in upwelling regions, due to the dense food aggregations that occur as a result of the rapid development of frequent phytoplankton blooms during the upwelling season.

INTRODUCTION

One of the goals of ecology is to derive general principles which serve as the basis for understanding the functioning of whole ecosystems. For many years the marine planktonic food chain was believed to be one of the best understood systems in ecology (Steele 1974, quoted by Fenchel 1987), but today few would dispute that the classic diatom-copepod-fish food chain does not adequately describe all processes occurring in the plankton (Williams 1981, Landry *et al.* 1984). This hypothesis of food-chain structure, exemplified in the model of Steele (1974) for a North Sea food chain, was revised largely as a result of improved technology; new reliable methods of assessing standing stocks and production of very small organisms (see Joint and Morris (1982) for a review) assigned a hitherto unsuspected importance to pico- and nano-plankton, both as primary producers and as consumers. In the last 10 years a number of field and laboratory studies have been undertaken to try and elucidate the role of pico- (< 2 μm), nano- (2-20) μm and micro- (20-200 μm) plankton in marine planktonic communities. The result has been a number of conflicting hypotheses as to the role of very small autotrophs and heterotrophs in carbon flow and nutrient (principally nitrogen) regeneration in planktonic ecosystems.

Marine ecologists generally recognise the need to distinguish between different sizes of phytoplankton, and many studies in recent years have used size-fractionated samples to estimate standing stocks and primary production (e.g. Malone 1977, Furnas 1982, 1983, Larsson and Hagstrom 1982, Bienfang and Takahashi 1983, Gieskes and Kraay 1983, Bienfang 1985, Herbland *et al.* 1985, Probyn 1985; 1987). In both coastal and oceanic waters small phytoplankton have been identified at times as comprising the major proportion of standing crop (e.g. Gieskes and Kraay 1983, Mitchell-Innes and Winter 1987) and of primary production (Glibert *et al.* 1982, Joint and Pomroy 1983). However, the presence of autotrophic pico- and nano-plankton within the food web is still ignored in many system models, which class phytoplankton as a single component when representing ecosystem structure (e.g. Tett *et al.* 1986, Jones and Henderson 1987). Thus, despite the evidence to the contrary, conventional diatom-dominated phytoplankton communities still are used as the basis for many food-web models.

The focus of attention away from pico-phytoplankton may be partially due to the focus on the role of bacterioplankton, which are the same size as pico-phytoplankton but are heterotrophs, obtaining their carbon from dissolved amd particulate organic matter. Traditionally regarded as remineralizers, bacterioplankton attained a potentially important role in utilizing the products of primary production (Wolter 1982), and the microbial loop (Azam *et al.* 1983) was hypothesized as an important pathway through which carbon fixed during photosynthesis eventually reached large organisms (Sorokin 1979, Gast 1985, Laake *et al.* 1983b, Jones and Henderson 1987, Lochte and Turley 1985). However, some studies have questioned the validity of this hypothesis, claiming that the microbial loop is a very inefficient transfer route (Joint and Pomroy 1983, Landry *et al.* 1984) or even a cul-de-sac, acting as a "sink" rather than a "link" (Ducklow *et al.* 1986, Smith *et al.* 1984).

The importance of the microbial loop in nutrient cycling has been the source of some controversy (e.g. Joint and Morris 1982, Lucas 1986). Small organisms with fast growth rates appear to remineralize nutrients rapidly, and field studies have demonstrated the importance of organisms < 10 μm in nitrogen regeneration (Harrison 1978, Glibert 1982, Probyn 1985; 1987). It was initially believed that bacteria were primarily responsible for nitrogen regeneration by this size fraction (e.g. Newell and Linley 1984), but recent work has implicated bactivorous protozoa as the chief agents of nitrogen regeneration (Caron *et al.* 1985, Andersson *et al.* 1985, Goldman *et al.* 1985). However, modelling studies by Moloney *et al.* (1986) and Newell *et al.* (1988) suggest that in dynamic systems there is a time sequence in which different size fractions play roles of varying importance in nitrogen regeneration. Because most data are collected as discrete samples within a dynamic process, different data sets appear to support different hypotheses.

There is a vast literature describing planktonic data from many disparate systems, and providing a spectrum of possible pathways for carbon and nitrogen flows through plankton comunities. In this chapter I assume that all of these data sets are derived from systems which are governed by the same basic processes (viz. carbon fixation, respiration, nitrogen uptake, excretion and grazing), and that the structures of the food webs and the rates of all the processes are determined by the sizes of the organisms involved. I use output from size-based simulation models

of typical coastal and oceanic food webs to examine the dynamic features of planktonic food webs, and to resolve some of the controversies surrounding the major pathways of carbon and nitrogen flows. I discuss the importance of phytoplankton cell sizes in determining production rates, and discuss the role of the microbial loop in carbon flows and nitrogen regeneration. An hypothesis is developed to explain the high productivity of pelagic fish in upwelling systems, and a model is presented which summarises the dynamic features of carbon and nitrogen flows in planktonic ecosystems.

THE SIZE STRUCTURE OF PHYTOPLANKTON COMMUNITIES

Pico-phytoplankton have fast growth rates and and take up nutrients efficiently at low ambient concentrations (Chapters 1 and 2). They appear particularly suited to outcompete large cells and dominate phytoplankton assemblages, but in nature large cells also occur, so there must be some factors that favour the growth of large cells. Some of these factors can be explained by body size. Kooijman (1986) used body-size relationships to model components of the energy budget of an animal. He concluded that the environment will select for small organisms when food concentrations are consistently reduced, because small organisms are efficient at taking up food at low ambient concentrations. However, in environments in which food is supplied in pulses, the pulses interspersed by conditions of little or no food, large organisms will dominate, because they have large storage capacities, and are well suited to surviving periods of starvation (Kooijman 1986). A similar argument can be used to relate phytoplankton cell-size to nutrient concentrations in the water.

The size-based model output shows that pico-phytoplankton dominate model systems when nutrients are limiting, because large phytoplankton cannot successfully compete for limited nitrogen (Parsons and Takahashi 1973, Chapter 4). In periodically eutrophic waters (e.g. upwelling regions), large phytoplankton cells may dominate, because they survive periods of reduced nutrients by developing dormant cysts, which form the seeding crop when nutrients are introduced to the euphotic zone (Estrada and Blasco 1985, Chapter 4). The formation of dense cysts has been suggested as a mechanism by which net-phytoplankton ensure that they are not

advected off the continental shelf, but sink rapidly to the bottom to await a mixing or upwelling event that will transport them into the euphotic zone in nutrient-rich water (Anderson *et al.* 1985). Pico-phytoplankton presumably do not have as strong a selection pressure as net-phytoplankton to form dense cysts to ensure that they remain on the continental shelf, because thay are able to grow in nutrient deficient oceanic waters (Chapter 6).

Size differences in phytoplankton assemblages may be partially attributed to nutrient concentrations. Differences in nutrient uptake capacities explain why large cells typically only are found in eutrophic coastal waters, but not why small cells do not outcompete large cells in these regions. Model output (Chapters 3, 4 and 5) indicates that predatory control of small cells precludes them from dominating for long periods in eutrophic waters. Small cells are eaten by small grazers, and are preyed upon at faster rates than are large cells, which are grazed by relatively slow-growing, large zooplankton (Chapter 1). In stratified coastal waters with a relatively stable nutrient supply, such as on the Agulhas Bank (Chapter 4), pico-phytoplankton are present as a variable proportion of the phytoplankton community. In eutrophic coastal areas, pico-phytoplankton may dominate the phytoplankton for limited periods, as was shown by the upwelling model (Chapter 4). However, predator control sets up oscillations and prevents them from persisting, and large phytoplankton cells form the bulk of protracted phytoplankton blooms.

THE ROLE OF THE MICROBIAL LOOP

Simulation studies allow one to view a system as a functional unit, and to assess the potential roles of different components. In this section I discuss the average role of the microbial loop in planktonic food webs on the basis of output produced by simulation models (Chapters 4 and 5). Average is used here in a stochastic sense, to express the energy flow or nutrient cycling, integrated over a suitable time interval, that follows any given pathway. There has been much speculation about the role of bacterioplankton in carbon transfer in the food web (see Joint and Morris 1982). To date, very little experimental work has been conducted to rigorously test the hypotheses, and much of the speculation is based on extrapolations from detailed studies on bacterioplankton, and not on the food web as a whole. This is the essence of a reductionist

approach. In the whole-system analysis used in this thesis, it has been shown that the dynamic oscillating nature of microplankton systems precludes the microbial loop from being an efficient pathway for carbon flows to large zooplankton and pelagic fish.

The average carbon flows through the bacterioplankton in the Agulhas Bank and the west coast upwelling simulations (Fig. 5.14, Chapter 5) indicate that very little of the carbon taken up by the bacterioplankton reaches large zooplankton. This supports the experimental work of Ducklow *et al.* (1986), who concluded that bacterioplankton act as a sink for carbon. Carbon is rapidly respired by micro-organisms, because of their fast metabolic rates (Chapter 1). The size fractions that comprise the different trophic steps in the microbial loop exhibit rapid population fluctuations (Chapters 3 and 4), and there are temporal mismatches between predator and prey populations, resulting in production being "wasted" in respiration (Chapter 5). The importance of mismatches in time has been overlooked in many system studies, which tend to view systems as static entities. Temporal mismatches appear to be important in eutrophic waters, where population fluctuations can be rapid (Chapter 4). It has been shown in network analyses of simulated plankton communities that up to six trophic positions can occur in microplankton communities (Chapter 5), but only the first three trophic positions are important as pathways of material flow. Temporal mismatches occur chiefly between populations of different sizes of heterotrophs, becauset there is a relatively persistent population of autotrophs. Consequently, the first two trophic steps dominate carbon flows in simulated food webs, and it is probable that a similar situation occurs in nature.

The fast metabolism of small organisms results in carbon rapidly being lost in respiration. This attribute of the microbial loop makes it inefficient in carbon transfer, but contributes to nitrogen recycling. If equivalent amounts of nitrogen are given off in excretion when carbon is respired (Chapter 3), the microbial loop would be important in nitrogen recycling, because of the rapid metabolic rates of small organisms. In Chapter 5 the importance of different size fractions in regenerating nitrogen in the model systems is discussed. All components of the microbial loop are shown to be important as remineralizers. However, because their populations undergo rapid fluctuations, their importance as remineralizers is transitory, and generally each size fraction

dominates, but at different times. Discrete samples from nature do not have sufficient resolution to test hypotheses about dynamic processes like recycling (see Chapter 7). Extrapolations from such data result in conflicting hypotheses about processes that are really part of a continuum.

WHY ARE UPWELLING SYSTEMS PRODUCTIVE?

Upwelling regions in eastern boundary current areas support the most productive commercial fisheries in the world (Cushing 1971). Ryther (1969) attempted to explain this very high productivity on the basis that the food chains in these areas are very short, encompassing only one or two trophic steps. However, with the introduction of the microbial loop hypothesis into the food web, a previously ignored pathway for primary production had to be incorporated into the calculations, which then did not balance. Assuming that the estimates of fish production are correct, this imbalance may be corrected in three ways:

1) Estimates of primary production may be increased, and trophic efficiencies left unchanged. This implies that primary production has been underestimated in the past (Jones 1984, Fenchel 1987), and the "unmeasured" production is the proportion that is lost in the microbial loop.
2) Estimates of primary production and trophic efficiencies may be left unchanged, and the additional microbial loop pathway can be incorporated as a very efficient pathway. Primary production then reaches fish through an alternative but efficient route. The problem with this hypothesis is that in each transfer step some energy or material is dissipated, so the gains decrease as one adds more steps into the food web.
3) Primary production may be left unchanged, but trophic efficiencies made larger than is generally believed. Very little primary production is directly available to pelagic fish, but this production is efficiently transferred. The remainder is channelled to the microbial loop, because much primary production is by organisms too small to be eaten by zooplankton such as copepods. This third option will be discussed below, because it appears to be viable, based on my studies with simulation models (Chapter 5), and on experimental data of the feeding of pelagic fish in the southern Benguela region (James 1988).

Food concentrations and trophic efficiencies

The growth and production of any organism is a function of the amount of food that it eats. It is well known that ingestion rates saturate at large food concentrations (Mullin *et al.* 1975, Chapter 2) and are sub-maximal when food concentrations are small. Trophic efficiencies are defined as the amount of production at one trophic position that is utilized by the next trophic position. In marine food chains, trophic efficiencies are generally assumed to 10 % . However, many factors will affect the efficiency of transfer, and it is invalid to assume that trophic efficiency is a constant (May 1979).

Trophic efficiencies are usually based on energy flows, but carbon flows will be used in the following example. Consider a system with three trophic categories, where the trophic categories refer to the integer number of trophic transfers that occur in the food web, starting with some external input (Ulanowicz and Kemp 1979). In the pelagic environment, this system might represent a three step trophic transfer from net-phytoplankton to zooplankton to fish (Fig. 8.1).

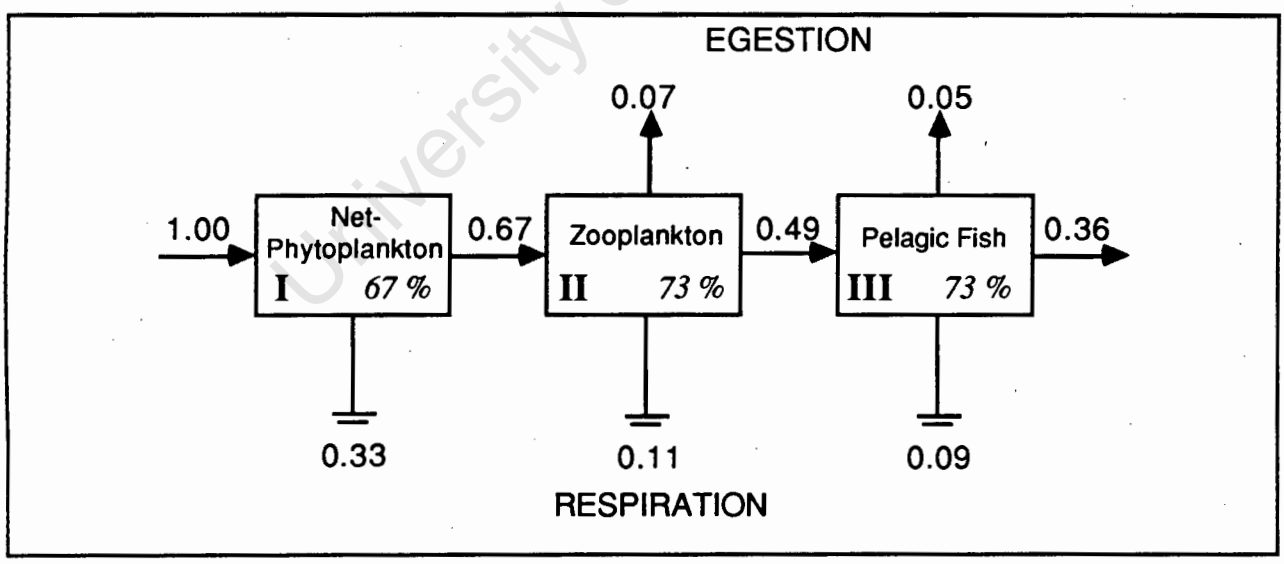

Fig. 8.1. Theoretical carbon flows in an idealized upwelling food chain. The trophic categories are in Roman numerals, and trophic efficiencies are italicized.

Carbon fixation during photosynthesis represents the external input to the system. Optimal conditions for carbon fixation occur when nutrients and light are not limiting. Under these

conditions, a unit of carbon may enter trophic category I during photosynthesis (Fig. 8.1). Some of this carbon will be respired, and according to mass balance calculations this should be about 33 % of primary production under optimal conditions (Chapter 1). If it is assumed that sinking and other losses are negligible in this ideal situation, 0.67 units are left in the first trophic category, and are available to trophic category II. If all 0.67 units enter the second trophic category, with an assimilation efficiency of 90 % (Chapter 1), 0.60 units are retained. Under the optimal conditions that are assumed to pertain, 19 % will be respired (Chapter 1), and the remainder made available to the next trophic category. Again, 10 % of this is egested and 19 % is respired, but 0.49 units of the original carbon fixed have reached the fish, and fish production is 36 % of primary production. Trophic efficiencies are large; 67 % in trophic category I and 73 % in trophic categories II and III. This food chain is thus very efficient.

These ideal conditions do not persist in nature. However, in order to approach the ideal described in Fig. 8.1, an important factor is that food densities should be large, because the concentration of available food is an important factor governing the ingestion rate (Chapter 2). In the southern Benguela region, phytoplankton blooms develop rapidly after upwelling, reaching maximum standing stocks of up to 1600 mg $C.m^{-3}$ after 3-5 days (Brown and Hutchings 1987b, Chapter 4). If these patches of phytoplankton are encountered by zooplankton swarms, feeding will be rapid, because maximum ingestion rates of zooplankton occur at food concentrations of approximately 300 mg $C.m^{-3}$ (Chapter 2). Similarly for fish schools encountering a zooplankton bloom. James (1988) has shown that in the southern Benguela region, anchovy *Engraulis capensis* may obtain all their daily carbon requirements within a few minutes at field concentrations of large zooplankton prey, with a net growth efficiency of up to 60 %, taking metabolic expenditure during active feeding into account. In the ideal model presented in Fig. 8.1, the net growth efficiency (NGE) of the third category (i.e. pelagic fish) is 73 % (NGE's correspond to trophic efficiencies in this example). Simulations of microplankton food chains in the upwelling area suggest that trophic efficiencies of the first two categories may be up to 62 % (Chapter 5). These are smaller than the theoretical maximum values, as would be expected, but are much larger than values

usually assumed to operate (e.g. Ryther 1969), suggesting that in dynamic systems high trophic efficiencies are possible.

The productivity of food chains is determined by the magnitude of primary production, the trophic efficiencies and the number of trophic steps. Ryther (1969) assumed that trophic efficiencies in upwelling regions were constant at 20 %, and that the great productivity of fish was due to the short food chain and the large initial primary production. Here it is suggested that trophic efficiencies in upwelling areas may be much larger than 20 %. The extent to which this high "efficiency" is dampened by mismatches between predator and prey in time and space is not known. The temporal and spatial scales on which important biological interactions occur need to be compared with those on which physical processes occur in upwelling regions. If one uses Ryther's (1969) estimate of primary production of upwelling regions and trophic efficiencies of 60 % for the short food chain, there is a large "surplus" of primary production. This surplus is either not available to pelagic fish, or reaches them through longer, less efficient pathways (James 1988). The average relative importance of the different pathways is also not known, but is likely to fluctuate in time and space.

A GENERALIZED PLANKTON MODEL

A modified version of the average food web described by Azam *et al.* (1983) is presented in Fig. 8.2. In this food web model, primary producers cover as wide a range of sizes as the micro-heterotrophs which form the microbial loop (Fig. 8.2). Thus, each of the components of the microbial loop eats not only heterotrophs but also phytoplankton cells smaller than itself. In general, all protozooplankton are capable of obtaining carbon from suitably-sized phytoplankton (Azam *et al.* 1983, Chapter 3). In addition to increasing sizes as one progresses along the food web (Fig. 8.2), there is a tendency towards longer time scales. Descriptive models are limited in this respect, because they give no indication of the dynamic nature of the system when all the components are interacting.

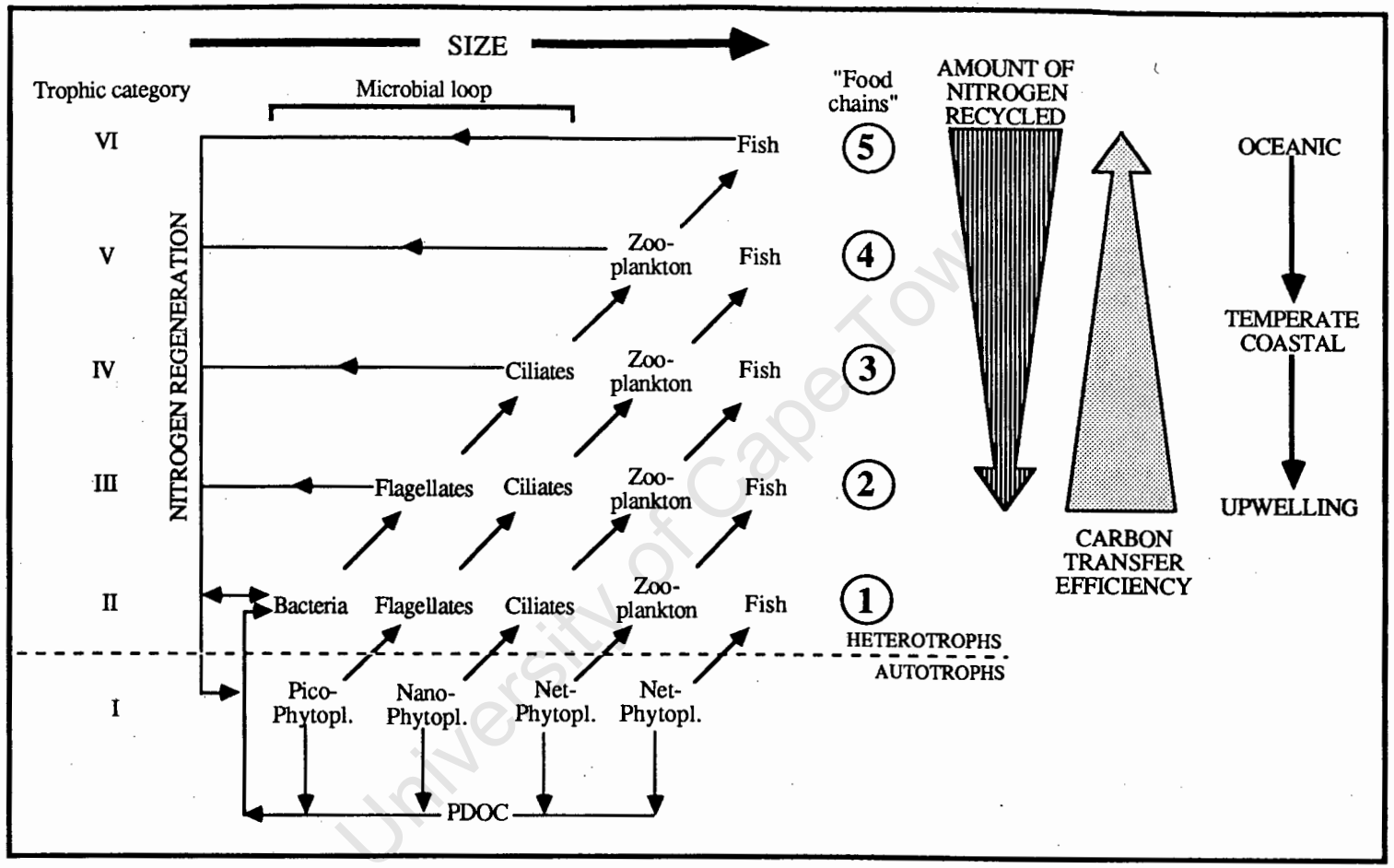

Fig. 8.2. Carbon and nitrogen flows in a plankton food web, modified after Azam *et al.* (1983). The trophic categories on the right refer to the integer number of steps from the primary producers. The "food chains" 2-5 refer to the diagonal flows in the food web, and are numbered to correspond to the number of trophic steps. Shaded arrows depict the qualitative changes in the amount of nitrogen recycled and the carbon transfer efficiencies of the 4 "food chains", which are believed to dominate to varying degrees in different marine ecosystems. Note that, in general, an ecosystem will tend to have all food chains that are longer than its shortest food chain.

In many recent studies, the role of the microbial loop ("food chain" 5, Fig. 8.2) has been emphasized, and the shorter chains ("food chains" 1, 2, 3 and 4, Fig. 8.2) from phytoplankton to fish have been de-emphasized. However, the microbial loop pathway is possibly the most unlikely pathway for the products of primary production to reach pelagic fish, because this route is the longest through the food web, and is likely to be very inefficient (Caron *et al.* 1985). The most efficient pathway in carbon transfer should be the shortest pathways (food chains 1and 2), with intermediate food chains 3 and 4 decreasing in terms of efficiency of carbon transfer. The converse is true for nitrogen regeneration. Long food chains will result in large amounts of nitrogen being regenerated through egestion and excretion, particularly because the long food chains are composed of small organisms, which are prolific remineralizers because of their fast turnover rates (Chapter 5).

Different marine planktonic systems have one or more of these food chains operating; in Chapter 5 it was shown that the simulated Agulhas Bank and upwelling food webs contain all four "food chains" in varying degrees of importance at different times. What are the features that determine which of the pathways will be most important? I hypothesise that nutrient / food concentrations are an important factor, and that these in turn determine the size structure of the phytoplankton community. If all phytoplankton are small (i.e. < 5 μm), the only available pathways are food chains 4 and 5. If the dominant phytoplankton are large species, food chains 1 and 2 can occur, but will only be efficient if food / prey concentrations are large enough. If food chain 1 occurs, it is probable that all of the food chains are present in some degree, because pico-phytoplankton are ubiquitous components of marine plankton communities (Johnson and Sieburth 1979, Joint and Pomroy 1983). Carbon flows in productive upwelling ecosystems (in terms of pelagic fish) will move along food chains 1 and 2 (Fig. 8.2) more often or more efficiently than will those of temperate coastal ecosystems, whereas carbon flows in unproductive oceanic waters will primarily pass along food chain 5. This implies that the productive systems have more complex food webs than the unproductive waters, which is the opposite to the traditional view of planktonic food webs (e.g. King 1987). The short "efficient" food chains may be fortuitous during "boom" periods when food densities are abundant, whereas the long "inefficient" food

chains may be important during lean periods when food concentrations are low. The total fish production in an ecosystem will depend on the extent to which the different food chains are averaged in time and space.

CONCLUSIONS

Analysis of output from a size-based model of plankton communities provides invaluable insight into the factors determining the dynamics of marine planktonic food webs. Many of the controversies regarding carbon and nitrogen flows in plankton communities have arisen because of a non-dynamic approach to analysing data, and a tendency to extrapolate from single data sets to the general. Controversies can be resolved to some extent by complementing field studies with dynamic system models. These models can guide field and experimental studies, providing an whole-system perspective of the problems being tackled.

LITERATURE CITED

Andersen, V., Nival, P., Harris, R. 1987. Modelling of a planktonic ecosystem in an enclosed water column. *J. mar. biol. Ass. U.K.* **67:** 407-430

Anderson, D.M., Lively, J.J., Reardon, E.M., Price, C.A. 1985. Sinking characteristics of dinoflagellate cysts. *Limnol. Oceanogr.* **30:** 1000-1009

Andersson, A., Lee, C., Azam, F., Hagstrom, A. 1985. Release of amino acids and inorganic nutrients by heterotrophic marine microflagellates. *Mar. Ecol. Prog. Ser.* **23:** 99-106

Andrews, W.R.H., Hutchings, L. 1980. Upwelling in the southern Benguela. *Prog. Oceanogr.* **9:** 1-81

Arashkevich, Y.G., Vinogradov, G.M., Semenova, T.N. 1986. Sinking speed of fecal pellets of the Barents Sea mysid *Praunus inermis* (Rathke) in the laboratory. *Oceanology* **26:** 370-374

Armstrong, D.A., Mitchell-Innes, B.A., Verheye-Dua, F., Waldron, H., Hutchings, L. 1987. Physical and biological features across an upwelling front in the southern Benguela. In: Payne, A.I.L., Gulland, J.A., Brink, K.H. [eds]. The Benguela and comparable ecosystems. *S. Afr. J. mar. Sci.* **5:** 171-189

Azam, F., Fenchel, T., Field, J.G., Gray, J.S., Meyer-Reil, L.A., Thingstad, F. 1983. The ecological role of water-column microbes in the sea. *Mar. Ecol. Prog. Ser.* **10:** 257-263

Azam, F., Hodson, R.E. 1977. Size distribution and activity of marine microheterotrophs. *Limnol. Oceanogr.* **22:** 492-502

Baldock, B.M., Baker, J.H., Sleigh, M.A. 1980. Laboratory growth rates of six species of freshwater Gymnamoebia. *Oecologia (Berl.)* **47:** 156-159

Banse, K. 1976. Rates of growth, respiration and photosynthesis of unicellular algae as related to cell size - a review. *J. Phycol.* **12:**135-140

Banse, K. 1982. Mass-scaled rates of respiration and intrinsic growth in very small invertebrates. *Mar. Ecol. Prog. Ser.* **9:** 281-297

Barlow, R.G. 1982. Phytoplankton ecology in the southern Benguela current. I. Biochemical composition. *J. exp. mar. Biol. Ecol.* **63:** 209-227

Barthel, K.-G. 1983. Food uptake and growth efficiency of *Eurytemora affinis* (Copepoda: Calanoida). *Mar. Biol.* **74:** 269-274

Bauerfeind, S. 1985. Degradation of phytoplankton detritus by bacteria: estimation of bacterial consumption and respiration in an oxygen chamber. *Mar. Ecol. Prog. Ser.* **21:** 27-36

Bell, W.H. 1980. Bacterial utilisation of algal extracellular products. I. The kinetic approach. *Limnol. Oceanogr.* **25:** 1007-1020

Bell, W.H., Sakshaug, E. 1980. Bacterial utilisation of algal extracellular products. 2. A kinetic study of natural populations. *Limnol. Oceanogr.* **25:** 1021-1033

Berman, T., Holm-Hansen, O. 1974. Release of photoassimilated carbon as dissolved organic matter by marine phytoplankton. *Mar. Biol.* **28:** 305-310

Bienfang, P.K. 1985. Size structure and sinking rates of various microparticulate constituents in oligotrophic Hawaiian waters. *Mar. Ecol. Prog. Ser.* **23:** 143-151

Bienfang, P.K., Harrison, P.J. 1984. Co-variation of sinking rate and cell quota among nutrient replete marine phytoplankton. *Mar. Ecol. Prog. Ser.* **14:** 297-300

Bienfang, P.K., Takahashi, M. 1983. Ultraplankton growth rates in a subtropical ecosystem. *Mar. Biol.* **76:** 213-218

Billen, G. 1984. Heterotrophic utilization and regeneration of nitrogen. In: Hobbie, J.E., Williams, P.J.leB. [eds]. *Heterotrophic activity in the sea.* Plenum Press, New York, 313-356

Blueweiss, L., Fox, H., Kudzma, V., Nakashima, D., Peters, R., Sams, S. 1978. Relationships between body size and some life history parameters. *Oecologia (Berl.)* **37:** 257-272

Bϕrsheim, K.Y. 1984. Clearance rates of bacteria sized particles by freshwater ciliates, measured with monodisperse fluorescent latex beads. *Oecologia (Berl.)* **63:** 286-288

Boyd, C.M. 1976. Selection of particle sizes by filter-feeding copepods: A plea for reason. *Limnol. Oceanogr.* **21:** 175-180

Bratbak, G., Thingstad, T.F. 1985. Phytoplankton-bacteria interactions: an apparent paradox? Analysis of a model system with both competition and commensalism. *Mar. Ecol. Prog. Ser.* **25:** 23-30

Brody, S., Procter, R.C., Ashworth, U.S. 1934. Basal metabolism, endogenous nitrogen, creatinine and neutral sulphur excretions as functions of body weight. *Missouri Agr. Exp. Sta. Res. Bull.* **220:** 1-40

Brooks, J.L., Dodson, S.I. 1965. Predation, body size, and composition of plankton. *Science* **150:** 28-35

Brown, P.C. 1984. Primary productivity at two contrasting nearshore sites in the southern Benguela upwelling region, 1977-1979. *S. Afr. J. mar. Sci.* **2:** 205-215

Brown, P.C., Field, J.G. 1985. Diel variation in production rates of natural phytoplankton populations in the southern Benguela upwelling region. *Bot. Mar.* **28:** 201-208

Brown, P.C., Field, J.G. 1986. Factors limiting phytoplankton production in a nearshore upwelling area. *J. Plankt. Res.* **8:** 55-68

Brown, P.C., Hutchings, L. 1987a. The development and decline of phytoplankton blooms in the southern Benguela upwelling system. 1. Drogue movements, hydrography and bloom development. In: Payne, A.I.L., Gulland, J.A., Brink, K.H. [eds]. The Benguela and comparable ecosystems. *S. Afr. J. mar. Sci.* **5:** 357-391

Brown, P.C., Hutchings, L. 1987b. The development and decline of phytoplankton blooms in the southern Benguela upwelling system. 2. Nutrient relationships. In: Payne, A.I.L., Gulland, J.A., Brink, K.H. [eds]. The Benguela and comparable ecosystems. *S. Afr. J. mar. Sci.* **5:** 393-409

Bruland, K.W., Silver, M.W. 1981. Sinking rates of fecal pellets from gelatinous zooplankton (Salps, Pteropods, Doliolids). *Mar. Biol.* **63:** 295-300

Burns, N.M., Rosa, F. 1980. *In situ* measurement of the settling velocity of organic carbon particles and 10 species of phytoplankton. *Limnol. Oceanogr.* **25:** 855-864

Calder, W. A. III. 1985. Size and metabolism in natural systems. In: Ulanowicz, R.E., Platt, T. [eds]. Ecosystem theory for biological oceanography. *Can. Bull. Fish. Aquat. Sci.* **213:** 65-75

Calow, P. 1977. Conversion efficiencies in heterotrophic organisms. *Biol. Rev.* **52:** 385-409

Cammen, L. M. 1980. Ingestion rate: an empirical model for aquatic deposit feeders and detritivores. *Oecologia (Berl.)* **44:** 303-310

Capriulo, G.M. 1982. Feeding of field collected tintinnid micro-zooplankton on natural food. *Mar. Biol.* **71:** 73-86

Caron, D.A., Goldman, J.C., Andersen, O.K., Dennett, M.R. 1985. Nutrient cycling in a microflagellate food chain: II. Population dynamics and carbon cycling. *Mar. Ecol. Prog. Ser.* **24:** 243-254

Carter, R.A., Bartlett, P.D., Swart, V.P. 1986. Estimates of the nitrogen flux required for the maintenance of subsurface chlorophyll maxima on the Agulhas Bank. In: Nihoul, J.C.J. [ed.]. *Marine interfaces ecohydrodynamics*. Elsevier, Amsterdam, 331-339

Carter, R.A., McMurray, H.F., Largier, J.L. 1987. Thermocline characteristics and phytoplankton dynamics in Agulhas Bank waters. In: Payne, A.I.L., Gulland, J.A., Brink, K.H. [eds]. The Benguela and comparable ecosystems. *S. Afr. J. mar. Sci.* **5:** 327-335

Cole, J.J., Likens, G.E., Strayer, D.L. 1982. Photosynthetically-produced dissolved organic carbon: an important carbon source for planktonic bacteria. *Limnol. Oceanogr.* **27:** 1080-1090

Cousins, S.H. 1980. A trophic continuum model derived from plant structure, animal size and a detritus cascade. *J. theor. Biol.* **82:** 607-618

Cousins, S.H. 1985. The trophic continuum in marine ecosystems: structure and equations for a predictive model. In: Ulanowicz, R.E., Platt, T. [eds]. Ecosystem theory for biological oceanography. *Can. Bull. Fish. Aquat. Sci.* **213:** 76-93

Cowles, T.J. 1979. The feeding response of copepods from the Peru upwelling system: food size selection. *J. mar. Res.* **37:** 601-622

Crawford, R.J.M., Shannon, L.V., Pollock, D.E. 1987. The Benguela ecosystem. Part IV. The major fish and invertebrate resources. *Oceanogr. Mar. Biol. Ann. Rev.* **25:** 353-505

Cushing, D.H. 1971. Upwelling and the production of fish. *Adv. mar. Biol.* **9:** 255-334

Dagg, M. J. 1976. Complete carbon and nitrogen budgets for the carnivorous amphipod, *Calliopius laeviusculus* (Krøyer). *Int. Revue. ges. Hydrobiol.* **61:** 297-357

Davis, P.G., Sieburth, J.McN. 1982. Differentiation of phototrophic and zooplanktonic nanoplankton populations in marine waters by epifluorescence microscopy. *Ann. Inst. océanogr., Paris* **58:** 249-260

De Decker, A. 1973. Agulhas Bank plankton. In: Zeitzschel, B. [ed.]. *The biology of the Indian Ocean*. Springer-Verlag, Berlin, 189-219

DeMott, W.R. 1988. Discrimination between algae and artificial particles by freshwater and marine copepods. *Limnol. Oceanogr.* **33:** 397-408

Dewey, J.M. 1976. Rates of feeding, respiration, and growth for the rotifer *Brachionus plicatilis* and the dinoflagellate *Noctiluca miliaris* in the laboratory. PhD Thesis, Univ. Washington, 149pp

Dickie, L.M., Kerr, S.R., Boudreau, P.R. 1987. Size-dependent processes underlying regularities in ecosystem structure. *Ecol. Monogr.* **57:** 233-250

Douglas, D.J. 1984. Microautoradiography-based enumeration of photosynthetic picoplankton with estimates of carbon-specific growth rates. *Mar. Ecol. Prog. Ser.* **14:** 223-228

Drebes, G. 1974. *Marines Phytoplankton. Eine Auswahl der Helgoländer Planktonalgen (Diatomeen, Peridineen)*. Georg Thieme Verlag, Stuttgart. 186 pp

Ducklow, H.W., Purdie, D.A., Williams, P.J.leB., Davies, J.M. 1986. Bacterioplankton: a sink for carbon in a coastal marine plankton community. *Science* **232:** 865-867

Dugdale, R.C., Goering, J.J. 1967. Uptake of new and regenerated forms of nitrogen in primary productivity. *Limnol. Oceanogr.* **12:** 196-206

Eberlein, K., Brockmann, U.H., Hammer, K.D., Kattner, G., Laake, M. 1983. Total dissolved carbohydrates in an enclosure experiment with unialgal *Skeletonema costatum* culture. *Mar. Ecol. Prog. Ser.* **14:** 45-58

Economos, A.C. 1979. On structural theories of basal metabolic rate. *J. theor. Biol.* **80:** 445-450

Eppley, R.W. 1981. Relations between nutrient assimilation and growth in phytoplankton with a brief review of estimates of growth rate in the ocean. In: Platt, T. [ed.]. Physiological bases of phytoplankton ecology. *Can. Bull. Fish. Aquat. Sci.* **210:** 251-263

Eppley, R.W., Peterson, B.J. 1979. Particulate organic matter and planktonic new production in the deep ocean. *Nature* **282:** 677-680

Eppley, R.W., Rogers, J.N., McCarthy, J.J. 1969. Half-saturation constants for uptake of nitrate and ammonium by marine phytoplankton. *Limnol. Oceanogr.* **14:** 912-920

Eppley, R.W., Sharp, J.H., Renger, E.H., Perry, M.J., Harrison, W.G. 1977. Nitrogen assimilation by phytoplankton and other microorganisms in the surface waters of the central North Pacific Ocean. *Mar. Biol.* **39:** 111-120

Estrada, M. 1980. Phytoplankton biomass and production in the upwelling region of NW Africa. Relationships with hydrographic parameters. *Mar. Biol.* **60:** 63-71

Estrada, M., Blasco, D. 1985. Phytoplankton assemblages in coastal upwelling areas. *Int. Symp. Upw. W. Afr., Inst. Inv. Pesq., Barcelona 1985* **1:** 370-402

Falkowski, P.G., Vidal, J., Hopkins, T.S., Rowe, G.T., Whitledge, T.E., Harrison, W.G. 1983. Summer nutrient dynamics in the Middle Atlantic Bight: primary production and utilisation of phytoplankton carbon. *J. Plankt. Res.* **5:** 515-537

Fenchel, T. 1974. Intrinsic rate of natural increase: the relationship with body size. *Oecologia (Berl.)* **14:** 317-326

Fenchel, T. 1980a. Relation between particle size selection and clearance in suspension-feeding ciliates. *Limnol. Oceanogr.* **25:** 733-738

Fenchel, T. 1980b. Suspension feeding in ciliated protozoa: functional response and particle size selection. *Microb. Ecol.* **6:** 1-11

Fenchel, T. 1980c. Suspension feeding in ciliated protozoa: feeding rates and their ecological significance. *Microb. Ecol.* **6:** 13-25

Fenchel, T. 1982a. Ecology of heterotrophic microflagellates. I. Some important forms and their functional morphology. *Mar. Ecol. Prog. Ser.* **8:** 211-223

Fenchel, T. 1982b. The bioenergetics of a heterotrophic microflagellate. *Ann. Inst. oceanogr.* **58:** 55-60

Fenchel, T. 1984. Suspended marine bacteria as a food source. In: Fasham, M.J.R. [ed.].*Flows of energy and material in marine ecosystems*. Plenum Press, New York, 301-315

Fenchel, T. 1987. *Ecology - potentials and limitations*. Ecology Institute, Oldendorf/Luhe

Fenchel, T., Finlay, B.J. 1983. Respiration rates in heterotrophic, free-living protozoa. *Microb. Ecol.* **9:** 99-122

Field, J.G., Wulff, F.V., Allen, P.M., Fasham, M.J.R., Flos, F., Fronteir, S., Kay, J.J., Silvert, W., Trainor, L. 1985. Ecosystem theory in relation to unexploited marine ecosystems. In: Ulanowicz, R.E., Platt, T. [eds]. Ecosystem theory for biological oceanography. *Can. Bull. Fish. Aquat. Sci.* **213:** 241-247

Finlay, B.J. 1977. The dependence of reproductive rate on cell size and temperature in freshwater ciliated protozoa. *Oecologia (Berl.)* **30:** 75-81

Frost, B.W. 1972. Effects of size and concentration of food particles on the feeding behaviour of the marine planktonic copepod *Calanus pacificus*. *Limnol. Oceanogr.* **17:** 805-815

Frost, B.W. 1975. A threshold feeding behaviour in *Calanus pacificus*. *Limnol. Oceanogr.* **20:** 263-266

Furnas, M.J. 1982. Growth rates of summer nanoplankton (< 10 μm) populations in lower Narragansett Bay, Rhode Island, USA. *Mar. Biol.* **70:** 105-115

Furnas, M.J. 1983. Nitrogen dynamics in lower Narragansett Bay, Rhode Island. I. Uptake by size-fractionated phytoplankton populations. *J. Plankt. Res.* **5:** 657-676

Gast, V. 1985. Bacteria as a food source for microzooplankton in the Schlei Fjord and Baltic Sea with special reference to ciliates. *Mar. Ecol. Prog. Ser.* **22:** 107-120

Gaudy, R., Boucher, J. 1983. Relation between respiration, excretion (ammonia and inorganic phosphorous) and activity of amylase and trypsin in different species of pelagic copepods from an Indian Ocean equatorial area. *Mar. Biol.* **75:** 37-45

Gieskes, W.W.C., Kraay, G.W. 1983. Dominance of Cryptophyceae during the phytoplankton spring bloom in the central North Sea detected by HPLC analysis of pigments. *Mar. Biol.* **75:** 179-185

Glibert, P.M. 1982. Regional studies of daily, seasonal and size fraction variability in ammonium remineralization. *Mar. Biol.* **70:** 209-222

Glibert, P.M., Goldman, J.C., Carpenter, E.J. 1982. Seasonal variations in the utilization of ammonium and nitrate by phytoplankton in the Vineyard Sound, Massachusetts, USA. *Mar. Biol.* **70:** 237-249

Goldman, J.C., Caron, D.A., Andersen, O.K., Dennett, M.R. 1985. Nutrient cycling in a microflagellate food chain: I. Nitrogen dynamics. *Mar. Ecol. Prog. Ser.* **24:** 231-242

Goldman, J.C., McCarthy, J.J., Peavey, D.G. 1979. Growth rate influence on the chemical composition of phytoplankton in oceanic waters. *Nature* **279:** 210-215

Gowing, M.M., Silver, M.W. 1985. Minipellets: a new and abundant size class of marine fecal pellets. *J. mar. Res.* **43:** 395-418

Gray, J.S., Field, J.G., Azam, F., Fenchel, T., Meyer-Reil, L.A., Thingstad, F. 1984. The role of free bacteria and bactivory. In: Fasham, M.J.R. [ed.]. *Flows of energy and material in marine ecosystems*. Plenum Press, New York, 301-315

Hagström, Å., Ammerman, J.W., Henrichs, S., Azam, F. 1984. Bacterioplankton growth in seawater: II. Organic matter utilization during steady-state growth in seawater cultures. *Mar. Ecol. Prog. Ser.* **18:** 41-48

Hahm, W., Langton, R. 1984. Prey selection based on predator / prey weight ratios for some northwest Atlantic fish. *Mar. Ecol. Prog. Ser.* **19:** 1-5

Hall, D.J., Threlkeld, S.T., Burns, C.W., Crowley, P.H. 1976. The size-efficiency hypothesis and the size structure of zooplankton communities. *Ann. Rev. Ecol. Syst.* **7:** 177-208

Harding, L.W.Jr., Prezelin, B.B., Sweeney, B.M., Cox, J.L. 1982. Diel oscillations of the phytoplankton-irradiance (P-I) relationship in natural assemblages of phytoplankton. *Mar. Biol.* **67:** 167-178

Hargrave, B.T., Harding, G.C., Drinkwater, K.F., Lambert, T.C., Harrison, W.G. 1985. Dynamics of the pelagic food web in St Georges Bay, southern Gulf of St Lawrence. *Mar. Ecol. Prog. Ser.* **20:** 221-240

Harrison, W.G. 1978. Experimental measures of nitrogen remineralisation in coastal waters. *Limnol. Oceanogr.* **23:** 684-694

Harrison, W.G., Fulton, J.D., Taylor, F.J.R., Parsons, T.R. 1983. Review of the biological oceanography of the Strait of Georgia pelagic environment. *Can. J. Fish. Aquat. Sci.* **40:** 1064-1094

Harrison, W.G., Li, W.K.W., Smith, J.C., Head, E.J.H., Longhurst, A.R. 1987. Depth profiles of plankton, particulate organic matter amd microbial activity in the Eastern Canadian Arctic during summer. *Polar Biol.* **7:** 207-224

Hemmingsen, A. M. 1960. Energy metabolism as related to body size and respiratory surfaces and its evolution. *Reports of the Steno Memorial Hospital and the Nordisk Insulinlaboratorium* **9(2):** 1-110

Herbland, A., le Bouteiller, A., Raimbault, P. 1985. Size structure of phytoplankton biomass in the equatorial Atlantic Ocean. *Deep-Sea Res.* **32:** 819-836

Heusner, A.A. 1982a. Energy metabolism and body size. I. Is the 0.75 mass exponent of Kleiber's equation a statistical artefact? *Resp. Physiol.* **48:** 1-12

Heusner, A.A. 1982b. Energy metabolism and body size. II. Dimensional analysis and energetic non-similarity. *Resp. Physiol.* **48:** 13-25

Holligan, P.M., Williams, P.J.leB., Purdie, D., Harris, R.P. 1984. Photosynthesis, respiration and nitrogen supply of plankton populations in stratified, frontal and tidally mixed shelf waters. *Mar. Ecol. Prog. Ser.* **17:** 201-213

Humphreys, W. F. 1979. Production and respiration in animal populations. *J. Anim. Ecol.* **48:** 427-453

Huntley, M.E., Barthel, K.-G., Star, J.L. 1983. Particle rejection by *Calanus pacificus*: discrimination between similarly sized particles. *Mar. Biol.* **74:** 151-160

Hutchings, L., Holden, C., Mitchell-Innes, B. 1984. Hydrological and biological shipboard measurements of upwelling off the Cape Peninsula. *S. Afr. J. Sci.* **80:** 83-89

Ikeda, T. 1970. Relationship between respiration rate and body size in marine plankton animals as a function of the temperature of habitat. *Bull. Fac. Fish., Hokkaido Univ.* **21:** 91-112.

Ikeda, T. 1977. Feeding rates of planktonic copepods from a tropical sea. *J. exp. mar. Biol. Ecol.* **29:** 263-277

Ikeda, T., Motoda, S. 1978. Zooplankton production in the Bering Sea calculated from 1956-1970 *Oshoro Maru* data. *Mar. Sci. Commns* **4:** 329-346

Isaacs, J.D. 1973. Potential trophic biomasses and trace-substance concentrations in unstructured marine food webs. *Mar. Biol.* **22:** 97-104

Ivleva, I.V. 1980. The dependence of crustacean respiration rate on body mass and habitat temperature. *Int. Rev. ges. Hydrobiol.* **65:** 1-47

Jackson, G.A. 1980. Phytoplankton growth and zooplankton grazing in oligotrophic oceans. *Nature* **284:** 439-441

James, A.G. 1987. Feeding ecology, diet and field-based studies on feeding selectivity of the Cape anchovy *Engraulis capensis* Gilchrist. In: Payne, A.I.L., Gulland, J.A., Brink, K.H. [eds]. The Benguela and comparable ecosystems. *S. Afr. J. mar. Sci.* **5:** 673-692

James, A.G. 1988. Feeding ecology and carbon and nitrogen budgets of the Cape anchovy, *Engraulis capensis* (Gilchrist). Ph.D. Thesis, University of Cape Town

Jensen, L.M. 1983. Phytoplankton release of extracellular organic carbon, molecular weight composition, and bacterial assimilation. *Mar. Ecol. Prog. Ser.* **11:** 39-48

Johnson, K.M., Burney, C.M., Sieburth, J.McN. 1981. Enigmatic marine ecosystem metabolism measured by direct diel ΣCO_2 and O_2 flux in conjunction with DOC release and uptake. *Mar. Biol.* **65:** 49-60

Johnson, P.W., Sieburth, J.McN. 1979. Chroococcoid cyanobacteria in the sea: a ubiquitous and diverse phototrophic biomass. *Limnol. Oceanogr.* **24:** 928-935

Joint, I.R., Morris. R.J. 1982. The role of bacteria in the turnover of organic matter in the sea. *Oceanogr. Mar. Biol. Ann. Rev.* **20:** 65-118

Joint, I.R., Pomroy, A.J. 1983. Production of picoplankton and small nanoplankton in the Celtic Sea. *Mar. Biol.* **77:** 19-27

Jones, R. 1984. Some observations on energy transfer through the North Sea and Georges Bank food webs. *Rapp. P.-v. Reun.Cons. perm. int. Explor. Mer* **183:** 204-217

Jones, R., Henderson, E.W. 1987. The dynamics of energy transfer in marine food chains. In: Payne, A.I.L., Gulland, J.A., Brink, K.H. [eds]. The Benguela and comparable ecosystems. *S. Afr. J. mar. Sci.* **5:** 447-465

Jonsson, P.R. 1986. Particle size selection, feeding rates and growth dynamics of marine planktonic oligotrichous ciliates (Ciliophora: Oligotrichia). *Mar. Ecol. Prog. Ser.* **33:** 265-277

Kanda, J., Saino, T., Hattori, A. 1985. Nitrogen uptake by natural populations of phytoplankton and primary production in the Pacific Ocean: regional variability of uptake capacity. *Limnol. Oceanogr.* **30:** 987-999

Kerr, R.A. 1986. The ocean's deserts are blooming. *Science* **232:** 1345

Kerr, S.R. 1974. Theory of size distribution in ecological communities. *J. Fish. Res. Bd Can.* **31:** 1859-1862

Kiefer, D.A., Atkinson, C.A. 1984. Cycling of nitrogen by plankton: A hypothetical description based upon efficiency of energy conversion. *J. mar. Res.* **42:** 655-675

King, F.D. 1987. Nitrogen recycling efficiency in steady-state oceanic environments. *Deep-Sea Res.* **34:** 843-856````

Kleiber, M. 1932. Body size and metabolism. *Hilgardia* **6:** 315-353

Kleiber, M. 1947. Body size and metabolic rate. *Physiol. Rev.* **27:** 511-541`

Kooijman, S.A.L.M. 1986. Energy budgets can explain body size relations. *J. theor. Biol.* **121:** 269-282

Laake, M., Dahle, A.B., Eberlein, K., Rein, K. 1983a. A modelling approach to the interplay of carbohydrates, bacteria and non-pigmented flagellates in a controlled ecosystem experiment with *Skeletonema costatum. Mar. Ecol. Prog. Ser.* **14:** 71-79

Laake, M., Dahle, A.B., Hentzschel, G. 1983b. Productivity and population diversity of marine organotrophic bacteria in enclosed planktonic ecosystems. *Mar. Ecol. Prog. Ser.* **14:** 59-69

Lampert, W. 1977. Studies on the carbon balance of *Daphnia pulex* de Geer as related to environmental conditions II. The dependence of carbon assimilation on animal size, temperature, food concentration and diet species. *Arch. Hydrobiol., Suppl.* **48:** 310-335

Lampitt, R.S., Gamble, J.C. 1982. Diet and respiration of the small planktonic copepod *Oithona nana. Mar. Biol.* **66:** 185-190

Lancelot, C. 1983. Factors affecting phytoplankton extracellular release in the southern bight of the North Sea. *Mar. Ecol. Prog. Ser.* **12:** 115-121

Landry, M.R., Hassett, R.P., Fagerness, V., Downs, J., Lorenzen, C.J. 1984. Effect of food acclimation on assimilation efficiency of *Calanus pacificus. Limnol. Oceanogr.* **29**: 361-364

Lapidus, L., Seinfeld, J.H. 1971. *Numerical solution of ordinary differential equations*. Academic Press, New York

Larsson, U., Hagström, Å. 1982. Fractionated phytoplankton primary production, exudate release and bacterial production in a Baltic eutrophication gradient. *Mar. Biol.* **67:** 57-70

Lavigne, D.M. 1982. Similarity in energy budgets of animal populations. *J. Anim. Ecol.* **51:** 195-206

Laws, E.A. 1975. The importance of respiration losses in controlling the size distribution of marine phytoplankton. *Ecology* **56:** 419-426

Laws, E.A., Archie, J.W. 1981. Appropriate use of regression analysis in marine biology. *Mar. Biol.* **65:** 12-16

Laws, E.A., Redalje, D.G., Haas, L.W., Bienfang, P.K., Eppley, R.W., Harrison, W.G., Karl, D.M., Marra, J. 1984. High phytoplankton growth and production rates in oligotrphic Hawaiian coastal waters. *Limnol. Oceanogr.* **29:** 1161-1169

Laybourn, J., Finlay, B.J. 1976. Respiratory energy losses related to cell weight and temperature in ciliated Protozoa. *Oecologia (Berl.)* **24:** 349-355

Lehman, J.T. 1980. Release and cycling of nutrients between planktonic algae and herbivores. *Limnol. Oceanogr.* **25:** 620-632

Lehman, J.T., Sandgren, C.D. 1985. Species-specific rates of growth and grazing loss among freshwater algae. *Limnol. Oceanogr.* **30:** 34-46

Levine, S. 1980. Several measures of trophic structure applicable to complex food webs. *J. theor. Biol.* **83:** 195-207

Linley, E.A.S., Newell, R.C. 1984. Estimates of bacterial growth yields based on plant detritus. *Bull. Mar. Sci.* **35:** 409-425

Lochte, K. 1985. Biological studies in the vicinity of a shallow-sea tidal mixing front III. Seasonal and spatial distribution of heterotrophic uptake of glucose. *Phil. Trans. R. Soc. Lond.* **B 310:** 445-469

Lochte, K., Turley, C.M. 1985. Heterotrophic activity and carbon flow via bacteria in waters associated with a todal mixing front. In: Gibbs, P.E. [ed.]. *Proc. 19th European Marine Biology Symposium*, Cambridge University Press, 73-85

Lucas, M. I. 1986. Decomposition in pelagic marine ecosystems. *J. Limnol. Soc. sth. Afr.* **12:** 99-122

Lucas, M.I., Painting, S.J., Muir, D.G. 1986. Estimates of carbon flow through bacterioplankton in the S. Benguela upwelling region based on ^{3}H thymidine incorporation and predator-free incubations. *GERBAM - Second International Colloquium of Marine Bacteriology, CNRS, Brest, October 1984, IFREMER, Actes de Coll.* **3:** 375-383

Lucas, M.I., Probyn, T.A., Painting, S.J. 1987. An experimental study of microflagellate bacterivory: further evidence for the importance and complexity of microplanktonic interactions. In: Payne, A.I.L., Gulland, J.A., Brink, K.H. [eds]. The Benguela and comparable ecosystems. *S. Afr. J. mar. Sci.* **5:** 791-810

Lynch, M. 1977. Fitness and optimal body size in zooplankton populations. *Ecology* **58:** 763-774

MacIsaac, J.J., Dugdale, R.C. 1969. The kinetics of nitrate and ammonia uptake by natural populations of marine phytoplankton. *Deep-Sea Res.* **16:** 45-57

Madin, L.P. 1982. Production, composition and sedimentation of salp fecal pellets in oceanic waters. *Mar. Biol.* **67:** 39-45

Malone, T.C. 1977. Light-saturated photosynthesis by phytoplankton size fractions in the New York Bight, USA. *Mar. Biol.* **42:** 281-292

Mann, K.H. 1982. *Ecology of coastal waters. A systems approach.* Blackwell, Oxford, 322 pp

May, R.M. 1979. Production and respiration in animal communities. *Nature* **282:** 443-444

McCarthy, J. J. 1981. The kinetics of nutrient utilisation. In: Platt, T. [ed.]. Physiological bases of phytoplankton ecology. *Can. Bull. Fish. Aquat. Sci.* **210:** 211-233

McCarthy, J. J., Goldman, J.C. 1979. Nitrogenous nutrition of marine phytoplankton in nutrient-depleted waters. *Science* **223:** 670-672

Miller, C.A., Landry, M.R. 1984. Ingestion-independent rates of ammonium excretion by the copepod *Calanus pacificus*. *Mar. Biol.* **78:** 265-270

Mitamura, O., Saijo, Y. 1980. *In situ* measurement of the urea decomposition rate and its turnover rate in the Pacific Ocean. *Mar. Biol.* **58:** 147-152

Mitchell-Innes, B.A., Winter, A. 1987. Coccolithophores: a major phytoplankton component in mature upwelled water off the Cape Peninsula, South Africa in March, 1983. *Mar. Biol.* **95:** 25-30

Moloney, C.L., Bergh, M.O., Field, J.G., Newell, R.C. 1986. The effect of sedimentation and microbial nitrogen regeneration in a plankton community: a simulation investigation. *J. Plankt. Res.* **8:** 427-445

Moloney, C.L., Field, J.G. 1985. Use of particle-size data to predict potential pelagic-fish yields of some southern African areas. *S. Afr. J. mar. Sci.* **3:** 119-128

Monod, J. 1949. The growth of bacterial cultures. *Ann. Rev. Microbiol.* **3:** 371-394

Morita, R.Y. 1984. Substrate capture by marine heterotrophic bacteria in low nutrient waters. In: Hobbie, J.E., Williams, P.J.leB. [eds].*Heterotrophic activity in the sea.* Plenum Press, New York, 83-100

Morris, I. 1981. Photosynthetic products, physiological state, and phytoplankton growth. In: Platt, T. [ed.]. Physiological bases of phytoplankton ecology. *Can. Bull. Fish. Aquat. Sci.* **210:** 83-102

Mullin, M.M., Stewart, E.F., Fuglister, F.J. 1975. Ingestion by planktonic grazers as a function of concentration of food. *Limnol. Oceanogr.* **20:** 259-262

Newell, G.E., Newell, R.C. 1963. *Marine plankton. A practical guide*. Hutchinson Educational, London. 244pp

Newell, R.C., Linley, E.A.S. 1984. Significance of microheterotrophs in the decomposition of phytoplankton: estimates of carbon and nitrogen flow based on the biomass of plankton communities. *Mar. Ecol. Prog. Ser.* 16: 105-119

Newell, R.C. , Moloney, C.L., Field, J.G., Lucas, M.I., Probyn, T.A. 1988. Nitrogen models at the community level: plant-animal-microbe interactions. In: Blackburn, T.H., Sørenson, J. [eds]. *Nitrogen cycling in coastal marine environments.* SCOPE, Cheltenham, U.K., Wiley, 379-414

Nissen, H., Nissen, P., Azam, F. 1984. Multiphasic uptake of D-glucose by an oligotrophic marine bacterium. *Mar. Ecol. Prog. Ser.* **16:** 155-160

Norris, R.E. 1983. *Proceedings of the Fifth National Oceanographic Symposium, Grahamstown, South Africa, January 1983,* S288, paper B17 (abstract)

O'Connors, H.B., Small, L.F., Donaghay, P.L. 1976. Particle size modification by two size classes of the estuarine copepod *Acartia clausi*. *Limnol. Oceanogr.* **21:** 300-308

Olivieri, E.T. 1985. Phytoplankton growth and zooplankton grazing in the southern Benguela current. Ph.D. Thesis, University of Cape Town, 214pp

Paffenhöfer, G.A. 1971. Grazing and ingestion rates of nauplii, copepodids and adults of the marine planktonic copepod *Calanus helgolandicus*. *Mar. Biol.* **11:** 286-298

Painting, S.J., Lucas, M.I., Muir, D.G. 1988. Fluctuations in heterotrophic bacterial production, activity and community structure in response to development and decay of phytoplankton in a microcosm. *Mar. Ecol. Prog. Ser.* (submitted)

Parkin, H., Cousins, S. 1981. *Towards a global model of large ecosystems: equations for a trophic continuum*. Energy Research Group Report 041, The Open University, Milton Keynes, U.K. 41pp

Parsons, T.R., Strickland, J.D.H. 1962. On the production of particulate organic carbon by heterotrophic processes in sea water. *Deep-Sea Res.* **8:** 211-222

Parsons, T.R., Takahashi, M., Hargrave, B. 1977. *Biological oceanographic processes, 2nd edition*. Pergamon Press,

Parsons, T.R., Takahashi, M. 1973. Environmental control of phytoplankton cell size. *Limnol. Oceanogr.* **18:** 511-515

Parsons, T.R., Takahashi, M. 1974. A rebuttal to the comment by Hecky and Kilham. *Limnol. Oceanogr.* **19:** 366-368

Pearre, S.Jr. 1980. Feeding by Chaetognatha: the relation of prey size to predator size in several species. *Mar. Ecol. Prog. Ser.* **3:** 125-134

Pearre, S.Jr. 1986. Ratio-based trophic niche breadths of fish, the Sheldon spectrum, and the size-efficiency hypothesis. *Mar. Ecol. Prog. Ser.* **27:** 299-314

Pengerud, B., Skjoldal, E.F., Thingstad, T.F. 1987. The reciprocal interaction between degradation of glucose and ecosystem structure. Studies in mixed chemostat cultures of marine bacteria, algae, and bacterivorous nanoflagellates. *Mar. Ecol. Prog. Ser.* **35:** 111-117

Penning de Vries, F.W.T., Brünsting, A.H.M., van Laar, H.H. 1974. Products, requirements and efficiency of biosynthesis: a quantitative approach. *J. theor. Biol.* **45:** 339-377

Peters, R.H. 1983. *The ecological implications of body size*. Cambridge University Press, Cambridge

Pillar, S.C. 1986. Temporal and spatial variations in copepod and euphausiid biomass off the southern and south-western coasts of South Africa in 1977/78. *S. Afr. J. mar. Sci.* **4:** 219-230

Platt, T. 1985. Structure of the marine ecosystem: its allometric basis. In: Ulanowicz, R.E., Platt, T. [eds]. Ecosystem theory for biological oceanography. *Can. Bull. Fish. Aquat. Sci.* **213:** 55-64

Platt, T., Denman, K. 1978. The structure of pelagic marine ecosystems. *Rapp. P.-v. Reun.Cons. perm. int. Explor. Mer* **173:** 60-65

Platt, T., Mann, K.H., Ulanowicz, R.E. 1981. *Mathematical models in biological oceanography.* The Unesco Press, Paris

Platt, T., Silvert, W. 1981. Ecology, physiology, allometry and dimensionality. *J. theor. Biol.* **93:** 855-860

Poulet, S.A. 1973. Grazing of *Pseudocalanus minutus* on naturally occurring particulate matter. *Limnol. Oceanogr.* **18:** 564-573

Prigogine, I. 1987. Exploring complexity. In: Allen, P.J., Schieve, W.C., Adams, R.N. [eds]. *Eur. J. Op. Res.* **30:** 97-103

Probyn, T.A. 1985. Nitrogen uptake by size-fractionated phytoplankton populations in the southern Benguela upwelling system. *Mar. Ecol. Prog. Ser.* **22:** 249-258

Probyn, T.A. 1987. Ammonium regeneration by microplankton in an upwelling environment. *Mar. Ecol. Prog. Ser.* **37:** 53-64

Probyn, T.A., Lucas, M.I. 1987. Ammonium and phosphorous flux through the microplankton community in Agulhas Bank waters. In: Payne, A.I.L., Gulland, J.A., Brink, K.H. [eds]. The Benguela and comparable ecosystems. *S. Afr. J. mar. Sci.* **5:** 209-221

Quetin, L.B., Ross, R.M. 1985. Feeding by Antarctic krill, *Euphausia superba*: Does size matter? In: Siegfried, W.R., Condy, P.R., Laws, R.M. [eds]. *Antarctic nutrient cycles and food webs.* Springer-Verlag, Berlin, 372-377

Raymont, J.E.G. 1980. *Plankton and productivity in the oceans (second edition). Volume 1 - Phytoplankton.* Pergamon Press, Oxford

Ricker, W. E. 1984. Computation and uses of central trend lines. *Can. J. Zool.* **62:** 1897-1905

Ricker, W.E. 1973. Linear regressions in fisheries research. *J. Fish. Res. Bd Can.* **30:** 409-434

Robison, B.H., Bailey, T.G. 1981. Sinking rates and dissolution of midwater fish fecal matter. *Mar. Biol.* **65:** 135-142

Rodriguez, J., Mullin, M.M. 1986. Relation between biomass and body weight of plankton in a steady state oceanic ecosystem. *Limnol. Oceanogr.* **31:** 361-370

Ross, R. M. 1982a. Energetics of *Euphausia pacifica.* I. Effects of body carbon and nitrogen and temperature on measured and predicted production. *Mar. Biol.* **68:** 1-13

Ross, R. M. 1982b. Energetics of *Euphausia pacifica.* II. Complete carbon and nitrogen budgets at 8°C and 12°C throughout the life span. *Mar. Biol.* **68:** 15-23

Ryther, J.H. 1969.Photosynthesis and fish production in the sea. *Science* **166:** 72-76

Sakshaug, E. 1980. Problems in the methodology of studying phytoplankton. In: Morris, I. [ed.].*The physiological bases of phytoplankton ecology.* Blackwell, Oxford, 57-91

Schlesinger, D.A., Molot, L.A., Shuter, B.J. 1981. Specific growth rates of freshwater algae in relation to cell size and light intensity. *Can. J. Fish. Aquat. Sci.* **38:** 1052-1058

Schmidt-Nielsen, K. 1970. Energy metabolism, body size, and problems of scaling. *Proc. Fed. Am. Soc. Exp. Biol.* **29:** 1524-1532

Shannon, L.V. 1985. The Benguela ecosystem. Part I. Evolution of the Benguela, physical features and processes. *Oceanogr. Mar. Biol. Ann. Rev.* **23:** 105-182

Shannon, L.V., Field, J.G. 1985. Are fish stocks food-limited in the southern Benguela pelagic ecosystem? *Mar. Ecol. Prog. Ser.* **22:** 7-19

Shannon, L.V., Pillar, S.C. 1986. The Benguela ecosystem. Part III. Plankton. *Oceanogr. Mar. Biol. Ann. Rev.* **23:** 105-182

Sheldon, R.W. 1984. Phytoplankton growth rates in the tropical ocean. *Limnol. Oceanogr.* **29:** 1342-1346

Sheldon, R.W., Kerr, S.R. 1972. The population density of monsters in Loch Ness. *Limnol. Oceanogr.* **17:** 796-798

Sheldon, R.W., Prakash, A., Sutcliffe, Jnr W.H. 1972. The size distribution of particles in the ocean. *Limnol. Oceanogr.* **17:** 327-340

Sheldon, R.W., Sutcliffe, Jnr W.H. 1978. Generation times of 3 h for Sargasso Sea microplankton determined by ATP analysis. *Limnol. Oceanogr.* **23:** 1051-1055

Sheldon, R.W., Sutcliffe, Jnr W.H., Paranjape, M.A. 1977. Structure of pelagic food chain and relationship between plankton and fish production. *J. Fish. Res. Bd Can.* **34:** 2344-2353

Sheldon, R.W., Sutcliffe, Jnr W.H., Prakash, A. 1973. The production of particles in the surface waters of the ocean with particular reference to the Sargasso Sea. *Limnol. Oceanogr.* **18:** 719-733

Shuter, B.J. 1978. Size dependence of phosphorous and nitrogen subsistence quotas in unicellular microorganisms. *Limnol. Oceanogr.* **23:** 1248-1255

Sieburth, J.M., Smetacek, V., Lenz, J. 1978. Pelagic ecosystem structure: heterotrophic compartments of the plankton and their relationship to plankton size fractions. *Limnol. Oceanogr.* **23:** 1256-1263

Silvert, W., Platt. T. 1980. Dynamic energy flow model of the particle size distribution in pelagic ecosystems. In: Kerfoot, W.C. [ed.]. *Evolution and ecology of zooplankton communities.* The University Press of New England, Dartmouth, N.H., 754-763

Small, L.F., Fowler, S.W., Unlu, M.Y. 1979. Sinking rates of natural copepod fecal pellets. *Mar. Biol.* **51:** 233-241

Smayda, T.J. 1970. The suspension and sinking of phytoplankton in the sea. *Oceanogr. Mar. Biol. Ann. Rev.* **8:** 353-414

Smith, R.E.H., Geider, R.J., Platt, T. 1984. Microplankton productivity in the oligotrophic ocean. *Nature* **311:** 252-254

Smith, R.J. 1980. Rethinking allometry. *J. theor. Biol.* **87:** 97-111

Smith, R.J. 1984. Allometric scaling in comparative biology: problems of concept and method. *Am. J. Physiol.* **246:** R152-R160

Sorokin, Y.I. 1979. Zooflagellates as a component of the community of eutrophic and oligotrophic waters in the Pacific Ocean. *Oceanology* **19:** 316-319

Sprules, W.G., Casselman, J.M., Shuter, B.J. 1983. Size distribution of pelagic particles in lakes. *Can. J. Fish. Aquat. Sci.* **40:** 1761-1769

Stahl, W. R. 1962. Similarity and dimensional methods in biology. *Science* **137:** 205-212

Starfield, A.M., Bleloch, A.L. 1986. *Building models for conservation and wildlife management.* MacMillan, New York, 253pp

Steele, J.H. 1974. *The structure of marine ecosystems.* Blackwell, Oxford

Stoecker, D.K. 1984. Particle production by planktonic ciliates. *Limnol. Oceanogr.* **29:** 930-940

Stoecker, D., Guillard, R.R.L., Kavee, R.M. 1981. Selective predation by *Favella ehrenbergii* (Tintinnia) on and among dinoflagellates. *Biol. Bull.* **160:** 136-145

Stoecker, D.K., Sanders, N.K. 1985. Differential grazing by *Acartia tonsa* on a dinoflagellate and a tintinnid. *J. Plankt. Res.* **7:** 85-100

Strathmann, R.R. 1967. Estimating the organic carbon content of phytoplankton from cell volume or plasma volume. *Limnol. Oceanogr.* **12:** 411-418

Strickland, J.D.H., Parsons, T.R. 1968. A practical handbook of seawater analysis. *Bull. Fish. Res. Bd Can.* **167:** 311pp

Stuart, V. 1986. Feeding and metabolism of *Euphausia lucens* (Euphausiacea) in the southern Benguela current. *Mar. Ecol. Prog. Ser.* **30:** 117-125

Sukhanova, I.N., Konovalova, G.V., Ratikova, T.N. 1978. Phytoplankton numbers and species structure in the Peruvian upwelling region. *Oceanology* **18:** 72-76

Sushchenya, L. M. 1970. Food rations, metabolism and growth of crustaceans. In: Steele, J. H. [ed.]. *Marine food chains.* Oliver and Boyd, Edinburgh, 127-141

Swart, V.P., Largier, J.L. 1987. Thermal structure of Agulhas Bank water. In: Payne, A.I.L., Gulland, J.A., Brink, K.H. [eds]. The Benguela and comparable ecosystems. *S. Afr. J. mar. Sci.* **5:** 243-253

Syrett, P.J. 1981. Nitrogen metabolism of microalgae. In: Platt, T. [ed.]. Physiological bases of phytoplankton ecology. *Can. Bull. Fish. Aquat. Sci.* **210:** 182-210

Taguchi, S. 1976. Relationship between photosynthesis and cell size of marine diatoms. *J. Phycol.* **12:** 185-189

Takahashi, M., Bienfang, P.K. 1983. Size structure of phytoplankton biomass and photosynthesis in subtropical Hawaiian waters. *Mar. Biol.* ***76:*** 203-211

Taylor, W.D., Shuter, B.J. 1981. Body size, genome size, and intrinsic rate of increase in ciliated protozoa. *Am. Nat.* **118:** 160-172

Tempest, D.W., Neijssel, O.M. 1978. Eco-physiological aspects of microbial growth in aerobic nutrient-limited environments. *Adv. Microb. Ecol.* **2:** 105-153

Terry, K.L. 1982. Nitrate uptake and assimilation in *Thalassiosira weissflogii* and *Pageodactylum tricornutum*: interactions with photosynthesis and with the uptake of other ions. *Mar. Biol.* **69:** 21-30

Tett, P., Edwards, A., Jones, K. 1986. A model for the growth of shelf-sea phytoplankton in summer. *Est. Coast. Shelf Sci.* **23:** 641-672

Turner, J.T. 1977. Sinking rates of fecal pellets from the marine copepod *Pontella meadii*. *Mar. Biol.* **40:** 249-259

Ulanowicz, R.E. 1986. *Growth and development: ecosystems phenomenology*. Springer-Verlag, New York

Ulanowicz, R.E., Kemp, W.M. 1979. Toward canonical trophic aggregations. *Am. Nat.* **114:** 871-883

Van Wambeke, F., Bianchi, M.A. 1985. Bacterial biomass production and ammonium regeneration in Mediterranean sea water supplemented with amino acids. I. Correlations between bacterial biomass, bacterial activities and environmental parameters. *Mar. Ecol. Prog. Ser.* **23:** 107-115

Verheye-Dua, F., Lucas, M.I. 1988. The southern Benguela frontal region: I. Hydrology, phytoplankton and bacterioplankton. *Mar. Ecol. Prog. Ser.* (in press)

Verheye, H.M., Hutchings, L. 1988. Horizontal and vertical distribution of zooplankton biomass in the southern Benguela, May 1983. *S. Afr. J. mar. Sci.* **6:** 255-266

Vezina, A.F. 1985. Empirical relationships between predator and prey size among terrestrial vertebrate predators. *Oecologia (Berl.)* **67:** 555-565

Wadsworth Professional Software. 1984. *Statpro, the statistics and graphics database workstation*. Wadsworth, Boston

Walsh, J.J., Kelley, J.C., Dugdale, R.C., Frost, B.W. 1971. Gross features of the Peruvian upwelling system with special reference to possible diel variation. *Inv. Pesq.* **35:** 25-42

Ware, D.M. 1978. Bioenergetics of pelagic fish: theoretical changes in swimming speed and ration with body size. *J. Fish. Res. Bd Can.* **35:** 220-228

Williams, P.J.leB. 1981. Incorporation of microheterotrophic processes into the classical paradigm of the planktonic food web. *Kieler Meeresforsch., Sonderh.* **5:** 1-28

Wilson,D.S. 1973. Food size selection among copepods. *Ecology* **54:** 909-914

Wolter, K. 1982. Bacterial incorporation of organic substances released by natural phytoplankton populations. *Mar. Ecol. Prog. Ser.* **7:** 287-295

Wroblewski, J.S. 1977. A model of phytoplankton plume formation during variable Oregon upwelling. *J. mar. Res.* **35:** 357-394

Yen, J. 1983. Effects of prey concentration, prey size, predator life stage, predator starvation, and season on predation rates of the carnivorous copepod *Euchaeta elongata*. *Mar. Biol.* **75:** 69-77

Zar, J. H. 1968. Calculation and miscalculation of the allometric equation as a model in biological data. *Bioscience* **18:** 1118-1120.

Zar, J. H. 1984. *Biostatistical analysis (second edition)*. Prentice-Hall, Englewood Cliffs, 718pp

APPENDIX I

DOCUMENTATION OF PROGRAM

COLMOL*THESIS.TC1

A PROGRAM TO DEVELOP THE STRUCTURE OF A TROPHIC CONTINUUM MODEL OF A PLANKTON / PELAGIC COMMUNITY

1. Program Specification

This program defines the structure and limits of a model plankton community. The community consists of autotrophs and heterotrophs, the latter being divided into bacterioplankton, epibacteria, bactivorous protozoa and microzooplankton. Information about the size ranges of these different components is input to the program, as is the log base to be used in designating size classes. The program uses this information to divide the autotrophs and heterotrophs into size classes. It also quantifies certain attributes of the size classes, such as body masses, predator and prey sizes, position in the food web, etc. In order to simulate flows of carbon and nitrogen through the community (see program *TC2*), it is necessary to quantify the flow parameters. All model parameters are body-size dependent, and this program calculates the values of parameters for each size class. It also initializes state variables, which are the standing stocks of carbon and nitrogen in each size class, and the concentrations of carbon and nitrogen in abiotic pools. Additional information is read in to the program concerning options to be used in executing the second program, which simulates the dynamics of the model. All the options and variable- and parameter- values are written to a data file, from where they are input to the second program.

2. Instructions for use

2.1 Runstream

The program was written for use on the Sperry 1100 series mainframe computer at the University of Cape Town. It is run in batch mode from CTS (Conversational Time Sharing). An example runstream is given below.

```
@RUN,/N Runid,ACCNT/USER,Projid,time,pages
@ASG,A COLMOL*THESIS.                    assigns program file
@ASG,A TC1*DATFIL.                       assigns input data file
@USE 12.,TC1*DATFIL.                     assigns internal name (12)
@ASG,A TC2*DATFIL.                       assigns output data file
@DELETE,C TC2*DATFIL.                    deletes output data file
@ASG,UP TC2*DATFIL.,F50                  reassigns output data file
@USE,13.,TC2*DATFIL.                     assigns internal name (13)
@XQT COLMOL*THESIS.TC1                   execute the program
@ADD TC1*DATFIL.                         add the input data file
@DATA,L TC1*DATFIL.                      list input data
@END                                     terminate DATA command
@FIN                                     terminate run
```

2.2 Input specifications

Input to the program is contained in a single data file. Records are read in free format at the start of each run, assigning limits and initial values to variables and parameters, and options for execution of the program. The data read from the data file are presented below, with the right hand column showing typical values.

The first line contains a title, which can be up to 72 characters long. The second line specifies the manner and amount of new nitrogen to be input to the model community. The first variable indicates the manner of input; 'PULSED' = a pulsed, single input, 'CONTIN' = a continuous input, or 'CNSTNT' = no input but a constant concentration. The next variable respectively specifies the constant new nitrogen concentration (if NITRO = 'CNSTNT') or the initial new nitrogen concentration (if NITRO = 'CONTIN'), and the third variable sets the input rate for the continuous input. The values of these variables do not matter if one of the other options is chosen.

The third line contains the number of loops (ILOOP) to be executed (the time equivalent in days is obtained by dividing by 20), a variable (III) which sets the loop increment in which data is written to data files for plotting, and a variable (IPRINT) which sets the loop increment in which output is sent to the printer. These varables thus control the total amount of output that is saved and is printed.

The fourth line contains the variable which activates the diurnal cycle, and DIURN can be switched on ('Y') or off ('N'). The variable PERCON allows PER to be set as constant ('CNSTNT') or variable ('CHANGE'). Line 5 contains the factors which determine the size range of prey organisms for each predator relative to the predator's size (U1, U2, U3). The sixth line inputs the value of the absorption efficiency of predators (ASSIM), and two variables which determine the refuge standing stocks of prey organisms. Line 7 contains the variables which determine the preferences of predators for different prey size classes, and line 8 the variables that are used to calculate the initial standing stocks in each size class of autotrophs (ASPEC1, ASPEC2) and heterotrophs (HSPEC1, HSPEC2). The logarithmic base (ESDINT) used to separate size classes is input in line 9, together with the initial carbon standing stock in the detrital compartment (INITD). Initial concentrations in the PDOC, new nitrogen and regenerated nitrogen pools are input from line 10. The value for the new nitrogen pool is ignored if NITRO is 'CNSTNT' or 'CONTIN'.

Lines 11 and 12 contain the minimum and maximum sizes (μm esd) of the autotroph and heterotroph continuums respectively. The factors that are used to convert wet masses to carbon for the model size classes are input from line 13, and the C : N ratios of different components are on line 14. The minumum and maximum esd's of the heterotroph groups are input from line 15, and lines 16 to 21 contain the values used in estimating model parameters.

1.	TITLE	'Standard Simulation'
2.	NITRO NCON NINCRE	'PULSED' 100 5

3.	ILOOP III IPRINT	400 2 10
4.	DIURN PERCON	'N' 'CNSTNT'
5.	U1 U2 U3	0.04 0.06 0.125
6.	ASSIM SMALL1 SMALL2	0.90 1 0
7.	PREF1 PREF2	1 1
8.	ASPEC1 ASPEC2 HSPEC1 HSPEC2	1000 0.95 1000 0.95
9.	ESDINT INITD	10 0
10.	PDOC(1) NEWN(1) REGN(1)	0 1500 0
11.	AMIN AMAX	0.2 200
12.	HMIN HMAX	0.2 2000
13.	ASTOW ASTOW1 HSTOW HSTOW1	0.07 1 0.07 1
14.	ACN PBCN EBCN BVCN ZPCN	6 4 4 4.5 4.5
15.	PBMIN PBMAX EBMIN EBMAX BVMIN BVMAX ZPMIN ZPMAX	0.2 2 2 2 2 20 20 2000
16.	ALPH1 ALPH2 ALPH2A ALPH3 ALPH4 ALPH4A	5.1 5.1 73 1.7 5.1 73
17.	ALPH5 ALPH7 ALPH11 ALPH13 ALPH15 ALP15A ALP15B	0 0 0 0.3 78 54 0
18.	ALPH17 ALPH19 ALPH23	0 15 0
19.	BETA1 BETA2 BETA2A BETA3 BETA4 BETA4A	-0.25 -0.25 940 -0.25 -0.25 940
20.	BETA5 BETA7 BETA11 BETA13 BETA15 BET15A	1 0 0 1 -0.25 0.08
21.	BETA17 BETA19 BETA23	1 -0.25 0

2.3 Output format

All values that are read in and calculated by the program are sent as output to the printer. In addition, values to be used in the second program are written to a data file.

2.4 Restrictions on generality

Two program parameters (SIZE and TIME) assign maximum dimensions to arrays and matrices. The model is thus constrained by the values of these two parameters.

2.5 Run time

Run times are no longer than 20 seconds of computer time. They are determined by the number of size classes; the more size classes there are, the more iterations the program has to perform. The number of size classes is determined by the logarithmic interval used; the smaller the interval the greater the number of size classes. Similarly, the minimum and maximum sizes in the continuums will affect the number of size classes.

3. Conceptual overview

3.1 Construction of the trophic continuum model

There are a number of steps involved in constructing the model. Autotroph and heterotroph groups are divided into size classes using the logarithmic interval set by the user, and the specified minimum and maximum sizes. The number of size classes is calculated, as are their size boundaries on the scale being used. The heterotroph continuum is then grouped into bacterioplankton, epibacteria, bactivores and zooplankton, each group with its own C:N ratio. All autotrophs are assumed to have the same C:N ratio.

Various parameters associated with each size class are calculated. These include average esd's, volumes, surface areas, surface : volume ratios and individual carbon and nitrogen weights. The minimum, optimum and maximum sizes of potential prey are calculated for each predator size class (bactivores and zooplankton), and from these the number of prey size classes available to each predator size class and their positions within the total prey array. Similarly, the minimum, optimum and maximum sizes of potential predators are calculated for each prey size class, as are the number of potential predators for each prey size class and their position within the total heterotroph array.

3.2 Initialization of the model

Size-dependent parameters are calculated, each size class having its own set of parameters. For each autotroph size class there are rate parameters for nitrogen uptake, carbon fixation, respiration and sinking, as well as half saturation constants for nitrogen uptake. For bacterioplankton and epibacteria uptake rates and half saturation constants for nitrogen- and carbon- uptake rates and respiration rates are calculated, and ingestion and respiration rates are calculated for bactivores and zooplankton.

Initial biomasses and numbers in each size class and total biomasses and numbers in each group are calculated. Certain variables read at the start of the run determine which methods of nitrogen input and PDOC release will be used in calculations, and whether or not the simulation is to have a diurnal cycle.

4. Program design

4.1 Overall description

The program is written in FORTRAN, and compiled using the FORTRAN V compiler. It has no subroutines. Initial values are read in at the beginning, calculations are performed and output is sent to the printer and an output data file.

4.2 Data structures

Most data are stored in the form of arrays, with the model structure being that of an array of size classes. The size of the array is determined by the minimum and maximum sizes specified at the beginning of the run, and the size interval being used. Maximum potential size is set by the value of the parameter SIZE in the program.

4.3 Program structure diagram

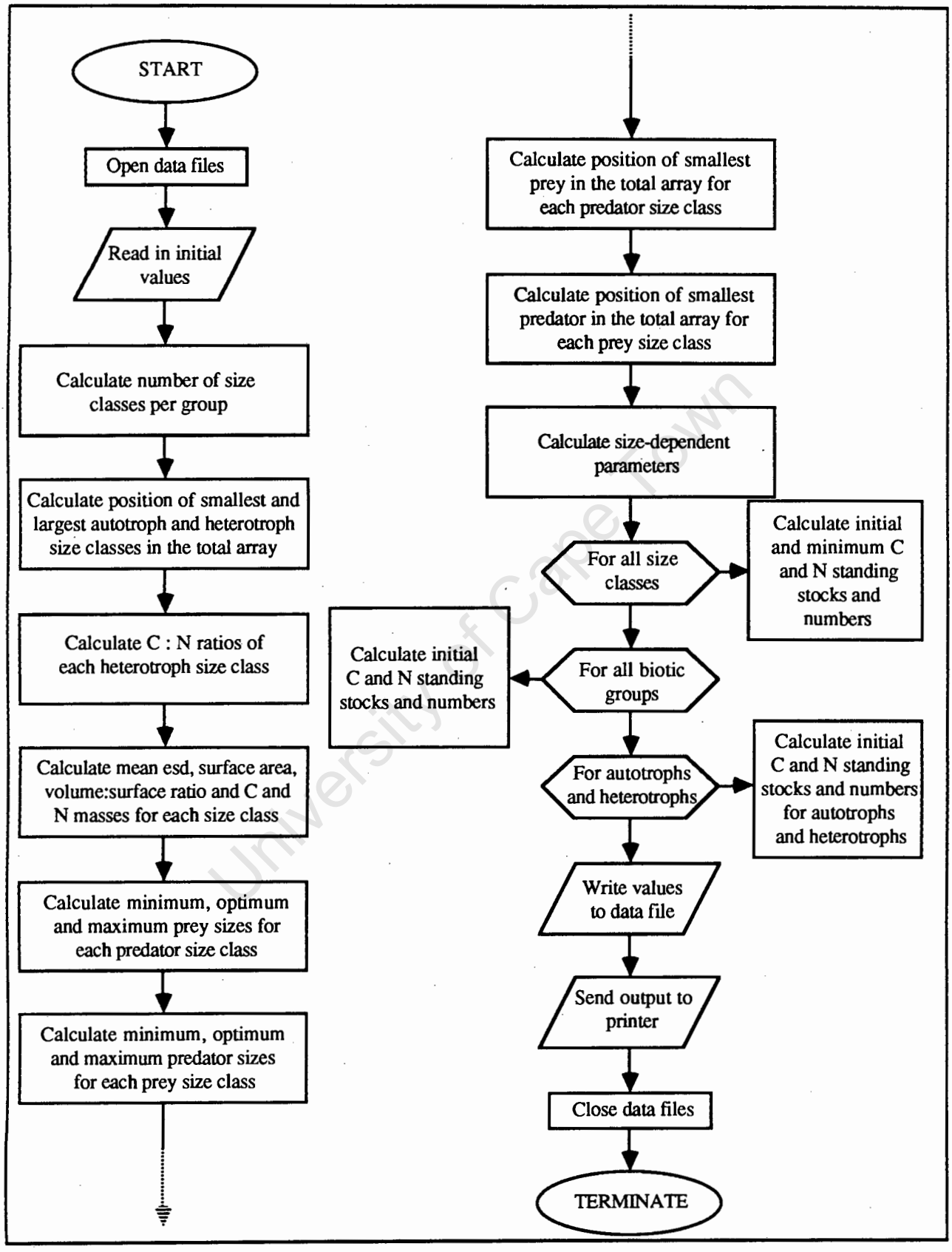

5. Program validation

The program was subjected to a number of checks and test runs to ascertain whether all calculations were carried out correctly. At present there is a problem involved in the calculations that estimate the sizes classes of prey for each predator, and the size classes of predators for each prey size class. The problem appears to be caused by machine rounding errors, and has only been found when the log base (ESDINT) is set to a value of 10. It is recommended that the output data file be checked for this error whenever the log base or size range is altered.

6. Extensions and improvements

The program could be made more interactive and user-friendly, which would make it easier to use.

7. Program listing

```
      ******************************** TC1 ********************************

            CHARACTER*21  VER$N  @ LAST UPDATED ON
     5      &                    /06 SEP 88 AT 09:20:15'/

            CHARACTER*1, DIURN
            CHARACTER*6, NITRO, PERCON
            CHARACTER *72, TITLE
     10
            INTEGER SIZE, TIME, ACLASS, HCLASS, ILOOP
            INTEGER TCLASS, UCLASS, UMINUS, UPLUS
            INTEGER VCLASS, VPLUS, VMINUS
            INTEGER PBCLAS, EBCLAS, BVCLAS, ZPCLAS
     15     INTEGER IA1, IA2, IH1, IH2, UPOS, VPOS, III
            INTEGER IPB1, IEB1, IBV1, IZP1
            INTEGER IPB2, IEB2, IBV2, IZP2
            INTEGER ICHECK, K, IPRINT

     20     PARAMETER SIZE = 100
            PARAMETER TIME = 2

            REAL A, AMIN, AMAX, AESD, AWTC, AWTN, ASTOW, ASTOW1, ACN
            REAL H, HMIN, HMAX, HESD, HWTC, HWTN, HSTOW, HSTOW1, HCN
     25     REAL T, TMIN, TMAX, TW1, TW2, TESD
            REAL ARAD, ASA, AVOL, ASAVOL
            REAL HRAD, HSA, HVOL, HSAVOL, ASSIMH
            REAL PB, PBMIN, PBMAX, PBCN
            REAL EB, EBMIN, EBMAX, EBCN
     30     REAL BV, BVMIN, BVMAX, BVCN
            REAL ZP, ZPMIN, ZPMAX, ZPCN
            REAL PBC, EBC, BVC, ZPC
            REAL PBN, EBN, BVN, ZPN
            REAL PBNUM, EBNUM, BVNUM, ZPNUM
     35     REAL ESDINT, INITD
```

```
      REAL A1, A2, A2A, A3, A4, A4A, A5, A7, A11, A13
      REAL H15, H15A, H17, H19, H23, K15
      REAL ALPH1, ALPH2, ALPH2A, ALPH3, ALPH4, ALPH4A
      REAL ALPH5, ALPH7, ALPH11, ALPH13, ALPH15
40    REAL ALP15A, ALP15B, ALPH17, ALPH19, ALPH23
      REAL BETA1, BETA2, BETA2A, BETA3, BETA4, BETA4A
      REAL BETA5, BETA7, BETA11, BETA13, BETA15, BET15A
      REAL BETA17, BETA19, BETA23
      REAL AC, HC, DC, PDOC
45    REAL AN, HN, DN, NEWN, REGN
      REAL ASUM, HSUM
      REAL AMASSC, AMASSN, ANUM
      REAL HMASSC, HMASSN, HNUM
      REAL TMASSC
50    REAL U, U1, U2, U3, UMAX, UMIN, UOPT
      REAL V, VMAX, VMIN, VOPT
      REAL PREF1, PREF2
      REAL RA, RH, RPB, REB, RBV, RZP
      REAL NCON, NINCRE
55    REAL ASPEC1, ASPEC2, HSPEC1, HSPEC2
      REAL ASSIM, ASMALC, HSMALC, SMALL1, SMALL2

      DIMENSION AESD(SIZE), ARAD(SIZE), ASA(SIZE), AVOL(SIZE)
      DIMENSION HESD(SIZE), HRAD(SIZE), HSA(SIZE), HVOL(SIZE)
60    DIMENSION HCN(SIZE), UPOS(SIZE), VPOS(SIZE), ASSIMH(SIZE)
      DIMENSION TESD(SIZE)
      DIMENSION ASAVOL(SIZE), AWTC(SIZE), AWTN(SIZE)
      DIMENSION HSAVOL(SIZE), HWTC(SIZE), HWTN(SIZE)
      DIMENSION ASMALC(SIZE), HSMALC(SIZE)
65    DIMENSION UMIN(SIZE), UOPT(SIZE), UMAX(SIZE)
      DIMENSION UCLASS(SIZE), UPLUS(SIZE), UMINUS(SIZE)
      DIMENSION VMIN(SIZE), VOPT(SIZE), VMAX(SIZE)
      DIMENSION VCLASS(SIZE), VPLUS(SIZE), VMINUS(SIZE)

70    DIMENSION A1(SIZE), A2(SIZE), A2A(SIZE), A3(SIZE), A4(SIZE)
      DIMENSION A4A(SIZE), A5(SIZE), A7(SIZE), A11(SIZE), A13(SIZE)
      DIMENSION H15(SIZE), H15A(SIZE), H17(SIZE)
      DIMENSION H19(SIZE), H23(SIZE), K15(SIZE)
      DIMENSION TMASSC(TIME,SIZE)
75    DIMENSION AMASSC(TIME,SIZE), AMASSN(TIME,SIZE), ANUM(TIME,SIZE)
      DIMENSION HMASSC(TIME,SIZE), HMASSN(TIME,SIZE), HNUM(TIME,SIZE)
      DIMENSION PBC(TIME), EBC(TIME), BVC(TIME), ZPC(TIME)
      DIMENSION PBN(TIME), EBN(TIME), BVN(TIME), ZPN(TIME)
      DIMENSION PBNUM(TIME), EBNUM(TIME), BVNUM(TIME), ZPNUM(TIME)
80    DIMENSION AC(TIME), AN(TIME), ASUM(TIME)
      DIMENSION HC(TIME), HN(TIME), HSUM(TIME)
      DIMENSION DC(TIME), DN(TIME)
      DIMENSION NEWN(TIME), REGN(TIME), PDOC(TIME)

85
    5   FORMAT ( )
    15  FORMAT ('1',A38,A21/////)
    25  FORMAT ('0',7X,A5,2X,I6,13X,A3,3X,I2,17X,A2,2X,F6.3//,7X,A6,
       &2X,F6.3,11X,A5,4X,A1,17X,A2,2X,F6.3//,8X,A5,2X,F6.3,11X,A5,
90     &2X,A6,14X,A2,2X,F6.3//,
       &7X,A6,2X,A6,12X,A4,2X,F6.1,11X,A5,
       &2X,F6.3//,8X,A5,2X,F6.2,10X,A6,2X,F6.3,11X,A5,2X,F6.3////)
    35  FORMAT ('0',6X,2(A5,1X,F7.3,6X),7X,2(A5,1X,F7.3,6X),6X,A6,1X,F7.3,
```

```
     &5X,A6,1X,F7.3//,2(7X,2(A5,1X,F7.3,6X),7X,2(A5,1X,F7.2,6X),6X,A6,
95   &1X,F7.3,5X,A6,1X,F7.3//),2(6X,2(A6,1X,F7.3,5X),7X,2(A6,1X,
     &F7.3,5X),7X,A6,1X,F7.3,5X,A6,1X,F7.3//),6X,A6,1X,F7.3////)
    45  FORMAT ('0',7X,A4,1X,F9.3,10X,A4,1X,E9.3,8X,A6,1X,I3,11X,A3,
     &1X,I3,8X,A3,1X,I3,4X,A6,1X,F10.1,3X,A3,1X,F4.2//,8X,A4,1X,F9.3,
     &10X,A4,1X,E9.3,8X,A6,1X,I3,11X,A3,1X,I3,8X,A3,1X,I3,4X,A6,1X,
100  &F10.1//,2(7X,A5,1X,F9.3,9X,A5,1X,E9.3,8X,A6,1X,I3,10X,A4,1X,I3,
     &7X,A4,1X,I3,4X,A6,1X,F10.1//),
     &2(7X,A5,1X,F9.3,9X,A5,1X,E9.3,8X,A6,1X,I3,10X,A4,1X,I3,
     &7X,A4,1X,I3,4X,A6,1X,F10.1//),8X,A4,1X,F9.3,10X,A4,1X,E9.3,8X,A6,
     &1X,I3,9X,A5,1X,F4.2,5X,A5,1X,F4.2,4X,A5,1X,F6.2,2X,A6,1X,F4.2////)
105  55  FORMAT ('1',30X,A40////)
     65  FORMAT ('0',A5,3X,A7,4X,2(A11,2X),2X,A7,5X,A7,6X,A5,5X,A9,3X,A9,
    &5X,A7,5X,A9)
     75  FORMAT ('0',A5,3X,A7,4X,2(A11,2X),2X,A7,5X,A7,6X,A5,5X,A9,3X,A9,
    &5X,A7,5X,A9//)
110  85  FORMAT ('0',I4,3X,E8.3,2X,E12.3,3X,4(E10.3,2X),2(F10.2,2X),
    &E10.3,8X,F5.2)
     95  FORMAT ('0',2X,A15,2X,F8.3,4X,A1,1X,F8.3,4X,I3,1X,A12//,
     &3X,A11,6X,F8.3,4X,A1,1X,F8.3,4X,I3,1X,A12//,
     &3X,A10,7X,F8.3,4X,A1,1X,F8.3,4X,I3,1X,A12//,
115  &3X,A11,6X,F8.3,4X,A1,1X,E8.3,4X,I3,1X,A12////)
    105  FORMAT ('0',3X,A8,7(2X,A8),4(2X,A10))
    115  FORMAT ('0',3X,A8,7(2X,A8),4(2X,A10)//)
    125  FORMAT ('0',8(F8.2,2X),4(E10.3,2X)////)
    135  FORMAT ('0',20X,A72////)
120 145  FORMAT ('0',28X,A15,4X,A17,4X,A13)
    155  FORMAT ('0',28X,A15,4X,A17,4X,A13//)
    165  FORMAT ('0',5X,A13,11X, 2(F8.2,12X),E10.3//,5X,A13,12X,
    &2(F8.2,12X),E10.3//,5X,A13,12X,2(F8.2,12X)//)
    175  FORMAT ('0',7X,A6,4X,3(A9,5X),A9,4X,A6,2X,A6,3X,A5,3X,A4)
125 185  FORMAT ('0',7X,A6,4X,3(A9,5X),A9,4X,A6,2X,A6,3X,A5,3X,A4//)
    195  FORMAT ('0',8X,I3,4(5X,E9.3),4(5X,I3))
    205  FORMAT ('0',7X,A6,4X,3(A9,5X),A9,4X,A6,2X,A6,3X,A5,3X,A4,2X,A15)
    215  FORMAT ('0',7X,A6,4X,3(A9,5X),A9,4X,A6,2X,A6,3X,A5,3X,A4,2X,A15//)
    225  FORMAT ('0',8X,I3,4(5X,E9.3),4(5X,I3),9X,E8.3)
130 235  FORMAT ('0',A5,1X,A7,2X,A3,3X,9(A6,1X),2X,5(A6,3X))
    245  FORMAT ('0',A5,1X,A7,2X,A3,3X,9(A6,1X),2X,5(A6,3X)//)
    255  FORMAT ('0',1X,I2,1X,E8.3,1X,9(F6.3,1X),6(E8.3,1X))


135 *        ****************************
    *        ***                      ***
    *        ***  INITIALISATION      ***
    *        ***                      ***
    *        ****************************
140
       OPEN (12)
       OPEN (13)


145    READ (12,5) TITLE
       READ (12,5) NITRO, NCON, NINCRE
       READ (12,5) ILOOP, III, IPRINT
       READ (12,5) DIURN, PERCON
       READ (12,5) U1, U2, U3
150    READ (12,5) ASSIM, SMALL1, SMALL2
       READ (12,5) PREF1, PREF2
```

```
      READ (12,5) ASPEC1, ASPEC2, HSPEC1, HSPEC2
      READ (12,5) ESDINT, INITD
      READ (12,5) PDOC(1), NEWN(1), REGN(1)
155   READ (12,5) AMIN, AMAX
      READ (12,5) HMIN, HMAX
      READ (12,5) ASTOW, ASTOW1, HSTOW, HSTOW1
      READ (12,5) ACN, PBCN, EBCN, BVCN, ZPCN
      READ (12,5) PBMIN, PBMAX, EBMIN, EBMAX, BVMIN, BVMAX, ZPMIN, ZPMAX
160   READ (12,5) ALPH1, ALPH2, ALPH2A, ALPH3, ALPH4, ALPH4A
      READ (12,5) ALPH5, ALPH7, ALPH11, ALPH13, ALPH15, ALP15A, ALP15B
      READ (12,5) ALPH17, ALPH19, ALPH23
      READ (12,5) BETA1, BETA2, BETA2A, BETA3, BETA4, BETA4A
      READ (12,5) BETA5, BETA7, BETA11, BETA13, BETA15, BET15A
165   READ (12,5) BETA17, BETA19, BETA23

*     ****************************************************************
*     ***                                                          ***
170   *** CALCULATE THE NUMBER OF SIZE CLASSES PER GROUP            ***
*     ***                                                          ***
*     ****************************************************************

      IF (AMIN .LE. HMIN) TMIN = AMIN
175   IF (HMIN .LE. AMIN) TMIN = HMIN

      IF (AMAX .GE. HMAX) TMAX = AMAX
      IF (HMAX .GE. AMAX) TMAX = HMAX

180   A = (LOG (AMAX / AMIN)) / (LOG (ESDINT))
      H = (LOG (HMAX / HMIN)) / (LOG (ESDINT))
      T = (LOG (TMAX / TMIN)) / (LOG (ESDINT))
      PB = (LOG (PBMAX / PBMIN)) / (LOG(ESDINT))
      EB = (LOG (EBMAX / EBMIN)) / (LOG (ESDINT))
185   BV = (LOG (BVMAX / BVMIN)) / (LOG (ESDINT))
      ZP = (LOG (ZPMAX / ZPMIN)) / (LOG (ESDINT))

      ACLASS = ANINT(A)
      HCLASS = ANINT(H)
190   PBCLAS = ANINT(PB)
      EBCLAS = ANINT(EB)
      BVCLAS = ANINT(BV)
      ZPCLAS = ANINT(ZP)
      TCLASS = ANINT(T)
195

*     ********************************************************************
*     ***                                                              ***
*     *** WORK OUT POSITION OF BIGGEST AND SMALLEST AUTOTROPH        ***
200   *** AND HETEROTROPH CLASSES IN THE PREY ARRAY                  ***
*     ***                                                              ***
*     ********************************************************************

      RA = LOG (AMIN / TMIN) / (LOG (ESDINT))
205   RH = LOG (HMIN / TMIN) / (LOG (ESDINT))
      RPB = LOG (PBMIN / TMIN) / LOG (ESDINT)
      REB = LOG (EBMIN / TMIN) / LOG (ESDINT)
      RBV = LOG (BVMIN / TMIN) / LOG (ESDINT)
      RZP = LOG (ZPMIN / TMIN) / LOG (ESDINT)
```

```
      IA1 = ANINT(RA) + 1
      IH1 = ANINT(RH) + 1
      IPB1 = ANINT(RPB) + 1
      IEB1 = ANINT(REB) + 1
      IBV1 = ANINT(RBV) + 1
      IZP1 = ANINT(RZP) + 1


      IA2 = IA1 + ACLASS - 1
      IH2 = IH1 + HCLASS - 1
      IPB2 = IPB1 + PBCLAS - 1
      IEB2 = IEB1 + EBCLAS - 1
      IBV2 = IBV1 + BVCLAS - 1
      IZP2 = IZP1 + ZPCLAS - 1

*************************************************************************
****                                                                 ***
****  CALCULATE THE C N RATIO OF EACH HETEROTROPH SIZE CLASS         ***
****                                                                 ***
*************************************************************************

   DO 100 J = IPB1, IPB2
      HCN(J) = PBCN
100  CONTINUE

   DO 110 J = IEB1, IEB2
      HCN(J) = EBCN
110  CONTINUE

   DO 120 J = IBV1, IBV2
      HCN(J) = BVCN
120  CONTINUE

   DO 130 J = IZP1, IZP2
      HCN(J) = ZPCN
130  CONTINUE


*************************************************************************
****                                                                 ***
****  CALCULATE THE MEAN INDIVIDUAL ESD, CARBON WEIGHT,              ***
**** NITROGEN WEIGHT & SA,VOLUME RATIO FOR EACH SIZE CLASS          ***
****            FOR EACH GROUP                                       ***
****                                                                 ***
*************************************************************************

*---------------------- PREY ARRAY ----------------------
   TW1 = TMIN
   TW2 = TMIN * ESDINT

   DO 140 J = 1, TCLASS
     TESD(J) = SQRT (TW1 * TW2)
     TW1 = TW2
     TW2 = TW2 * ESDINT
140  CONTINUE
*---------------------- AUTOTROPHS ----------------------
 DO 150 J = IA1, IA2
```

```
          AESD(J) = TESD(J)
          ARAD(J) = AESD(J) / 2
270       ASA(J)  = 4 * 3.1415926 * ARAD(J)**2
          AVOL(J) = ASA(J) * ARAD(J) / 3
          ASAVOL(J) = ASA(J) / AVOL(J)
          AWTC(J) = ASTOW * AVOL(J) ** ASTOW1
          AWTN(J) = AWTC(J) / ACN
275     150 CONTINUE
        *-------------------- HETEROTROPHS --------------------
          DO 160 J = IH1, IH2
            HESD(J) = TESD(J)
            HRAD(J) = HESD(J) / 2
280         HSA(J)  = 4 * 3.1415926 * HRAD(J)**2
            HVOL(J) = HSA(J) * HRAD(J) / 3
            HSAVOL(J) = HSA(J) / HVOL(J)
            HWTC(J) = HSTOW * HVOL(J) ** HSTOW1
            HWTN(J) = HWTC(J) / HCN(J)
285     160 CONTINUE
        * ***************************************************************************
        * ***                                                                     ***
        * ***   WORK OUT MIN, MAX & OPT PREY SIZES FOR EACH PREDATOR CLASS    ***
        * ***                                                                     ***
290     * ***************************************************************************

          DO 170 J = IBV1, IH2
            UMIN(J) = U1 * HESD(J)
            IF (UMIN(J) .LT. TESD(1)) UMIN(J) = TESD(1)
295         UOPT(J) = U2 * HESD(J)
            IF (UOPT(J) .LT. TESD(1)) UOPT(J) = TESD(1)
            UMAX(J) = U3 * HESD(J)
            IF (UMAX(J) .LT. TESD(1)) UMAX(J) = TESD(1)
              DO 172 K = IH1, IH2
300             IF(UMIN(J).GE.TESD(K).AND.UMIN(J).LT.TESD(K+1))THEN
                  UMIN(J) = TESD(K)
                ENDIF
                IF(UOPT(J).GE.TESD(K).AND.UOPT(J).LT.TESD(K+1))THEN
                  UOPT(J) = TESD(K)
305             ENDIF
                IF(UMAX(J).GT.TESD(K).AND.UMAX(J).LE.TESD(K+1))THEN
                  UMAX(J) = TESD(K+1)
                ENDIF
            172 CONTINUE
310         U = LOG (UMAX(J) / UMIN(J)) / (LOG (ESDINT))
            UCLASS(J) = ANINT(U) + 1
            U = LOG (UOPT(J) / UMIN(J)) / (LOG (ESDINT))
            UMINUS(J) = ANINT(U)
            U = LOG (UMAX(J) / UOPT(J)) / (LOG (ESDINT))
315         UPLUS(J) = ANINT(U)
        170 CONTINUE

        * ***************************************************************************
        * ***                                                                     ***
320     * ***   WORK OUT MIN, MAX & OPT PREDATOR SIZES FOR EACH PREY CLASS    ***
        * ***                                                                     ***
        * ***************************************************************************

          DO 180 J = 1, IH2
325         VMIN(J) = TESD(J) / U3
```

```
            VOPT(J) = TESD(J) / U2
            VMAX(J) = TESD(J) / U1

           IF (VMIN(J) .LT. TESD(IBV1) .AND. VMAX(J) .GE. TESD(IBV1))
330       &     VMIN(J) = TESD(IBV1)
           IF (VMIN(J) .GT. TESD(IH2) .AND. J .EQ. IH2) VMIN(J) = 9999999
            IF (VMIN(J).GT.TESD(IH2).AND.VMIN(J).LE.TMAX) THEN
              VMIN(J) = TESD(IH2)
            ENDIF
335        IF (VMIN(J) .LT. TESD(IBV1) .AND. VMAX(J) .LT. TESD(IBV1))
          &     VMIN(J) = 9999999

           IF (VOPT(J) .LT. TESD(IBV1) .AND. VMAX(J) .GE. TESD(IBV1))
          &     VOPT(J) = TESD(IBV1)
340        IF (VOPT(J) .GT. TESD(IH2) .AND. VMIN(J) .LE. TESD(IH2))
          &     VOPT(J) = TESD(IH2)
           IF (VOPT(J) .LT. TESD(IBV1) .AND. VMAX(J) .LT. TESD(IBV1))
          &     VOPT(J) = 9999999
           IF (VOPT(J) .GT. TESD(IH2) .AND. VMIN(J) .GT. TESD(IH2))
345       &     VOPT(J) = 9999999

           IF (VMAX(J) .LT. TESD(IBV1)) VMAX(J) = 9999999
           IF (VMAX(J) .GT. TESD(IH2) .AND. VMIN(J) .LE. TESD(IH2))
          &     VMAX(J) = TESD(IH2)
350        IF (VMAX(J) .GT. TESD(IH2) .AND. VMIN(J) .GT. TESD(IH2))
          &     VMAX(J) = 9999999
           DO 182 K = IBV1, IH2
            IF (VMIN(J).GE.TESD(K).AND.VMIN(J).LT.TESD(K+1))THEN
              VMIN(J) = TESD(K)
355         ENDIF
            IF (VOPT(J).GE.TESD(K).AND.VOPT(J).LT.TESD(K+1))THEN
              VOPT(J) = TESD(K)
            ENDIF
            IF (VMAX(J).GT.TESD(K).AND.VMAX(J).LE.TESD(K+1))THEN
360           VMAX(J) = TESD(K+1)
            ENDIF
       182  CONTINUE

           V = LOG (VMAX(J) / VMIN(J)) / (LOG (ESDINT))
365        VCLASS(J) = ANINT(V) + 1
           V = LOG (VOPT(J) / VMIN(J)) / (LOG (ESDINT))
           VPLUS(J) = ANINT(V)
           V = LOG (VMAX(J) / VOPT(J)) / (LOG (ESDINT))
           VMINUS(J) = ANINT(V)
370        IF (VMAX(J) .EQ. 9999999) VCLASS(J) = 0
           IF (VMIN(J) .EQ. 9999999) VCLASS(J) = 0
           IF (VOPT(J) .EQ. 9999999) VCLASS(J) = 0
           IF (VCLASS(J) .EQ. 0) THEN
             VPLUS(J) = 0
375          VMINUS(J) = 0
           ENDIF
       180 CONTINUE

       * ********************************************************************
380    * ***                                                            ***
       * ***       CALCULATE POSITION OF SMALLEST PREY IN PREY          ***
       * ***             ARRAY FOR EACH PREDATOR                        ***
       * ***                                                            ***
```

```
      * ****************************************************************
385
          ICHECK = 0

          DO 200 J = IBV1, IH2
            K = 1
390       190   CONTINUE
            IF (UMIN(J) .GE. TESD(K) .AND. UMIN(J) .LT. TESD(K+1)) THEN
              UPOS(J) = K
            ELSEIF (UMIN(J) .GT. TESD(K) .AND. UMIN(J) .GE. TESD(K+1)) THEN
              K = K + 1
395           GO TO 190
            ELSEIF (UMIN(J) .LT. TESD(K)) THEN
              UPOS(J) = 1
              UMINUS(J) = ICHECK
              ICHECK = ICHECK + 1
400         ENDIF
          200 CONTINUE


      * ****************************************************************
405   * ***                                                          ***
      * ***       CALCULATE POSITION OF SMALLEST PREDATOR IN         ***
      * ***            PREDATOR ARRAY FOR EACH PREY                  ***
      * ***                                                          ***
      * ****************************************************************
410
          ICHECK = 0

          DO 220 J = 1, IH2
            K = IBV1
415       210   CONTINUE
            IF (K .EQ. IH2) THEN
              IF (VMIN(J) .LE. TESD(K)) THEN
                VPOS(J) = K
              ELSEIF (VMIN(J) .GT. TESD(K)) THEN
420             VPOS(J) = 0
              ENDIF
            ELSEIF (K .LT. IH2) THEN
              IF (VMIN(J).GT.TESD(K).AND.VMIN(J) .LE. TESD(K+1)) THEN
                VPOS(J) = K + 1
425           ELSEIF (VMIN(J) .EQ. TESD(IBV1)) THEN
                VPOS(J) = IBV1
              ELSEIF (VMIN(J).GT.TESD(K).AND.VMIN(J) .GE. TESD(K+1)) THEN
                K = K + 1
                GO TO 210
430           ELSEIF(VMIN(J).LT.TESD(IBV1).AND.VMAX(J).GE.TESD(IBV1))THEN
                VPOS(J) = IBV1
                VMINUS(J) = ICHECK
                ICHECK = ICHECK + 1
              ELSEIF(VMIN(J).LT.TESD(IBV1).AND.VMAX(J).LT.TESD(IBV1))THEN
435             VPOS(J) = 0
              ENDIF
            ENDIF
          220 CONTINUE

440
      *       ***************************************************
```

```
*        ***                                                  ***
*        ***  CALCULATE SIZE-DEPENDENT PARAMETERS             ***
*        ***                                                  ***
*        ******************************************************
      DO 230 J = 1, TCLASS
        TMASSC(1,J) = 0
        A1(J)  = 0
        A2(J)  = 0
        A2A(J) = 0
        A3(J)  = 0
        A4(J)  = 0
        A4A(J) = 0
        A5(J)  = 0
        A7(J)  = 0
        A11(J) = 0
        A13(J) = 0
        H15(J) = 0
        H15A(J) = 0
        H17(J) = 0
        H19(J) = 0
        H23(J) = 0
  230 CONTINUE

      DO 250 J = 1, TCLASS
        IF (AWTC(J) .EQ. 0) GO TO 240
        A1(J)  = ALPH1 * AWTC(J)** BETA1
        A2(J)  = ALPH2 * AWTC(J)** BETA2
        A2A(J) = ALPH2A * AWTC(J) / (BETA2A + AWTC(J))
        A3(J)  = ALPH3 * AWTC(J)** BETA3
        A4(J)  = ALPH4 * AWTC(J)** BETA4
        A4A(J) = ALPH4A * AWTC(J) / (BETA4A + AWTC(J))
        A5(J)  = ALPH5 * AWTC(J)** BETA5
        A7(J)  = ALPH7 * AWTC(J)** BETA7
        A11(J) = ALPH11 * AWTC(J)** BETA11
        A13(J) = ALPH13 ** BETA13
  240   CONTINUE

        IF (HWTC(J) .EQ. 0) GO TO 250
        IF (J .GE. IPB1 .AND. J .LE. IEB2) THEN
          K15(J) = ALPH2A * HWTC(J) / (BETA2A + HWTC(J))
        ELSEIF (J .LT. IPB1 .OR. J .GT. IEB2) THEN
          K15(J) = 0
        ENDIF
        IF (J .GE. IPB1 .AND. J .LE. IEB2) THEN
          H15(J) = ALPH2 * HWTC(J)** BETA2
        ELSEIF (J .GT. IEB2) THEN
          H15(J) = ALPH15 * HWTC(J)** BETA15
        ENDIF
        H15A(J) = ALP15B + ALP15A * HWTC(J) ** BET15A
        H17(J) = ALPH17 * HWTC(J)** BETA17
        IF (J .GE. IPB1 .AND. J .LE. IEB2) THEN
          H19(J) = ALPH3 * HWTC(J) **BETA3
        ELSEIF (J .GT. IEB2) THEN
          H19(J) = ALPH19 * HWTC(J)** BETA19
        ENDIF
        H23(J) = ALPH23 * HWTC(J)** BETA23
        IF (J .GE. IPB1 .AND. J .LE. IEB2) ASSIMH(J) = 1
```

```
500         IF (J .GT. IEB2) ASSIMH(J) = ASSIM

      250 CONTINUE

      * ****************************************************************
505   * ***                                                          ***
      * ***  CALCULATE THE INITIAL BIOMASSES (ug) AND MINIMUM    ***
      * ***        BIOMASSES (ug) FOR EACH SIZE CLASS             ***
      * ***                                                          ***
      * ****************************************************************
510
        DO 260 J = IA1, IA2
          AMASSC(1,J) = (ASPEC1 * AWTC(J) **ASPEC2) / 1000000
          AMASSN(1,J) = AMASSC(1,J) / ACN
          ANUM(1,J) = AMASSC(1,J) * 1000000 / AWTC(J)
515       TMASSC(1,J) = AMASSC(1,J)
          ASMALC(J) = (SMALL1 * AWTC(J) ** SMALL2) / 1000000
      260 CONTINUE

        DO 270 J = IPB1, IPB2
520       HMASSC(1,J) = (HSPEC1 * HWTC(J) **HSPEC2) / 1000000
          HMASSN(1,J) = HMASSC(1,J) / HCN(J)
          HNUM(1,J) = HMASSC(1,J) * 1000000 / HWTC(J)
          TMASSC(1,J) = TMASSC(1,J) + HMASSC(1,J)
          HSMALC(J) = (SMALL1 * HWTC(J) ** SMALL2) / 1000000
525   270 CONTINUE

        DO 280 J = IEB1, IEB2
          HMASSC(1,J) = (HSPEC1 * HWTC(J) **HSPEC2) / 1000000
          HMASSN(1,J) = HMASSC(1,J) / HCN(J)
530       HNUM(1,J) = HMASSC(1,J) * 1000000 / HWTC(J)
          TMASSC(1,J) = TMASSC(1,J) + HMASSC(1,J)
          HSMALC(J) = (SMALL1 * HWTC(J) ** SMALL2) / 1000000
      280 CONTINUE

535     DO 290 J = IBV1, IBV2
          HMASSC(1,J) = (HSPEC1 * HWTC(J) **HSPEC2) / 1000000
          HMASSN(1,J) = HMASSC(1,J) / HCN(J)
          HNUM(1,J) = HMASSC(1,J) * 1000000 / HWTC(J)
          TMASSC(1,J) = TMASSC(1,J) + HMASSC(1,J)
540       HSMALC(J) = (SMALL1 * HWTC(J) ** SMALL2) / 1000000
      290 CONTINUE

        DO 300 J = IZP1, IZP2
          HMASSC(1,J) = (HSPEC1 * HWTC(J) **HSPEC2) / 1000000
545       HMASSN(1,J) = HMASSC(1,J) / HCN(J)
          HNUM(1,J) = HMASSC(1,J) * 1000000 / HWTC(J)
          TMASSC(1,J) = TMASSC(1,J) + HMASSC(1,J)
          HSMALC(J) = (SMALL1 * HWTC(J) ** SMALL2) / 1000000
      300 CONTINUE
550
      * ****************************************************************
      * ***                                                          ***
      * *** CALCULATE THE INITIAL BIOMASSES (ug) AND NUMBERS     ***
      * ***          FOR EACH HETEROTROPH GROUP                    ***
555   * ***                                                          ***
      * ****************************************************************
```

```
      PBC(1) = 0
      PBN(1) = 0
560   PBNUM(1) = 0

      DO 310 J = IPB1, IPB2
         PBC(1) = PBC(1) + HMASSC(1,J)
         PBN(1) = PBN(1) + HMASSN(1,J)
565      PBNUM(1) = PBNUM(1) + HNUM(1,J)
  310 CONTINUE

      EBC(1) = 0
      EBN(1) = 0
570   EBNUM(1) = 0

      DO 320 J = IEB1, IEB2
         EBC(1) = EBC(1) + HMASSC(1,J)
         EBN(1) = EBN(1) + HMASSN(1,J)
575      EBNUM(1) = EBNUM(1) + HNUM(1,J)
  320 CONTINUE

      BVC(1) = 0
      BVN(1) = 0
580   BVNUM(1) = 0

      DO 330 J = IBV1, IBV2
        BVC(1) = BVC(1) + HMASSC(1,J)
        BVN(1) = BVN(1) + HMASSN(1,J)
585     BVNUM(1) = BVNUM(1) + HNUM(1,J)
  330 CONTINUE

      ZPC(1) = 0
      ZPN(1) = 0
590   ZPNUM(1) = 0

      DO 340 J = IZP1, IZP2
        ZPC(1) = ZPC(1) + HMASSC(1,J)
        ZPN(1) = ZPN(1) + HMASSN(1,J)
595     ZPNUM(1) = ZPNUM(1) + HNUM(1,J)
  340 CONTINUE

*  ********************************************************************
*  ***                                                              ***
600*  *** CALCULATE THE INITIAL BIOMASSES (ug) AND NUMBERS          ***
*  ***          FOR EACH FUNCTIONAL GROUP                           ***
*  ***                                                              ***
*  ********************************************************************

605   AC(1) = 0
      HC(1) = 0
      DC(1) = 0
      AN(1) = 0
      HN(1) = 0
610   DN(1) = 0
      ASUM(1) = 0
      HSUM(1) = 0

      DO 350 J = 1, TCLASS
615     AC(1) = AC(1) + AMASSC(1,J)
```

```
            HC(1) = HC(1) + HMASSC(1,J)
            AN(1) = AN(1) + AMASSN(1,J)
            HN(1) = HN(1) + HMASSN(1,J)
            ASUM(1) = ASUM(1) + ANUM(1,J)
620         HSUM(1) = HSUM(1) + HNUM(1,J)
350   CONTINUE

*           **********************************
*           ***                            ***
625   *     ***  WRITE INITIAL VALUES      ***
*           ***                            ***
*           **********************************

      IF (NITRO .EQ. 'PULSED') THEN
630     WRITE (13,5) "'PULSED'", NCON, NINCRE
      ELSEIF (NITRO .EQ. 'CONTIN') THEN
        WRITE (13,5) "'CONTIN'", NCON, NINCRE
      ELSEIF (NITRO .EQ. 'CNSTNT') THEN
        WRITE (13,5) "'CNSTNT'", NCON, NINCRE
635   ENDIF
      WRITE (13,5) ILOOP, TCLASS, ACN
      DO 360 J = 1, TCLASS
        WRITE (13,5) AMASSC(1,J), AMASSN(1,J), HMASSC(1,J),
     &   HMASSN(1,J), TMASSC(1,J), ASMALC(J), HSMALC(J), HCN(J)
640   360  CONTINUE
      WRITE (13,5) DC(1), DN(1), NEWN(1), REGN(1), PDOC(1)
      WRITE (13,5) IBV1, IH1, IH2, ACN, PREF1, PREF2
      WRITE (13,5) IA1, IA2, IPB1, IPB2
      DO 370 J = 1, TCLASS
645     WRITE (13,5) UCLASS(J), UMINUS(J), UPLUS(J), UPOS(J)
        WRITE (13,5) VPOS(J), VCLASS(J)
370   CONTINUE
      DO 380 J = IH1, IH2
        WRITE (13,5) H15(J), H15A(J), HCN(J), A2(J), A2A(J), K15(J)
650   380  CONTINUE
      IF (DIURN .EQ. 'Y') THEN
        WRITE (13,5) IA1, IA2, ACN, "'Y'"
      ELSEIF (DIURN .EQ. 'N') THEN
        WRITE (13,5) IA1, IA2, ACN, "'N'"
655   ENDIF
      IF (PERCON .EQ. 'CNSTNT') THEN
        WRITE (13,5) "'CNSTNT'"
      ELSEIF (PERCON .EQ. 'CHANGE') THEN
        WRITE (13,5) "'CHANGE'"
660   ENDIF
      DO 390 J = IA1, IA2
        WRITE (13,5) A1(J), A2(J), A2A(J), A3(J), A4(J),
     &   A4A(J), A5(J), A7(J), A11(J), A13(J)
390   CONTINUE
665   WRITE (13,5) IH1, IH2, IPB1, IPB2, IEB1, IEB2, IBV1
      DO 400 J = IH1, IH2
        WRITE (13,5) H15(J), H15A(J), H17(J), H19(J),
     &   H23(J), ASSIMH(J), HCN(J), K15(J)
400   CONTINUE
670   WRITE (13,5) IPRINT
      WRITE (13,5) IA1, IA2, IH1, IH2, III
      WRITE (13,5) IPB1, IPB2, IEB1, IEB2, IBV1, IBV2, IZP1, IZP2
      WRITE (13,5) IPRINT
```

```
      WRITE (13,5) IA1, IA2, IPB1, IPB2, IEB1, IEB2, IBV1, IBV2,
675   &IZP1, IZP2

*     ************************************
*     ***                              ***
*     ***  PRINT INITIAL VALUES        ***
680   *     ***                              ***
*     ************************************

      PRINT 15, 'PROGRAMME THESIS.TC1 LAST UPDATED ON ', VER$N
      PRINT 5, TITLE, 'IPRINT =', IPRINT
685
      PRINT 25, 'ILOOP',ILOOP,'III',III,'U1',U1,'ESDINT',ESDINT,
     &'DIURN',DIURN,'U2',U2,'INITD',INITD,'NITRO',NITRO,'U3',U3,
      &'PERCON',PERCON,'NCON',NCON,'PREF1',PREF1,
      &'ASSIM',ASSIM,'NINCRE',NINCRE,'PREF2',PREF2
690   PRINT 35, 'ALPH1',ALPH1,'BETA1',BETA1,
     &        'ALPH2',ALPH2,'BETA2',BETA2,'ALPH2A',ALPH2A,
     &        'BETA2A',BETA2A,'ALPH3',ALPH3,'BETA3',BETA3,
     &        'ALPH4',ALPH4,'BETA4',BETA4,'ALPH4A',ALPH4A,
     &        'BETA4A',BETA4A,'ALPH5',ALPH5,'BETA5',BETA5,
695   &        'ALPH7',ALPH7,'BETA7',BETA7,'ALPH11',ALPH11,
     &        'BETA11',BETA11,'ALPH13',ALPH13,'BETA13',BETA13,
     &        'ALPH15',ALPH15,'BETA15',BETA15,'ALP15A',ALP15A,
     &        'BET15A',BET15A,'ALPH17',ALPH17,
     &        'BETA17',BETA17,'ALPH19',ALPH19,
700   &        'BETA19',BETA19,'ALPH23',ALPH23,'BETA23',BETA23,
     &        'ALP15B',ALP15B
      PRINT 45, 'AMIN',AMIN,'AMAX',AMAX,'ACLASS',ACLASS,'IA1',IA1,
      &        'IA2',IA2,'ASPEC1',ASPEC1,'ACN',ACN,'HMIN',HMIN,
      &        'HMAX',HMAX,'HCLASS',HCLASS,'IH1',IH1,'IH2',IH2,
705   &        'ASPEC2',ASPEC2,'PBMIN',PBMIN,'PBMAX',PBMAX,'PBCLAS',
      &        PBCLAS,'IPB1',IPB1,'IPB2',IPB2,'HSPEC1',HSPEC1,
      &        'EBMIN',EBMIN,'EBMAX',
     &        EBMAX,'EBCLAS',EBCLAS,'IEB1',IEB1,'IEB2',IEB2,
      &        'HSPEC2',HSPEC2,'BVMIN',BVMIN,'BVMAX',BVMAX,'BVCLAS',
710   &        BVCLAS,'IBV1',IBV1,'IBV2',IBV2,'SMALL1',SMALL1,
      &        'ZPMIN',ZPMIN,'ZPMAX',ZPMAX,'ZPCLAS',ZPCLAS,
      &        'IZP1',IZP1,'IZP2',IZP2,'SMALL2',SMALL2,'TMIN',TMIN,
      &        'TMAX',TMAX,'TCLASS',TCLASS,'ASTOW',ASTOW,'HSTOW',HSTOW,
     &       'ASTOW1',ASTOW1,'HSTOW1',HSTOW1
715
      PRINT 55, '**********  AUTOTROPHS  **********'
      PRINT 65, 'CLASS','ESD(UM)','VOLUME(UM3)','S AREA(UM2)',
     &       'CWT(PG)','NWT(PG)','SAVOL','CMASS(UG)','NMASS(UG)',
     &       'NUMBERS','C N RATIO'
720   PRINT 75, '*****','*******','***********','***********',
     &       '*******','*******','*****','*********','*********',
     &       '*******','*********'

      DO 410 J = IA1, IA2
725     PRINT 85, J, AESD(J), AVOL(J), ASA(J), AWTC(J), AWTN(J),
     &         ASAVOL(J), AMASSC(1,J),AMASSN(1,J), ANUM(1,J), ACN
410   CONTINUE

      PRINT 55, '*********  HETEROTROPHS  *********'
730   PRINT 65, 'CLASS','ESD(UM)','VOLUME(UM3)','S AREA(UM2)',
     &       'CWT(PG)','NWT(PG)','SAVOL','CMASS(UG)','NMASS(UG)',
```

```
     &        'NUMBERS','C N RATIO'
      PRINT 75, '*****','*******','**********','**********',
     &        '*******','*******','*****','*********','*********',
735  &        '*******','*********'

     DO 420 J = IH1, IH2
       PRINT 85, J, HESD(J),HVOL(J), HSA(J), HWTC(J), HWTN(J),
     &        HSAVOL(J), HMASSC(1,J), HMASSN(1,J), HNUM(1,J),
740  &        HCN(J)
420  CONTINUE

     PRINT 55, '*****  HETEROTROPH GROUPS  *****'
     PRINT 95, 'PLANKTOBACTERIA', PBMIN, '-', PBMAX, PBCLAS,
745  &        'SIZE CLASSES', 'EPIBACTERIA', EBMIN, '-', EBMAX,
     &        EBCLAS, 'SIZE CLASSES', 'BACTIVORES', BVMIN, '-',
     &        BVMAX, BVCLAS, 'SIZE CLASSES', 'ZOOPLANKTON',
     &        ZPMIN, '-', ZPMAX, ZPCLAS, 'SIZE CLASSES'
     PRINT 105, 'PB C(UG)','EB C(UG)','BV C(UG)','ZP C(UG)',
750  &       'PB N(UG)','EB N(UG)','BV N(UG)','ZP N(UG)',
     &       'PB NUMBERS','EB NUMBERS','BV NUMBERS','ZP NUMBERS'
     PRINT 115, '********','********','********','********',
     &        '********','********','********','********',
     &        '**********','**********','**********','**********'
755  PRINT 125, PBC(1), EBC(1), BVC(1), ZPC(1), PBN(1), EBN(1),
     &       BVN(1), ZPN(1), PBNUM(1), EBNUM(1), BVNUM(1), ZPNUM(1)

     PRINT 135, '*****  TOTAL BIOMASSES AND NUMBERS FOR FUNCTIONAL GRO
    &UPS  *****'
760  PRINT 145, 'CARBON MASS(UG)', 'NITROGEN MASS(UG)', 'TOTAL NUMBERS'
     PRINT 155, '***************', '*****************', '*************'
     PRINT 165, 'AUTOTROPHS  ', AC(1), AN(1), ASUM(1),
     &        ' HETEROTROPHS', HC(1), HN(1), HSUM(1),
     &        ' DETRITUS   ', DC(1), DN(1)
765
     PRINT 55, '**********  PREDATORS  **********'
     PRINT 175, 'CLASS',' ESD (UM)','UMIN (UM)','UOPT (UM)',
     &        'UMAX (UM)','UCLASS','UMINUS','UPLUS','UPOS'
     PRINT 185, '*****',' ********','*********','*********',
770  &        '*********','******','******','******','****'
     DO 430 J = IH1, IH2
       PRINT 195, J, TESD(J), UMIN(J), UOPT(J), UMAX(J), UCLASS(J),
    &        UMINUS(J), UPLUS(J), UPOS(J)
430  CONTINUE
775
     PRINT 55, '**********    PREY    **********'
     PRINT 205, 'CLASS',' ESD (UM)','VMIN (UM)','VOPT (UM)',
     &        'VMAX (UM)','VCLASS','VMINUS','VPLUS','VPOS',
     &       'PREY K (UGCL-1)'
780  PRINT 215, '*****',' ********','*********','*********',
     &        '*********','******','******','******','****',
     &        '***************'
     DO 440 J = IH1, IH2
       PRINT 225, J, TESD(J), VMIN(J), VOPT(J), VMAX(J), VCLASS(J),
785  &        VMINUS(J), VPLUS(J), VPOS(J), H15A(J)
440  CONTINUE

     PRINT 55, '****  RATE PARAMETERS - PER DAY  ****'
     PRINT 235, 'CLASS','ESD(UM)','P/S','NEWN V','NEWN K','A RESP',
```

```
790         &       'REGN V','REGN K','ADEATH','A SINK','A GROW','PDOC V',
            &       'PRED V','UPT KS','ASSIMH','H RESP','H GROW'
             PRINT 245, '******','*******','***','******','******','******',
            &       '******','******','******','******','******','******',
            &       '******','******','******','******','******'
795
            DO 450 J = 1, TCLASS
              PRINT 255, J,TESD(J),A1(J),A2(J),A2A(J),A3(J),A4(J),A4A(J),
           &        A5(J),A7(J),A11(J),A13(J),H15(J),K15(J),ASSIMH(J),
           &        H19(J),H23(J)
800      450 CONTINUE

            CLOSE (12)
            CLOSE (13)

805         END
```

8. Program variable and parameter definitions

A	The real number of autotroph size classes (ACLASS is the integer form of A)
A1	An array of size-dependent carbon fixation rates by autotrophs
A2	An array of size-dependent new-nitrogen uptake rates by autotrophs
A2A	An array of size-dependent half saturation constants for new-nitrogen uptake by autotrophs
A3	An array of size-dependent respiration rates for autotrophs
A4	An array of size-dependent regenerated-nitrogen uptake rates by autotrophs
A4A	An array of size-dependent half saturation constants for regenerated-nitrogen uptake by autotrophs
A5	An array of size-dependent death rates for autotrophs
A7	An array of size-dependent sinking rates for autotrophs
A11	An array of size-dependent growth rates for autotrophs
A13	An array of size-dependent PDOC production rates for autotrophs
AC	An array of total carbon standing stocks (µg) for autotrophs at each time step (sum of all the AMASSC's)
ACLASS	The integer number of autotroph size classes
ACN	The carbon : nitrogen ratio for autotrophs
AESD	An array of mean individual esd's for each autotroph size class
ALPH1	The rate coefficient for calculating size-dependent maximum carbon fixation rates of autotroph size classes
ALPH2	The rate coefficient for calculating size-dependent maximum new-nitrogen uptake rates of autotrophs size classes
ALPH2A	The "rate coefficient" for calculating size-dependent half saturation constants for new-nitrogen uptake rates of autotroph size classes
ALPH3	The rate coefficient for calculating size-dependent maximum respiration rates of autotroph size classes
ALPH4	The rate coefficient for calculating size-dependent maximum regenerated-nitrogen uptake rates by autotroph size classes
ALPH4A	The "rate coefficient" for calculating size-dependent half saturation constants for regenerated-nitrogen uptake rates of autotroph size classes
ALPH5	The rate coefficient for calculating size-dependent death rates of autotroph size classes
ALPH7	The maximum sinking rate for phytoplankton cells
ALPH11	The rate coefficient for calculating size-dependent growth rates of autotroph size classes
ALPH13	The rate coefficient for calculating size-dependent PDOC production rates of autotroph size classes
ALPH15	The rate coefficient for calculating size-dependent maximum ingestion rates of heterotroph size classes
ALP15A	A variable for calculating size-dependent half saturation constants for maximum ingestion rates of heterotroph size classes
ALP15B	A variable for calculating size-dependent half saturation constants for maximum ingestion rates of heterotroph size classes
ALPH17	The "rate coefficient" for calculating size-dependent assimilation rates of heterotroph size classes

ALPH19	The rate coefficient for calculating size-dependent maximum respiration rates of heterotroph size classes
ALPH23	The rate coefficient for calculating size-dependent growth rates of heterotroph size classes
AMASSC	An array of carbon standing stocks (µg) in each autotroph size class at each time step
AMASSN	An array of nitrogen standing stocks (µg) in each autotroph size class at each time step
AMAX	The maximum esd for autotrophs
AMIN	The minimum esd for autotrophs
AN	An array of total nitrogen standing stocks (µg) for autotrophs at each time step (sum of all the AMASSN's)
ANUM	An array of total numbers of individuals in each autotroph size class at each time step
ARAD	An array of mean individual radii (µm) for each autotroph size class
ASA	An array of mean individual surface areas (μm^2) (assuming spheres) for each autotroph size class
ASAVOL	An array of mean individual surface area : volume ratios for each autotroph size class
ASMALC	An array of minimum carbon standing stocks (µg) for each autotroph size class
ASMALN	An array of minimum nitrogen standing stocks (µg) for each autotroph size class
ASPEC1	A variable which determines the initial standing stocks in each autotroph size class at the start of each simulation
ASPEC2	A variable which scales the initial standing stocks to autotroph body size at the start of each simulation (if ASPEC2 equals one, there is no scaling factor; if ASPEC2 equals zero, the initial biomass spectrum is flat)
ASSIM	The assimilation efficiency of non-bacteria heterotrophs
ASSIMH	An array of assimilation efficiencies for each heterotroph size class
ASTOW	Factor used to convert autotroph volumes (μm^3) to carbon masses (pg C)
ASTOW1	Scaling factor used to scale body masses when converting autotroph volumes (μm^3) to carbon masses (pg C)
ASUM	The total number of autotrophs at each time step (the sum of all the ANUM's)
AVOL	An array of mean individual volumes (μm^3) for each autotroph size class
AWTC	An array of mean individual carbon weights (pg C) for a "typical" organism in each autotroph size class
AWTN	An array of mean individual nitrogen weights (pg N) for a "typical" organism in each autotroph size class
BETA1	The scaling parameter for calculating size-dependent carbon fixation of autotroph size classes
BETA2	The scaling parameter for calculating size-dependent new-nitrogen uptake of autotroph size classes
BETA2A	The scaling parameter for calculating size-dependent half saturation constants for new-nitrogen uptake of autotroph size classes
BETA3	The scaling parameter for calculating size-dependent respiration rates of autotroph size classes
BETA4	The scaling parameter for calculating size-dependent regenerated-nitrogen uptake of autotroph size classes
BETA4A	The scaling parameter for calculating size-dependent half saturation constants for regenerated nitrogen uptake of autotroph size classes
BETA5	The scaling parameter for calculating size-dependent death rates of autotroph size classes
BETA7	The half saturation constant for calculating size-dependent sinking rates of autotroph size classes
BETA11	The scaling parameter for calculating size-dependent growth rates of autotroph size classes
BETA13	The scaling parameter for calculating size-dependent PDOC production rates of autotroph size classes
BETA15	The scaling parameter for calculating size-dependent carbon ingestion / uptake rates of heterotroph size classes
BET15A	The scaling parameter for calculating half saturation constants for size-dependent carbon ingestion / uptake rates of heterotroph size classes
BETA17	The scaling parameter for calculating size-dependent assimilation rates of heterotroph size classes
BETA19	The scaling parameter for calculating size-dependent respiration rates of heterotroph size classes
BETA23	The scaling parameter for calculating size-dependent growth rates of heterotroph size classes
BV	he real number of bactivore size classes (BVCLAS is the integer form of BV)
BVC	An array of total carbon standing stocks (µg) for bactivores at each time step (sum of all the HMASSC's between IBV1 and IBV2)
BVCLAS	The integer number of bactivore size classes
BVCN	The carbon : nitrogen ratio for bactivores
BVMAX	The maximum esd for bactivores
BVMIN	The minimum esd for bactivores

BVN	An array of total nitrogen standing stocks (µg) for bactivores at each time step (sum of all the HMASSN's between IBV1 and IBV2)
BVNUM	An array of total numbers of individuals in the bactivore group at each time step
DC	The total amount of carbon (µg) in the detrital pool at each time step
DIURN	Character variable ('Y' or 'N') for setting a diurnal cycle in the model community
DN	The total amount of nitrogen (µg) in the detrital pool at each time step
EB	The real number of epibacteria size classes (EBCLAS is the integer form of EB)
EBC	An array of total carbon standing stocks (µg) for epibacteria at each time step (sum of all the HMASSC's between IEB1 and IEB2)
EBCLAS	The integer number of epibacteria size classes
EBCN	The carbon : nitrogen ratio for epibacteria
EBMAX	The maximum esd for epibacteria
EBMIN	The minimum esd for epibacteria
EBN	An array of total nitrogen standing stocks (µg) for epibacteria at each time step (sum of all the HMASSN's between IEB1 and IEB2)
EBNUM	An array of total numbers of individuals in the epibacteria group at each time step
ESDINT	The logarithmic factor that is used to define the size classes
H	The real number of heterotroph size classes (HCLASS is the integer form of H)
H15	An array of size-dependent carbon ingestion / uptake rates of heterotrophs
H15A	An array of prey-size dependent half saturation constants for carbon ingestion rates by predators
H17	An array of size-dependent assimilation rates of heterotrophs
H19	An array of size-dependent respiration rates of heterotrophs
H23	An array of size-dependent growth rates of heterotrophs
HC	An array of total carbon standing stocks (µg) for heterotrophs at each time step (sum of all the HMASSC's)
HCLASS	The integer number of heterotroph size classes
HCN	An array of carbon : nitrogen ratios for each of the heterotroph size classes
HESD	An array of mean individual esd's for each heterotroph size class
HMASSC	An array of carbon standing stocks (µg) in each heterotroph size class at each time step
HMASSN	An array of nitrogen standing stocks (µg) in each heterotroph size class at each time step
HMAX	The maximum esd for heterotrophs
HMIN	The minimum esd for heterotrophs
HN	An array of total nitrogen standing stocks (µg) for heterotrophs at each time step (sum of all the HMASSN's)
HNUM	An array of total numbers of individuals in each heterotroph size class at each time step
HRAD	An array of mean individual radii (µm) for each heterotroph size class
HSA	An array of mean individual surface areas (μm^2) (assuming spheres) for each heterotroph size class
HSAVOL	An array of mean individual surface area : volume ratios for each heterotroph size class
HSMALC	An array of minimum carbon standing stocks for each heterotroph size class
HSMALN	An array of minimum nitrogen standing stocks for each heterotroph size class
HSPEC1	A variable which determines the initial standing stock in each heterotroph size class at the start of each simulation
HSPEC2	A variable which scales the initial standing stocks to heterotroph body size at the start of each simulation (if HSPEC2 equals one, there is no scaling factor; if HSPEC2 equals zero, the initial biomass spectrum is flat)
HSTOW	Factor used to convert heterotroph volumes (μm^3) to carbon masses (pg C)
HSTOW1	Scaling factor used to scale body masses when converting heterotroph volumes (μm^3) to carbon masses (pg C)
HSUM	The total number of heterotrophs at each time step (the sum of all the HNUM's)
HVOL	An array of mean individual volumes (μm^3) for each heterotroph size class)
HWTC	An array of mean individual carbon weights (pg C) for a "typical" organism in each heterotroph size class
HWTN	An array of mean individual nitrogen weights (pg N) for a "typical" organism in each heterotroph size class
IA1	An integer subscript denoting the starting position of autotrophs in the prey array
IA2	An integer subscript denoting the end position of autotrophs in the prey array
IBV1	An integer subscript denoting the starting position of bactivores in the prey array
IBV2	An integer subscript denoting the end position of bactivores in the prey array

ICHECK	An internal program counter used in calculating the number of predator and prey size classes
IEB1	An integer subscript denoting the starting position of epibacteria in the prey array
IEB2	An integer subscript denoting the end position of epibacteria in the prey array
IH1	An integer subscript denoting the starting position of heterotrophs in the prey array
IH2	An integer subscript denoting the end position of heterotrophs in the prey array
III	An internal program counter
ILOOP	An integer variable denoting the number of loops to be executed in each simulation
INITD	The starting carbon standing stock in the detrital pool
IPB1	An integer subscript denoting the starting position of bacterioplankton in the prey array
IPB2	An integer subscript denoting the end position of bacterioplankton in the prey array
IZP1	An integer subscript denoting the starting position of zooplankton in the prey array
IZP2	An integer subscript denoting the end position of heterotrophs in the prey array
K	An integer subscript used to denote position in the total array
K15	An array of size-dependent half saturation constants for carbon and nitrogen uptake by bacteria
NCON	The constant amount of nitrogen (µg) always in the model system if the method of nitrogen input is chosen to be a constant level (i.e. NITRO is "CNSTNT")
NEWN	The total nitrogen biomass (µg N) in the new-nitrogen pool at any time step
NINCRE	The amount of new-nitrogen entering the system at any time step if the method of nitrogen input is chosen to be a small continuous amount (i.e. NITRO is "CONTIN")
NITRO	A character variable which determines the method of nitrogen input into the system: a single large input at the beginning of the run which simulates upwelling (PULSED), a small continuous input which simulates diffusion across the pycnocline (CONTIN) or a constant unchanging level (CNSTNT)
PB	The real number of bacterioplankton size classes (PBCLAS is the integer form of PB)
PBC	An array of total carbon standing stocks (µg) for bacterioplankton at each time step (sum of all the HMASSC's between IPB1 and IPB2)
PBCLAS	The integer number of bacterioplankton size classes
PBCN	The carbon : nitrogen ratio for bacterioplankton
PBMAX	The maximum esd for bacterioplankton
PBMIN	The minimum esd for bacterioplankton
PBN	An array of total nitrogen standing stocks (µg) for bacterioplankton at each time step (sum of all the HMASSN's between IPB1 and IPB2)
PBNUM	An array of total numbers of individuals in the bacterioplankton group at each time step
PDOC	An array of total amounts of carbon (µg) in the PDOC pool at each time step
PERCON	A character variable which determines whether PER is a constant fraction of gross carbon fixation (CNSTNT) or whether it depends on external nitrogen concentrations (CHANGE)
PREF1	A real variable which determines the preference of predators for their optimum prey size class (usually set at 1)
PREF2	A real variable which determines the factor by which the preference of each predator class for its prey classes is decreased as one moves successively away from the optimum prey class
RA	A real subscript denoting the position of the smallest autotroph size class in the total array (IA1 is the integer form of RA)
RH	A real subscript denoting the position of the smallest heterotroph size class in the total array (IH1 is the integer form of RH)
RBV	A real subscript denoting the position of the smallest bactivore size class in the total array (IBV1 is the integer form of RBV)
REB	A real subscript denoting the position of the smallest epibacteria size class in the total array (IEB1 is the integer form of REB)
REGN	An array of total amounts of nitrogen (µg) in the regenerated-nitrogen pool at each time step
RPB	A real subscript denoting the position of the smallest bacterioplankton size class in the total array (IPB1 is the integer form of RPB)
RZP	A real subscript denoting the position of the smallest zooplankton size class in the total array (IZP1 is the integer form of RZP)
SIZE	An integer parameter denoting the maximum possible number of size classes in each functional group (denotes maximum width of matrices and size of some arrays in the program)
SMALL1	A variable which determines the minimum biomasses in each size class i.e. the "refuge" biomasses
SMALL2	A variable which scales the minimum biomasses to body size (if SMALL2 equals one, minimum biomasses are proportional to body weight; if SMALL2 equals zero, all biomasses are the same in each size class

T	The real number of size classes in the total array (TCLASS is the integer form of T)
TCLASS	The integer number of size classes in the total array
TESD	An array of mean individual esd's for each size class in the total array
TIME	An integer parameter denoting the maximum possible number of loops that the program will execute in any one run (denotes the maximum length of matrices and size of some arrays in the program)
TITLE	A character parameter which gives a title to each simulation
TMASSC	An array of total carbon standing stocks (µg) in each size class at each time step
TMAX	The maximum esd in the total array
TMIN	The minimum esd in the total array
TW1	An internal program variable used in calculating mean esd's in each size class of the total array
TW2	An internal program variable used in calculating mean esd's in each size class of the total array
U	An array of real numbers of prey size classes available to each predator size class (UCLASS is the integer form of U)
U1	The factor used to calculate the esd of the minimum sized prey for any predator relative to that predator's esd
U2	The factor used to calculate the esd of the optimum sized prey for any predator relative to that predator's esd
U3	The factor used to calculate the esd of the maximum sized prey for any predator relative to that predator's esd
UCLASS	An array of integer numbers of prey size classes available to each predator size class
UMAX	An array of maximum-sizes of prey that can be ingested by each of the predator size classes
UMIN	An array of minimum-sizes of prey that can be ingested by each of the predator size clases
UMINUS	An array of the number of size classes in each predators prey range that are smaller than the optimum prey size for each predator
UOPT	An array of optimum prey esd's for each predator size class
UPLUS	An array of the number of prey size classes in the predator's prey range that are larger than the optimum prey size class for each predator
UPOS	An array of subscripts denoting the position of the smallest prey size class in the total array for each predator
V	An array of real numbers of predator size classes preying on each prey size class (VCLASS is the integer form of V)
VCLASS	An array of integer numbers of predator size classes preying on each prey size class
VER$N	A character parameter that records the date at which the program was last updated. VER$N changes whenever the routine UPDATE is called from CTS
VMAX	An array of maximum sizes of predator preying on each of the prey size classes
VMIN	An array of minimum sizes of predator preying on each of the prey size classes
VMINUS	An array of numbers of size classes in each prey's predator range that are smaller than the optimum predator size for each prey
VOPT	An array of "optimum" predator esd's for each prey size class
VPLUS	An array of numbers of predator size classes in the prey's predator range that are larger than the optimum predator size class for each prey
VPOS	An array of subscripts denoting the position of the smallest predator size class in the total array for each prey
ZP	The real number of zooplankton size classes (ZPCLAS is the integer form of ZP)
ZPC	An array of total carbon standing stocks (µg) for zooplankton at each time step (sum of all the HMASSC's between IZP1 and IZP2)
ZPCLAS	The integer number of zooplankton size classes
ZPCN	The carbon : nitrogen ratio for zooplankton
ZPMAX	The maximum esd for zooplankton
ZPMIN	The minimum esd for zooplankton
ZPN	An array of total nitrogen standing stocks (µg) for zooplankton at each time step (sum of the HMASSN's between IZP1 and IZP2)
ZPNUM	An array of total numbers of individuals in the zooplankton group at each time step

APPENDIX II

DOCUMENTATION OF PROGRAM

COLMOL*THESIS.TC2

A PROGRAM TO SIMULATE THE FLOWS OF CARBON AND NITROGEN THROUGH A SIZE-BASED MODEL OF A PLANKTON COMMUNITY

1. Program specification

The program uses a second order Runge-Kutta method, operating within a repeating time loop, to solve a set of differential equations. The equations calculate the flows of carbon and nitrogen within and between components of a model plankton community. It receives input from another program (Appendix I), which initializes the structure of the model, calculates certain parameters and initializes state variables. The changes with time of the standing stocks of all model components are presented in the form of tables and figures. Three-dimensional plots may be produced, which show changes in standing stocks in different size components of the model community with time. Relationships between the fluxes of different components are also calculated.

2. Instructions for use

2.1 Runstream

The program was written for use on the Sperry 1100 Series mainframe computer at the University of Cape Town. It is run in batch mode from CTS (Conversational Time Sharing). An example runstream is given below:

```
@RUN,/N Userid,ACCNT/USER,Projid,Time,Pages
@ASG,A COLMOL*THESIS.                  - assign program file
@ASG,A TC2*DATFIL.                     - assign input data file
@USE 13., TC2*DATFIL.                  - assign internal name
@ASG,T TC2*OUT.,F///500                - assign temporary data file
@USE 23.,TC2*OUT.                      - assign internal name
@ASG,A TC2*TOUT.                       - assign output file
@DELETE,C TC2*TOUT.                    - delete output file
@ASG,UP TC2*TOUT.,F50                  - create output file
@USE 14.,TC2*TOUT.                     - assign internal name
@ASG,A TC2*AOUT.                       - assign output file
@DELETE,C TC2*AOUT.                    - delete output file
@ASG,UP TC2*AOUT.,F50                  - create output file
@USE 20.,TC2*AOUT.                     - assign internal name
@ASG,A TC2*HOUT.                       - assign output file
@DELETE,C TC2*HOUT.                    - delete output file
@ASG,UP TC2*HOUT.,F50                  - create output file
@USE 21.,TC2*HOUT.                     - assign internal name
@ASG,A TC2*RELT.                       - assign output file
@DELETE,C TC2*RELT.                    - delete output file
@ASG,UP TC2*RELT.,F50                  - create output file
@USE 15.,TC2*RELT.                     - assign internal name
@ASG,A TC2*RELA.                       - assign output file
@DELETE,C TC2*RELA.                    - delete output file
```

```
@ASG,UP TC2*RELA.,F50                          - create output file
@USE 16.,TC2*RELA.                             - assign internal name
@ASG,A TC2*RELH.                               - assign output file
@DELETE,C TC2*RELH.                            - delete output file
@ASG,UP TC2*RELH.,F50                          - create output file
@USE 17.,TC2*RELH.                             - assign internal name
@ASG,T TC2*BMDP.,F50                           - assign temporary data file
@USE 22.,TC2*BMDP.                             - assign internal name
@XQT,F COLMOL*THESIS.TC2                       - execute program
@BMDP*85.BMDP BMDP6D,30000                     - assign BMDP package
/PROBLEM TITLE IS 'TROPHIC CONTINUUM MODEL'.   |
/INPUT VARIABLES ARE 9.                        |
     FORMAT IS '(F6.2, 8 F8.1)'.               |
/VARIABLE NAMES ARE TIME, AC, PBC,             |        BMDP
    EBC, BVC, ZPC, PDOC, NEWN, REGN            |        control
/PLOT YVAR ARE AC, PBC, EBC, BVC, ZPC,         |        language
    PDOC, NEWN, REGN.                          |
    XVAR ARE TIME, TIME, TIME, TIME,           |
    TIME, TIME, TIME, TIME.                    |
/END                                           |
@ADD TC2*BMDP.                                 - add BMDP data file
@DATA,L TC2*AOUT.                              - list contents of data file
@END                                           - terminate DATA command
@DATA,L TC2*HOUT.                              - list contents of data file
@END                                           - terminate DATA command
@DATA,L TC2*TOUT.                              - list contents of data file
@END                                           - terminate DATA command
@FIN                                           - terminate run
```

In practice, two programs (TC1 and TC2) are involved in execution of the model and can be called together by the following runstream:

```
@RUN,/N Userid,ACCNT/USER,Projid,Time,Pages
@ASG,A COLMOL*THESIS.                          - assign program file
@ASG,A TC1*DATFIL.                             - assign input file
@USE 12., TC1*DATFIL.                          - assign internal name
@ASG,A TC2*DATFIL.                             - assign output file
@DELETE,C TC2*DATFIL.                          - delete output file
@ASG,UP TC2*DATFIL.,F50                        - create output file
@USE 13., TC2*DATFIL.                          - assign internal name
@XQT COLMOL*THESIS.TC1.                        - execute first program
@DATA,L TC1*DATFIL.                            - list contents of data file
@END                                           - terminate DATA command
@ASG,T TC2*OUT.,F///500                        - assign temporary data file
@USE 23.,TC2*OUT.                              - assign internal name
@ASG,A TC2*TOUT.                               - assign output file
@DELETE,C TC2*TOUT.                            - delete output file
@ASG,UP TC2*TOUT.,F50                          - create output file
@USE 14.,TC2*TOUT.                             - assign internal name
@ASG,A TC2*AOUT.                               - assign output file
@DELETE,C TC2*AOUT.                            - delete output file
@ASG,UP TC2*AOUT.,F50                          - create output file
@USE 20.,TC2*AOUT.                             - assign internal name
@ASG,A TC2*HOUT.                               - assign output file
@DELETE,C TC2*HOUT.                            - delete output file
@ASG,UP TC2*HOUT.,F50                          - create output file
```

```
@USE 21.,TC2*HOUT.                          - assign internal name
@ASG,A TC2*RELT.                            - assign output file
@DELETE,C TC2*RELT.                         - delete output file
@ASG,UP TC2*RELT.,F50                       - create output file
@USE 15.,TC2*RELT.                          - assign internal name
@ASG,A TC2*RELA.                            - assign output file
@DELETE,C TC2*RELA.                         - delete output file
@ASG,UP TC2*RELA.,F50                       - create output file
@USE 16.,TC2*RELA.                          - assign internal name
@ASG,A TC2*RELH.                            - assign output file
@DELETE,C TC2*RELH.                         - delete output file
@ASG,UP TC2*RELH.,F50                       - create output file
@USE 17.,TC2*RELH.                          - assign internal name
@ASG,T TC2*BMDP.,F50                        - assign temporary data file
@USE 22.,TC2*BMDP.                          - assign internal name
@XQT,F COLMOL*THESIS.TC2                    - execute program file
@BMDP*85.BMDP BMDP6D,30000                  - assign BMDP package
/PROBLEM TITLE IS 'TROPHIC CONTINUUM MODEL'.
/INPUT VARIABLES ARE 9.
      FORMAT IS '(F6.2, 8 F8.1)'.
/VARIABLE NAMES ARE TIME, AC, PBC, EBC, BVC,        BMDP
     ZPC, PDOC, NEWN, REGN                          control
/PLOT YVAR ARE AC, PBC, EBC, BVC, ZPC, PDOC,        language
    NEWN, REGN.
    XVAR ARE TIME, TIME, TIME, TIME, TIME,
    TIME, TIME, TIME.
/END
@ADD TC2*BMDP.
@DATA,L TC2*AOUT.                           - list contents of data file
@END                                        - terminate DATA command
@DATA,L TC2*HOUT.                           - list contents of data file
@END                                        - terminate DATA command
@DATA,L TC2*TOUT.                           - list contents of data file
@END                                        - terminate DATA command
@FIN                                        - terminate run
```


2.2 Input specifications

Input of initial values to the program is done through a single data file, which in turn receives its data from the first program. Data from this data file are read by the different subroutines during the execution of the the first loop of the program. In addition, values calculated by subroutines AUTSUB and HETSUB are written to a temporary data file for storage, before being read by subroutine EXTRAS for further calculations. All data is read in free format.

2.3 Output format

Carbon and nitrogen standing stocks calculated in subroutine MASSES are sent as output to the printer, as are the additional variables calculated in subroutine EXTRAS. Carbon standing stocks for the biotic and abiotic groups are sent to temporary data files for use in plotting routines from BMDP. Carbon standing stocks of autotroph and heterotroph size classes and of the combined array of size classes are sent to three separate data files for use in 3-dimensional (3-D)

plotting routines using SACLANT. Also saved and plotted are the proportions of the standing stocks of each group relative to the maximum value for the three groups. The following data files receive output from the program:

TC2*OUT. A temporary data file which stores the data matrices that are calculated by subroutines AUTSUB and HETSUB and used as input to the subroutine EXTRAS.

TC2*BMDP. An output data file which stores the standing stocks of autotrophs, bacterioplankton, epibacteria, bactivores, zooplankton, PDOC, new nitrogen and regenerated nitrogen from each time step. Data in this file is used to produce plots of standing stocks versus time using a BMDP plotting routine.

TC2*AOUT. An output data file which stores a data matrix of carbon standing stocks in each autotroph size class at each time step; the rows of the matrix represent time and the columns of the matrix the autotroph size classes. These data are used in producing a three dimensional plot of the autotroph biomass spectrum over time, using the SACLANT 3-D plotting package.

TC2*HOUT. An output data file which stores a data matrix of carbon standing stocks in each heterotroph size class at each time step; the rows of the matrix representing time and the columns of the matrix the heterotroph size classes. These data are used in producing a three dimensional plot of the heterotroph biomass spectrum over time, using the SACLANT 3-D plotting package.

TC2*TOUT. An output data file which stores a data matrix of the proportion of the carbon standing stock in each autotroph size class at each time step relative to the maximum autotroph carbon standing stock in any autotroph size class at any time; the rows of the matrix represent time and the columns the size classes. These data are used in producing a three dimensional plot of the total biomass spectrum over time, using the SACLANT 3-D plotting package.

TC2*RELA. An output data file which stores a data matrix of the proportions of the carbon standing stocks in each autotroph size class at each time step relative to the maximum carbon standing stock in any autotroph size class at any time; the rows represent time and the columns the autotroph size classes. These data are used to produce a three dimensional plot of the relative autotroph biomass spectrum with time, using the SACLANT 3-D plotting package.

TC2*RELH. An output data file which stores a data matrix of the proportions of the carbon standing stocks in each heterotroph size class at each time step relative to the maximum carbon standing stock in any heterotroph size class at any time; the rows represent time and the columns the heterotroph size classes. These data are used to produce a three dimensional plot of the relative heterotroph biomass spectrum with time, using the SACLANT 3-D plotting package.

TC2*RELT. An output data file which stores a data matrix of the proportions of the total carbon standing stocks in each size class at each time step relative to the maximum carbon standing stock in any size class at any time; the rows represent time and the columns the size classes. These data are used to produce a three dimensional plot of the relative total biomass spectrum with time, using the SACLANT 3-D plotting package.

2.4 Restrictions on generality

The program is limited by available memory, and this is reflected in the sizes of matrices and arrays. The maximum number of time steps that can be used is about 600 if the maximum number of size classes is 50. The limits are defined by internal parameters TIME and SIZE. If required, these parameters can be altered to allow, for example, more time steps and fewer size classes.

2.5 Run time

Run times are affected by the number of size clases and the number of loops to be executed. Example times are presented below.

Number of size classes	Number of loops	Approximate run time (minutes)
5	1000	4
10	1000	7
50	600	12

3. Conceptual overview

3.1 Initializing variables

Within the first loop of the program, initial values are read from a data file by the MAIN program and relevant subroutines.

3.2 Calculation of carbon and nitrogen flows at each time step

Subroutines PREDS, AUTSUB, HETSUB and DETSUB calculate the rates of flow of carbon and nitrogen into and out of each size class in the trophic continuum at each time step. The differences between carbon and nitrogen input and output are computed for the biotic groups in subroutines AUTSUB and HETSUB, and for the abiotic pools in subroutine DETSUB.

3.3 Solving the differential equations

Changes in the biotic and abiotic groups with time are represented by a series of differential equations. These equations are solved numerically using a second order Runge-Kutta method in the subroutines ISUB1, INCRE1, ISUB2 and INCRE2.

3.4 Calculating standing stocks and flow relationships

Size classes are grouped to give total standing stocks for the different functional groups (autotrophs, bacterioplankton, epibacteria, bactivores and zooplankton) in subroutine MASSES. Carbon and nitrogen flows and relationships between these flows and the standing stocks are calculated in subroutine EXTRAS.

4. Program design

4.1 Overall description

The program is written in FORTRAN and compiled using the FORTRAN V compiler. It consists of a main program and ten subroutines. The sequence of the programming logic is presented in Fig. A-II.1:

4.3 Data structures

Most data are stored in the form of arrays, because the model is structured as arrays of size classes. Some variables, which are input into the first program by the user, determine which of a series of options will be used in executing the dynamic form of the model. These options are entered and stored as character variables (for a more detailed description see Appendix I).

Fig. A-II.1. Program structure diagram of Main program:

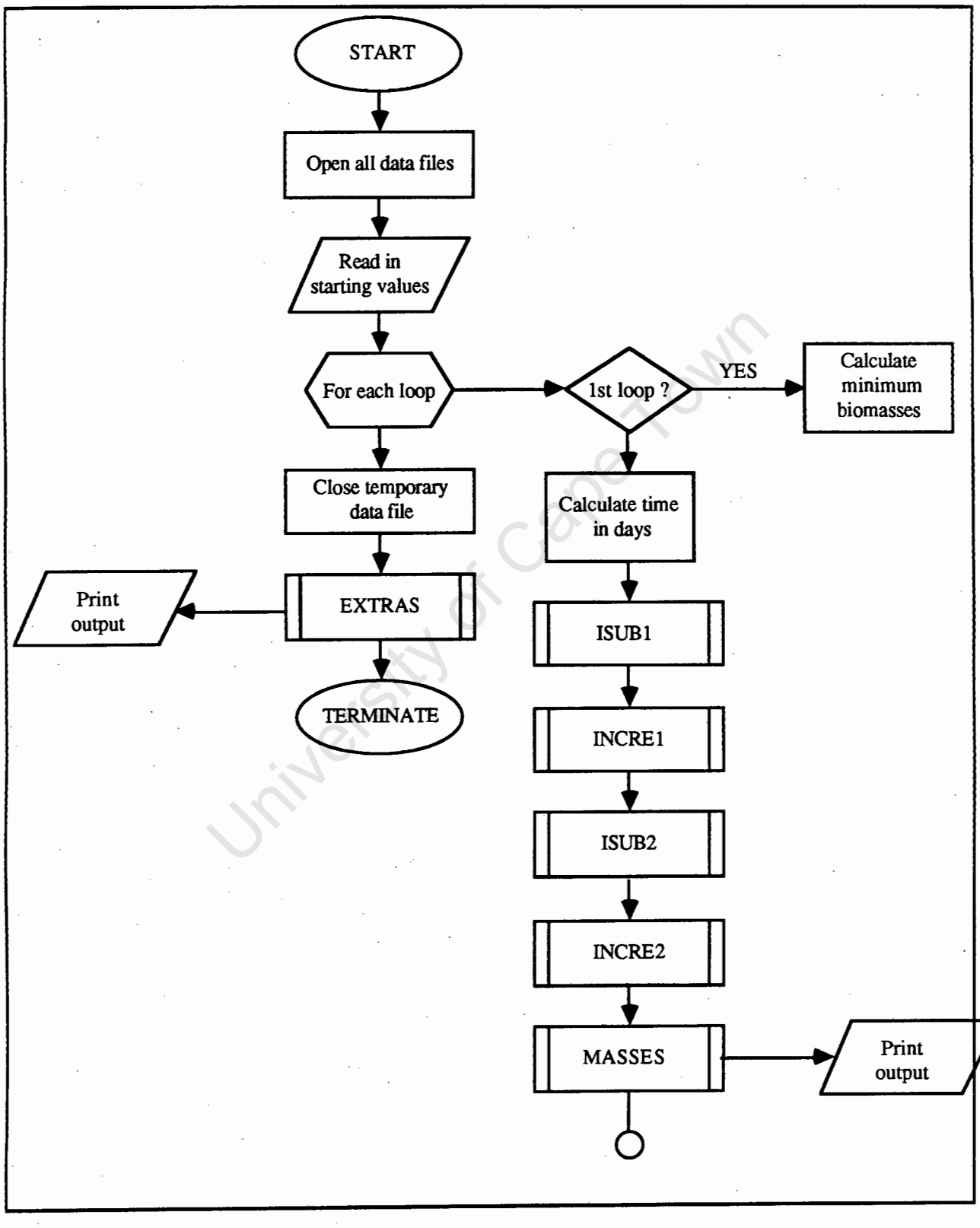

4.4. Subroutines

4.4.1. Subroutine ISUB1

CALLED BY: MAIN program

CALLS: PREDS, AUTSUB, HETSUB, DETSUB

This subroutine controls the first set of calculations in the Runge-Kutta procedure for the terms on the RHS of the differential equations. It receives values from the MAIN program for I, ITAB, TCLASS, AMASSC, AMASSN, HMASSC, HMASSN, TMASSC, NEWN, REGN, PDOC, DC, DN, ASMALC, HSMALC, NITRO and NINCRE. ISUB1 calls subroutines and returns variables DAMASC, DAMASN, DHMASC, DHMASN, DDC, DDN, DNEWN, DREGN, DPDOC, DAY, IH1, IH2 and EBCT15 to the MAIN program. The programming logic is as follows:

Fig. A-II.2. Program structure diagram of subroutine ISUB1.

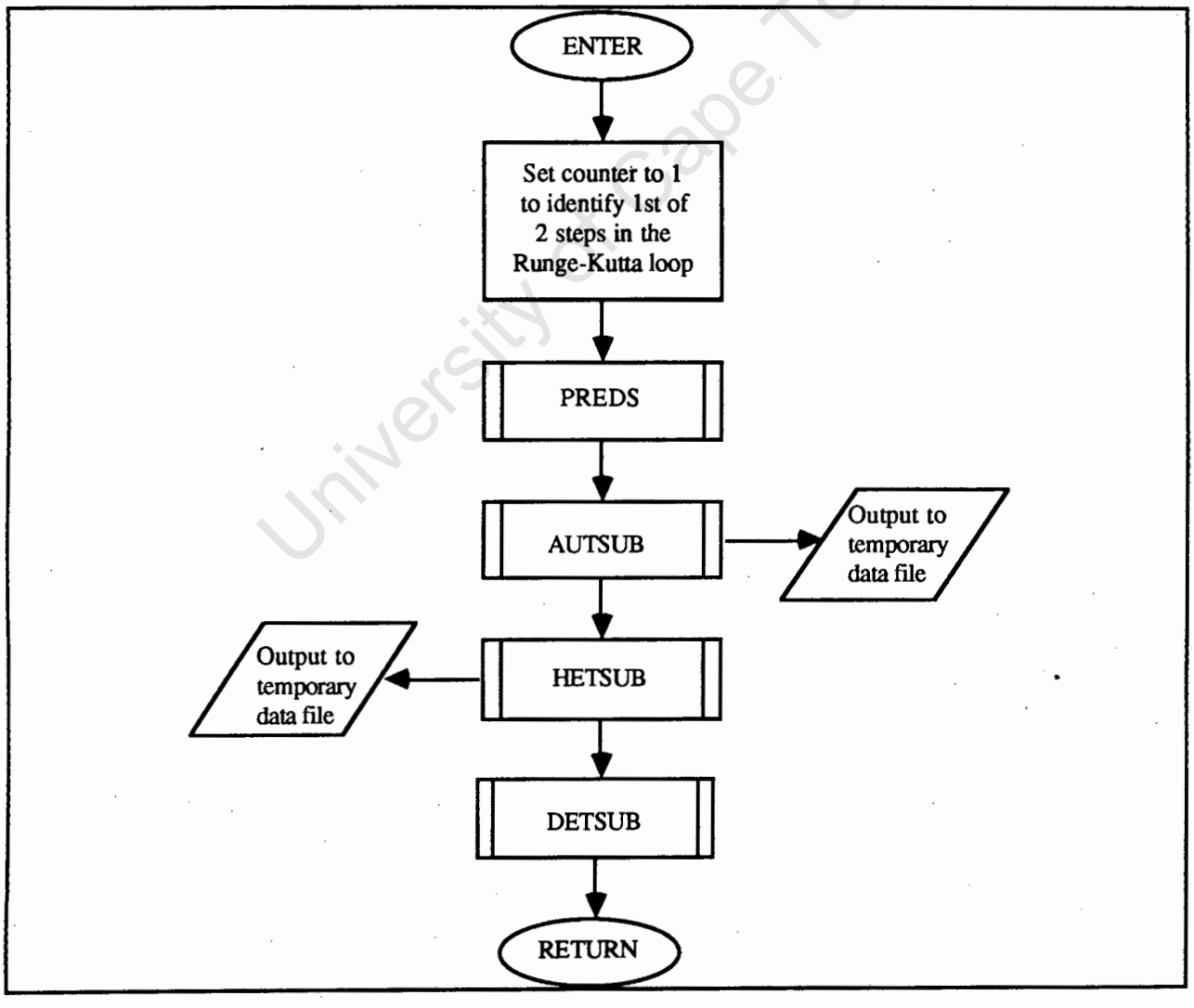

4.4.2 Subroutine INCRE1

CALLED BY: MAIN program

This subroutine calculates the first increment in the Runge-Kutta procedure to be added to each standing stock in each trophic size class and abiotic pool. It receives values from the MAIN program for variables I, DAMASC, DAMASN, DHMASC, DHMASN, DDC, DDN, DNEWN, DREGN, DPDOC, TCALSS, NCON, NITRO, ASMALC, ASMALN, HSMALC and HSMALN. It returns values to the MAIN program for variables AMASSC, AMASSN, HMASSC, HMASSN, DC, DN, NEWN, REGN and PDOC. The programming logic is as follows:

Fig. A-II.3. Program structure diagram of subroutine INCRE1.

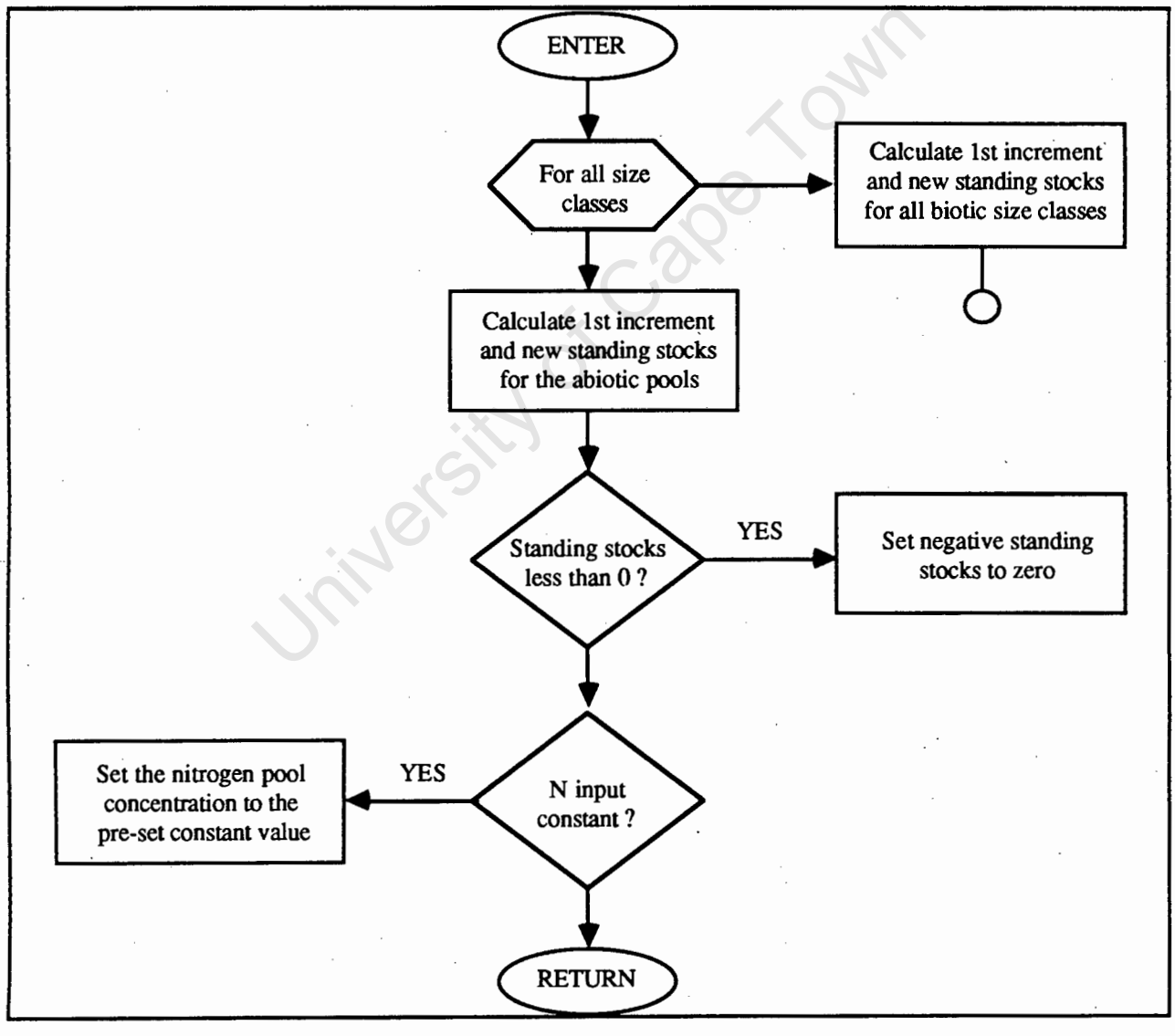

4.4.4 Subroutine ISUB2

CALLED BY: MAIN program

CALLS: PREDS, AUTSUB, HETSUB, DETSUB

This subroutine controls the second set of calculations for the Runge-Kutta procedure for the terms on the RHS of the differential equations. It receives values from the MAIN program for I, TCLASS, AMASSC, AMASSN, HMASSC, HMASSN, TMASSC, NEWN, REGN, PDOC, DC, DN, ASMALC and HSMALC. ISUB2 calls subroutines and returns variables DAMASC, DAMASN, DHMASC, DHMASN, DDC, DDN, DNEWN, DREGN, DPDOC, DAY, ITAB, IH1, IH2 and EBCT15 to the MAIN program. The programming logic is as follows:

Fig. A-II.4. Program structure diagram of subroutine ISUB2.

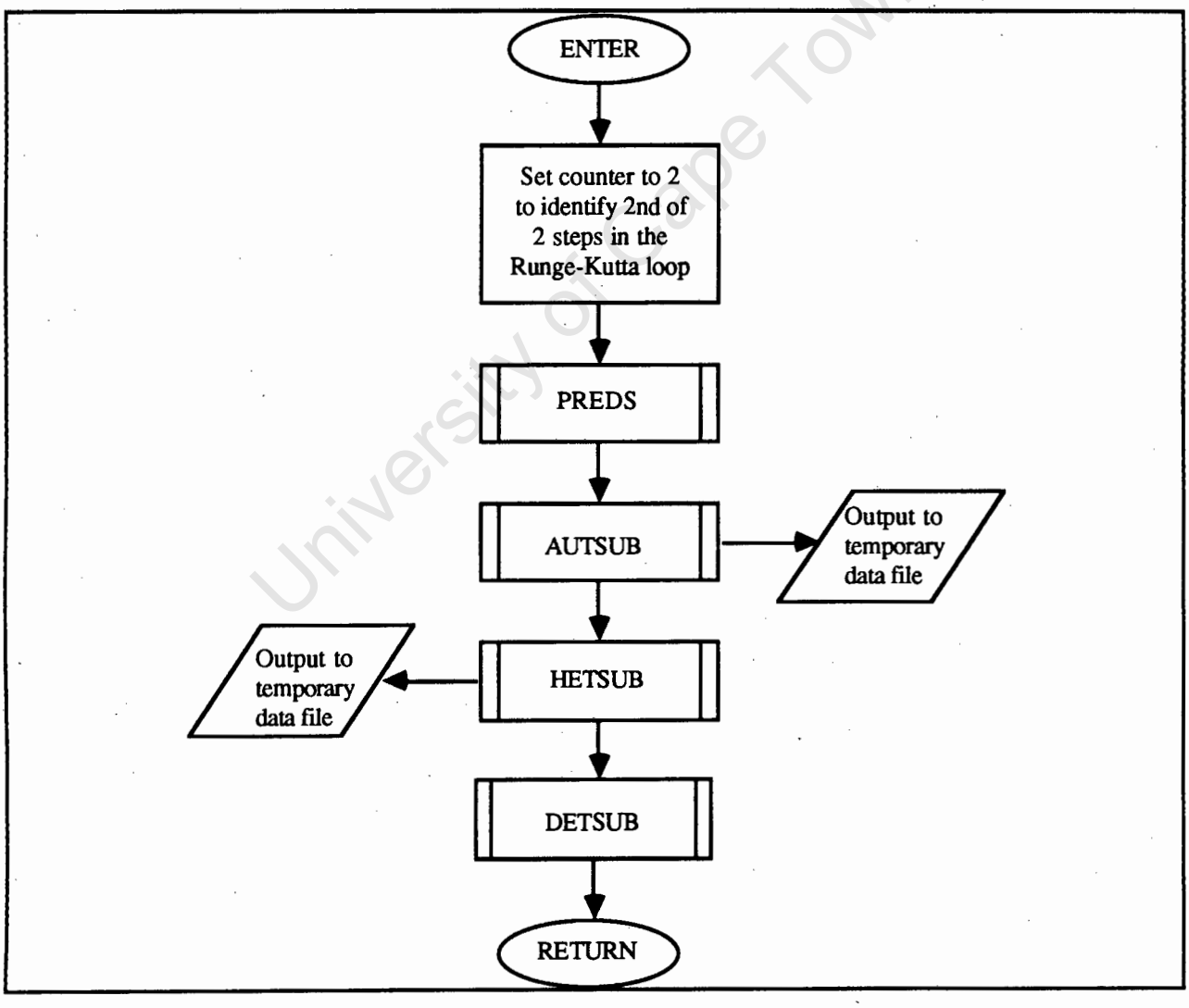

4.4.5 Subroutine INCRE2

CALLED BY: MAIN program

This subroutine calculates the second increment in the Runge-Kutta procedure to be added to each standing stock in each trophic size class and abiotic pool. It receives values from the MAIN program for variables I, DAMASC, DAMASN, DHMASC, DHMASN, DDC, DDN, DNEWN, DREGN, DPDOC, TCLASS, NCON, NITRO, ASMALC, ASMALN, HSMALC and HSMALN. It returns values to the MAIN program for variables AMASSC, AMASSN, HMASSC, HMASSN, DC, DN, NEWN, REGN and PDOC. The programming logic is as follows:

Fig. A-II.5. Program structure diagram of subroutine INCRE2.

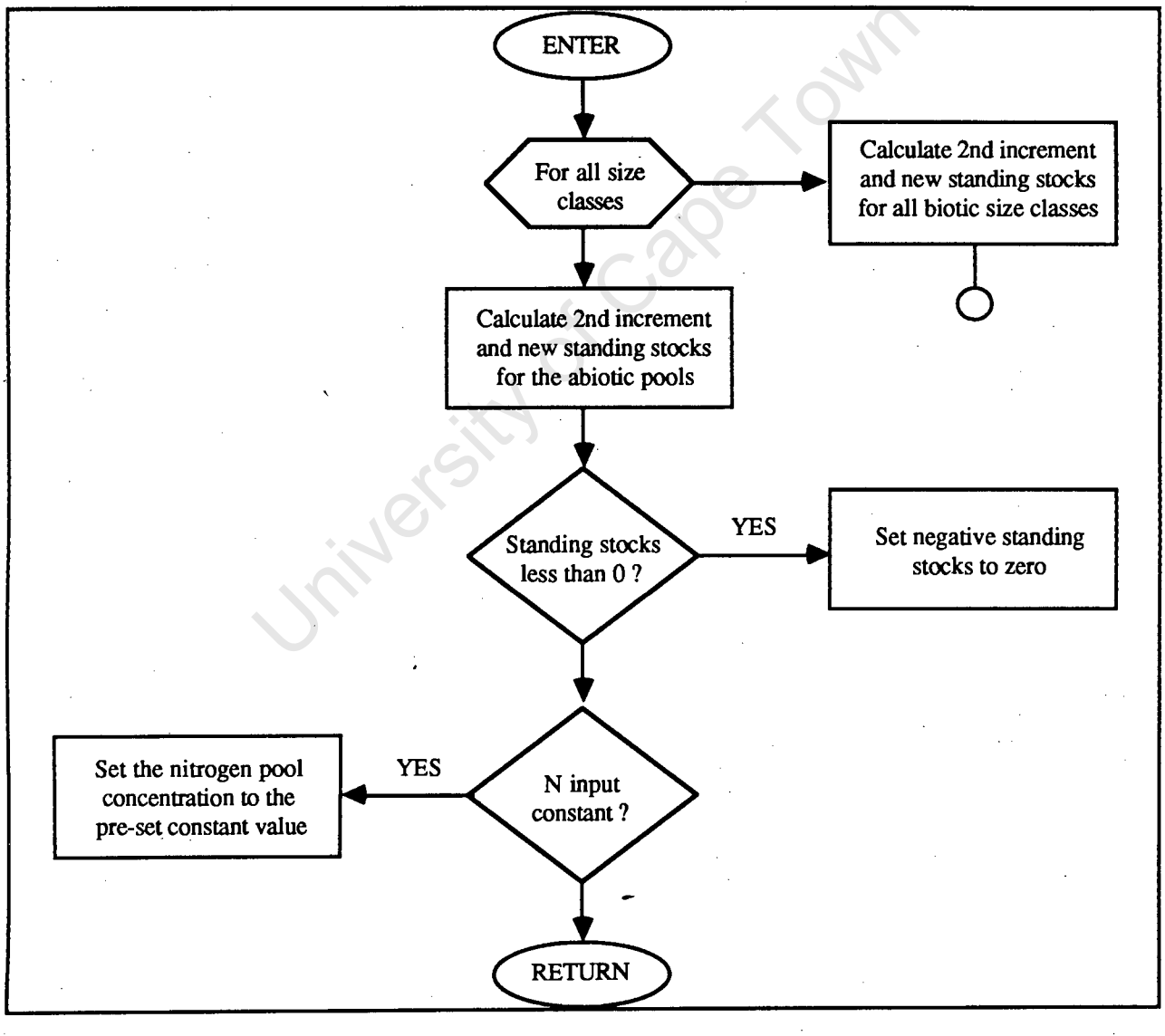

4.2.6 Subroutine PREDS

- CALLED BY: ISUB1, ISUB2

This subroutine calculates the predation losses from prey size classes into predator size classes. It also calculates the total potential uptake of new-nitrogen and regenerated-nitrogen from the respective pools. The programming logic is as follows:

Fig. A-II.6. Program structure diagram of subroutine PREDS.

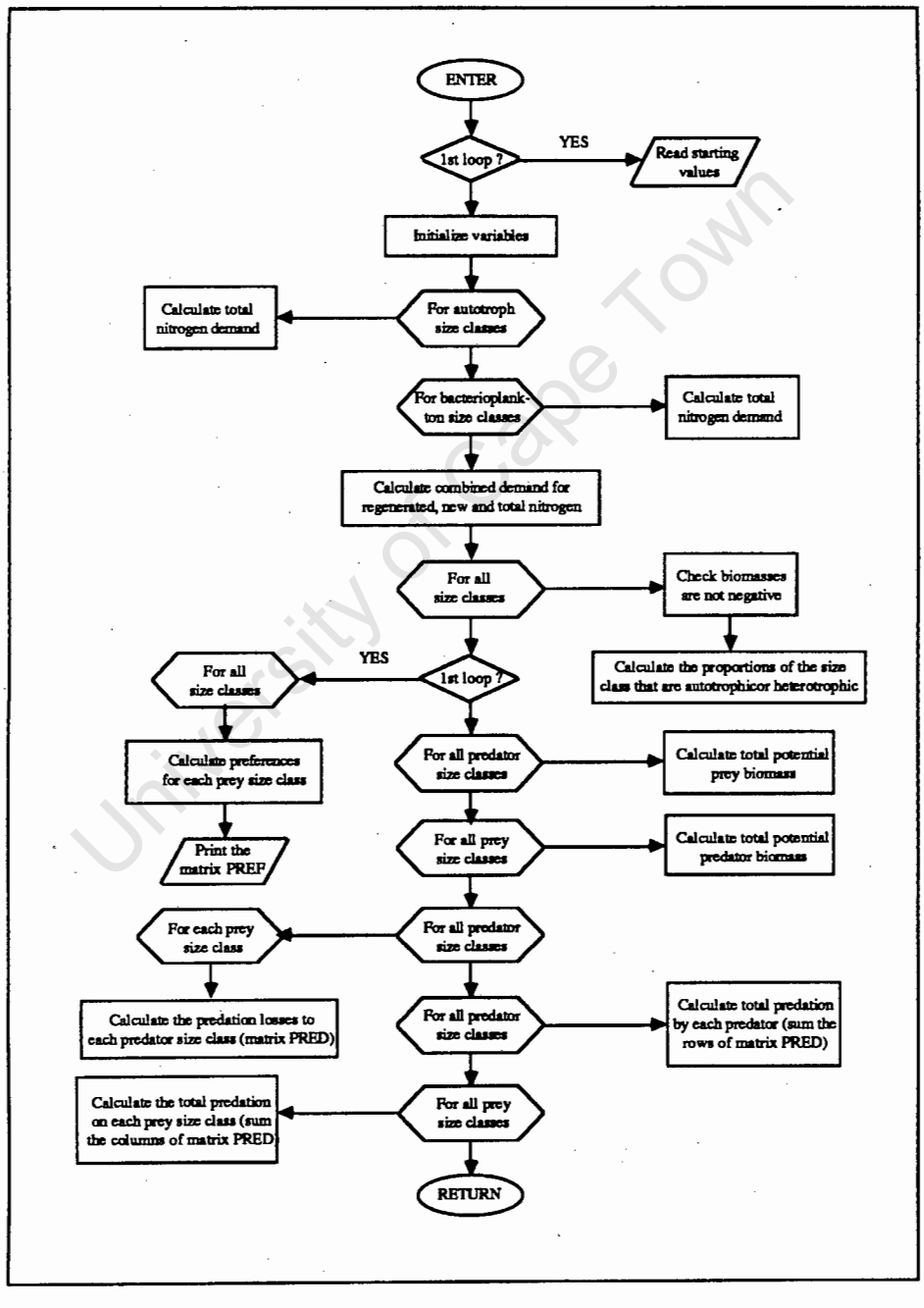

4.2.7 Subroutine AUTSUB

CALLED BY: ISUB1, ISUB2

This subroutine computes the flows in to and out of each autotroph size class, and then calculates the daily increment of each size class. It receives values from ISUB1 and ISUB2 for variables I, ICOUNT, DAY, AMASSC, AMASSN, NEWN, REGN, FLOW9, FLOW10, ITAB, UTOTNN, UTOTRN and AFRAC, and returns to ISUB1 and ISUB2 values for variables DAMASC, DAMASN, CDIN, NDIN, DOCIN, REGIN, NEWOUT and REGOUT. The programming logic is as follows:

Fig. A-II.7. Program structure diagram of subroutine AUTSUB.

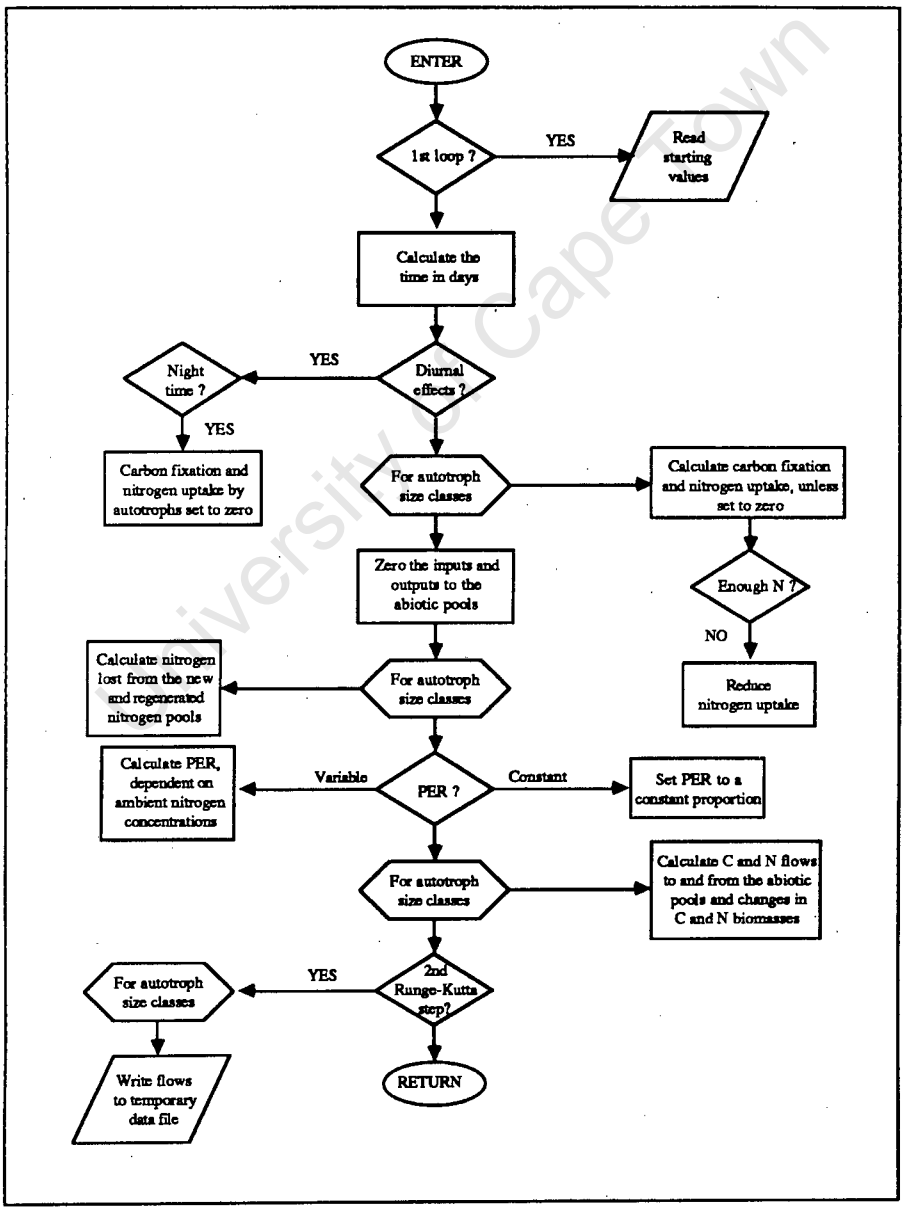

4.2.8 Subroutine HETSUB

CALLED BY: ISUB1, ISUB2

This subroutine computes carbon and nitrogen flows in to and out of each heterotroph size class, and calculates the daily increment for each size class. It receives values from ISUB1 and ISUB2 for variables I, ICOUNT, HMASSC, HMASSN, NEWN, REGN, PDOC, DC, DN, FLOW15, FLOW16, FLOW21, FLOW22, HFRAC, ITAB, HSMALC and UTOTN, and returns to ISUB1 and ISUB2 values for variables DHMASC, DHMASN, EBCT15, CDIN, NDIN, REGIN, CDOUT, NDOUT, NEWOUT, REGOUT and DOCOUT. The programming logic is as follows:

Fig. A-II.8. Program structure diagram of subroutine HETSUB.

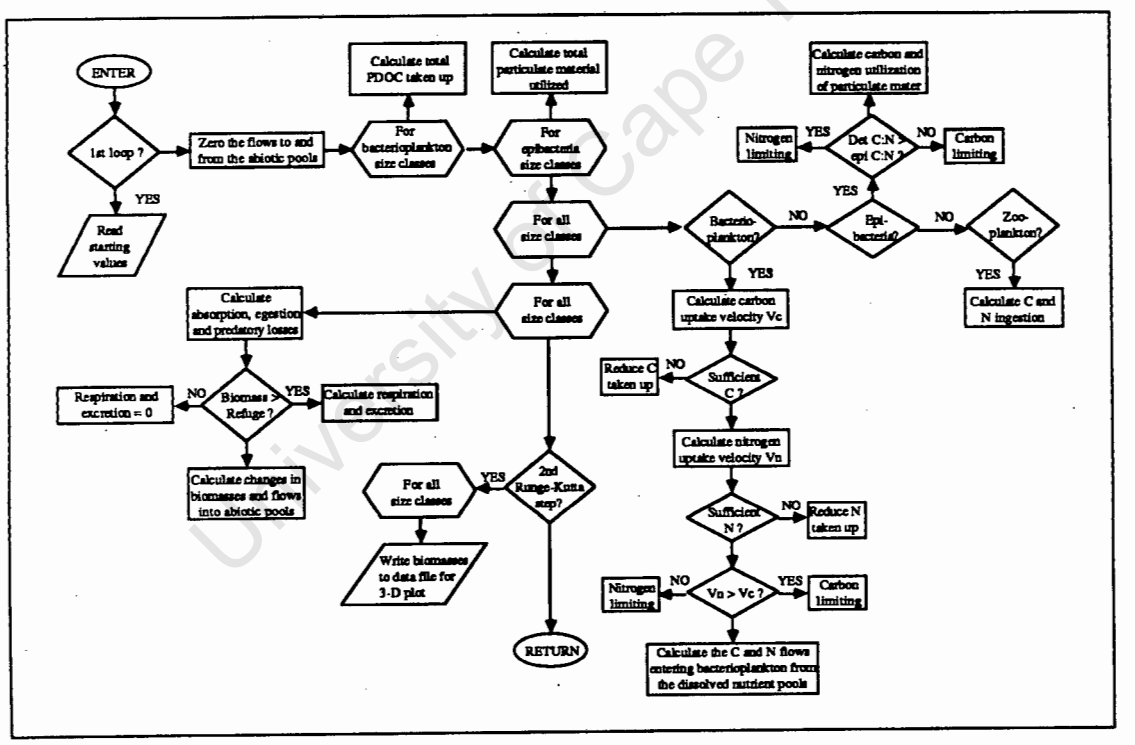

4.2.9 Subroutine DETSUB

CALLED BY: ISUB1, ISUB2

This subroutine computes the differences between carbon and nitrogen flows in to and out of the new-nitrogen, regenerated-nitrogen, PDOC, detrital carbon and detrital pools. It receives values from ISUB1 and ISUB2 for variables CDIN, NDIN, DOCIN, REGIN, CDOUT, NDOUT, DOCOUT, NEWOUT, NITRO, NINCRE and REGOUT, and returns to ISUB1 and ISUB2 values for variables DDC, DDN, DPDOC, DNEWN and DREGN. The programming logic is as follows:

Fig. A-II.9. Program structure diagram of subroutine DETSUB.

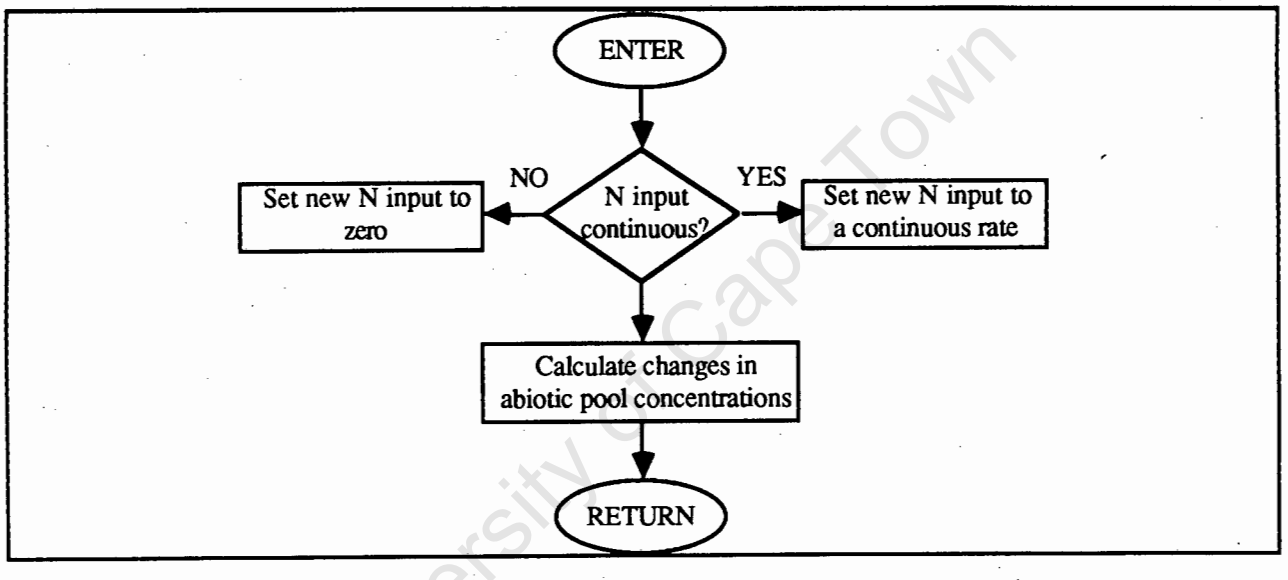

4.2.10 Subroutine MASSES

CALLED BY: MAIN program

This subroutine computes the total carbon and nitrogen standing stocks at each time step for autotrophs, planktobacteria, epibacteria, bactivores and zooplankton. It receives values from the MAIN program for variables I, AMASSC, AMASSN, HMASSC, HMASSN, DC, DN, NEWN, REGN, PDOC, DAY, ITAB and ILOOP, and returns to the main program values for variables AC, AN, PBC, PBN, EBC, EBN, BVC, BVN, ZPC and ZPN. It writes size-class standing stocks to six data files for three dimensional graphics output: TC2*AOUT., TC2*HOUT. and TC2*TOUT. for autotrophs, heterotrophs and the total biomass spectrum respectively; TC2*RELA., TC2*RELH. and TC2*RELT. for relative standing stocks of autotrophs, heterotrophs and the total spectrum respectively. The programming logic is as follows:

Fig. A-II.10. Program structure diagram of subroutine MASSES.

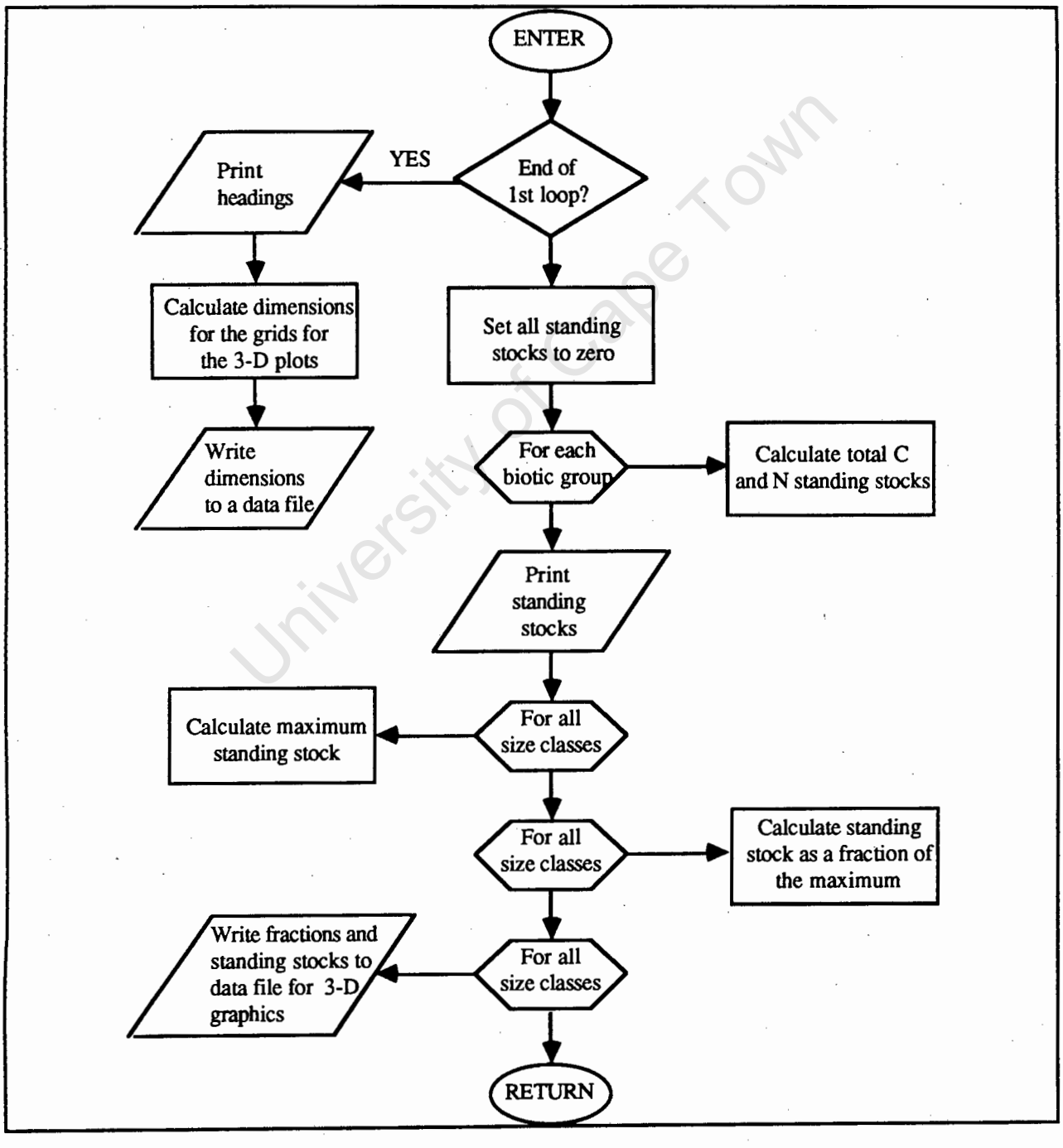

4.2.11 Subroutine EXTRAS

CALLED BY: Main program

This subroutine computes different flows and relationships between the flows and standing stocks in the trophic continuum. It receives values from the MAIN program for variables ILOOP, AC, AN, PBC, PBN, EBC, EBN, BVC, BVN, ZPC, ZPN, NEWN, REGN, EBCT15, DC, DN, TCLASS, IH1 and IH2. It returns no values to the MAIN program; all output is sent to the printer. The programming logic is as follows:

Fig. A-II.11. Program structure diagram of subroutine EXTRAS.

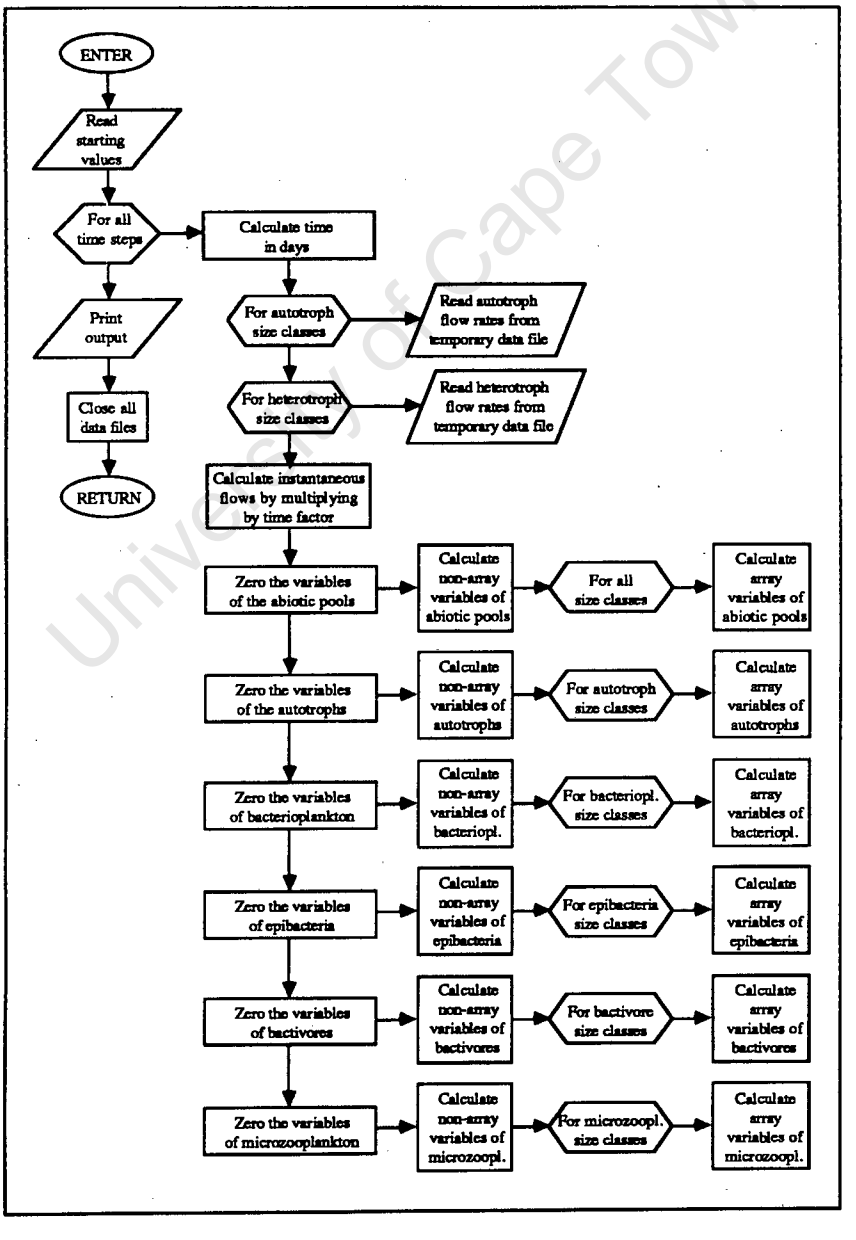

5. Program validation

The program was subjected to a number of checks and test runs to ascertain whether all calculations were carried out correctly. The units and dimensions used throughout and indicated on the printer output have been checked, and no inconsistencies have been found.

6. Extensions and improvements

In the programs' present forms, the structure of the model is relatively flexible, but the programs are not very easy to use for someone unfamiliar with them. It would be ideal to work with the model in interactive mode, so that changes to parameters and starting values could easily be done.

7. Program listing

```
      ****************************** TC2 ******************************

            CHARACTER*21  VER$N  @ LAST UPDATED ON
           &                '/09 JUN 88 AT 19:55:29'/
        5   CHARACTER*1, EBCT15
            CHARACTER*6, NITRO

            REAL AMASSC, AMASSN, HMASSC, HMASSN, DC, DN
            REAL NEWN, REGN, PDOC, NCON, NINCRE
       10   REAL DAMASC, DAMASN, DHMASC, DHMASN, DDC, DDN
            REAL DNEWN, DREGN, DPDOC
            REAL TMASSC, DAY, STEP
            REAL AC, AN, PBC, PBN, EBC, EBN, BVC, BVN, ZPC, ZPN
            REAL ASMALC, ASMALN, HSMALC, HSMALN
       15   REAL ACN, HCN

            INTEGER ILOOP, TCLASS, ITAB, IH1, IH2, SIZE, TIME
            PARAMETER STEP = 0.05
            PARAMETER SIZE = 25
       20   PARAMETER TIME = 1000

            DIMENSION AMASSC(SIZE), AMASSN(SIZE), HMASSC(SIZE), HMASSN(SIZE)
            DIMENSION DAMASC(SIZE), DAMASN(SIZE), DHMASC(SIZE), DHMASN(SIZE)
            DIMENSION TMASSC(SIZE), EBCT15(TIME)
       25   DIMENSION AC(TIME), AN(TIME), PBC(TIME), PBN(TIME), EBC(TIME)
            DIMENSION EBN(TIME), BVC(TIME), BVN(TIME), ZPC(TIME), ZPN(TIME)
            DIMENSION DC(TIME), DN(TIME), NEWN(TIME), REGN(TIME), PDOC(TIME)
            DIMENSION ASMALC(SIZE), ASMALN(SIZE), HSMALC(SIZE), HSMALN(SIZE)
            DIMENSION HCN(SIZE)
       30
          5   FORMAT ( )
          15  FORMAT ('1', A38, A21///)

            OPEN (13)
       35   OPEN (14)
            OPEN (15)
            OPEN (16)
            OPEN (17)
            OPEN (18)
       40   OPEN (20)
            OPEN (21)
            OPEN (22)
            OPEN (23)
```

```
      READ (13,5) NITRO, NCON, NINCRE
      READ (13,5) ILOOP, TCLASS, ACN
      DO 100 J = 1, TCLASS
        READ (13,5) AMASSC(J), AMASSN(J), HMASSC(J), HMASSN(J),
     &   TMASSC(J), ASMALC(J), HSMALC(J), HCN(J)
  100 CONTINUE
      READ (13,5) DC(1), DN(1), NEWN(1), REGN(1), PDOC(1)
      IF (NITRO .EQ. 'CONTIN') THEN
        NEWN(1) = NCON
      ELSEIF (NITRO .EQ. 'CNSTNT') THEN
        NEWN(1) = NCON
      ENDIF
      ITAB = 1

      PRINT 15, 'PROGRAM THESIS.TC2 LAST UPDATED ON ', VER$N

      DO 120 I = 1, ILOOP
      IF (I .EQ. 1) THEN
        DO 110 J = 1, TCLASS
          ASMALN(J) = ASMALC(J) / ACN
          HSMALN(J) = HSMALC(J) / HCN(J)
  110   CONTINUE
      ENDIF
        DAY = I * STEP
        CALL ISUB1 (I, AMASSC, AMASSN, HMASSC, HMASSN, TMASSC, NEWN,
     &            REGN, PDOC, DC, DN, DAMASC, DAMASN, DHMASC,
     &            DHMASN, DDC, DDN, DNEWN, DREGN, DPDOC, DAY,
     &            TCLASS, ITAB, IH1, IH2, EBCT15, ASMALC, HSMALC,
     &            NITRO, NINCRE)

        ITAB = ITAB + 1
        CALL INCRE1 (I, DAMASC, DAMASN, DHMASC, DHMASN, DDC, DDN,
     &            DNEWN, DREGN, DPDOC, AMASSC, AMASSN, HMASSC,
     &            HMASSN, DC, DN, NEWN, REGN, PDOC, TCLASS, NCON,
     &            NITRO, ASMALC, ASMALN, HSMALC, HSMALN)

        CALL ISUB2 (I, AMASSC, AMASSN, HMASSC, HMASSN, TMASSC, NEWN,
     &            REGN, PDOC, DC, DN, DAMASC, DAMASN, DHMASC,
     &            DHMASN, DDC, DDN, DNEWN, DREGN, DPDOC,
     &            DAY, EBCT15, TCLASS, ITAB, IH1, IH2, ASMALC,
     &            HSMALC, NITRO, NINCRE)

        CALL INCRE2 (I, DAMASC, DAMASN, DHMASC, DHMASN, DDC, DDN,
     &            DNEWN, DREGN, DPDOC, AMASSC, AMASSN, HMASSC,
     &            HMASSN, DC, DN, NEWN, REGN, PDOC, TCLASS, NCON,
     &            NITRO, ASMALC, ASMALN, HSMALC, HSMALN)

        CALL MASSES (I, AMASSC, AMASSN, HMASSC, HMASSN, DC, DN, NEWN,
     &            REGN, PDOC, AC, AN, PBC, PBN, EBC, EBN, BVC,
     &            BVN, ZPC, ZPN, DAY, ITAB, ILOOP)

  120 CONTINUE

      CLOSE (23)

      CALL EXTRAS (ILOOP, AC, AN, PBC, PBN, EBC, EBN, BVC, BVN,
     &            ZPC, ZPN, NEWN, REGN, EBCT15, DC, DN, TCLASS,
     &            IH1, IH2)

      END

*****************************  ISUB1  *****************************

      SUBROUTINE ISUB1 (I, AMASSC, AMASSN, HMASSC, HMASSN, TMASSC, NEWN,
     &            REGN, PDOC, DC, DN, DAMASC, DAMASN, DHMASC,
     &            DHMASN, DDC, DDN, DNEWN, DREGN, DPDOC, DAY,
     &            TCLASS, ITAB, IH1, IH2, EBCT15, ASMALC, HSMALC,
     &            NITRO, NINCRE)
```

```
      REAL AMASSC, AMASSN, HMASSC, HMASSN, TMASSC, DC, DN
      REAL NEWN, REGN, PDOC
      REAL DAMASC, DAMASN, DHMASC, DHMASN, DDC, DDN
      REAL DNEWN, DREGN, DPDOC
      REAL FLOW9, FLOW10, FLOW15, FLOW16, FLOW21, FLOW22
      REAL CDIN, NDIN, CDOUT, NDOUT, REGIN, REGOUT, NEWOUT
      REAL DOCIN, DOCOUT, NINCRE
      REAL DAY, AFRAC, HFRAC
      REAL ASMALC, HSMALC, UTOTN, UTOTNN, UTOTRN

      CHARACTER*1, EBCT15
      CHARACTER *6, NITRO

      INTEGER SIZE, TIME, TCLASS, ITAB, IH1, IH2, ICOUNT

      PARAMETER SIZE = 25
      PARAMETER TIME = 1000

      DIMENSION AMASSC(SIZE), AMASSN(SIZE), HMASSC(SIZE), HMASSN(SIZE)
      DIMENSION TMASSC(SIZE), NEWN(TIME), REGN(TIME), PDOC(TIME)
      DIMENSION DAMASC(SIZE), DAMASN(SIZE), DHMASC(SIZE), DHMASN(SIZE)
      DIMENSION FLOW9(SIZE), FLOW10(SIZE), FLOW15(SIZE), FLOW16(SIZE)
      DIMENSION FLOW21(SIZE), FLOW22(SIZE), AFRAC(SIZE), HFRAC(SIZE)
      DIMENSION DC(TIME), DN(TIME), EBCT15(TIME)
      DIMENSION ASMALC(SIZE), HSMALC(SIZE)

      ICOUNT = 1

      CALL PREDS (I, AMASSC, HMASSC, TMASSC, FLOW9, FLOW10, FLOW15,
     &          FLOW16, FLOW21, FLOW22, AFRAC, HFRAC, TCLASS,
     &          ITAB, IH1, IH2, UTOTN, ASMALC, HSMALC, NEWN,
     &          REGN, UTOTNN, UTOTRN)

      CALL AUTSUB (I, ICOUNT, DAY, AMASSC, AMASSN, NEWN, REGN, FLOW9,
     &          FLOW10, DAMASC, DAMASN, CDIN, NDIN, DOCIN, REGIN,
     &          NEWOUT, REGOUT, AFRAC, ITAB, UTOTNN, UTOTRN)

      CALL HETSUB (I, ICOUNT, HMASSC, HMASSN, NEWN, REGN, PDOC, DC, DN,
     &          FLOW15, FLOW16, FLOW21, FLOW22, DHMASC, DHMASN,
     &          EBCT15, CDIN, NDIN, REGIN, CDOUT, NDOUT, NEWOUT,
     &          REGOUT, DOCOUT, HFRAC, ITAB, HSMALC, UTOTN)

      CALL DETSUB (CDIN, NDIN, DOCIN, REGIN, CDOUT, NDOUT, DOCOUT,
     &          NEWOUT, REGOUT, DDC, DDN, DPDOC, DNEWN, DREGN,
     &          NITRO, NINCRE)

      RETURN
      END

********************************* INCRE1 ****************************

      SUBROUTINE INCRE1 (I, DAMASC, DAMASN, DHMASC, DHMASN, DDC, DDN,
     &            DNEWN, DREGN, DPDOC, AMASSC, AMASSN, HMASSC,
     &            HMASSN, DC, DN, NEWN, REGN, PDOC, TCLASS, NCON,
     &           NITRO, ASMALC, ASMALN, HSMALC, HSMALN)

      CHARACTER*6, NITRO
      INTEGER SIZE, TCLASS, TIME

      REAL STEP

      REAL DAMASC, DAMASN, DHMASC, DHMASN
      REAL DDC, DDN, DNEWN, DREGN, DPDOC, NCON
      REAL AMASSC, AMASSN, HMASSC, HMASSN, DC, DN, NEWN, REGN, PDOC
      REAL C1, C2, C3, C4, C5, C6, C7, C8, C9
      REAL ASMALC, ASMALN, HSMALC, HSMALN
```

```
      PARAMETER SIZE = 25
      PARAMETER STEP = 0.05
185   PARAMETER TIME = 1000

      DIMENSION DAMASC(SIZE), DAMASN(SIZE), DHMASC(SIZE), DHMASN(SIZE)
      DIMENSION AMASSC(SIZE), AMASSN(SIZE), HMASSC(SIZE), HMASSN(SIZE)
      DIMENSION ASMALC(SIZE), ASMALN(SIZE), HSMALC(SIZE), HSMALN(SIZE)
190   DIMENSION C1(SIZE), C2(SIZE), C3(SIZE), C4(SIZE)
      DIMENSION NEWN(TIME), REGN(TIME), PDOC(TIME)
      DIMENSION DC(TIME), DN(TIME)

      DO 100 J = 1, TCLASS
195     C1(J) = STEP * DAMASC(J)
        C2(J) = STEP * DAMASN(J)
        C3(J) = STEP * DHMASC(J)
        C4(J) = STEP * DHMASN(J)
        AMASSC(J) = AMASSC(J) + 0.5 * C1(J)
200     AMASSN(J) = AMASSN(J) + 0.5 * C2(J)
        HMASSC(J) = HMASSC(J) + 0.5 * C3(J)
        HMASSN(J) = HMASSN(J) + 0.5 * C4(J)
        IF (AMASSC(J) .LT. ASMALC(J)) AMASSC(J) = ASMALC(J)
        IF (AMASSN(J) .LT. ASMALN(J)) AMASSN(J) = ASMALN(J)
205     IF (HMASSC(J) .LT. HSMALC(J)) HMASSC(J) = HSMALC(J)
        IF (HMASSN(J) .LT. HSMALN(J)) HMASSN(J) = HSMALN(J)
  100 CONTINUE
        C5 = STEP * DDC
        C6 = STEP * DDN
210     C7 = STEP * DNEWN
        C8 = STEP * DREGN
        C9 = STEP * DPDOC

        DC(I) = DC(I) + 0.5 * C5
215     DN(I) = DN(I) + 0.5 * C6
        NEWN(I) = NEWN(I) + 0.5 * C7
        REGN(I) = REGN(I) + 0.5 * C8
        PDOC(I) = PDOC(I) + 0.5 * C9

220     IF (DC(I) .LT. 0) DC(I) = 0
        IF (DN(I) .LT. 0) DN(I) = 0
        IF (NEWN(I) .LT. 0) NEWN(I) = 0
        IF (REGN(I) .LT. 0) REGN(I) = 0
        IF (PDOC(I) .LT. 0) PDOC(I) = 0
225
        IF (NITRO .EQ. 'CNSTNT') THEN
          NEWN(I) = NCON
        ENDIF

230     RETURN
        END

      ****************************** ISUB2 ******************************
235
        SUBROUTINE ISUB2 (I, AMASSC, AMASSN, HMASSC, HMASSN, TMASSC, NEWN,
       &                  REGN, PDOC, DC, DN, DAMASC, DAMASN, DHMASC,
       &                  DHMASN, DDC, DDN, DNEWN, DREGN, DPDOC, DAY,
       &                  EBCT15, TCLASS, ITAB, IH1, IH2, ASMALC, HSMALC,
240    &                  NITRO, NINCRE)

        REAL AMASSC, AMASSN, HMASSC, HMASSN, TMASSC, DC, DN
        REAL NEWN, REGN, PDOC
        REAL DAMASC, DAMASN, DHMASC, DHMASN, DDC, DDN
245     REAL DNEWN, DREGN, DPDOC
        REAL FLOW9, FLOW10, FLOW15, FLOW16, FLOW21, FLOW22
        REAL CDIN, NDIN, CDOUT, NDOUT, REGIN, REGOUT, NEWOUT
        REAL DOCIN, DOCOUT, NINCRE
        REAL DAY, AFRAC, HFRAC
250     REAL ASMALC, HSMALC, UTOTN, UTOTNN, UTOTRN
```

```
      CHARACTER*1, EBCT15
      CHARACTER *6, NITRO

255   INTEGER SIZE, TIME, TCLASS, ITAB, IH1, IH2, ICOUNT

      PARAMETER SIZE = 25
      PARAMETER TIME = 1000

260   DIMENSION AMASSC(SIZE), AMASSN(SIZE), HMASSC(SIZE), HMASSN(SIZE)
      DIMENSION TMASSC(SIZE), AFRAC(SIZE), HFRAC(SIZE), EBCT15(TIME)
      DIMENSION DAMASC(SIZE), DAMASN(SIZE), DHMASC(SIZE), DHMASN(SIZE)
      DIMENSION FLOW9(SIZE), FLOW10(SIZE), FLOW15(SIZE), FLOW16(SIZE)
      DIMENSION FLOW21(SIZE), FLOW22(SIZE)
265   DIMENSION NEWN(TIME), REGN(TIME), PDOC(TIME)
      DIMENSION DC(TIME), DN(TIME)
      DIMENSION ASMALC(SIZE), HSMALC(SIZE)

      ICOUNT = 2
270
      CALL PREDS (I, AMASSC, HMASSC, TMASSC, FLOW9, FLOW10, FLOW15,
     &          FLOW16, FLOW21, FLOW22, AFRAC, HFRAC, TCLASS,
     &          ITAB, IH1, IH2, UTOTN, ASMALC, HSMALC, NEWN,
     &          REGN, UTOTNN, UTOTRN)
275
      CALL AUTSUB (I, ICOUNT, DAY, AMASSC, AMASSN, NEWN, REGN, FLOW9,
     &          FLOW10, DAMASC, DAMASN, CDIN, NDIN, DOCIN, REGIN,
     &          NEWOUT, REGOUT, AFRAC, ITAB, UTOTNN, UTOTRN)

280   CALL HETSUB (I, ICOUNT, HMASSC, HMASSN, NEWN, REGN, PDOC, DC, DN,
     &          FLOW15, FLOW16, FLOW21, FLOW22, DHMASC, DHMASN,
     &          EBCT15, CDIN, NDIN, REGIN, CDOUT, NDOUT, NEWOUT,
     &          REGOUT, DOCOUT, HFRAC, ITAB, HSMALC, UTOTN)

285   CALL DETSUB (CDIN, NDIN, DOCIN, REGIN, CDOUT, NDOUT, DOCOUT,
     &          NEWOUT, REGOUT, DDC, DDN, DPDOC, DNEWN, DREGN,
     &          NITRO, NINCRE)

      RETURN
290   END

*********************************  INCRE2  ****************************

295   SUBROUTINE INCRE2 (I, DAMASC, DAMASN, DHMASC, DHMASN, DDC, DDN,
     &          DNEWN, DREGN, DPDOC, AMASSC, AMASSN, HMASSC,
     &          HMASSN, DC, DN, NEWN, REGN, PDOC, TCLASS, NCON,
     &          NITRO, ASMALC, ASMALN, HSMALC, HSMALN)

300   INTEGER SIZE, TCLASS, TIME

      CHARACTER*6, NITRO

      REAL STEP
305   REAL DAMASC, DAMASN, DHMASC, DHMASN
      REAL DDC, DDN, DNEWN, DREGN, DPDOC, NCON
      REAL AMASSC, AMASSN, HMASSC, HMASSN, DC, DN, NEWN, REGN, PDOC
       REAL C1, C2, C3, C4, C5, C6, C7, C8, C9
       REAL ASMALC, ASMALN, HSMALC, HSMALN
310
      PARAMETER SIZE = 25
      PARAMETER STEP = 0.05
      PARAMETER TIME = 1000

315   DIMENSION DAMASC(SIZE), DAMASN(SIZE), DHMASC(SIZE), DHMASN(SIZE)
      DIMENSION AMASSC(SIZE), AMASSN(SIZE), HMASSC(SIZE), HMASSN(SIZE)
      DIMENSION C1(SIZE), C2(SIZE), C3(SIZE), C4(SIZE)
      DIMENSION NEWN(TIME), REGN(TIME), PDOC(TIME)
      DIMENSION DC(TIME), DN(TIME)
320   DIMENSION ASMALC(SIZE), ASMALN(SIZE), HSMALC(SIZE), HSMALN(SIZE)
```

```
      DO 100 J = 1, TCLASS
        C1(J) = STEP * DAMASC(J)
        C2(J) = STEP * DAMASN(J)
325     C3(J) = STEP * DHMASC(J)
        C4(J) = STEP * DHMASN(J)
        AMASSC(J) = AMASSC(J) + C1(J)
        AMASSN(J) = AMASSN(J) + C2(J)
        HMASSC(J) = HMASSC(J) + C3(J)
330     HMASSN(J) = HMASSN(J) + C4(J)
        IF (AMASSC(J) .LT. ASMALC(J)) AMASSC(J) = ASMALC(J)
        IF (AMASSN(J) .LT. ASMALN(J)) AMASSN(J) = ASMALN(J)
        IF (HMASSC(J) .LT. HSMALC(J)) HMASSC(J) = HSMALC(J)
        IF (HMASSN(J) .LT. HSMALN(J)) HMASSN(J) = HSMALN(J)
335   100 CONTINUE
        C5 = STEP * DDC
        C6 = STEP * DDN
        C7 = STEP * DNEWN
        C8 = STEP * DREGN
340     C9 = STEP * DPDOC

        DC(I+1) = DC(I) + C5
        DN(I+1) = DN(I) + C6
        NEWN(I+1) = NEWN(I) + C7
345     REGN(I+1) = REGN(I) + C8
        PDOC(I+1) = PDOC(I) + C9

        IF (DC(I+1) .LT. 0) DC(I+1) = 0
        IF (DN(I+1) .LT. 0) DN(I+1) = 0
350     IF (NEWN(I+1) .LT. 0) NEWN(I+1) = 0
        IF (REGN(I+1) .LT. 0) REGN(I+1) = 0
        IF (PDOC(I+1) .LT. 0) PDOC(I+1) = 0

        IF (NITRO .EQ. 'CNSTNT') THEN
355       NEWN(I+1) = NCON
        ENDIF

      RETURN
      END
360

*****************************  MASSES  ****************************

      SUBROUTINE MASSES (I, AMASSC, AMASSN, HMASSC, HMASSN, DC, DN,
365   &                   NEWN, REGN, PDOC, AC, AN, PBC, PBN, EBC, EBN,
      &                   BVC, BVN, ZPC, ZPN, DAY, ITAB, ILOOP)

      INTEGER IA1, IA2, IH1, IH2, IPB1, IPB2, IEB1, IEB2, IBV1, IBV2
      INTEGER IZP1, IZP2, ITAB, III
370   INTEGER SIZE, TIME
      INTEGER NX, NY, IPRINT, ISPACE

      PARAMETER SIZE = 25
      PARAMETER TIME = 1000
375
      REAL AMASSC, AMASSN, HMASSC, HMASSN, TMASSC
      REAL NEWN, REGN, PDOC, DC, DN, DAY
      REAL AC, AN, PBC, PBN, EBC, EBN, BVC, BVN, ZPC, ZPN
      REAL X1, XL, Y1, YL
380   REAL TOPT, TOPA, TOPH
      REAL BST, BSA, BSH

      DIMENSION AMASSC(SIZE), AMASSN(SIZE), HMASSC(SIZE), HMASSN(SIZE)
      DIMENSION TMASSC(SIZE)
385   DIMENSION BST(SIZE), BSA(SIZE), BSH(SIZE)
      DIMENSION AC(TIME), AN(TIME), PBC(TIME), PBN(TIME), EBC(TIME)
      DIMENSION EBN(TIME), BVC(TIME), BVN(TIME), ZPC(TIME), ZPN(TIME)
      DIMENSION DC(TIME), DN(TIME), NEWN(TIME), REGN(TIME), PDOC(TIME)
```

```
    5   FORMAT ( )
   15   FORMAT ('1', 30X, A50)
   25   FORMAT (' ', 30X, A50)
   35   FORMAT (' ', 30X, A50////)
   45   FORMAT (' ',1X,A4,3X,A13,2X,2(A10,3X),A10,2X,A11,4X,A8,7X,
  &        A4,6X,A9,4X,A9)
   55   FORMAT (' ',A6,4X,9(A10,3X)/,11X,5(A10,3X),A10,3(2X,A11))
   65   FORMAT (' ',1X,A4,3X,A13,2X,2(A10,3X),A10,2X,A11,4X,A8,7X,
  &        A4,6X,A9,4X,A9//)
   75   FORMAT (' ',F5.2,5X,9(E9.3,4X)/,11X,9(E9.3,4X)/)
   85   FORMAT (14(6(F10.3,1X),:/),6(F10.3,1X))
   95   FORMAT (14(6(F10.3,1X),:/),6(F10.3,1X))
  105   FORMAT (F6.2,8(F8.1))
  115   FORMAT (I3,3X,I4)
  125   FORMAT (4(F6.1, 2X))

      IF (ITAB .EQ. 2) THEN
        READ (13,5) IPRINT
        ISPACE = IPRINT
        READ (13,5) IA1, IA2, IH1, IH2, III
        READ (13,5) IPB1, IPB2, IEB1, IEB2, IBV1, IBV2, IZP1, IZP2

        PRINT 15, '***************************'
        PRINT 25, '***                     ***'
        PRINT 25, '***   STANDING STOCKS   ***'
        PRINT 25, '***                     ***'
        PRINT 35, '***************************'
        PRINT 45, 'TIME','PHYTOPLANKTON','P-BACTERIA','E-BACTERIA',
       &          'BACTIVORES','ZOOPLANKTON','DETRITUS','PDOC',
       &          'NEW NITRO','REG NITRO'
        PRINT 55, '(DAYS)','(MG.C.M-3)','(MG.C.M-3)','(MG.C.M-3)',
       &          '(MG.C.M-3)','(MG.C.M-3)','(MG.C.M-3)','(MG.C.M-3)',
       &          '(MG.N.M-3)','(MG.N.M-3)','(MG.N.M-3)','(MG.N.M-3)',
       &          '(MG.N.M-3)','(MG.N.M-3)','(MG.N.M-3)','(MG.N.M-3)',
       &          '(UG.AT.L-1)','(UG.AT.L-1)','(UG.AT.L-1)'
        PRINT 65, '****','************','**********','**********',
       &          '**********','**********','********','****',
       &          '*********','*********'
        PRINT 75, DAY, AC(I), PBC(I), EBC(I), BVC(I), ZPC(I), DC(I),
       &       PDOC(I), NEWN(I), REGN(I), AN(I), PBN(I), EBN(I),
       &       BVN(I), ZPN(I), DN(I), PDOC(I)/12, NEWN(I)/14,
       &        REGN(I)/14
        NX = IZP2
        NY = ILOOP / 2
        X1 = REAL (IPB1)
        XL = REAL (IZP2)
        Y1 = 1
        YL = REAL (ILOOP) / 2
        WRITE (14,115) NX, NY
        WRITE (14,125) X1, XL, Y1, YL
        WRITE (15,115) NX, NY
        WRITE (15,125) X1, XL, Y1, YL
        NX = IA2 - IA1 + 1
        X1 = REAL (IA1)
        XL = REAL (IA2)
        WRITE (20,115) NX, NY
        WRITE (20,125) X1, XL, Y1, YL
        WRITE (16,115) NX, NY
        WRITE (16,125) X1, XL, Y1, YL
        NX = IZP2
        X1 = REAL (IPB1)
        XL = REAL (IZP2)
        WRITE (21,115) NX, NY
        WRITE (21,125) X1, XL, Y1, YL
        WRITE (17,115) NX, NY
        WRITE (17,125) X1, XL, Y1, YL
      ENDIF

      AC(I), AN(I) = 0
```

```
      PBC(I), PBN(I) = 0
      EBC(I), EBN(I) = 0
      BVC(I), BVN(I) = 0
      ZPC(I), ZPN(I) = 0

      DO 100 J = IA1, IA2
        AC(I) = AC(I) + AMASSC(J)
        AN(I) = AN(I) + AMASSN(J)
  100 CONTINUE

      DO 110 J = IPB1, IPB2
        PBC(I) = PBC(I) + HMASSC(J)
        PBN(I) = PBN(I) + HMASSN(J)
  110 CONTINUE

      DO 120 J = IEB1, IEB2
        EBC(I) = EBC(I) + HMASSC(J)
        EBN(I) = EBN(I) + HMASSN(J)
  120 CONTINUE

      DO 130 J = IBV1, IBV2
        BVC(I) = BVC(I) + HMASSC(J)
        BVN(I) = BVN(I) + HMASSN(J)
  130 CONTINUE

      DO 140 J = IZP1, IZP2
        ZPC(I) = ZPC(I) + HMASSC(J)
        ZPN(I) = ZPN(I) + HMASSN(J)
  140 CONTINUE

      DO 150 J = IPB1, IZP2
        TMASSC(J) = AMASSC(J) + HMASSC(J)
  150 CONTINUE

      IF (I .EQ. IPRINT) THEN
        PRINT 75, DAY, AC(I), PBC(I), EBC(I), BVC(I), ZPC(I), DC(I),
     &        PDOC(I), NEWN(I), REGN(I), AN(I), PBN(I), EBN(I),
     &        BVN(I), ZPN(I), DN(I), PDOC(I)/12, NEWN(I)/14,
     &         REGN(I)/14
        IPRINT = IPRINT + ISPACE
      ENDIF

      TOPT = 0
      TOPA = 0
      TOPH = 0

      DO 160 J = IPB1, IZP2
        IF (TMASSC(J) .GT. TOPT) TOPT = TMASSC(J)
        IF (AMASSC(J) .GT. TOPA) TOPA = AMASSC(J)
        IF (HMASSC(J) .GT. TOPH) TOPH = HMASSC(J)
  160 CONTINUE

      DO 170 J = IPB1, IZP2
        BST(J) = 100 * TMASSC(J) / TOPT
        BSA(J) = 100 * AMASSC(J) / TOPA
        BSH(J) = 100 * HMASSC(J) / TOPH
  170 CONTINUE

      IF (I .EQ. III) THEN
        WRITE (14,85) (TMASSC(J), J = IPB1, IZP2)
        WRITE (20,95) (AMASSC(J), J = IA1, IA2)
        WRITE (21,85) (HMASSC(J), J = IPB1, IZP2)
        WRITE (15,85) (BST(J), J = IPB1, IZP2)
        WRITE (16,95) (BSA(J), J = IA1, IA2)
        WRITE (17,85) (BSH(J), J = IPB1, IZP2)
        WRITE (22,105) I*0.05, AC(I), PBC(I), EBC(I),
     &              BVC(I), ZPC(I), PDOC(I),
     &              NEWN(I), REGN(I)
        III = III + 2
```

```
      ENDIF
      RETURN
      END

*****************************  PREDS  *****************************

      SUBROUTINE PREDS (I, AMASSC, HMASSC, TMASSC, FLOW9, FLOW10,
     &            FLOW15, FLOW16, FLOW21, FLOW22, AFRAC, HFRAC,
     &            TCLASS, ITAB, IH1, IH2, UTOTN, ASMALC, HSMALC,
     &           NEWN, REGN, UTOTNN, UTOTRN)

      INTEGER IBV1, IH1, IH2, UPOS, VPOS, SIZE, TIME, ITAB, I2, I3
      INTEGER IA1, IA2, IPB1, IPB2
      INTEGER TCLASS, UCLASS, UMINUS, UPLUS, VCLASS

      PARAMETER SIZE = 25
      PARAMETER TIME = 1000

      REAL AMASSC, AFRAC, ACN
      REAL HMASSC, HFRAC, HCN
      REAL TMASSC
      REAL UMASSC, VMASSC
      REAL PREF, PRED
      REAL PREF1, PREF2, PREF3
      REAL CPREDA, CPREDH, NPREDA, NPREDH
      REAL H15, H15A, A2, A2A, K15
      REAL FLOW9, FLOW10, FLOW15, FLOW16, FLOW21, FLOW22
      REAL UTOTAN, UTOTPN, UTOTN, UTOTNN, UTOTRN
      REAL ASMALC, HSMALC, NEWN, REGN

      DIMENSION UPOS(SIZE), UCLASS(SIZE), UMINUS(SIZE), UPLUS(SIZE)
      DIMENSION VPOS(SIZE), VCLASS(SIZE)
      DIMENSION AMASSC(SIZE), AFRAC(SIZE)
      DIMENSION HMASSC(SIZE), HFRAC(SIZE), HCN(SIZE)
      DIMENSION UMASSC(SIZE), VMASSC(SIZE), TMASSC(SIZE)
      DIMENSION H15(SIZE), H15A(SIZE), A2(SIZE), A2A(SIZE), K15(SIZE)
      DIMENSION FLOW9(SIZE), FLOW10(SIZE), FLOW15(SIZE)
      DIMENSION FLOW16(SIZE), FLOW21(SIZE), FLOW22(SIZE)
      DIMENSION PRED(SIZE,SIZE), PREF(SIZE,SIZE)
      DIMENSION NEWN(TIME), REGN(TIME)
      DIMENSION ASMALC(SIZE), HSMALC(SIZE)

    5  FORMAT ( )
   15  FORMAT (' ',30X,A36////)
   25  FORMAT (' ', 6X,20(I2,3X)//)
   35  FORMAT (' ',I2,3X,20F5.3)
   45  FORMAT ('1',6X,20(I2,3X)//)
   55  FORMAT ('1',6X,I2,24(3X,I2)//)
   65  FORMAT (' ',I2,2X,F5.3,24F5.3)

      IF (ITAB .EQ. 1) THEN
        READ (13,5) IBV1, IH1, IH2, ACN, PREF1, PREF2
        READ (13,5) IA1, IA2, IPB1, IPB2
        DO 100 J = 1, TCLASS
          READ (13,5) UCLASS(J), UMINUS(J), UPLUS(J), UPOS(J)
          READ (13,5) VPOS(J), VCLASS(J)
  100   CONTINUE

        DO 110 J = IH1, IH2
          READ (13,5) H15(J), H15A(J), HCN(J), A2(J), A2A(J), K15(J)
  110   CONTINUE
      ENDIF

*  ***********************************************************
*  ***                                                     ***
*  ***     WORK OUT TOTAL COMPETITION FOR NITROGEN         ***
*  ***                                                     ***
```

```
*  ************************************************************

      UTOTAN = 0
600   DO 120 J = IA1, IA2
        UTOTAN = UTOTAN + A2(J) * AMASSC(J) / ACN * (NEWN(I) +
     &   REGN(I)) / (A2A(J) + NEWN(I) + REGN(I))
120   CONTINUE

605   UTOTPN = 0
      DO 130 J = IPB1, IPB2
        UTOTPN = UTOTPN + H15(J) * HMASSC(J) / HCN(J) * (NEWN(I) +
     &   REGN(I)) / (K15(J) + NEWN(I) + REGN(I))
130   CONTINUE
610
      UTOTN = UTOTAN + UTOTPN
      UTOTNN = UTOTN * NEWN(I) / (NEWN(I) + REGN(I))
      UTOTRN = UTOTN * REGN(I) / (NEWN(I) + REGN(I))

615
*  ************************************************************
*  ***                                      ***
*  ***   WORK OUT THE RELATIVE PROPORTIONS OF AUTOTROPHS   ***
*  ***     AND HETEROTROPHS IN EACH OF THE CLASSES       ***
620*  ***             IN THE PREY ARRAY                 ***
*  ***                                      ***
*  ************************************************************


625   DO 140 J = 1, TCLASS
        IF (AMASSC(J) .LT. 0) PRINT *, 'NEGATIVE AMASSC, PREDS'
        IF (HMASSC(J) .LT. 0) PRINT *, 'NEGATIVE HMASSC, PREDS'
        TMASSC(J) = AMASSC(J) + HMASSC(J)
        IF (TMASSC(J) .GT. 0) THEN
630       AFRAC(J) = (AMASSC(J) - ASMALC(J)) / (TMASSC(J) - ASMALC(J)
     &     - HSMALC(J))
          HFRAC(J) = (HMASSC(J) - HSMALC(J)) / (TMASSC(J) - ASMALC(J)
     &     - HSMALC(J))
        ELSEIF (TMASSC(J) .LE. 0) THEN
635       AFRAC(J) = 0
          HFRAC(J) = 0
        ENDIF
140   CONTINUE

640
*  ****************************************************
*  ***                                    ***
*  ***  WORK OUT THE PREDATOR PREFERENCES FOR EACH   ***
*  ***  PREY CLASS FOR EACH PREDATOR - MATRIX PREF   ***
645*  ***                                    ***
*  ****************************************************


      IF (ITAB .EQ. 1) THEN
650     DO 160 J = IH1, IH2
          PREF3 = PREF1
          I2 = UPOS(J) + UMINUS(J)
          PREF(J,I2) = PREF3
          DO 150 K = IH1, IH2
655         PREF3 = PREF3 / PREF2
            IF (K .LE. UPLUS(J) .AND. K. LE. UMINUS(J)) THEN
              PREF(J,I2+K) = PREF3
              PREF(J,I2-K) = PREF3
            ELSEIF (K .LE. UPLUS(J) .AND. K .GT. UMINUS(J)) THEN
660           PREF(J,I2+K) = PREF3
              IF (I2-K .GE. IH1) PREF(J,I2-K) = 0
            ELSEIF (K .GT. UPLUS(J) .AND. K .LE. UMINUS(J)) THEN
              IF (I2+K .LE. IH2) PREF(J,I2+K) = 0
              PREF(J,I2-K) = PREF3
665         ELSEIF (K .GT. UPLUS(J) .AND. K .GT. UMINUS(J)) THEN
```

```
                IF (I2+K .LE. IH2) PREF(J,I2+K) = 0
                IF (I2-K .GE. IH1) PREF(J,I2-K) = 0
              ENDIF
150         CONTINUE
160       CONTINUE

          PRINT 15, '******  MATRIX PREF  ******'
          I2 = 1
          I3 = 20
          PRINT 25, (K, K = I2, I3)
          DO 170 J = IH1, IH2
            PRINT 35, J, (PREF(J,K), K = I2, I3)
170       CONTINUE
          I2 = I3 + 1
          I3 = I3 + 20
          DO 190 II = 1, 2
            PRINT 45, (K, K = I2, I3)
            DO 180 J = IH1, IH2
              PRINT 35, J, (PREF(J,K), K = I2, I3)
180         CONTINUE
            I2 = I3 + 1
            I3 = I3 + 20
190       CONTINUE
          PRINT 55, (K, K = I2, I3)
          DO 200 J = IH1, IH2
            PRINT 65, J, (PREF(J,K), K = I2, SIZE)
200       CONTINUE

        ENDIF

*   ************************************************************
*   ***                                                      ***
*   ***  WORK OUT THE TOTAL PREY BIOMASS FOR EACH PREDATOR   ***
*   ***                                                      ***
*   ************************************************************

        DO 220 J = IH1,IH2
          I2 = UPOS(J)
          I3 = UPOS(J) + UCLASS(J) - 1
          IF (I3 .GT. IH2) I3 = IH2
          IF (I3 .LT. 0) I3 = 0
          UMASSC(J) = 0
          DO 210 K = I2, I3
            UMASSC(J) = UMASSC(J) + TMASSC(K) - ASMALC(K) - HSMALC(K)
210       CONTINUE
220     CONTINUE


*   ************************************************************
*   ***                                                      ***
*   ***     WORK OUT THE TOTAL PREDATION FOR EACH PREY       ***
*   ***                                                      ***
*   ************************************************************

        DO 240 K = IH1, IH2
          I2 = VPOS(K)
          I3 = VPOS(K) + VCLASS(K) - 1
          IF (I3 .LT. 0) I3 = 0
          VMASSC(K) = 0
          DO 230 J = I2, I3
            VMASSC(K) = VMASSC(K) + HMASSC(J) * H15(J) * PREF(J,K)
     &    * (TMASSC(K) - ASMALC(K) - HSMALC(K)) / (H15A(K) + UMASSC(J))
230       CONTINUE
240     CONTINUE


*   ************************************************************
*   ***                                                      ***
```

```
735   *  ***  WORK OUT THE PREDATION LOSSES FROM EACH PREY CLASS  ***
      *  ***          TO EACH PREDATOR - MATRIX PRED           ***
      *  ***                                                   ***
      *  ***********************************************************

740         DO 260 J = IH1, IH2
              DO 250 K = IH1, IH2
               IF (UMASSC(J) .LE. 0 .OR. VMASSC(K) .LE. 0) THEN
                PRED(J,K) = 0
               ELSE
745             PRED(J,K) = H15(J) * HMASSC(J) * PREF(J,K) * (TMASSC(K) -
           &      ASMALC(K) - HSMALC(K)) / (H15A(K) + UMASSC(J))
               ENDIF
      250    CONTINUE
      260  CONTINUE
750       DO 265 J = IH1, IH2
            WRITE (18,5) (PRED(J,K), K = IH1, IH2)
      265  CONTINUE


755   *  ********************************************************
      *  ***                                                  ***
      *  ***  WORK OUT THE TOTAL PREDATION BY EACH PREDATOR   ***
      *  ***   SUM THE ROWS OF MATRIX PRED - FLOWS 15 & 16    ***
      *  ***                                                  ***
760   *  ********************************************************

         DO 280 J = IH1, IH2
            FLOW15(J) = 0
            FLOW16(J) = 0
765         DO 270 K = IH1, IH2
               CPREDA = AFRAC(K) * PRED(J,K)
               NPREDA = CPREDA / ACN
               CPREDH = HFRAC(K) * PRED(J,K)
               NPREDH = CPREDH / HCN(K)
770            FLOW15(J) = FLOW15(J) + CPREDH + CPREDA
               FLOW16(J) = FLOW16(J) + NPREDA + NPREDH
      270    CONTINUE
      280  CONTINUE

775
      *  ************************************************************
      *  ***                                                      ***
      *  ***  WORK OUT THE TOTAL PREDATION ON EACH PREY - SUM THE  ***
      *  ***    COLUMNS OF MATRIX PRED - FLOWS 9, 10, 21 & 22     ***
780   *  ***                                                      ***
      *  ************************************************************

         DO 300 K =IH1,IH2
            FLOW9(K) = 0
785         FLOW10(K) = 0
            FLOW21(K) = 0
            FLOW22(K) = 0
            DO 290 J = IH1, IH2
               CPREDA = AFRAC(K) * PRED(J,K)
790            NPREDA = CPREDA / ACN
               CPREDH = HFRAC(K) * PRED(J,K)
               NPREDH = CPREDH / HCN(K)
               FLOW9(K)  = FLOW9(K)  + CPREDA
               FLOW10(K) = FLOW10(K) + NPREDA
795            FLOW21(K) = FLOW21(K) + CPREDH
               FLOW22(K) = FLOW22(K) + NPREDH
      290      CONTINUE
      300  CONTINUE

800

         RETURN
         END
```

```
805
      ********************************* AUTSUB **************************

          SUBROUTINE AUTSUB (I, ICOUNT, DAY, AMASSC, AMASSN, NEWN, REGN,
          &                  FLOW9, FLOW10, DAMASC, DAMASN, CDIN, NDIN,
810       &                  DOCIN, REGIN, NEWOUT, REGOUT, AFRAC, ITAB,
          &                  UTOTNN, UTOTRN)

          CHARACTER *1, DIURN
          CHARACTER *6, PERCON
815
          INTEGER IDAY, IA1, IA2, SIZE, TIME, ICOUNT, ITAB

          PARAMETER SIZE = 25
          PARAMETER TIME = 1000
820
          REAL AMASSC, AMASSN, ACN
          REAL DAMASC, DAMASN, DAY
          REAL NEWN, REGN, AFRAC
          REAL CDIN, NDIN, DOCIN, REGIN, NEWOUT, REGOUT
825       REAL A1, A2, A2A, A3, A4, A4A, A5, A7, A11, A13
          REAL FLOW1, FLOW1A, FLOW2, FLOW3, FLOW4, FLOW5, FLOW6, FLOW7
          REAL FLOW8, FLOW9, FLOW10, FLOW11, FLOW12, FLOW13, FLOW14
          REAL UTOTNN, UTOTRN, PER

830       DIMENSION AMASSC(SIZE), AMASSN(SIZE), AFRAC(SIZE)
          DIMENSION DAMASC(SIZE), DAMASN(SIZE)
          DIMENSION NEWN(TIME), REGN(TIME)
          DIMENSION A1(SIZE), A2(SIZE), A2A(SIZE), A3(SIZE), A4(SIZE)
          DIMENSION A4A(SIZE), A5(SIZE), A7(SIZE), A11(SIZE), A13(SIZE)
835       DIMENSION FLOW1(SIZE), FLOW1A(SIZE), FLOW2(SIZE)
          DIMENSION FLOW3(SIZE), FLOW4(SIZE), FLOW5(SIZE)
          DIMENSION FLOW6(SIZE), FLOW7(SIZE), FLOW8(SIZE)
          DIMENSION FLOW9(SIZE), FLOW10(SIZE), FLOW11(SIZE)
          DIMENSION FLOW12(SIZE), FLOW13(SIZE), FLOW14(SIZE)
840
      5   FORMAT ( )
      15  FORMAT (2(5(E9.3,1X)/),5(E9.3,1X),F7.3)

          IF (ITAB .EQ. 1) THEN
845         READ (13,5) IA1, IA2, ACN, DIURN
            READ (13,5) PERCON
            DO 100 J = IA1, IA2
              READ (13,5) A1(J), A2(J), A2A(J), A3(J), A4(J), A4A(J),
          &     A5(J), A7(J), A11(J), A13(J)
850   100   CONTINUE
          ENDIF

          IDAY = INT (DAY)

855
          IF (DIURN .EQ. 'Y') GO TO 110
          IF (DIURN .EQ. 'N') GO TO 130

      110 CONTINUE
860       IF (DAY-IDAY .GE. 0.5 .AND. DAY-IDAY .LT. 1) THEN
            DO 120 J = IA1, IA2
              FLOW1(J) = 0
              FLOW2(J) = 0
              FLOW4(J) = 0
865   120     CONTINUE
            GO TO 160
          ELSEIF (DAY-IDAY .GE. 0 .AND. DAY-IDAY .LT. 0.5) THEN
            GO TO 130
          ENDIF
870   130 CONTINUE
```

```
            DO 140 J = IA1, IA2
              FLOW2(J) = A2(J) * AMASSN(J) * NEWN(I) / (A2A(J) +
875         &          NEWN(I) + REGN(I))
              FLOW4(J) = A4(J) * AMASSN(J) * REGN(I) / (A4A(J) +
            &          NEWN(I) + REGN(I))
              IF (UTOTNN .GT. NEWN(I)) THEN
                FLOW2(J) = FLOW2(J) * NEWN(I) / UTOTNN
880           ELSEIF (UTOTNN .LE. NEWN(I)) THEN
                FLOW2(J) = FLOW2(J)
              ENDIF
              IF (UTOTRN .GT. REGN(I)) THEN
                FLOW4(J) = FLOW4(J) * REGN(I) / UTOTRN
885           ELSEIF (UTOTRN .LE. REGN(I)) THEN
                FLOW4(J) = FLOW4(J)
              ENDIF
          140 CONTINUE
            REGOUT = 0
890         NEWOUT = 0
            DO 150 J = IA1, IA2
              NEWOUT = NEWOUT + FLOW2(J)
              REGOUT = REGOUT + FLOW4(J)
          150 CONTINUE
895       160 CONTINUE

            CDIN = 0
            NDIN = 0
            DOCIN = 0
900         REGIN = 0

            IF (PERCON .EQ. 'CNSTNT') THEN
              PER = A13(IA1)
            ELSEIF (PERCON .EQ. 'CHANGE') THEN
905           PER = EXP (-0.00405 * (NEWN(I) + REGN(I)))
            ENDIF

            DO 170 J = IA1, IA2
              FLOW1A(J) = ACN * (FLOW2(J) + FLOW4(J))
910           FLOW1(J) = FLOW1A(J) / (1 - PER)
              FLOW3(J)  = A3(J) * AMASSC(J)
              FLOW5(J)  = A5(J) * AMASSC(J)
              FLOW6(J)  = FLOW5(J) / ACN
              FLOW7(J)  = A7(J) * AMASSC(J)
915           FLOW8(J)  = FLOW7(J) / ACN
              FLOW9(J)  = FLOW9(J)
              FLOW10(J) = FLOW10(J)
              FLOW11(J) = A11(J) * AMASSC(J)
              FLOW12(J) = FLOW11(J) / ACN
920           FLOW13(J) = FLOW1(J) - FLOW1A(J)
              FLOW14(J) = FLOW3(J) / ACN

              CDIN = CDIN + FLOW5(J)
              NDIN = NDIN + FLOW6(J)
925           DOCIN = DOCIN + FLOW13(J)
              REGIN = REGIN

            if (j .eq. ia1) then
              DAMASC(J) = FLOW1(J) - FLOW3(J) - FLOW5(J) -
930         &         FLOW7(J) - FLOW9(J) - FLOW11(J) - FLOW13(J)
              DAMASN(J) = FLOW2(J) + FLOW4(J) - FLOW6(J) -
            &         FLOW8(J) - FLOW10(J) - FLOW12(J) - FLOW14(J)
            elseif (j .gt. ia1 .and. j .LT. ia2) then
              DAMASC(J) = FLOW1(J) + flow11(j-1) - FLOW3(J) - FLOW5(J) -
935         &         FLOW7(J) - FLOW9(J) - FLOW11(J) - FLOW13(J)
              DAMASN(J) = FLOW2(J) + FLOW4(J) + flow12(j-1) - FLOW6(J) -
            &         FLOW8(J) - FLOW10(J) - FLOW12(J) - FLOW14(J)
            ELSEIF (J .EQ. IA2) THEN
              DAMASC(J) = FLOW1(J) + flow11(j-1) - FLOW3(J) - FLOW5(J) -
940         &         FLOW7(J) - FLOW9(J) - FLOW13(J)
              DAMASN(J) = FLOW2(J) + FLOW4(J) + flow12(j-1) - FLOW6(J) -
```

```
     &         FLOW8(J) - FLOW10(J) - FLOW14(J)
      endif

945  170  CONTINUE
      IF (ICOUNT .EQ. 2) THEN
        DO 180 J = IA1, IA2
          WRITE (23,15) FLOW1(J), FLOW1A(J), FLOW2(J), FLOW3(J),
     &     FLOW4(J), FLOW5(J), FLOW6(J), FLOW7(J), FLOW8(J),
950  &     FLOW9(J), FLOW10(J), FLOW11(J), FLOW12(J), FLOW13(J),
     &     FLOW14(J), AFRAC(J)
     180  CONTINUE
      ELSEIF (ICOUNT .EQ. 1) THEN
        GO TO 190
955   ENDIF

     190  CONTINUE

      RETURN
960   END


     ***************************** HETSUB *****************************

965   SUBROUTINE HETSUB (I, ICOUNT, HMASSC, HMASSN, NEWN, REGN, PDOC,
     &            DC, DN, FLOW15, FLOW16, FLOW21, FLOW22,
     &            DHMASC, DHMASN, EBCT15, CDIN, NDIN, REGIN,
     &            CDOUT, NDOUT, NEWOUT, REGOUT, DOCOUT, HFRAC,
     &            ITAB, HSMALC, UTOTN)
970
      CHARACTER *1, EBCT15

      INTEGER IH1, IH2, IPB1, IPB2, IEB1, IEB2, IBV1, ICOUNT, ITAB
      INTEGER SIZE, TIME
975
      PARAMETER SIZE = 25
      PARAMETER TIME = 1000


980   REAL HMASSC, HMASSN, HCN
      REAL ASIMHC, ASIMHN, PBCV, PBNV, ASSIMH
      REAL DHMASC, DHMASN, HFRAC
      REAL CDIN, NDIN, REGIN
      REAL CDOUT, NDOUT, DOCOUT, NEWOUT, REGOUT
985   REAL DC, DN, PDOC, NEWN, REGN
      REAL H15, H15A, H17, H19, H23, K15
      REAL FLOW15, FLOW16, FLW16A, FLW16B, FLW16C, FLOW17, FLOW18
      REAL FLOW19, FLOW20, FLOW21, FLOW22, FLOW23, FLOW24
      REAL HSMALC, UTOTD, UTOTC, UTOTN
990
      DIMENSION HMASSC(SIZE), HMASSN(SIZE), HCN(SIZE)
      DIMENSION ASIMHC(SIZE), ASIMHN(SIZE), HFRAC(SIZE)
      DIMENSION DHMASC(SIZE), DHMASN(SIZE), ASSIMH(SIZE)
      DIMENSION NEWN(TIME), REGN(TIME), PDOC(TIME), EBCT15(TIME)
995   DIMENSION H15(SIZE), H15A(SIZE), H17(SIZE), H19(SIZE), H23(SIZE)
      DIMENSION FLOW15(SIZE), FLOW16(SIZE), FLW16A(SIZE)
      DIMENSION FLW16B(SIZE), FLW16C(SIZE), FLOW17(SIZE)
      DIMENSION FLOW18(SIZE), FLOW19(SIZE), FLOW20(SIZE)
      DIMENSION FLOW21(SIZE), FLOW22(SIZE), FLOW23(SIZE)
1000  DIMENSION FLOW24(SIZE), K15(SIZE)
      DIMENSION DC(TIME), DN(TIME)
      DIMENSION HSMALC (SIZE)

     5   FORMAT ( )
1005 15   FORMAT (2(5(E9.3,1X)/),3(E9.3,1X),F7.3)

      IF (ITAB .EQ. 1) THEN
        READ (13,5) IH1, IH2, IPB1, IPB2, IEB1, IEB2, IBV1

1010    DO 100 J = IH1, IH2
```

```
          READ (13,5) H15(J), H15A(J), H17(J), H19(J), H23(J),
     &      ASSIMH(J), HCN(J), K15(J)
  100    CONTINUE
       ENDIF
1015

       DOCOUT = 0
       CDOUT = 0
       NDOUT = 0
1020

       UTOTC = 0
       DO 110 J = IPB1, IPB2
          UTOTC = UTOTC + H15(J) * HMASSC(J) * PDOC(I) / (K15(J) *
1025   &    HCN(J) + PDOC(I))
  110  CONTINUE

       UTOTD = 0
       DO 120 J = IEB1, IEB2
1030      UTOTD = UTOTD + H15(J) * HMASSC(J)
  120  CONTINUE

       DO 130 J = IH1, IH2

1035      IF (J .GE. IPB1 .AND. J .LE. IPB2) THEN
             PBCV = H15(J) * PDOC(I) / (K15(J) * HCN(J) +
     &            PDOC(I))
             IF (UTOTC .GT. PDOC(I)) THEN
                PBCV = PBCV * PDOC(I) / UTOTC
1040         ELSEIF (UTOTC .LE. PDOC(I)) THEN
                PBCV = PBCV
             ENDIF
             PBNV = H15(J) * (NEWN(I) + REGN(I)) /
     &            (K15(J) + NEWN(I) + REGN(I))
1045         IF (UTOTN .GT. NEWN(I) + REGN(I)) THEN
                PBNV = PBNV * (NEWN(I) + REGN(I)) / UTOTN
             ELSEIF (UTOTN .LE. NEWN(I) + REGN(I)) THEN
                PBNV = PBNV
             ENDIF
1050         IF (PBNV .LT. PBCV) THEN
               FLOW15(J) = PBNV * HMASSC(J)
               FLOW16(J) = FLOW15(J) / HCN(J)
             ELSEIF (PBNV .GE. PBCV) THEN
               FLOW15(J) = PBCV * HMASSC(J)
1055           FLOW16(J) = FLOW15(J) / HCN(J)
             ENDIF
            FLW16A(J) = FLOW16(J) * NEWN(I) / (NEWN(I) + REGN(I))
            FLW16B(J) = FLOW16(J) * REGN(I) / (NEWN(I) + REGN(I))
          ELSEIF (J .GE. IEB1 .AND. J .LE. IEB2) THEN
1060        IF (DC(I)/DN(I) .LE. HCN(J)) THEN
               FLOW15(J) = H15(J) * HMASSC(J) * DC(I) / (K15(J) *
     &                HCN(J) + DC(I))
               FLOW16(J) = FLOW15(J) / HCN(J)
               EBCT15(I) = 'C'
1065           FLW16C(J) = 0
            ELSEIF (DC(I)/DN(I) .GT. HCN(J)) THEN
               FLOW16(J) = H15(J) * HMASSN(J) * DN(I) / (K15(J) +
     &                DN(I))
               FLOW15(J) = FLOW16(J) * HCN(J)
1070           EBCT15(I) = 'N'
               FLW16C(J) = 0
            ENDIF
          ELSEIF (J .GE. IBV1) THEN
            FLOW15(J) = FLOW15(J)
1075        FLOW16(J) = FLOW16(J)
          ENDIF

          ASIMHC(J) = ASSIMH(J) * FLOW15(J)
          ASIMHN(J) = ASIMHC(J) / HCN(J)
```

```
1080          FLOW17(J) = FLOW15(J) - ASIMHC(J)
              FLOW18(J) = FLOW16(J) - ASIMHN(J)
              IF (HMASSC(J) .LE. HSMALC(J)) THEN
                 FLOW19(J) = 0
                 FLOW20(J) = 0
1085          ELSEIF (HMASSC(J) .GT. HSMALC(J)) THEN
                 FLOW19(J) = H19(J) * HMASSC(J)
                 FLOW20(J) = H19(J) * HMASSN(J)
              ENDIF
              FLOW21(J) = FLOW21(J)
1090          FLOW22(J) = FLOW22(J)
              FLOW23(J) = H23(J) * HMASSC(J)
              FLOW24(J) = FLOW23(J) / HCN(J)

              CDIN = CDIN + FLOW17(J)
1095          NDIN = NDIN + FLOW18(J)
              REGIN = REGIN + FLOW20(J)

            if (j .eq. ih1) then
              DHMASC(J) = FLOW15(J) - FLOW17(J) - FLOW19(J)
1100        &          - FLOW21(J) - FLOW23(J)
              DHMASN(J) = FLOW16(J) - FLOW18(J) - FLOW20(J)
            &          - FLOW22(J) - FLOW24(J)
             elseif (j .gt. ih1 .and. j .LT. ih2) then
              DHMASC(J) = FLOW15(J) - FLOW17(J) - FLOW19(J)
1105        &          - FLOW21(J) - FLOW23(J) + FLOW23(J-1)
              DHMASN(J) = FLOW16(J) - FLOW18(J) - FLOW20(J)
            &          - FLOW22(J) - FLOW24(J) + FLOW24(J-1)
             ELSEIF (J .EQ. IH2) THEN
              DHMASC(J) = FLOW15(J) - FLOW17(J) - FLOW19(J)
1110        &          - FLOW21(J) + FLOW23(J-1)
              DHMASN(J) = FLOW16(J) - FLOW18(J) - FLOW20(J)
            &          - FLOW22(J) + FLOW24(J-1)
            endif
          130  CONTINUE
1115
            IF (ICOUNT .EQ. 2) THEN
              DO 140 J = IH1, IH2
                WRITE (23,15) FLOW15(J), FLOW16(J), FLW16A(J),
            &    FLW16B(J), FLW16C(J), FLOW17(J), FLOW18(J),
1120        &    FLOW19(J), FLOW20(J), FLOW21(J), FLOW22(J),
            &    FLOW23(J), FLOW24(J), HFRAC(J)
          140    CONTINUE
            ELSEIF (ICOUNT .EQ. 1) THEN
              GO TO 150
1125        ENDIF

          150  CONTINUE

            DO 160 J = IPB1, IPB2
1130          NEWOUT = NEWOUT + FLW16A(J)
              REGOUT = REGOUT + FLW16B(J)
          160  CONTINUE

            DO 170 J = IPB1, IPB2
1135          DOCOUT = DOCOUT + FLOW15(J)
          170  CONTINUE

            DO 180 J = IEB1, IEB2
              CDOUT = CDOUT + FLOW15(J)
1140          NDOUT = NDOUT + FLOW16(J)
          180  CONTINUE

            RETURN
            END
1145

          ****************************** DETSUB ******************************
```

```
      SUBROUTINE DETSUB (CDIN, NDIN, DOCIN, REGIN, CDOUT, NDOUT,
1150  &                  DOCOUT, NEWOUT, REGOUT, DDC, DDN, DPDOC,
      &                  DNEWN, DREGN, NITRO, NINCRE)

      REAL CDIN, NDIN, DOCIN, REGIN, NINCRE
      REAL CDOUT, NDOUT, DOCOUT, REGOUT, NEWOUT
1155  REAL DDC, DDN, DPDOC, DNEWN, DREGN
      CHARACTER *6, NITRO

      DDC = CDIN - CDOUT
      DDN = NDIN - NDOUT
1160
      DPDOC = DOCIN - DOCOUT


      IF (NITRO .EQ. 'CONTIN') THEN
1165    DNEWN = NINCRE - NEWOUT
      ELSEIF (NITRO .NE. 'CONTIN') THEN
        DNEWN = - NEWOUT
      ENDIF
      DREGN = REGIN - REGOUT
1170  RETURN
      END


C     ************************** EXTRAS ****************************
1175
      SUBROUTINE EXTRAS (ILOOP, AC, AN, PBC, PBN, EBC, EBN, BVC,
      &                  BVN, ZPC, ZPN, NEWN, REGN, EBCT15, DC, DN,
      &                  TCLASS, IH1, IH2)

1180  CHARACTER*1, EBCT15

      INTEGER SIZE, TIME
      INTEGER TCLASS, ILOOP, IH1, IH2
      INTEGER IA1, IA2, IPB1, IPB2, IEB1, IEB2, IBV1, IBV2, IZP1, IZP2
1185  REAL STEP

      PARAMETER TIME = 1000
      PARAMETER SIZE = 25
      PARAMETER STEP = 0.05
1190
      REAL AC, AN, PBC, PBN, EBC, EBN, BVC, BVN, ZPC, ZPN, NEWN, REGN
      REAL DC, DN, DAY
      REAL AUTO1, AUTO2, AUTO3, AUTO4, AUTO5, AUTO6
      REAL AUTO7, AUTO8, AUTO9, AUTO10, AUTO11, AUTO12
1195  REAL AUTO13, AUTO14, AUTO15, AUTO16, AUTO17, AUTO18
      REAL PBCT1, PBCT2, PBCT3, PBCT4, PBCT5, PBCT6, PBCT7, PBCT8
      REAL PBCT9, PBCT10, PBCT11, PBCT12, PBCT13, PBCT14, PBCT15
      REAL EBCT1, EBCT2, EBCT3, EBCT4, EBCT5, EBCT6, EBCT7, EBCT8
      REAL EBCT9, EBCT10, EBCT11, EBCT12, EBCT13, EBCT14
1200  REAL BVOR1, BVOR2, BVOR3, BVOR4, BVOR5, BVOR6
      REAL BVOR7, BVOR8, BVOR9, BVOR10, BVOR11, BVOR12
      REAL ZOOP1, ZOOP2, ZOOP3, ZOOP4, ZOOP5, ZOOP6
      REAL ZOOP7, ZOOP8, ZOOP9, ZOOP10, ZOOP11, ZOOP12
      REAL HET1, DET1, DET2, DET3, DET4, DET5, DET6, DET7, DET8
1205  REAL FLOW1, FLOW1A, FLOW2, FLOW3, FLOW4, FLOW5, FLOW6
      REAL FLOW7, FLOW8, FLOW9, FLOW10, FLOW11, FLOW12, FLOW13
      REAL FLOW14, FLOW15, FLOW16, FLW16A, FLW16B, FLW16C, FLOW17
      REAL FLOW18, FLOW19, FLOW20, FLOW21, FLOW22, FLOW23, FLOW24
      REAL AFRAC, HFRAC
1210
      DIMENSION FLOW1(SIZE), FLOW1A(SIZE), FLOW2(SIZE)
      DIMENSION FLOW3(SIZE), FLOW4(SIZE), FLOW5(SIZE)
      DIMENSION FLOW6(SIZE), FLOW7(SIZE), FLOW8(SIZE)
      DIMENSION FLOW9(SIZE), FLOW10(SIZE), FLOW11(SIZE)
1215  DIMENSION FLOW12(SIZE), FLOW13(SIZE), FLOW14(SIZE)
      DIMENSION FLOW15(SIZE), FLOW16(SIZE), FLW16A(SIZE)
      DIMENSION FLW16B(SIZE), FLW16C(SIZE), FLOW17(SIZE)
```

```
      DIMENSION FLOW18(SIZE), FLOW19(SIZE), FLOW20(SIZE)
      DIMENSION FLOW21(SIZE), FLOW22(SIZE), FLOW23(SIZE)
1220  DIMENSION FLOW24(SIZE)
      DIMENSION AUTO1(TIME), AUTO2(TIME), AUTO3(TIME), AUTO4(TIME)
      DIMENSION AUTO5(TIME), AUTO6(TIME), AUTO7(TIME), AUTO8(TIME)
      DIMENSION AUTO9(TIME), AUTO10(TIME), AUTO11(TIME), AUTO12(TIME)
      DIMENSION AUTO13(TIME), AUTO14(TIME), AUTO15(TIME), AUTO16(TIME)
1225  DIMENSION AUTO17(TIME), AUTO18(TIME)
      DIMENSION PBCT1(TIME), PBCT2(TIME), PBCT3(TIME), PBCT4(TIME)
      DIMENSION PBCT5(TIME), PBCT6(TIME), PBCT7(TIME), PBCT8(TIME)
      DIMENSION PBCT9(TIME), PBCT10(TIME), PBCT11(TIME), PBCT12(TIME)
      DIMENSION PBCT13(TIME), PBCT14(TIME), PBCT15(TIME)
1230  DIMENSION EBCT1(TIME), EBCT2(TIME), EBCT3(TIME), EBCT4(TIME)
      DIMENSION EBCT5(TIME), EBCT6(TIME), EBCT7(TIME), EBCT8(TIME)
      DIMENSION EBCT9(TIME), EBCT10(TIME), EBCT11(TIME), EBCT12(TIME)
      DIMENSION EBCT13(TIME), EBCT14(TIME), EBCT15(TIME)
     DIMENSION BVOR1(TIME), BVOR2(TIME), BVOR3(TIME), BVOR4(TIME)
1235  DIMENSION BVOR5(TIME), BVOR6(TIME), BVOR7(TIME), BVOR8(TIME)
      DIMENSION BVOR9(TIME), BVOR10(TIME), BVOR11(TIME), BVOR12(TIME)
      DIMENSION ZOOP1(TIME), ZOOP2(TIME), ZOOP3(TIME), ZOOP4(TIME)
      DIMENSION ZOOP5(TIME), ZOOP6(TIME), ZOOP7(TIME), ZOOP8(TIME)
      DIMENSION ZOOP9(TIME), ZOOP10(TIME), ZOOP11(TIME), ZOOP12(TIME)
1240  DIMENSION HET1(TIME), DET1(TIME), DET2(TIME), DET3(TIME)
      DIMENSION DET4(TIME), DET5(TIME), DET6(TIME), DET7(TIME)
      DIMENSION DET8(TIME), AFRAC(SIZE), HFRAC(SIZE), DAY(TIME)
      DIMENSION AC(TIME), AN(TIME), PBC(TIME), PBN(TIME)
      DIMENSION EBC(TIME), EBN(TIME), BVC(TIME), BVN(TIME)
1245  DIMENSION ZPC(TIME), ZPN(TIME), DC(TIME), DN(TIME)
      DIMENSION NEWN(TIME), REGN(TIME)

    5   FORMAT ( )
    15  FORMAT ('1', 30X, A50)
1250  25  FORMAT (' ', 30X, A50)
    35  FORMAT (' ', 30X, A50////)
    45  FORMAT (' ',1X,A4,5X,A9,4X,A9,5X,A7,6X,A7,4X,A11,2X,A11,3X,
       &      A10,4X,A8,5X,A7/,1X,A6,3X,2(A12,4X,A5,5X),4(A12,1X))
    55  FORMAT (' ',A6,3X,A12,2X,A9,3X,A12,3X,A7,4X,3(A12,1X),A12,
1255   &      3X,A7//)
    65  FORMAT (' ',F5.2,5X,9(E9.3,4X))
    75  FORMAT (' ',1X,A4,6X,A7,5X,A9,5X,A8,4X,A10,2X,A11,4X,A8,3X,
       &      A11,2X,A11,3X,A9/,1X,A6,3X,3(A12,1X),1X,A10,3X,A9,4X,
       &      A11,1X,A12,1X,A12)
1260  85  FORMAT (' ',A6,3X,3(A12,1X),1X,A10,2X,A11,3X,A11,1X,A12,1X,
       &      A12,2X,A9//)
    95  FORMAT (' ',1X,A4,2(2X,A7),4X,A4,3X,A6,1X,A9,1X,A7,1X,A6,
       &      3(2X,A7),1X,A6,2X,A6,2X,A5,3X,A7,2X,A3/,1X,A6,3(1X,A8),
       &      9X,A8,25X,A8,1X,A8,16X,A8)
1265  105 FORMAT (' ',A6,3(1X,A8),1X,A6,1X,A9,1X,A7,1X,A6,2X,A7,2(1X,A8),
       &      1X,A6,2X,A6,1X,A8,1X,A7,2X,A3//)
    115 FORMAT (' ',F5.2,1X,E8.3,1X,E9.3,1X,E8.3,1X,F6.2,2X,
       &      E8.3,1X,3(F6.2,2X),2(E8.3,1X),F6.2,2X,F6.2,1X,
       &      E8.3,1X,F6.2,2X,F5.2)
1270  125 FORMAT (' ',1X,A4,2(2X,A7),4X,A4,3X,A6,1X,A9,1X,A7,1X,A6,
       &      3(2X,A7),2X,A5,3X,A7,2X,A5,3X,A3,2X,A5/,1X,A6,3(1X,A8),
       &      9X,A8,25X,A8,2(1X,A8))
    135 FORMAT (' ',A6,3(1X,A8),1X,A6,1X,A9,1X,A7,1X,A6,2X,A7,3(1X,A8),
       &      1X,A7,2X,A5,3X,A3,2X,A5//)
1275  145 FORMAT (' ',F5.2,1X,E8.3,1X,E9.3,1X,E8.3,1X,F6.2,2X,
       &      E8.3,1X,3(F6.2,2X),3(E8.3,1X),2(F6.2,2X),F5.2,2X,A1)
    155 FORMAT (' ',1X,A4,2X,A7,3X,A7,5X,A4,5X,A6,3X,A6,4X,A5,2X,A9,
       &      2X,A7,3X,A6,3X,A5,4X,A7,3X,A3/,1X,A6,1X,3(A8,2X),9X,A8,
       &      11X,A8,20X,A8)
1280  165 FORMAT (' ',A6,1X,3(A8,2X),1X,A6,2X,A8,3X,A5,2X,A9,2X,A7,
       &      3X,A6,2X,A8,2X,A7,3X,A3//)
    175 FORMAT (' ',F5.2,3(1X,E9.3),2X,F7.2,2X,E8.3,2X,F7.2,2X,E8.3,
       &      2(2X,F7.2),2X,E8.3,2X,F7.2,2X,F5.2)
    185 FORMAT (' ',A4,3X,A7,4X,A6,3X,A6,2X,A7,5X,A4,5X,A6,3X,A6,4X,
1285   &      A5,2X,A9,3X,A6,3X,A6,4X,A3/,1X,A6,1X,A8,20X,A8,2X,A8,11X,
       &      A8,11X,A8)
```

```
      195   FORMAT (' ',A6,1X,A8,3X,A6,3X,A6,2X,A8,2X,A8,3X,A6,2X,A8,3X,
     &        A5,2X,A9,3X,A6,3X,A6,4X,A3//)
      205   FORMAT (' ',F5.2,2X,E8.3,2X,2(F7.2,2X),2(E9.3,1X),F7.2,2X,
1290  &        E8.3,2X,F7.2,2X,E8.3,2X,2(F7.2,2X),1X,F5.2)
      215   FORMAT (' ',A4,4X,A9,4X,A8,4X,A6,5X,A6,4X,A8,1X,A11,2X,A7,2X,
     &        A11,4X,A3/,A6,1X,2(A12,1X),8X,A12,11X,A12,10X,A12)
      225   FORMAT (' ',A6,1X,2(A12,1X),A6,2X,A12,1X,A8,1X,A12,1X,A7,2X,
     &        A12,3X,A3//)
1295  235   FORMAT (' ',F5.2,3X,2(E9.3,3X),F7.2,3X,E9.3,3X,F7.2,3X,E9.3,
     &        3X,F7.2,3X,E9.3,4X,F5.2)
      245   FORMAT (2(5(E9.3,1X)/),5(E9.3,1X),F7.3)
      255   FORMAT (2(5(E9.3,1X)/),3(E9.3,1X),F7.3)

1300        OPEN (23)

            READ (13,5) IPRINT
            READ (13,5) IA1, IA2, IPB1, IPB2, IEB1, IEB2,
            &           IBV1, IBV2, IZP1, IZP2
1305
            DO 180 I = 1, ILOOP
              DAY(I) = I * STEP
              DO 100 J = IA1, IA2
                READ (23,245) FLOW1(J), FLOW1A(J), FLOW2(J),
1310        &       FLOW3(J), FLOW4(J), FLOW5(J), FLOW6(J), FLOW7(J),
            &       FLOW8(J), FLOW9(J), FLOW10(J), FLOW11(J),
            &       FLOW12(J), FLOW13(J), FLOW14(J), AFRAC(J)
      100     CONTINUE
              DO 110 J = IH1, IH2
1315            READ (23,255) FLOW15(J), FLOW16(J), FLW16A(J),
            &       FLW16B(J), FLW16C(J), FLOW17(J), FLOW18(J),
            &       FLOW19(J), FLOW20(J), FLOW21(J), FLOW22(J),
            &       FLOW23(J), FLOW24(J), HFRAC(J)
      110     CONTINUE
1320
            HET1(I) = 0
            DET1(I) = 0
            DET3(I) = 0
            DET5(I) = 0
1325        DET7(I) = 0

            DO 120 J = 1, TCLASS
              HET1(I) = HET1(I) + FLOW20(J)
              DET1(I) = DET1(I) + FLOW5(J)
1330          DET3(I) = DET3(I) + FLOW17(J)
      120   CONTINUE

            DET2(I) = 100 * DET1(I) / (DET1(I) + DET3(I))
            DET4(I) = 100 * DET3(I) / (DET1(I) + DET3(I))
1335        DET8(I) = DC(I) / DN(I)



1340        AUTO1(I) = 0
            AUTO3(I) = 0
            AUTO5(I) = 0
            AUTO6(I) = 0
            AUTO10(I) = 0
1345        AUTO11(I) = 0
            AUTO12(I) = 0
            AUTO16(I) = 0
            AUTO17(I) = 0

1350        DO 130 J = IA1, IA2
              AUTO1(I)  = AUTO1(I) + FLOW1(J)
              AUTO3(I)  = AUTO3(I)  + FLOW1A(J)
              AUTO5(I)  = AUTO5(I)  + FLOW3(J)
              AUTO6(I)  = AUTO6(I)  + FLOW13(J)
1355          AUTO10(I) = AUTO10(I) + FLOW5(J)
```

```
            AUTO11(I) = AUTO11(I) + FLOW7(J)
            AUTO12(I) = AUTO12(I) + FLOW9(J)
            AUTO16(I) = AUTO16(I) + FLOW2(J)
            AUTO17(I) = AUTO17(I) + FLOW4(J)
130     CONTINUE

        AUTO2(I)  = AUTO1(I) / AC(I)
        AUTO4(I)  = AUTO3(I) / AC(I)
        AUTO7(I)  = 100 * AUTO6(I) / AUTO1(I)
        AUTO8(I)  = 100 * EXP (- 0.00405 * (NEWN(I) + REGN(I)))
        AUTO9(I)  = AUTO8(I) / 100 * AUTO1(I)
        AUTO13(I) = 100 * AUTO10(I) / AC(I)
        AUTO14(I) = 100 * AUTO11(I) / AC(I)
        AUTO15(I) = 100 * AUTO12(I) / AC(I)
        AUTO18(I) = AC(I) / AN(I)

        PBCT1(I) = 0
        PBCT3(I) = 0
        PBCT5(I) = 0
        PBCT9(I) = 0
        PBCT10(I) = 0
        PBCT13(I) = 0

        DO 140 J = IPB1, IPB2
          PBCT1(I)  = PBCT1(I) + FLOW15(J)
          PBCT3(I)  = PBCT3(I) + FLOW19(J)
          PBCT5(I)  = PBCT5(I) + FLOW21(J)
          PBCT9(I)  = PBCT9(I) + FLW16A(J)
          PBCT10(I) = PBCT10(I) + FLW16B(J)
          PBCT13(I) = PBCT13(I) + FLOW20(J)
140     CONTINUE

        PBCT2(I) = PBCT1(I) - PBCT3(I)
        PBCT4(I) = 100 * PBCT3(I) / PBCT1(I)
        PBCT6(I) = 100 * PBCT5(I) / PBC(I)
        PBCT7(I) = 100 * PBCT2(I) / PBCT1(I)
        PBCT8(I) = 100 * PBCT2(I) / AUTO1(I)
        PBCT11(I)= 100 * (PBCT9(I) + PBCT10(I)) / (PBCT9(I) + PBCT10(I)
       &          + AUTO16(I) + AUTO17(I))
        PBCT12(I)= 100 * PBCT10(I) / (PBCT10(I) + PBCT9(I))
        PBCT14(I)= 100 * PBCT13(I) / HET1(I)
        PBCT15(I)= PBC(I) / PBN(I)

        EBCT1(I) = 0
        EBCT3(I) = 0
        EBCT5(I) = 0
        EBCT9(I) = 0
        EBCT10(I) = 0
        EBCT11(I) = 0

        DO 150 J = IEB1, IEB2
          EBCT1(I)  = EBCT1(I) + FLOW15(J)
          EBCT3(I)  = EBCT3(I) + FLOW19(J)
          EBCT5(I)  = EBCT5(I) + FLOW21(J)
          EBCT9(I)  = EBCT9(I) + FLW16A(J) + FLW16B(J)
          EBCT10(I) = EBCT10(I) + FLOW16(J)
          EBCT11(I) = EBCT11(I) + FLOW20(J)
150     CONTINUE

        EBCT2(I)  = EBCT1(I) - EBCT3(I)
        EBCT4(I)  = 100 * EBCT3(I) / EBCT1(I)
        EBCT6(I)  = 100 * EBCT5(I) / EBC(I)
        EBCT7(I)  = 100 * EBCT2(I) / EBCT1(I)
        EBCT8(I)  = 100 * EBCT1(I) / AUTO1(I)
        EBCT12(I) = 100 * EBCT11(I) / HET1(I)
        EBCT13(I) = 100 * EBC(I) / (EBC(I) + PBC(I))
        EBCT14(I) = EBC(I) / EBN(I)

        BVOR1(I) = 0
```

```
1425        BVOR3(I) = 0
            BVOR5(I) = 0
            BVOR7(I) = 0
            BVOR10(I) = 0

1430        DO 160 J = IBV1, IBV2
              BVOR1(I)  = BVOR1(I) + FLOW15(J)
              BVOR3(I)  = BVOR3(I) + FLOW19(J)
              BVOR5(I)  = BVOR5(I) + FLOW17(J),
              BVOR7(I)  = BVOR7(I) + FLOW21(J)
1435          BVOR10(I) = BVOR10(I) + FLOW20(J)
          160 CONTINUE

            BVOR2(I)  = BVOR1(I) - BVOR3(I) - BVOR5(I)
            BVOR4(I)  = 100 * BVOR3(I) / BVOR1(I)
1440        BVOR6(I)  = 100 * BVOR5(I) / DET3(I)
            BVOR8(I)  = 100 * BVOR7(I) / BVOR1(I)
            BVOR9(I)  = 100 * BVOR2(I) / BVOR1(I)
            BVOR11(I) = 100 * BVOR10(I) / HET1(I)
            BVOR12(I) = BVC(I) / BVN(I)
1445
            ZOOP1(I) = 0
            ZOOP2(I) = 0
            ZOOP3(I) = 0
            ZOOP5(I) = 0
1450        ZOOP7(I) = 0
            ZOOP9(I) = 0

            DO 170 J = IZP1, IZP2
              ZOOP1(I) = ZOOP1(I) + FLOW15(J)
1455          ZOOP2(I) = ZOOP2(I) + AFRAC(J) * FLOW15(J)
              ZOOP3(I) = ZOOP3(I) + HFRAC(J) * FLOW15(J)
              ZOOP5(I) = ZOOP5(I) + FLOW19(J)
              ZOOP7(I) = ZOOP7(I) + FLOW17(J)
              ZOOP9(I) = ZOOP9(I) + FLOW21(J)
1460      170 CONTINUE

            ZOOP4(I) = ZOOP1(I) - ZOOP5(I) - ZOOP7(I)
            ZOOP2(I) = 100 * ZOOP2(I) / ZOOP1(I)
            ZOOP3(I) = 100 * ZOOP3(I) / ZOOP1(I)
1465        ZOOP6(I) = 100 * ZOOP5(I) / ZOOP1(I)
            ZOOP8(I) = 100 * ZOOP7(I) / DET3(I)
            ZOOP10(I) = 100 * ZOOP9(I) / ZOOP4(I)
            ZOOP11(I) = 100 * (ZOOP4(I) - ZOOP9(I)) / ZOOP1(I)
            ZOOP12(I) = ZPC(I) / ZPN(I)
1470
            DET5(I) = EBCT1(I)
            DET7(I) = EBCT10(I)
            DET6(I) = 100 * DET5(I) / DC(I)

1475
          180 CONTINUE

            PRINT 15, '*************************'
            PRINT 25, '***                   ***'
1480        PRINT 25, '***  PHYTOPLANKTON    ***'
            PRINT 25, '***                   ***'
            PRINT 35, '*************************'
             PRINT 45, 'TIME','GROSS P/S','GROSS P/B','NET P/S','NET P/B',
            &'RESPIRATION','ACTUAL PDOC','ACTUAL PER','EST PDOC',
1485        &'EST PER','(DAYS)','(MG.M-3.D-1)','(D-1)',
            &'(MG.M-3.D-1)','(D-1)','(MG.M-3.D-1)','(MG.M-3.D-1)',
            &'(PDOC/GROSS)','(MG.M-3.D-1)'
             PRINT 55, '******','***********','*********','***********',
            &'********','***********','***********','***********',
1490        &'***********','*******'
            DO 190 I = 1, ILOOP, IPRINT
              PRINT 65, DAY(I),AUTO1(I),AUTO2(I),AUTO3(I),AUTO4(I),
           &   AUTO5(I),AUTO6(I),AUTO7(I),AUTO9(I),AUTO8(I)
```

```
      190  CONTINUE
1495
           PRINT 15, '*************************'
           PRINT 25, '***                   ***'
           PRINT 25, '***   PHYTOPLANKTON   ***'
           PRINT 25, '***                   ***'
1500       PRINT 35, '*************************'

           PRINT 75, 'TIME','C DEATH','C SINKING','C GRAZED','% THAT DIE',
          &'% THAT SINK','% GRAZED','NEWN UPTAKE','REGN UPTAKE','C N RATIO',
          &'(DAYS)','(MG.M-3.D-1)','(MG.M-3.D-1)','(MG.M-3.D-1)',
1505      &'(DEATH/AC)','(SINK/AC)','(GRAZED/AC)','(MG.M-3.D-1)',
          &'(MG.M-3.D-1)'
           PRINT 85, '******','************','************','************',
          &'**********','**********','**********','************',
          &'************','*********'
1510       DO 200 I = 1, ILOOP, IPRINT
             PRINT 65, DAY(I),AUTO10(I), AUTO11(I), AUTO12(I),AUTO13(I),
          &   AUTO14(I),AUTO15(I),AUTO16(I),AUTO17(I),AUTO18(I)
      200  CONTINUE

1515       PRINT 15, '*************************'
           PRINT 25, '***                   ***'
           PRINT 25, '***  PLANKTOBACTERIA  ***'
           PRINT 25, '***                   ***'
           PRINT 35, '*************************'
1520       PRINT 95, 'TIME','PDOC IN','GR PROD','RESP','% RESP',
          &'AMT EATEN','% EATEN','NET YG','%1 PROD','NEWN IN','REGN IN',
          &'% TOTN','% REGN','EXCRE','% REMIN','C N','(DAYS)','(MG.M-3)',
          &'(MG.M-3)','(MG.M-3)','(MG.M-3)','(MG.M-3)','(MG.M-3)',
          &'(MG.M-3)'
1525       PRINT 105, '******','********','********','********','******',
          &'*********','*******','******','*******','********',
          &'********','******','******','********','*******','***'
           DO 210 I = 1, ILOOP, IPRINT
             PRINT 115, DAY(I),PBCT1(I),PBCT2(I),PBCT3(I),PBCT4(I),
1530      &   PBCT5(I),PBCT6(I),PBCT7(I),PBCT8(I),PBCT9(I),PBCT10(I),
          &   PBCT11(I),PBCT12(I),PBCT13(I),PBCT14(I),PBCT15(I)
      210  CONTINUE

           PRINT 15, '*************************'
1535       PRINT 25, '***                   ***'
           PRINT 25, '***    EPIBACTERIA    ***'
           PRINT 25, '***                   ***'
           PRINT 35, '*************************'
           PRINT 125, 'TIME','DETC IN','GR PROD','RESP','% RESP',
1540      &'AMT EATEN','% EATEN','NET YG','%1 PROD','DISN IN','DETN IN',
          &'EXCRE','% REMIN','% EPI','C N','LIMIT','(DAYS)','(MG.M-3)',
          &'(MG.M-3)','(MG.M-3)','(MG.M-3)','(MG.M-3)','(MG.M-3)',
          &'(MG.M-3)'
           PRINT 135, '********','********','********','******',
1545      &'*********','*******','******','*******','********','********',
          &'********','*******','*****','***','*****'
           DO 220 I = 1, ILOOP, IPRINT
             PRINT 145, DAY(I),EBCT1(I),EBCT2(I),EBCT3(I),EBCT4(I),EBCT5(I),
          &  EBCT6(I),EBCT7(I),EBCT8(I),EBCT9(I),EBCT10(I),EBCT11(I),
1550      &  EBCT12(I),EBCT13(I),EBCT14(I),EBCT15(I)
      220  CONTINUE

           PRINT 15, '*************************'
           PRINT 25, '***                   ***'
1555       PRINT 25, '***   BACTIVORES      ***'
           PRINT 25, '***                   ***'
           PRINT 35, '*************************'
           PRINT 155, 'TIME','C EATEN','GR PROD','RESP','% RESP',
          &'FAECES','% DET','AMT EATEN','% EATEN','NET YG','EXCRE',
1560      &'% REMIN','C N','(DAYS)','(MG.M-3)','(MG.M-3)','(MG.M-3)',
          &'(MG.M-3)','(MG.M-3)','(MG.M-3)'
           PRINT 165, '******','********','********','********','******',
```

```
     &'********','******','*********','*******','******','********',
     &'*******','***'
1565  DO 230 I = 1, ILOOP, IPRINT
       PRINT 175, DAY(I),BVOR1(I),BVOR2(I),BVOR3(I),BVOR4(I),BVOR5(I),
     &  BVOR6(I),BVOR7(I),BVOR8(I),BVOR9(I),BVOR10(I),BVOR11(I),
     &  BVOR12(I)
    230  CONTINUE
1570
      PRINT 15, '*************************'
      PRINT 25, '***                   ***'
      PRINT 25, '***   ZOOPLANKTON     ***'
      PRINT 25, '***                   ***'
1575  PRINT 35, '*************************'
      PRINT 185, 'TIME','C EATEN','% HERB','% CARN','GR PROD',
     &'RESP','% RESP','FAECES','% DET','AMT EATEN','% HETS',
     &'NET YG','C N','(DAYS)','(MG.M-3)','(MG.M-3)','(MG.M-3)',
     &'(MG.M-3)','(MG.M-3)'
1580  PRINT 195, '******','********','******','******','********',
     &'********','******','********','*****','*********','******',
     &'******','***'
      DO 240 I = 1, ILOOP, IPRINT
       PRINT 205, DAY(I),ZOOP1(I),ZOOP2(I),ZOOP3(I),ZOOP4(I),ZOOP5(I),
1585  &  ZOOP6(I),ZOOP7(I),ZOOP8(I),ZOOP9(I),ZOOP10(I),ZOOP11(I),
     &  ZOOP12(I)
    240  CONTINUE

      PRINT 15, '*************************'
1590  PRINT 25, '***                   ***'
      PRINT 25, '***  ABIOTIC POOLS    ***'
      PRINT 25, '***                   ***'
      PRINT 35, '*************************'
      PRINT 215, 'TIME','TOT REMIN','A TO DET','% AUTO','FAECES',
1595  &'% FAECES','DET C EATEN','% EATEN','DET N EATEN','C N',
     &'(DAYS)','(MG.M-3.D-1)','(MG.M-3.D-1)','(MG.M-3.D-1)',
     &'(MG.M-3.D-1)','(MG.M-3.D-1)'
      PRINT 225, '******','************','************','******',
     &'************','********','************','*******',
1600  &'************','***'
      DO 250 I = 1, ILOOP, IPRINT
       PRINT 235, DAY(I),HET1(I),DET1(I),DET2(I),DET3(I),DET4(I),
     &  DET5(I),DET6(I),DET7(I),DET8(I)
    250  CONTINUE
1605
      CLOSE (13)
      CLOSE (14)
      CLOSE (15)
      CLOSE (16)
1610  CLOSE (17)
      CLOSE (20)
      CLOSE (21)
      CLOSE (22)
      CLOSE (23)
1615
      RETURN
      END
```

8. Definitions of program variables and parameters

A1	An array of size-dependent carbon fixation rates by autotrophs
A2	An array of size-dependent new-nitrogen uptake rates by autotrophs
A2A	An array of size-dependent half saturation constants for new-nitrogen uptake by autotrophs
A3	An array of size-dependent respiration rates for autotrophs
A4	An array of size-dependent regenerated-nitrogen uptake rates by autotrophs
A4A	An array of size-dependent half saturation constants for regenerated-nitrogen uptake by autotrophs
A5	An array of size-dependent death rates for autotrophs

A7	An array of size-dependent sinking rates for autotrophs
A11	An array of size-dependent growth rates for autotrophs
A13	An array of size-dependent PDOC production rates for autotrophs
AC	An array of total carbon standing stocks (µg) for autotrophs at each time step (sum of all the AMASSC's)
ACN	The carbon : nitrogen ratio for autotrophs
AFRAC	An array denoting the proportion of each size class in the total array which is composed of autotrophs
AMASSC	An array of the carbon standing stocks (µg) in each autotroph size class at each time step
AMASSN	An array of the nitrogen standing stocks (µg) in each autotroph size class at each time step
AN	An array of total nitrogen standing stocks (µg) for autotrophs at each time step (sum of all the AMASSN's)
ASIMHC	An array of amounts of carbon (µg) assimilated by each heterotroph size class at each time step
ASIMHN	An array of amounts of nitrogen (µg) assimilated by each heterotroph size class at each time step
ASMALC	An array of the minimum carbon standing stocks (µg) for each autotroph size class (the "refuge")
ASMALN	An array of minimum nitrogen standing stocks (µg) in each autotroph size class (the "refuge")
ASSIMH	An array of assimilation efficiencies for each heterotroph size class
AUT01	An array of gross amounts of carbon fixed by autotrophs at each time step
AUT02	An array of gross production : biomass ratios for autotrophs at each time step
AUT03	An array of net amounts of carbon fixed by autotrophs at each time step
AUT04	An array of net production : biomass ratios for autotrophs at each time step
AUT05	An array of total amounts of carbon lost through respiration by all autotrophs at each time step
AUT06	An array of total amounts of carbon lost through PDOC production by all autotrophs at each time step
AUT07	An array of total PER's by all autotrophs at each time step
AUT08	An array of PER's for all autotrophs calculated on the basis of ambient nitrogen concentrations at each time step
AUT09	An array of total amounts of carbon lost through PDOC production by all autotrophs at each time step, calculated on the basis of ambient nitrogen concentrations
AUT010	An array of total amounts of carbon lost through death by all autotrophs at each time step
AUT011	An array of total amounts of carbon lost through sinking by all autotrophs at each time step
AUT012	An array of total amounts of carbon lost through grazing by zooplankton by all autotrophs at each time step
AUT013	An array of percentages of standing stocks of all autotrophs that die at each time step
AUT014	An array of percentages of standing stocks of all autotrophs that sink at each time step
AUT015	An array of percentages of standing stocks of all autotrophs that are grazed at each time step
AUT016	An array of total amounts of new-nitrogen taken up by autotrophs at each time step
AUT017	An array of total amounts of regenerated-nitrogen taken up by autotrophs at each time step
AUT018	An array of calculated C : N ratios of autotrophs at each time step
BSA	An array of percentages of the standing stocks in each autotroph size class of the maximum autotroph size class standing stock at each time step
BSH	An array of percentages of standing stocks in each heterotroph size class of the maximum heterotroph size class standing stock at each time step
BST	An array of percentages of standing stocks in each size class of the maximum size class standing stock at each time step
BVC	An array of total carbon standing stocks (µg) for bactivores at each time step (sum of all the HMASSC's between IBV1 and IBV2)
BVN	An array of total nitrogen standing stocks (µg) for bactivores at each time step (sum of all the HMASSN's between IBV1 and IBV2)
BVOR1	An array of total amounts of carbon consumed by bactivores at each time step
BVOR2	An array of total amounts of carbon channelled to gross production by bactivores at each time step
BVOR3	An array of total amounts of carbon lost through respiration by bactivores at each time step
BVOR4	An array of total percentages of consumption lost through respiration by bactivores at each time step
BVOR5	An array of total amounts of carbon lost as faeces from bactivores at each time step
BVOR6	An array of percentage contributions of bactivores to the detrital pool at each time step
BVOR7	An array of total amounts of carbon lost to grazers from bactivores at each time step
BVOR8	An array of total percentages of bactivore standing stocks lost to grazers at each time step
BVOR9	An array of net growth yields of bactivores at each time step
BVOR10	An array of total amounts of nitrogen lost through excretion by bactivores at each time step
BVOR11	An array of percentage contributions of bactivores to nitrogen regeneration at each time step

BVOR12	An array of calculated C : N ratios of bactivores at each time step
C1	An array of carbon increments times the time step (STEP) for autotroph size classes
C2	An array of nitrogen increments times the time step (STEP) for autotroph size classes
C3	An array of carbon increments times the time step (STEP) for heterotroph size classes
C4	An array of nitrogen increments times the time step (STEP) for heterotroph size classes
C5	The carbon increment times the time step (STEP) for the detrital pool
C6	The nitrogen increment times the time step (STEP) for the detrital pool
C7	The nitrogen increment times the time step (STEP) for the new-nitrogen pool
C8	The nitrogen increment times the time step (STEP) for the regenerated-nitrogen pool
C9	Carbon increment times the time step (STEP) for the PDOC pool
CDIN	The amount of carbon (µg) contributed to the detrital pool by autotrophs and heterotrophs at each time step
CDOUT	The amount of carbon (µg) removed from the detrital pool by heterotrophs at each time step
CPREDA	The amount of carbon (µg) in each autotroph size class consumed by predator size classes
CPREDH	The amount of carbon (µg) in each heterotroph size class consumed by predator size classes
DAMASC	An array of the differences between carbon inputs and carbon outputs in each autotroph size class, calculated twice in each loop in the program
DAMASN	An array of the differences between nitrogen inputs and nitrogen outputs in each autotroph size class, calculated twice in each loop in the program
DAY	The real time in days, calculated as STEP x I
DC	The total amounts of carbon (µg) in the detrital pool at each time step
DDC	The difference between carbon inputs and carbon outputs to the detrital pool, calculated twice in each loop in the program
DDN	The difference between nitrogen inputs and nitrogen outputs to the detrital pool, calculated twice in each loop in the program
DET1	An array of amounts of autotroph carbon entering the detrital pool at each time step
DET2	An array of percentage contributions of autotrophs to the detrital pool at each time step
DET3	An array of amounts of faecal carbon entering the detrital pool at each time step
DET4	An array of percentage contributions of faecal material to the detrital pool at each time step
DET5	An array of amounts of detrital carbon eaten from the detrital pool at each time step
DET6	An array of percentages of detrital material eaten at each time step
DET7	An array of amounts of detrital nitrogen eaten from the detrital pool at each time step
DET8	An array of calculated C : N ratios for the detrital pool at each time step
DHMASC	An array of the differences between carbon inputs and carbon outputs in each heterotroph size class, calculated twice in each loop in the program
DHMASN	An array of the differences between nitrogen inputs and nitrogen outputs in each heterotroph size class, calculated twice in each loop in the program
DIURN	Character variable (Y or N) for setting a diurnal cycle in the model community
DN	An array of total amounts of nitrogen (µg) in the detrital pool at each time step
DNEWN	The difference between nitrogen inputs and nitrogen outputs to the new-nitrogen pool, calculated twice in each loop in the program
DOCIN	The amount of carbon (µg) contributed to the PDOC pool by autotrophs at each time step
DOCOUT	The amount of carbon (µg) removed from the PDOC pool by heterotrophs at each time step
DPDOC	The difference between carbon inputs and carbon outputs to the PDOC pool, calculated twice in each loop in the program
DREGN	The difference between nitrogen inputs and nitrogen outputs to the regenerated-nitrogen pool, calculated twice in each loop in the program
EBC	An array of total carbon standing stocks (µg) for epibacteria at each time step (sum of all the HMASSC's between IEB1 and IEB2)
EBCT1	An array of amounts of detrital carbon eaten by epibacteria at each time step
EBCT2	An array of total amounts of carbon channelled to gross production by epibacteria at each time step
EBCT3	An array of amounts of carbon lost through respiration from epibacteria at each time step
EBCT4	An array of percentages of consumption lost through respiration by epibacteria at each time step
EBCT5	An array of total amounts of carbon lost to grazers from epibacteria at each time step
EBCT6	An array of total percentages of epibacteria standing stocks lost to grazers at each time step
EBCT7	An array of net growth yield of epibacteria at each time step
EBCT8	An array of percentages epibacteria production of primary production at each time step
EBCT9	An array of amounts of dissolved nitrogen taken up by epibacteria at each time step

EBCT10	An array of amounts of detrital nitrogen eaten by epibacteria at each time step
EBCT11	An array of total amounts of nitrogen lost through excretion by epibacteria at each time step
EBCT12	An array of percentage contributions of epibacteria to nitrogen regeneration at each time step
EBCT13	An array of percentages bacteria that are epibacteria at each time step
EBCT14	An array of C : N ratios of epibacteria at each time step
EBCT15	An array of character variables indicating whether carbon ('C') or nitrogen ('N') is limiting epibacteria growth at each time step
EBN	An array of total nitrogen standing stocks (μg) for epibacteria at each time step (sum of all the HMASSN's between IEB1 and IEB2)
FLOW1	An array of gross amounts of carbon (μg) fixed by each autotroph size class
FLOW1A	An array of net amounts of carbon (μg) fixed by each autotroph size class
FLOW2	An array of amounts of new-nitrogen taken up by each autotroph size class
FLOW3	An array of carbon losses (μg) through respiration by each autotroph size class
FLOW4	An array of amounts of regenerated-nitrogen ($(\mu g.d^{-1})$ for g) taken up by each autotroph size class
FLOW5	An array of carbon losses through natural death (μg) from each autotroph size class
FLOW6	An array of nitrogen losses through natural death (μg) from each autotroph size class
FLOW7	An array of carbon losses (μg) through sinking from each autotroph size class
FLOW8	An array of nitrogen losses (μg) through sinking from each autotroph size class
FLOW9	An array of carbon losses (μg) from each autotroph size class through predation (sum of CPREDA's for each prey class)
FLOW10	An array of nitrogen losses (μg) from each autotroph size class through predation (sum of NPREDA's for each prey class)
FLOW11	An array of carbon losses (μg) through growth from each autotroph size class
FLOW12	An array of nitrogen losses (μg) through growth from each autotroph size class
FLOW13	An array of carbon losses (μg) through PDOC excretion from each autotroph size class
FLOW14	An array of nitrogen losses (μg) through PDON excretion from each autotroph size class
FLOW15	An array of carbon gains (μg) into each heterotroph size class through ingestion / uptake (sum of CPREDA's and CPREDH's for each predator class)
FLOW16	An array of nitrogen gains (μg) into each heterotroph size class through ingestion / uptake (sum of NPREDA's and NPREDH's for each predator class)
FLOW17	An array of carbon losses (μg) from each heterotroph size class through egestion
FLOW18	An array of nitrogen losses (μg) from each heterotroph size class through egestion
FLOW19	An array of carbon losses (μg) from each heterotroph size class through respiration
FLOW20	An array of nitrogen losses (μg) from each heterotroph size class through excretion
FLOW21	An array of carbon losses (μg) from each heterotroph size class through predation (sum of CPREDH's for each prey class)
FLOW22	An array of nitrogen losses (μg) from each heterotroph size class through predation (sum of NPREDH's for each prey class)
FLOW23	An array of carbon losses (μg) from each heterotroph size class through growth
FLOW24	An array of nitrogen losses (μg) from each heterotroph size class through growth
FLW16A	An array of amounts of new-nitrogen (μg) taken up by each bacterioplankton size class
FLW16B	An array of amounts of regenerated-nitrogen (μg) taken up by each bacterioplankton size class
FLW16C	An array of amounts of dissolved nitrogen (μg) taken up by each epibacteria size class
H15	An array of size-dependent ingestion / uptake rates by heterotrophs
H15A	An array of prey-size dependent half saturation constants for carbon ingestion
H17	An array of size-dependent assimilation rates for each heterotroph size class
H19	An array of size-dependent respiration rates for each heterotroph size class
H23	An array of size-dependent growth rates for each heterotroph size class
HCN	An array of carbon : nitrogen ratios for each heterotroph size class
HET1	An array of total amounts of regenerated nitrogen entering the regenerated nitrogen pool at each time step
HFRAC	An array denoting the proportion of each size class in the total array which is composed of heterotrophs
HMASSC	An array of carbon standing stocks (μg) in each heterotroph size class at each time step
HMASSN	An array of nitrogen standing stocks (μg) in each heterotroph size class at each time step
HSMALC	An array of minimum carbon standing stocks (μg) for each heterotroph size class (the "refuge")
HSMALN	An array of minimum nitrogen standing stocks (μg) for each heterotroph size class (the "refuge")

I	An integer counter which records the number of the loop being executed (maximum value is set by ILOOP)
I2	An integer subscript used internally as a counter for prey and predator subscripts
I3	An integer subscript used internally as a counter for prey and predator subscripts
IA1	An integer subscript denoting the starting position of autotrophs in the total array
IA2	An integer subscript denoting the end position of autotrophs in the total array
IBV1	An integer subscript denoting the starting position of bactivores in the total array
IBV2	An integer subscript denoting the end position of bactivores in the total array
ICOUNT	An integer counter which determines when output is written to the temporary file TC2*OUT. for input to subroutine EXTRAS. ICOUNT is set to one in ISUB1 and to two in ISUB2, at which stage the flows are written to the temporary file
IDAY	The integer time in days, calculated as the integer (truncated) form of DAY
IEB1	An integer subscript denoting the starting position of epibacteria in the total array
IEB2	An integer subscript denoting the end position of epibacteria in the total array
IH1	An integer subscript denoting the starting position of heterotrophs in the total array
IH2	An integer subscript denoting the end position of heterotrophs in the total array
III	An integer variable determining when the data for 3-D plots should be written to the appropriate data files
ILOOP	An integer variable denoting the number of loops to be executed in each simulation
IPB1	An integer subscript denoting the starting position of bacterioplankton in the total array
IPB2	An integer subscript denoting the end position of bacterioplankton in the total array
IPRINT	An integer counter which specifies at what time interval in the program output should be printed
ISPACE	An internal integer counter which specifies at what time interval in the program output should be printed
ITAB	An integer counter used to determine when initial values should be read from data files; if ITAB is greater than one all READ statements are ignored, since initial values are only read in the first loop
IZP1	An integer subscript denoting the starting position of zooplankton in the total array
IZP2	An integer subscript denoting the end position of zooplankton in the total array
K15	An array of size-dependent half saturation constants for nitrogen uptake by bacterioplankton
NCON	The constant amount of nitrogen (µg) always in the model system if the method of nitrogen input is chosen to be a constant level i.e. NITRO is 'CNSTNT'
NDIN	The amount of nitrogen (µg) contributed to the detrital pool by autotrophs and heterotrophs at each time step
NDOUT	The amount of nitrogen (µg) removed from the detrital pool by heterotrophs at each time step
NEWN	An array of total amounts of nitrogen (µg) in the new-nitrogen pool at each time step
NEWOUT	The amount of nitrogen (µg) removed from the new-nitrogen pool by autotrophs and heterotrophs at each time step
NINCRE	The amount of new-nitrogen (µg) entering the system at each time step if the method of nitrogen input is chosen to be a small continuous amount i.e. NITRO is 'CONTIN'
NITRO	A character variable which determines the method of nitrogen input into the system: a single large input at the beginning of the run which simulates upwelling (PULSED), a small continuous input which simulates diffusion across the pycnocline (CONTIN) or a constant unchanging level (CNSTNT)
NPREDA	The amount of nitrogen (µg) in each autotroph size class consumed by predator size classes
NPREDH	The amount of nitrogen (µg) in each heterotroph size class consumed by predator size classes
NX	An integer variable used to determine the number of points on the X axis of the grid for the 3-D plot
NY	An integer variable used to determine the number of points on the Y axis of the grid for the 3-D plot
PBC	An array of total carbon standing stocks (µg) for bacterioplankton at each time step (sum of all the HMASSC's between IPB1 and IPB2)
PBCT1	An array of amounts of carbon taken up from the PDOC pool by bacterioplankton at each time step
PBCT2	An array of total amounts of carbon channelled to gross production by bacterioplankton at each time step
PBCT3	An array of amounts of carbon lost through respiration from bacterioplankton at each time step
PBCT4	An array of total percentages of consumption lost through respiration by bacterioplankton at each time step
PBCT5	An array of total amounts of carbon lost to grazers from bacterioplankton at each time step
PBCT6	An array of total percentages of bacterioplankton standing stocks lost to grazers at each time step
PBCT7	An array of net growth yields of bacterioplankton at each time step
PBCT8	An array of percentages bacterioplankton production of primary production at each time step

PBCT9	An array of amounts of new-nitrogen taken up by bacterioplankton at each time step
PBCT10	An array of amounts of regenerated-nitrogen taken up by bacterioplankton at each time step
PBCT11	An array of percentages total nitrogen taken up by bacterioplankton at each time step
PBCT12	An array of percentages regenerated-nitrogen taken up by bacterioplankton at each time step
PBCT13	An array of total amounts of nitrogen lost through excretion by bacterioplankton at each time step
PBCT14	An array of percentage contributions of bacterioplankton to nitrogen regeneration at each time step
PBCT15	An array of C : N ratios of bacterioplankton at each time step
PBCV	The mass-specific uptake rate of carbon from the PDOC pool by bacterioplankton
PBN	An array of total nitrogen standing stocks (μg) for bacterioplankton at each time step (sum of all the HMASSN's between IPB1 and IPB2)
PBNV	The mass-specific uptake rate of nitrogen from the nitrogen pool by bacterioplankton
PDOC	An array of total amounts of carbon (μg) in the PDOC pool at each time step
PER	The percentage extracellular release of PDOC from each autotroph size class; PER can be a constant fraction or dependent on ambient nitrogen concentrations
PERCON	A character variable which determines whether PER is a constant fraction of gross carbon fixation (CNSTNT) or whether it depends on ambient nitrogen concentrations (CHANGE)
PRED	A matrix containing predation losses from each prey size class to each predator size class
PREF	A matrix containing the "preference" factors for predation by each predator class on each prey class
PREF1	A real variable which determines the preference factor of predators for their optimum prey size class (usually set to 1)
PREF2	A real variable which determines the factor by which the preference of each predator class for its prey classes (PREF3) is decreased as one moves successively away from the optimum prey size class
PREF3	The preference factor of each predator class for each of its prey classes
REGIN	The amount of nitrogen (μg) contributed to the regenerated-nitrogen pool by heterotrophs at each time step
REGN	An array of total amounts of nitrogen (μg) in the regenerated-nitrogen pool at each time step
REGOUT	The amount of nitrogen (μg) removed from the regenerated-nitrogen pool by autotrophs and heterotrophs at each time step
SIZE	An integer parameter which sets the maximum number of size classes in some arrays
STEP	A real parameter which determines the time step used in solving the differential equations in the program (set equal to 0.05)
TCLASS	The integer number of size classes in the total array
TIME	An integer parameter which sets the maximum possible number of loops that the program can execute in each run, and thus determines the maximum size of some arrays
TMASSC	An array of total carbon standing stocks (μg) in each prey size class at each time step
TOPA	The maximum size class standing stock for autotrophs at each time step
TOPH	The maximum size class standing stock for heterotrophs at each time step
TOPT	The maximum size class standing stock for autotrophs and heterotrophs combined at each time step
UCLASS	An array of integer numbers of prey size classes available to each predator size class
UMASSC	An array of total amounts of prey carbon available to each predator size class
UMINUS	An array of numbers of size classes in each predator's prey range that are smaller than the optimum prey size for each predator
UPLUS	An array of numbers of size classes in each predator's prey range that are larger than the optimum prey size for each predator
UPOS	An array of subscripts denoting the position of the smallest prey size class in the total array for each predator
UTOTAN	The total amount of nitrogen (μg) potentially required by autotrophs
UTOTC	The total amount of carbon (μg) potentially required by bacterioplankton
UTOTD	The total amount of detrital carbon (μg) potentially required by epibacteria
UTOTN	The total amount of nitrogen (μg) potentially required by bacterioplankton and autotrophs
UTOTNN	The total amount of new-nitrogen (μg) potentially required by bacterioplankton and autotrophs
UTOTPN	The total amount of nitrogen (μg) potentially required by bacterioplankton
UTOTRN	The total amount of regenerated-nitrogen (μg) potentially required by bacterioplankton and autotrophs
VCLASS	An array of integer numbers of predator size classes preying on each prey size class
VER$N	A character parameter that records the date at which the program was last updated. VER$N changes whenever the routine UPDATE is called from CTS
VMASSC	An array of total predator standing stocks preying on each prey size class

VPOS	An array of subscripts denoting the position of the smallest predator size class in the total array for each prey size class
X1	A real variable setting the minimum X value for the grid for the 3-D plot
XL	A real variable setting the maximum X value for the grid for the 3-D plot
Y1	A real variable setting the minimum Y value for the grid for the 3-D plot
YL	A real variable setting the maximum Y value for the grid for the 3-D plot
ZOOP1	An array of total amounts of carbon consumed by zooplankton at each time step
ZOOP2	An array of percentages autotrophs in the diet of zooplankton at each time step
ZOOP3	An array of percentages heterotrophs in the diet of zooplankton at each time step
ZOOP4	An array of total amounts of carbon channelled to gross production by zooplankton at each time step
ZOOP5	An array of total amounts of carbon lost through respiration by zooplankton at each time step
ZOOP6	An array of total percentages of consumption lost through respiration by zooplankton at each time step
ZOOP7	An array of total amounts of carbon lost as faeces from zooplankton at each time step
ZOOP8	An array of percentage contributions of zooplankton to the detrital pool at each time step
ZOOP9	An array of total amounts of carbon lost to grazers from zooplankton at each time step
ZOOP10	An array of total percentages of zooplankton standing stocks lost to grazers at each time step
ZOOP11	An array of net growth yields of zooplankton at each time step
ZOOP12	An array of calculated C : N ratios of zooplankton at each time step
ZPC	An array of total carbon standing stocks (µg) for zooplankton at each time step (sum of all the HMASSC's between IZP1 and IZP2)
ZPN	An array of total nitrogen standing stocks (µg) for zooplankton at each time step (sum of all the HMASSN's between IZP1 and IZP2)